Geotechnical Investigation and Geologic Hazard Study Report

Berkeley City College – 2118 Milvia Street
Peralta Community College District
Berkeley, California

SUBMITTED TO:

Mr. Jeff Swinyer
Project Executive
XL Construction
jswinyer@xlconstruction.com

January 21, 2022

A3GEO

January 21, 2022

Mr. Jeff Swinyer
Project Executive
XL Construction
jswinyer@xlconstruction.com

Geotechnical Investigation and Geologic Hazard Study Report
Berkeley City College – 2118 Milvia Street
Peralta Community College District
Berkeley, California

Dear Mr. Swinyer:

This report presents the results of our geotechnical investigation and geologic hazards study for the Berkeley City College project at 2118 Milvia Street in Berkeley, California, which is part of the Peralta Community College District. Our work was performed in accordance with our proposal dated January 21, 2021 and our professional services agreement with XL Construction dated August 4, 2021.

This report includes data and interpretations pertaining to geotechnical and geologic conditions at the site and presents conclusions and recommendations for the geotechnical aspects of the project, as currently envisioned. This report is intended to be consistent with the State of California requirements for public school construction. The conclusions and recommendations presented in this report were developed in accordance with generally accepted geotechnical principles and practices at the time the report was prepared. No other warranty, expressed or implied, is made.

Thank you for inviting us to complete this work, and we look forward to our continued service during final design and subsequent construction phases of the project. Should you have questions or concerns regarding our findings, the design concepts discussed, or our recommendations, please do not hesitate to contact us.

Respectfully,

A3GEO, Inc.

Dillon Braud, PE
Project Engineer
dillon@a3geo.com

Timothy P. Sneddon, PE, GE
Principal Engineer
tim@a3geo.com

Lettis Consultants International, Inc.

John N. Baldwin, CEG
Sr. Principal Geologist
baldwin@lettisci.com

TABLE OF CONTENTS

List of Tables

List of Figures

List of Appendices

1. INTRODUCTION

This report presents the results of our geotechnical investigation and geologic hazards study for the Berkeley City College project at 2118 Milvia Street in Berkeley, California, which is part of the Peralta Community College District. We obtained information about the project from the design team, which includes XL Construction and Peralta Community College District. Our work was performed in accordance with our proposal dated January 21, 2021 and our professional services agreement with XL Construction dated August 4, 2021. This investigation was conducted by a project team that includes A3GEO, Inc. (geotechnical engineering) and Lettis Consultants International, Inc. (LCI; engineering geology and seismology).

1.01 Project Overview

The Berkeley City College project is located in downtown Berkeley, at the northwest corner of Milvia Street and Center Street (Figure 1). The site location is also indicated on a compilation of U.S. Geological Survey topographic quadrangle maps (Richmond, Briones Valley, Oakland West, and Oakland East Quadrangles) presented in Figure 2.

Based on review of the project documents, we understand the project will consist of demolition of the existing three-story building (approximately 25,000 square feet of floor space) and construction of a new six story building in the same location with a footprint of about 10,000 square feet and approximately 60,000 square feet of floor space. The new building will include classroom spaces, art studios, and an outdoor roof space for student activities as well as offices for faculty and administrators.

1.02 Objectives and Scope

The primary objectives of our study were to 1) evaluate site conditions and geologic hazards in a manner consistent with Division of the State Architect (DSA) / California Geological Society (CGS) Note 48, the 2019 California Building Code, ASCE 7-16 and other applicable state guidelines (CGS, 2019); and 2) develop geotechnical conclusions and recommendations for the design and construction of the planned work. The scope of our authorized services consisted of:

- Reviewing existing data;
- Performing site reconnaissance;
- Performing subsurface explorations and geophysical testing;
- Performing geotechnical laboratory testing;
- Characterizing geotechnical and geologic conditions;
- Developing a site-specific response spectrum in accordance with the 2019 California Building Code (CBC) and ASCE 7-16; and
- Preparing this design-level report in accordance with CGS Note 48.

Figures are provided, following the text of the report, to illustrate the information described in the report. Following the illustrative figures are appendices that present the data and results of our investigation:

- Appendix A – Exploratory Boring Logs
- Appendix B – Historical Boring Logs (Previous Consultants)
- Appendix C – Geotechnical Laboratory Testing Data
- Appendix D – Existing Building Foundation Plans
- Appendix E – Geophysical Data Report
- Appendix F – Site-Specific Seismic Hazard Analysis
- Appendix G – Liquefaction and Dynamic Settlement Analysis
- Appendix H – Vertical and Lateral Pile Analysis
- Appendix I – Modulus of Subgrade Reaction

Please note that our scope was limited to aspects of the project that are geotechnical and/or geologic in nature. The scope of our services did not include an environmental assessment or investigation for the presence of hazardous, toxic, or corrosive materials on, below, or around the site.

1.03 Elevation Datum

Elevations in this report are in feet (ft) and are based on the topographic map for the site prepared by CSW/Stuber-Stroeh Engineering Group, Inc. (CSW/ST2), dated January 29, 2015 (CSW/ST2, 2015). The topographic map references the North American Vertical Datum of 1988 (NAVD 88). Locations and elevations presented in this report should be considered approximate.

2. METHODS OF INVESTIGATION

2.01 Review of Geologic, Seismic and Historical Information

We reviewed published and unpublished references containing information on geologic, seismic, and historical conditions in the vicinity of the site. A list of references used in this analysis is presented at the end of this report; selected references are noted below:

2.01.1 Published Geologic, Seismic and Historical References

- U.S. Geological Survey (USGS) regional geologic maps by Graymer (2000), and Graymer and others (2006);
- California Geological Survey (CGS) maps titled “Earthquake Zones of Required Investigation” (CGS, 2003a), Fault Activity Map of California” (Jennings and Bryant, 2010), and “Tsunami Inundation Map for Emergency Planning” (CGS, 2009);
- USGS Liquefaction Susceptibility and Quaternary Deposits maps by Knudsen and others (2000), and Witter and others (2006);
- Federal Emergency Management Agency (FEMA) National Flood Insurance Rate Maps (FEMA, 2009);
- USGS topographic maps; and
- Historical creek maps from the City of Berkeley and the Oakland Museum (Sowers, 1993).

2.01.2 Historical Aerial Photographs

We obtained historic aerial photographs of the project area from Pacific Aerial Surveys (a Quantum Spatial Company) in Novato, California. Pacific Aerial Surveys provided 9 vintages of geo-referenced aerial photographs taken between 1930 and 2015.

2.01.3 Existing Building Drawings

We reviewed foundation plan drawings for the existing structure prepared by L. L. Freels and Associates, dated August 18, 1966 (Freels, 1966). The drawings are attached in Appendix D.

2.02 Previous Subsurface Investigations

We reviewed a previously prepared subsurface and geotechnical investigation report for the proposed Berkeley City College project at 2118 Milvia Street (Terraphase, 2017). Three soil borings were performed for this investigation, including one hollow-stem auger boring on Milvia Street to a depth of 50 feet below ground surface (bgs) and two limited access direct push borings inside the building to depths of 21-25 feet. Logs of the Terraphase borings are included in Appendix B and the boring locations are shown on Figures 3 and 4. Soil conditions interpreted from the boring logs are depicted graphically on Geologic Cross Sections A-A’ and B-B’ (Figures 5 and 6).

We also reviewed numerous other geotechnical and environmental studies conducted in the general vicinity of the proposed Berkeley City College project to assess general geological and hydrologic conditions. The locations of these studies are shown on Figure 7 and are listed in Section 9 of this report. A summary of the data reviewed is provided in Table 1.

Table 1 – Summary of Exploratory Borings from Nearby Investigations

Site Address/Name	Investigation Type	Type, Number, and Depth of Exploration Locations	Reference
Berkeley Community Theater	Geotechnical	6 CPTs (depths: 40 to 76 feet) 6 Borings (depths: 2 to 26.5 feet)	A3GEO, 2020
2211 Harold Way	Geotechnical	None	Engeo, 2013
2001 Allston Way	Geotechnical	4 Borings (depths: 24 to 40 feet)	Harza Kaldveer, 1992
2150 Shattuck Ave	Geotechnical	2 Borings (depths: 31.5 feet)	Subsurface Consultants, Inc., 2000
2025 Center Street	Geotechnical	5 CPTs (depths: 26 to 50 feet)	Rockridge Geotechnical, 2015
1900 Addison Street	Environmental	3 Borings (depths: 30 to 40 feet)	Aqua Resources Inc., 1987
1931 Addison Street	Environmental	5 Borings (depths: 20 to 40 feet)	Golden Gate Environmental, Inc., 2009
1974 University Ave	Geotechnical	1 Boring (depths: 51.5 feet)	Alan Kropp & Associates, Inc., 2013

2.03 A3GEO/LCI Subsurface Investigation (This Study)

On August 13 and 23, 2021, we undertook a subsurface investigation at the project site to inform design of the proposed construction project.

2.03.1 Soil Borings

On August 13, our drilling subcontractor (Taber Drilling of West Sacramento, California) advanced one exploratory soil boring outside the existing building (identified as B-1 at the location shown on Figure 3) on Center Street. Boring B-1 was advanced to a depth of 51½ feet below ground surface using a truck-mounted drill rig and mud-rotary drilling equipment.

On August 13, A3GEO staff also advanced two hand augers inside the existing building (identified as B-2 and B-3 at the locations shown on Figure 3). Boring B-2 was advanced to a depth of approximately 8½ feet and Boring B-3 was advanced to a depth of 2½ feet before encountering refusal due to cobble obstructions.

A summary of exploratory borings drilled as part of this investigation and the previous Terraphase (2017) investigation is presented in Table 2.

Table 2 – Summary of Site Exploratory Borings

Exploration ID	Boring Depth (feet)	Approximate Surface Elevation (feet)	Bottom of Boring Elevation (feet)	Drilling Method	Date Performed
B-1	51.5	167	115.5	Mud-Rotary	8/13/21
B-2	8.5	170	161.5	Hand Auger	8/13/21
B-3	2.5	170	167.5	Hand Auger	8/13/21
TP/B-1	25	170	145	Direct Push	3/21/17
TP/B-2	21	170	149	Direct Push	3/21/17
TP/B-3	50.5	170	119.5	Hollow Stem Auger	3/21/17

Note - Ground surface elevations were estimated based on the topographic contours from CSW/ST2 (2015) and should be considered approximate.

Prior to conducting field activities, we marked boring locations and contacted Underground Service Alert (USA) more than 48 hours prior to advancing borings, and subcontracted with GeoTech Utility Locating of Moraga, California, a private utility locating company, to screen each location for underground utilities. Additionally, we subcontracted with Bess Utility Solutions of Hayward, California, to core through the concrete at each boring location. Following drilling, the boreholes were grouted to the level of the soil subgrade and patched with rapid-set concrete. Borehole permits were obtained from the City of Berkeley.

During drilling and hand-augering, an A3GEO engineer supervised the drilling operations, obtained samples at frequent intervals, and prepared field logs of the subsurface conditions encountered.

Soil samples from Boring B-1 were obtained using either a 2-inch outside diameter (O.D.) Standard Penetration Test (SPT) split spoon sampler without liners, a 3-inch O.D. California Modified sampler with liners, or a 3-inch inside diameter Shelby tube sampler. The SPT and Modified California Modified samplers were driven with a 140-pound mechanically automated trip hammer with an approximate 30-inch fall. The hammer blows required to drive the sampler the final 12 inches of each 18-inch drive are presented on the boring logs. Where a full 12-inch drive could not be achieved, the number of blows and amount of penetration achieved is shown. Sampler blow counts (in blows per foot) obtained using the SPT sampler correspond to SPT N-values. The Modified California sampler blow counts shown on the logs have been adjusted by a factor of 0.63 to account for the larger sampler end area (Adjusted N-Values).

Soil samples from Borings B-2 and B-3 were obtained by collecting grab samples of cuttings from the hand auger. A dynamic cone penetrometer (DCP) was used to evaluate the penetration resistance of the subsurface soils of Borings B-2 and B-3. The DCP method utilizes a small weight dropped from a uniform height to drive a cone-shaped steel probe into the ground. The number of drops (blows) required to drive the probe in specified increments were recorded and are included on the boring logs.

Soils were visually/manually classified in general accordance with ASTM D2488 classifications which are based on the Unified Soil Classification System (USCS). John Baldwin (CEG) reviewed the draft field logs and soil samples at A3GEO's laboratory in Berkeley, CA, on August 18, 2021. Field classifications were subsequently checked and revised, where appropriate, based on laboratory test data. The logs of the borings are attached in Appendix A, preceded by a Key to Exploratory Boring Logs that describes the USCS and the symbols used on the logs.

The boring logs represent our interpretation of the subsurface materials at the boring locations at the time of drilling; the passage of time may result in changes in the subsurface conditions. The boring locations shown on Figure 3 were determined by measuring from existing site features and should be considered approximate. Ground surface elevations shown on the logs were estimated based on the topographic contours from CSW/ST2 (2015) and should be considered approximate.

2.03.2 Surface Geophysical Survey

On August 23, our geophysical subcontractor, GEO*Vision* Geophysical Services, Inc. (GeoVision), of Corona, California, performed a surface geophysical survey at the project site. The purpose of the survey was to provide a shear (S) wave velocity profile to a depth of approximately 200 ft, to estimate the average S-wave velocity in the upper 100 ft (V_{s100ft}), and, if possible, to estimate the depth to bedrock below the site. Seismic measurements were collected using both active-source (using the multi-channel analysis of surface waves [MASW] method), and passive-source (using horizontal over vertical spectral ratio [HVSR] and microtremor methods).

Microtremor measurements were made using an L-shaped array with both profiles (east-west and north-south oriented) of the array located along the sidewalks of Milvia Street and Center Street (Figure 3A). MASW measurements were made at an array along Center Street and HVSR measurements were made at one location at the public park on the south side of Center Street to support interpretation of surface wave data (Figure 3B). HVSR measurements were initially attempted on the sidewalk of Center Street next to the building; however, traffic noise created significant interference and disruption for any useful analysis. As such, a location further from the street and at the public park was then selected to support the interpretation of the surface wave data.

GeoVision's geophysical survey report is attached in Appendix E; locations of active and passive arrays and HSVR measurements are shown on Figure 5.

2.04 Geotechnical Laboratory Testing

Our geotechnical laboratory testing program was directed toward a quantitative and qualitative evaluation of the physical properties of the soils at the site. The following geotechnical laboratory tests were performed:

- Atterberg Limits per ASTM D4318;
- Particle Size Analysis per ASTM D422 or D1140;
- Moisture Content per ASTM D2216;
- Dry Density per ASTM D2937;
- Unconsolidated Undrained Triaxial per ASTM D2850; and
- Incremental Consolidation per ASTM D2435

Geotechnical laboratory testing was performed by B. Hillebrandt Soils Testing, Inc. and Cooper Testing Labs, Inc. The test results are included in Appendix C.

2.05 Geochemical Laboratory Tests

We screened for naturally occurring corrosive materials by conducting a suite of geochemical laboratory tests on a sample of soil obtained from a depth of 3.75-4.25 feet in Boring B-2. The geochemical laboratory tests were performed by Cooper Testing Labs, Inc. and included measurements of:

- Resistivity (100% saturated) per Caltrans 643;
- Chloride ion concentration per Caltrans 422 (modified);
- Sulfate ion concentration per Caltrans 417 (modified);
- pH per Caltrans 643; and
- Moisture per ASTM D2216.

The corrosivity test results are included in Appendix C.

3. GEOLOGIC, SEISMIC, AND HISTORICAL SETTING

3.01 Regional Geology

The San Francisco Bay Region (SFBR) is characterized by hills and valleys that generally trend southeast/northwest (Figure 8). This characteristic topography is partly the result of the SFBR's location at the boundary between the North American and Pacific crustal plates, which are in relative motion with respect to each other. Over geologic time, the topography of the region formed through a complex series of processes that have included deposition, accretion, faulting, folding, uplift, volcanism, and changes in sea level. San Francisco Bay and the adjacent flatlands presently occupy a structural depression between the East Bay Hills and the roughly parallel hills of the San Francisco Peninsula and Marin County.

The SFBR includes three "basement" rock complexes: the Great Valley Complex, the Franciscan Complex, and the Salinian Complex. All were formed during the Mesozoic Era (225 to 65 million years ago) and have been brought together by movement occurring along faults. These Mesozoic basement rock complexes are locally overlain by a diverse sequence of Cenozoic Era (younger than 65 million years) sedimentary and volcanic rocks. Since their deposition, the Mesozoic and Cenozoic rocks have been extensively deformed by repeated episodes of folding and faulting. Significantly, the Bay Area experienced several episodes of uplift and faulting during the late Tertiary Period (about 25 million to 2 million years ago), that produced the region's characteristic northwest-trending mountain ranges and valleys.

World-wide climate fluctuations during the Pleistocene (about 1.8 million to 11 thousand years ago) resulted in several distinct glacial periods. A lowering of sea level accompanied each glacial advance as water became stored in vast ice sheets. Melting of the continental glaciers during warm intervals caused corresponding rises in sea level. High sea levels favored rapid and widespread deposition in the bay and surrounding floodplains. Low sea levels during glacial advances steepened the gradients of streams and rivers draining to the sea thereby encouraging erosional downcutting. The most recent glacial interval ended about 15,000 years ago. Evidence suggests that during the maximum extent of this latest glaciation, sea level was 300 to 400 ft below its present elevation and the valley now occupied by San Francisco Bay drained to the Pacific Ocean more than 30 miles west of the Golden Gate.

Near the beginning of the Holocene (about 11 thousand years ago) the rising sea re-entered the Golden Gate, and sediments accumulated rapidly beneath the rising San Francisco Bay and on the surrounding floodplains. The sediments that now cover the bottom of the bay and blanket much of the adjacent lower flatlands are less than 11,000 years old. The Holocene-age surface deposits are generally less dense, weaker, and more compressible than the adjacent/deeper Pleistocene-age soils that pre-date the last sea level rise.

3.02 Regional Active Faults

Within the SFBR, the relative motion of the Pacific and North American crustal plates is presently accommodated by a series of active northwest-trending faults that exist over a width of more than 50 miles (Figure 8). Faults that are defined as active exhibit one or more of the following: (1) evidence of Holocene-age (within about the past 11,000 years) displacement, (2) measurable aseismic fault creep, (3) close proximity to linear concentrations or trends of earthquake epicenters, and (4) prominent tectonic-related geomorphology. Potentially active faults are defined as those that are not known to be active but have evidence of Quaternary-age displacement (within about the past 2 million years).

Major active faults within the region include the Hayward, Rogers Creek, San Andreas, San Gregorio, Concord-Green Valley, Calaveras, West Napa, and Greenville faults (Figure 8). These major faults are near-vertical and generally exhibit right-lateral strike-slip movement (which means that the movement is predominantly horizontal and when viewed from one side of the fault, the opposite side of the fault is observed as being displaced to the right). Approximate distances and directions from the Site to major Bay Area active faults as mapped by Jennings and Bryant (2010) are tabulated in Table 3.

Table 3 – Approximate Distances and Directions to Principal Bay Area Active Faults

Fault System	Approximate Distance from Site	Approximate Direction from Site
Hayward-Rodgers Creek	1 mile	East-Northeast
Calaveras	13 miles	East-Southeast
Concord-Green Valley	15 miles	East-Northeast
Pleasanton	17 miles	Southeast
Greenville – Clayton – Marsh Creek	17 miles	East-Northeast
San Andreas	18 miles	West-Southwest
West Napa	20 miles	North-Northeast
San Gregorio	20 miles	West-Southwest

As noted in the preceding table, the closest regional Holocene active fault to the site is the Hayward fault, located about 1 mile to the east-northeast of the site. The Hayward/Rodgers Creek fault system is one of the primary active faults in the SFBR, and overall has the highest probability of generating a large-magnitude earthquake within the next 30 years (WGCEP, 2008). The Hayward/Rodgers Creek fault system extends approximately 95 miles from Fremont to Healdsburg and is interpreted as stepping to the right beneath San Pablo Bay. Additional discussion of regional active faults is presented in Appendix F.

3.03 Regional Seismicity

The San Francisco Bay region is seismically active. Since 1800, five earthquakes of magnitude (M) ≥ 6.5 have occurred in the Bay Area (Bakun 1999). These include the: 1836 M6.5 event east of Monterey Bay; 1838 M6.8 event on the Peninsula section of the San Andreas fault; 1868 M6.8-7.0 Hayward event on the southern Hayward fault; 1906 M7.9 San Francisco earthquake on the San Andreas fault; and 1989 M6.9 Loma Prieta event in the Santa Cruz Mountains.

The Working Group on California Earthquake Probabilities (WGCEP) has developed authoritative estimates of the magnitude, location, and frequency of future earthquakes in California, which are published in Uniform California Earthquake Forecast (UCERF) reports. Table 4 summarizes the most recent UCERF3 forecast of likelihoods for one or more earthquake events of the specified magnitude occurring within the SFBR in the next 30 years (starting in 2014).

Table 4 – UCERF3 San Francisco Region Earthquake Likelihood Forecast

Earthquake Magnitude (greater than or equal to)	30-year Likelihood of one or more earthquake events
≥ 5.0	100%
≥ 6.0	98%
≥ 6.7	72%
≥ 7.0	51%
≥ 7.5	20%
≥ 8.0	4%

Compared to the previous UCERF forecast, the likelihood of moderate-sized earthquakes (magnitude 6.5 to 7.5) is generally lower whereas the magnitude of larger earthquakes is higher. While UCERF3 results are generally in line with previous forecasts, UCERF 3 indicates lower probabilities for earthquakes occurring on the most well-known faults of the SFBR (Hayward and San Andreas), while the probabilities for earthquakes on

lesser-known faults has increased substantially in some cases. These changes reflect a better understanding of the regional fault system and the potential for multi-fault ruptures on many faults.

3.04 Local Geology

The site is situated near the eastern edge of a broad, gently sloping alluvial plain deposited by streams flowing westward from the Berkeley Hills. Franciscan complex bedrock, which is present near the ground surface within the UC Berkeley Main Campus and in borings drilled previously for BART to the east-northeast, is interpreted to underly the alluvial deposits at the site. The USGS regional geologic map on Figure 9 (Graymer, 2000) maps the near surface soils at the site as alluvial and fluvial deposits of Holocene age (map symbol Qhaf). Knudsen et al. (2000) describes the Qhaf unit as follows:

> ***Qhaf:*** *Sediments deposited by streams emanating from mountain canyons onto alluvial valley floors or alluvial plans as debris flows, hyperconcentrated mudflows, or braided stream flows. Alluvial fan sediment includes sand, gravel, silt, and clay, and is moderately to poorly sorted and moderately to poorly bedded. Sediment clast size and general particle size typically decrease downslope from the fan apex. Many Holocene alluvial fans exhibit levee/interlevee topography, particularly the fans associated with the fans flowing west from the eastern San Francisco Bay hills. Alluvial fan deposits are identified primarily on the basis of fan morphology and topographic expression. Holocene alluvial fans are relatively undissected, especially when compared to older alluvial fans. In places, Holocene deposits may be only a thin veneer over Pleistocene deposits. Soils are typically entisols, inceptisols, mollisols, and vertisols. Greater than 5 percent of the nine-county San Francisco Bay Area is covered by Holocene alluvial fan deposits. It is the most extensive Quaternary map unit in the region.*

Witter et al. (2006) maps the surficial deposits at the site as alluvial fan deposits of Holocene age (map symbol Qhf) associated with Strawberry Creek that are bound to the north and south by Pleistocene alluvial fan deposits (map symbol Qpf, Figure 10). These deposits are mapped to the north and south of the site. Knudsen et al. (2000) describes the Qpf unit as follows:

> ***Qpf:*** *This unit is mapped on alluvial fans where latest Pleistocene age is indicated by greater dissection than is present on Holocene fans, and/or the development of alfisols. Latest Pleistocene alluvial fan sediment was deposited by streams emanating from mountain canyons onto alluvial valley floors or alluvial plains as debris flows, hyperconcentrated mudflows, or braided stream flows. Alluvial fan sediment typically includes sand, gravel, silt, and clay, and is moderately to poorly sorted, and moderately to poorly bedded. Sediment clast size and general particle size typically decreases downslope from the fan apex. Latest Pleistocene alluvial fan sediment is approximately 10 percent denser than Holocene alluvial fan sediment and has penetration resistance values about 50 percent greater than values for Holocene alluvial fan sediment* (Clahan et al., 2000). *Pleistocene alluvial fans may be veneered or incised by thin unmapped Holocene alluvial fan deposits. Along the west-facing hills of Oakland and Berkeley, where latest Pleistocene alluvial fan deposits are mapped, the age of these deposits is not well constrained and the deposits may actually be a combination of early to late Pleistocene alluvial fan and thin pediment deposits, and latest Pleistocene alluvial fan deposits.*

Witter et al. (2006) shows the presence of Artificial Channel Fill (map symbol acf) directly to the south of the site, below the Martin Luther King Jr. Civic Center Park by Center Street. The presence of the mapped Artificial Channel Fill coincides with the mapped location of the former historical location of Strawberry Creek (Figure 11), which has been routed into underground culverts and storm drains below the park (Sowers, 1993). In addition to this artificial channel fill of Strawberry Creek, based on the mapping of Sowers (Figure 11), another un-named former tributary creek is located at the project site. The Sowers map indicates that this former creek was buried or drained circa 1850 and was located near the North side of the property at 2118 Milvia Street, oriented in an east-west direction.

Franciscan complex sandstone (map symbol KJfs) and mélange (map symbol KJfm) are mapped on the UC Berkeley Main Campus to the east of the site (Figure 9). Graymer (2000) describes these basement rock units

as follows:

> ***KJfs**: Franciscan complex sandstone, undivided (Late Cretaceous to Late Jurassic) – Graywacke and meta-graywacke.*
>
> ***KJfm**: Franciscan complex mélange (Cretaceous and/or Late Jurassic) – Sheared black argillite, graywacke, and minor green tuff, containing blocks and lenses of graywacke and meta-graywacke (fs), chert (fc), shale, metachert, serpentinite (sp), greenstone (fg), amphibolite, tuff, eclogite, quartz schist, greenschist, basalt, marble, conglomerate, and glaucophane schist (fm). Blocks range in size from pebbles to several hundred meters in length. Only some of the largest blocks are shown on the map.*

3.05 Geologic Hazard Mapping

The official Seismic Hazard Map for the site (Figure 12) shows the site is outside of any Earthquake Zone of Required Investigation for liquefaction or earthquake-induced landsliding (CGS, 2003a). Additionally, the site is not within an Alquist-Priolo (A-P) Fault Zone (CGS, 2003a). A 2006 USGS liquefaction susceptibility map (Figure 13) shows the site as located within an area of "Moderate" liquefaction susceptibility (Witter et al., 2006). However, the historical creek channel mapped directly to the south side of the site is mapped as "Very High" liquefaction susceptibility.

3.06 Site Development History

A summary of the site development history is included in the Draft Phase I Environmental Site Assessment dated January 2015 by Terraphase Engineering (Terraphase, 2015). The summary is as follows:

> *"The 1899 15-minute USGS topographic map (San Francisco Quadrangle EDR 2014b) of the Site shows that Milvia Street had not yet been advanced between Center Street and Alston Way. There is a structure shown on the Site which likely would have been torn down or moved when Milvia was advanced between Center Street and Alston Way. Strawberry Creek is shown as an above-ground ephemeral stream.*
>
> *The 1915 15-minute USGS topographic map (San Francisco Quadrangle EDR 2014b) shows that Milvia Street had been completed, Strawberry Creek had been undergrounded and the Site was vacant. A review of historical aerial photographs and city directories (EDR 2014d,e) indicates that a gasoline service station was located on the Site by 1939. The 1929 Sanborn map indicates the Site was vacant. Based on aerial photographs and directory listings, the gasoline service station (Fairchild & White) was located on the Site (with the former address of 1999 Center Street) until before 1966 when the current structure was built. The 1968 aerial photograph (EDR 2014e) shows the gasoline station had been removed and been replaced with the existing office building. The Site remained as an office building, with various commercial occupants, until the present. (EDR, 2014d)."*

Some of the site developmental history described above can also be seen in the historical aerial photographs, which includes photographs taken between 1930 and 2015.

The foundation plan for the existing building is dated August 18, 1966 (Freels, 1966). Construction is assumed to have occurred within a few years after design plans. The plans, which are presented in Appendix D, show that interior columns are supported on 9-foot square spread footings with bottom bearing depths of approximately 3 feet below the top of slab. The southern and eastern walls are supported on spread footings varying in size from 7-foot by 7-foot to 9-foot by 3-foot footings bearing at depths approximately 3 feet below the slab. The northern wall is supported on a strip footing 3.33 feet wide at a depth of approximately 3 feet below the slab. The western wall is supported on 18-inch diameter drilled piers of unknown depth. The building plans indicate that the piles were to be installed as following: "bottom of pile to be 4 feet into the dense cohesionless strata, see soil report". Based on our findings during the subsurface geotechnical investigation and review of

existing site data, this suggests that the piles may be on the order of between 20 and 30 feet below existing grade where a coarse-grained deposit was encountered.

4. SITE CONDITIONS

4.01 Surface Conditions

The site is presently occupied by an existing three-story office building in downtown Berkeley. The site is bound by Center Street to the south and Milvia Street to the east, an apartment complex and parking lot to the north, and an-office building to the west (1947 Center Street). Public sidewalks, approximately 8 to 10 feet wide, currently exist between the roads and the existing structure. The structure to the west, 1947 Center Street, is a six-story office building with one-below grade basement used for City of Berkeley business.

Grades surrounding the structure are relatively flat, ranging from approximately 170 feet to 168 feet in elevation, with a gentle downward slope towards the west. While on site, we observed that the pavements and sidewalks around the structure appeared to be in fair to good condition.

4.02 Existing Building

The existing structure is a three-story facility with a footprint of approximately 11,000 square feet. During various site reconnaissance visits, we observed that the existing structure exterior appeared to be in fair condition. The exterior walls appear to be constructed of concrete. A temporary construction fence had been installed around the south wall sidewalk due to some concrete falling off a cantilevered overhang; however, we did not see any obvious indicators of significant distress related to underlying geotechnical or structural conditions. We did not perform a detailed reconnaissance of the structure's interior, nor should this reconnaissance of the outside and visible parts of the building be construed as an official structural analysis of the existing building.

4.03 Adjacent Structures

As discussed previously, the project site is bounded to the west and north by adjacent properties. Based on a review of design plans for the structure at 1947 Center Street, the structure includes one below-grade level of basement. The bottom of the basement wall is shown to extend to a depth of about 10 feet relative to the existing top of slab of 2118 Milvia St, which corresponds to an elevation of about 159 feet. The foundation system for 1947 Center Street is shown as pile-supported with pile caps. The property to the north of the project site (2108 Milvia Street) consists of a paved parking area within approximately 75 feet of the site. The foundation types and lowest level floor elevations for the structure to the northwest (2100 Milvia Street) were unknown at the time of writing this report.

Further evaluation of the foundation systems and locations of neighboring structures may be needed. Where excavations bear within a 2:1 zone of influence from existing structures, temporary shoring or similar mitigation measures should be provided. Additional recommendations to mitigate loading of the adjacent basement wall to the west are provided in the recommendations section of this report.

4.04 Site Soil and Bedrock Conditions

Generally, the soils encountered at the site consisted of undocumented fill over alluvial fan or fluvial deposits, which may be on the order of 250 feet thick. Soil conditions are described in the following sections and are depicted graphically on Geologic Cross Sections A-A' and B-B' (Figures 5 and 6).

4.04.1 Fill

The pavement section encountered in Boring B-1 consisted of 12 inches of asphalt underlain by 7 inches of concrete. Fill was encountered below the pavement section to a depth of 6 feet. This boring is close to the northern creekbank margin of historical Strawberry Creek as mapped by Witter et al., (2006) and Sowers (1993). The concrete slab section encountered in Borings B-2 and B-3 consisted of 4 to 5 inches of concrete underlain by a plastic liner and 3 inches of sand. Fill was encountered below the concrete section to a depth of

3 feet in Boring B-2 and to the depth explored of 2½ feet in B-3. The previous geotechnical investigation by Terraphase (2017) does not indicate soil units (alluvium versus fill) on the boring logs or in the report text.

Where fill was encountered in the borings, it was typically described as dark gray, moist, stiff, sandy lean clay; and dark brown to black, moist, medium dense, clayey sand with gravel. Steel and cobbles were also observed in the fill.

4.04.2 Alluvial/Fluvial Deposits

The fill is underlain by bedded, heterogeneous, alluvial/fluvial deposits, interpreted to be Quaternary in age. The full thickness of the alluvial/fluvial deposits was not encountered in the borings; however, based on the shear wave velocity profile from the geophysical survey, coupled with review of recent work performed in the vicinity of the project site (A3GEO, 2020), the alluvial/fluvial deposits are likely on the order of 250 feet thick at the site (shear wave velocity increases to about 3,150 feet per second [ft/s] at about 265 feet in depth). Typically, the alluvial/fluvial deposits encountered at the project site consist of dark brown to very dark gray medium stiff to very stiff, lean clay, with a trace of sand and gravel; as well as a dark brown, grayish brown to yellowish brown, medium dense clayey sand with gravel and dense clayey gravel with sand. Boring B-1 encountered a thicker deposit of sand and gravel material than Terraphase Boring TP/B-3 located about 150 feet to the north (Figure 3).

Based on laboratory test results, the undrained shear strength of the clay material at a depth of 8 feet (within the alluvial/fluvial deposits) from Boring B-1 is about 2,400 pounds per square foot (psf). Shear wave velocity measured in the geophysical survey increased with depth, ranging from approximately 600 to 1,450 ft/s in the upper 100 feet. The plasticity indices of three samples of the clayey units from depths of 6 feet, 35 feet, and 41 feet, within the alluvial/fluvial deposits, were measured as 29,11, and 10, respectively.

Based on the available data from the site, and similar exploratory borehole data reviewed for adjacent properties and projects, the coarse-grained deposits within the alluvial/fluvial deposits are likely related to alluvial fan deposition and/or a paleochannel deposit derived from a former west-flowing tributary or path associated with Strawberry Creek. Interpolation between borehole data points suggests that the coarse-grained deposits are lenticular and discontinuous across the site and may be more concentrated in the southwest part of the property.

4.04.3 Bedrock

Bedrock was not encountered in any of the recent or previous test borings performed at the site. As discussed in Section 3.04, bedrock of the Franciscan Complex is interpreted to underly the site based on regional geologic mapping and review of borehole and geophysical data in the vicinity. The top of bedrock is interpreted to be at a depth of about 265 feet based on the geophysical survey. A shear wave velocity of approximately 3,150 ft/s was measured near the interpreted alluvium/bedrock contact (Appendix E).

4.05 Groundwater Conditions

Groundwater was not measured in the recent soil borings. The mud rotary drilling method used for Boring B-1 utilizes fluids that obscure the natural groundwater level during and immediately after drilling. The relatively shallow hand-auger borings at B-2 and B-3 did not encounter groundwater. Groundwater was encountered in Terraphase Boring TP/B-3 at a depth of about 20 feet (elevation of approximately 150 feet).

The groundwater levels measured during drilling were obtained over a relatively short time period, and thus may not accurately reflect long term in-situ conditions. Groundwater levels can fluctuate significantly with location, season, precipitation, leakage in and out of utilities, and other factors.The CGS Seismic Hazard Zone Report (CGS, 2003b) shows the historic high groundwater at the site at approximately 10 feet below ground surface. Based on a review of publicly available environmental monitoring well data in the vicinity (Figure 4),

groundwater was generally measured at 10 to 20 feet below the ground surface. Based on the existing data, we recommend assuming the groundwater table at 10 feet below ground surface for design purposes.

5. GEOLOGIC HAZARD ASSESSMENT

5.01 Earthquake Ground Shaking

Strong earthquake shaking is a hazard shared throughout the region and the direct risks posed to structures by ground shaking are mitigated through the structural design provisions of the California Building Code (CBC). Structures at the site should be designed to resist strong ground shaking in accordance with the applicable building code(s) and local design practice.

A site-specific ground motion hazard analysis was performed in accordance with: 1) Section 1613A of the 2019 California Building Code (CBC); 2) American Society of Civil Engineers (ASCE) 7-16 Standard; and 3) CGS Note 48. A further discussion of the analysis is provided in Section 7.02 and a site-specific ground motion report is presented in Appendix F.

5.02 Surface Fault Rupture

Historically, earthquake fault rupture most often occurs along pre-existing active faults. The site is not within an AP Zone and no active faults are mapped in the direct vicinity of the site. The closest AP Zone surrounds the active Hayward fault, which is approximately 1 mile to the east (Figure 8). Based on the foregoing, we judge there to be very low hazard for surface fault rupture at the site.

5.03 Liquefaction

Liquefaction is a phenomenon whereby certain types of soils below groundwater may lose strength, compress (i.e., settle) and/or gain mobility (i.e., flow) in response to earthquake shaking. Soils that are most likely to experience liquefaction include loose, clean, coarse-grained soils (i.e., sands and gravels) that are below groundwater. These same types of soils, when unsaturated (i.e. above groundwater), may be susceptible to seismically-induced densification. The principal effect of seismic densification is settlement. Lateral spreading occurs when non-liquefied soils above groundwater move laterally on an underlying liquefied layer, sometimes toward an open “free face” such as a shoreline or creek bank.

Fine-grained soils (i.e., silts and clays) below groundwater with very low plasticity can also experience generally similar cyclic degradation in response to earthquake shaking and are considered susceptible to liquefaction, if certain criteria are met. Liquefaction within fine-grained soils is a topic of ongoing research. However, there appears to be an emerging consensus that: 1) the Plasticity Index (PI) is one good indicator of liquefaction susceptibility; and 2) there exists a fines content threshold (FC_{thr}) above which a soil will behave like the fines and not the coarser matrix soil. Typically, the FC_{thr} is between about 20 and 35 percent depending on factors such as the soil’s full gradational characteristics, mineralogical composition, particle shapes, and depositional environment.

5.03.1 Liquefaction Susceptibility

The two commonly used criterion for evaluating liquefaction susceptibility of soils with fines are papers from Idriss and Boulanger (2008) and Bray and Sancio (2006), which use Plasticity Index (PI), water content (w_c), and Liquid Limit (LL) to delineate liquefaction susceptibility. A brief summary of the key recommendations from these papers is presented as follows:

Idriss and Boulanger (2008) Criterion: Soils having a PI of less than 3 exhibit sand-like behavior and are susceptible to liquefaction and that the transition to clay-like behavior occurs as the plasticity index increases from 3 to 8. Based on these findings, Idriss and Boulanger (2008) include the following criterion: “In engineering practice, fine-grained soils can reasonably be expected to exhibit clay-like behavior if they have a PI greater than or equal to 7.”

Bray and Sancio (2006) Criterion: Work by Bray and Sancio (2006) includes the finding that liquefaction can

occur in soils with higher plasticity, based in part on data from the 1999 earthquake Kocaeli earthquake and the effects observed in Adapazari, Turkey. Based on these findings, Bray and Sancio's (2006) paper includes the following criterion: "Loose soils with PI less than 12 and a w_c/LL greater than 0.85 were susceptible to liquefaction, and loose soils with 12<PI<18 and w_c/LL< 0.80 were systematically more resistant to liquefaction. Soils with a PI >18 tested at low confining stresses were not susceptible to liquefaction." Bray and Sancio (2006) also notes that "other factors such as soil mineralogy, void ratio, overconsolidation ratio, age, etc. are also contributing factors to liquefaction susceptibility."

5.03.2 Liquefaction Analysis and Dynamic Settlement

A3GEO analyzed the liquefaction susceptibility and resulting vertical settlements using an in-house developed spreadsheet based on the methods of Boulanger and Idriss (2014). Materials that met the following criteria were considered not susceptible to liquefaction: 1) above the design groundwater level, and 2) fines content of 30 percent or more with a Plasticity Index (PI) of 7 or more (Idriss and Boulanger, 2008 criterion). The analysis involved assessing the seismic demand on a soil layer, expressed in terms of the cyclic stress ratio (CSR), and comparing this value to the capacity of the soil to resist liquefaction, expressed in terms of the cyclic resistance ratio (CRR). The factor of safety against liquefaction is determined by dividing the CRR by the CSR. Field blow counts were corrected for sampler type, overburden, and other factors as recommended in Boulanger and Idriss (2014) to obtain $N_{1,60CS}$ values. Where the calculated factor of safety was less than 1.3, dynamic settlement calculations were performed using an in-house developed spreadsheet and the procedure of Idriss and Boulanger (2008).

Our analysis used the following values:

- ***Mw = 7.6:*** the mean characteristic magnitude for the rupture of the Hayward Fault (the Maximum Considered Earthquake, or MCE);
- ***PGA = 1.14 g***; and
- ***Groundwater Depth = 10 feet***

Analysis was not performed on A3GEO Borings B-2 and B-3 as these did not extend below the groundwater depth. Analysis was also not performed on Terraphase Borings B-1 and B-2 as these did not include any driven samplers with blow count data. The computational spreadsheet used in our liquefaction triggering analyses is presented in Appendix G and the results of the analyses are summarized in Table 5.

Table 5 – Summary of Liquefaction and Dynamic Settlement Analysis

Boring	Depth Below Ground Surface of Liquefiable Material	Settlement (in)
B-1	36' to 38'	0.2
Terraphase/B-3	30.5' to 33'	0.3

We anticipate that any additional settlement due to seismic densification will be very small relative to the liquefaction-related settlements calculated above, which correspond to high ground water conditions. Under low groundwater conditions, densification settlement would potentially be greater; however, densification settlements would still be significantly less than the predicted liquefaction-related settlements.

Our liquefaction susceptibility analysis generally shows low-susceptible soils are present within the project site. The overall potential for significant liquefaction to occur in the project area as a result of a future large earthquake is low. Were liquefaction to occur, the principal consequence would be settlement, and based on the available data and our analyses, we estimate that seismic-related settlements at the site would be relatively small, with a total settlement of about ¼ inch and a differential settlement of about ¼ inch over a horizontal distance of 30 feet.

5.04 Expansive Soils

Expansive materials shrink and swell in response to changes in moisture and have the potential to damage improvements that are supported on them. Based on the results of our subsurface exploration, the near-surface soils consist of sandy lean clay or clayey sand with gravel (CL and SC). Laboratory testing indicates the near-surface materials generally have a plasticity index of 28 and 29, which is generally indicative of soil having a moderate expansion potential.

Based on the Atterberg Limits test results, we judge that expansive soils are a consideration for the design of the project. Recommendations for embedment depth and subgrade preparation are provided to mitigate the impact of expansive soils for concrete foundations. Recommendations for removal and replacement with select non-expansive fill are provided to create a zone of low expansion potential below flatwork and slab-on-grades. Chemical treatment to reduce the expansion characteristics could be used as an alternative to importing select fill. Recommendations for chemical treatment can be provided if needed.

5.05 Corrosion Potential

We screened for the presence of corrosive soils by conducting a suite of geochemical laboratory tests on a sample obtained from Boring B-2 at a depth of approximately 4 feet. California Department of Transportation (Caltrans) defines a corrosive environment as an area where the soil contains chloride concentration of 500 ppm or greater, soluble sulfate concentration of 1,500 ppm or greater, and a pH of 5.5 or less (Caltrans, 2018a). Based on the Caltrans guidelines, the tested samples would not be considered corrosive.

Table 6 – Corrosion Test Data and Guidelines

Geochemical Test	Sample ID and Test Results	Corrosion Threshold for Structural Elements
	Boring B-2 at 4 feet	
Resistivity @ 15.5° C (ohm-cm)	940	see below
Chloride (mg/kg or ppm)	10	≥ 500
Sulfate (mg/kg or ppm)	278	≥ 1,500
pH	7.3	≤ 5.5

The Caltrans guidelines indicate that a minimum resistivity value for soil of less than 1,100 ohm-cm indicates the presence of high quantities of soluble salts and a higher propensity for corrosion and requires testing for chlorides of such soils. The National Association of Corrosion Engineers (NACE) provides guidelines on soil resistivity and soil corrosion classification which are presented in Table 7.

Table 7 – NACE Corrosion Classifications

Soil Resistivity (ohm-cm)	Soil Classification
Below 500	Very Corrosive
500 – 1,000	Corrosive
1,000 – 2,000	Moderately Corrosive
2,000 – 10,000	Mildly Corrosive
Above 10,000	Progressively Less Corrosive

Based on the NACE criteria, the sample from Boring B-2 would classify as “Corrosive”. A qualified corrosion engineer should be consulted if additional interpretations or recommendations pertaining to corrosion are desired.

5.06 Other Geologic Hazards *Not* Present

Lateral Spreading - Lateral spreading is a phenomenon in which blocks of non-liquefied soil move laterally on top of an underlying continuous (or near-continuous) liquefied layer. Hazards posed by lateral spreading are typically greatest where there is a nearby topographic free face towards which spreading can occur. Because the potentially liquefiable layers are discontinuous and there is no significant topographic free face nearby, and Strawberry Creek remains buried, we conclude the potential for significant earthquake-induced lateral spreading to occur at the site to be very low.

Landsliding - The site is located within a gently sloping alluvial plain with no slopes in the direct vicinity of the site. The closest hills are about 1 mile to the east of the site. We judge there to be essentially no potential for large-scale landsliding to affect the site.

Inundation/Flooding - The site is near elevation 170 feet and is about 1½ miles inland from the tsunami zone shown on the CGS Tsunami Inundation Map (CGS, 2021). A flood map by FEMA shows the site outside of areas considered susceptible to significant flooding. A review of California Dam Breach Inundation Maps also shows the site to be outside areas considered susceptible to significant flooding due to dam breaches (DWSR-DSOD, 2021). We judge there to be a low potential for flooding to affect the project site.

6. GEOTECHNICAL EVALUATIONS AND CONCLUSIONS

6.01 Feasibility

Based on the results of our investigation, we conclude that the proposed project is feasible from a geotechnical standpoint, provided that the conclusions and recommendations presented in this report are appropriately incorporated into the design and construction of the project. Geologic and geotechnical considerations for the project are discussed in the following sections.

6.02 Undocumented Fill

Existing fills at the site are considered undocumented, unless records are found that demonstrate that the materials were placed and compacted under appropriate engineering controls. Undocumented fill is considered generally unsuitable for the support of the proposed building.

Undocumented fill was encountered below the proposed building footprint during our subsurface exploration to a depth of about 3 feet below the existing ground surface. The depth of fill may be greater in areas where paleochannels or depressions may have been filled (e.g., closer to Center Street). Remediation for undocumented fill typically consists of over-excavation and replacement with new engineered fill or designing foundations to bear below the depth of undocumented fill. Ground improvement, such as permeation grouting, can also be used to mitigate undocumented fill concerns. Recommendations to mitigate concerns related to undocumented fill are presented in Sections 7.03 and 7.07.

6.03 Foundation Support

Several foundation options were considered for support of the new structure, including: 1) deep foundations supported within the alluvial soils (i.e., *not* to bedrock); and 2) a mat foundation bearing on alluvial soils. The results of our investigation indicate that bedrock at the site is very deep (approximately 250 feet below the existing ground surface). Preliminary structural column loads provided by the project structural engineer indicate column loads that range from about 140 kips to 600 kips for dead loads and 170 kips to 740 kips for dead and live loads combined. Shear wall loads range from about 710 kips to 1380 kips for dead loads and 830 kips to 1660 kips for dead and live loads combined. Primary geotechnical design considerations for foundation design include near-surface soil having a moderate expansion potential and consolidation settlement of the alluvial soils under the weight of the new building.

Based on communications and review of documents, we understand that the adjacent building to the west (1947 Center Street) has a basement level. To mitigate potential new building loads from impacting the adjacent basement wall, the western portion of a proposed mat foundation can be structurally tied to and supported on Cast-In-Drilled-Hole (CIDH) reinforced concrete piles. The piles should be sleeved or cased to the bottom of the adjacent basement wall (estimated to be about 6 feet below the bottom of the mat) to prevent the transfer of axial loads to the adjacent basement wall. Similarly, a deep foundation system should case or sleeve the upper part of piles to the bottom of the adjacent basement wall along the western portion.

6.03.1 Foundation Settlement Analysis

The primary concern with using foundations deriving support in alluvial materials for support of the new structure is consolidation settlement of the underlying soils. Consolidation is a slow process that requires water to be expelled from between clay particles, and clay has very low permeability. Factors influencing the magnitude and rate of consolidation settlement include: 1) the magnitude of the proposed new building loads; 2) the thickness and consolidation characteristics of the underlying compressible deposits subject to increased loads; and 3) the length of the path by which water drains from the compressible soil layer(s).

To assess the relative magnitude and pattern of long-term settlements associated with the new foundation, A3GEO performed a three-dimensional settlement analysis using commercially available geotechnical software

(Settle3D by Rocscience). Primary inputs to our model included vertical soil stratigraphy, consolidation parameters, and the structure loads provided to us by the project structural engineer. Our evaluation included an iterative analysis of subgrade modulus, bearing pressures, and settlement in coordination with the project structural engineer. Based on the results of our analysis, we anticipate that maximum consolidation settlements will be up to about a total of 1¾ inches with a differential of 1 inch over a horizontal distance of 30 feet.

6.04 Construction Considerations

We anticipate that soil materials at the site can generally be excavated with conventional earth-moving equipment, however the Contractor should anticipate the presence of obstructions within the fill soils, including cobbles, boulders, old concrete slabs and foundation elements, bricks, and blocks, etc. The Contractor should anticipate that equipment capable of cutting steel and/or breaking concrete may be necessary to remove these obstructions within the fill.

The contractor is responsible for shoring, excavation safety, and the protection of adjacent offsite improvement throughout all phases of construction. All excavations deeper than 4 feet that will be entered by workers will need to be shored or sloped for safety in accordance with the applicable: (1) California Occupational Safety and Health Administration (Cal-OSHA) standards; and (2) any site-specific health and safety protocols and procedures required by the City of Berkeley.

The contractor's responsibilities should include: (1) documenting the condition of the adjacent improvements prior to the commencement of site demolition and excavation activities; (2) designing demolition, excavation and construction programs that will keep surface settlements and vibrations within acceptable limits; and (3) coordinating with the District and local agencies, as needed, to assure that adjacent facilities are not adversely affected during the geotechnical aspects of construction.

Although it is possible for excavation and/or construction to proceed during or immediately following the wet winter months, a number of geotechnical problems may occur which may increase costs and cause project delays. The water content of onsite soils may increase during the winter and rise significantly above optimum moisture content for compaction of subgrade or backfill materials. If this occurs, the contractor may be unable to achieve the specified levels of compaction. If utility or footing trenches are open during winter rains, caving of the trench walls may occur. Subgrade preparation beneath footings, mat foundations, slabs-on-grade, and pavement sections may prove difficult or infeasible. In general, we note that it has also been our experience that increased clean-up costs may be incurred, and greater safety hazards may exist, if the work proceeds during the wet winter months.

This geotechnical and geologic report does not address design or construction issues related to chemically impacted soils and groundwater as environmental services were not included in our scope.

7. RECOMMENDATIONS

7.01 General

The following presents our geotechnical recommendations for the design and construction of the proposed Berkeley City College project. If the project design differs significantly from that discussed previously in this report, we should be consulted regarding the applicability of the conclusions and recommendations presented herein, and be provided the opportunity to provide supplemental recommendations, where appropriate. Contractors responsible for the geotechnical aspects of the project should become familiar with the contents of this report and acknowledge:

- The site conditions, as described in this report and the attached Appendices;
- The construction considerations discussed in Section 6.04 of this report; and
- Any additional special project requirements (CGS, DSA, City of Berkeley, etc.).

We recommend that these and all other contractor responsibilities be clearly defined in the project plans and specifications.

7.02 Seismic Design

Structures at the site should be designed to resist strong ground shaking in accordance with the applicable building codes and local design practice. Appendix F contains our site-specific ground motion analysis report for the site. A summary of site-specific seismic design parameters is presented in Table 8.

Table 8 – Site-Specific Seismic Design Parameters

Parameter	Factor/Coefficient	Value
Short-Period MCE_R at 0.2s	S_s	2.16 g
1.0s Period MCE_R	S_1	0.833 g
Soil Profile Type	Site Class	D
Site Coefficient	F_a	1.0
Site Coefficient	F_v	2.5
Risk Coefficient	C_{RS}	0.904
Risk Coefficient	C_{R1}	0.895
Site-Specific Design Spectral Acceleration Parameters	S_{DS}	1.62
	S_{D1}	1.11
Site-Specific Peak Ground Acceleration from MCE_G	PGA_M	1.14 g

7.03 Shallow Foundations

7.03.1 Mat Foundations

As discussed previously, the proposed structure can be founded on a mat foundation. Based on the undocumented fill and expansive soil encountered during our subsurface exploration, we recommend that the bottom of the mat foundation be located at a distance of 3 feet, or more, below the existing ground surface. Where existing piles or other foundation elements are present, we recommend removing them to a depth of 5 feet below the bottom of the mat foundation. We recommend the mat be 12 inches, or more, in thickness and

include at least two layers (top and bottom) of steel reinforcement. The mat foundation should be designed to span an unsupported length of 10 feet.

The new mat slab below the structure should be evaluated using the allowable contact pressures in Table 9 (DL = Dead Loads; LL = Live Loads; Total = DL + LL + wind or seismic). These allowable contact pressures represent the total load that can be placed on the soil at foundation subgrade level. If these assumptions change, the allowable contact pressures may need to be revised.

Table 9 – Mat Allowable Contact Pressures

Load Case	Bearing Pressure * (psf)	Minimum Factor of Safety
DL Allowable	3,000	3.0
DL + LL Allowable	4,500	2.0
Total Allowable	6,000	1.5
Ultimate	9,000	1.0

* In localized areas of the mat, the bearing pressure can be increased by 10% if needed.

The allowable contact pressures and modulus of subgrade reaction were estimated in multiple iterations between the structural engineer and A3GEO to achieve deflection compatibility between structural mat deflection and soil settlement. As a result, the following modulus of subgrade reaction values are recommended for design:

- Variable values from the lowest (8 psi/in) at the centroid to the highest (20 psi/in) at the edge can be used for long-term loading of the entire mat footprint (See Appendix I).
- A uniform subgrade modulus (25 psi/in) can be used for a short-term seismic event.
- At isolated column locations and/or to evaluate concentrated loading, a value of 125 psi/in can be used.

7.03.2 Lateral Load Resistance

Resistance to lateral loads can be provided by passive pressures acting on the vertical faces of below-grade structural elements and by friction along the bottom of the mat. Where below-grade structural elements are surrounded by soil, passive resistance can be evaluated using an equivalent fluid weight of 300 pcf. This value can be increased by one-third for dynamic loading. At perimeter locations, the top of the assumed passive zone should be assumed to start at 1 foot below the lowest adjacent ground surface.

A friction coefficient can be used to evaluate frictional resistance along the bottoms of footings and slabs. The following friction coefficients can be used for design:

- concrete in contact with waterproofing layer: 0.20
- concrete in contact with native soil: 0.30
- concrete in contact with Caltrans Class 2 AB: 0.45

The preceding passive and frictional resistance values include a factor of safety of at least 1.5 and can be fully mobilized with deformations of less than ½- and ¼- inch, respectively.

7.04 Deep Foundations

The proposed structure can be founded on a deep pile foundation. To mitigate potential new building loads from impacting the adjacent basement wall, the western portion of the foundation piles should be sleeved or cased to the bottom of the adjacent basement wall (estimated to be about 6 feet below the bottom of a 4-foot-thick pile cap) to prevent the transfer of axial or lateral loads to the adjacent basement wall. Where existing piles or other foundation elements are present, we recommend locating new piles to achieve a minimum clearance of 18 inches. Pile axial capacity and lateral response charts are provided for two conditions: 1) the west side of the

building, where the upper 10 feet is neglected to prevent loading the adjacent building; and 2) the rest of the building footprint where the top of pile is assumed to start at the bottom of a 4-foot-thick pile cap.

7.04.1 Pile Axial Design

Foundation piles should be spaced no closer than three pile diameters, center-to-center to avoid group effects for axial capacity. Axial capacity was performed on a representative soil profile for the site. Graphical plots depicting allowable pile capacity versus depth for 18-inch and 30-inch diameter drilled piles are provided in Appendix H. The values shown in the charts can be increased by 1/3 for short term wind or seismic loading conditions. For uplift, the allowable capacity should be 80 percent of the values shown in the charts.

For drilled piles, we recommend that any contribution to axial capacity from end bearing be ignored due to difficulties associated with obtaining and/or assuring a clean bearing surface at the bottom of the holes and the pile displacement needed to mobilize end bearing resistance.

Preliminary estimates indicate structures supported on piles, consistent with these recommendations, should be designed for a total static settlement of up to ½ inch with a differential of ¼ inch over a lateral span of 30 feet for sustained loads. The actual settlement across the building will be dependent on the foundation system selected and loading conditions. If deep foundations are selected for the structure, additional settlement analysis should be conducted once the final building configuration, pile layout, pile diameter, and pile loading are known.

7.04.2 Pile Lateral Design

Piles will develop lateral resistance from their structural rigidity and from the surrounding soil pressures. The lateral resistance is related to the allowable horizontal displacements and bending moments generated in the pile. Lateral pile response was performed on a representative soil profile for 18-inch and 30-inch diameter drilled piles. Lateral pile analyses' results for free and fixed head conditions with ½-inch of pile head deflection are provided in Appendix H.

For lateral resistance in a direction with multiple piles, group effects should be considered. If the loading direction for a pile is perpendicular to the row, a multiplier of less than 1.0 shall only be used if the pile spacing is 4 times the pile diameter (B) or less. A P-multiplier of 0.80, 0.90, and 1.0 shall be used for pile spacings of 2.5B, 3B, and 4B, respectively. If the loading direction for the pile cap is parallel to the row, multipliers should be applied using the values in Table 10.

Table 10 – Pile P-Multipliers, Pm for Multiple Row Shading

Center-to-Center Spacing (in the direction of loading)	P-Multipliers, P_m		
	Row 1	Row 2	Row 3
2.0B	0.60	0.35	0.25
3.0B	0.75	0.55	0.40
5.0B	1.0	0.85	0.70
7.0B	1.0	1.0	0.90
8.0B	1.0	1.0	1.0

Resistance to lateral loads can also be provided by passive pressures acting on the vertical faces of grade beams and pile caps. Passive resistance can be evaluated using an equivalent fluid pressure of 300 pounds per cubic foot (pcf). This value can be increased by one-third for dynamic loading. In areas not confined by slabs or pavements, passive resistance should be neglected within 1 foot of the ground surface. The ultimate passive resistance can be considered fully mobilized when the lateral displacement of the pile cap or top of the pile is 6 percent of the height of the pile cap. For smaller lateral displacements, the values provided in Table 11 can be used for design.

Table 11 – Passive Resistance of Pile Caps

Lateral Displacement/Height of Pile Cap	Mobilized Passive/ Ultimate Passive (psf)
1%	55%
2%	70%
3%	82%
4%	90%
6%	100%

7.05 Moisture Vapor Barrier

We recommend a waterproofing design specialist be consulted regarding waterproofing and moisture vapor designs. The following general recommendations are provided based on experience with typical building construction and are not intended as specific design criteria.

The potential for migration of moisture through slabs underlying enclosed spaces or overlain by moisture sensitive floor coverings can be reduced by providing a moisture vapor retarding system between the subgrade soil and the bottom of slabs. A typical moisture vapor retarding system consists of a 4-inch-thick capillary break, overlain by a 15-mil-thick plastic membrane. The capillary break should be constructed of clean, compacted, open-graded crushed rock or angular gravel of ¾-inch nominal size. To reduce the potential for slab curling and cracking, an appropriate concrete mix with low shrinkage characteristics and a low water-to-cementitious-materials ratio should be specified. In addition, the concrete should be delivered and placed in accordance with ASTM C94 with attention to concrete temperature and elapsed time from batching to placement, and the slab should be cured in accordance with the ACI Manual of Concrete Practice (ACI, 2016), as appropriate. The plastic membrane should conform to the requirements in the latest version of ASTM Standard E 1745 for a Class A membrane (Stego® wrap 15-mil or an approved equivalent). The bottom of the moisture barrier system should be higher in elevation than the exterior grade, if possible. Positive drainage should be established and maintained adjacent to foundations and flatwork.

Where an unbonded topping slab is to be placed directly over the concrete mat foundation, the vapor barrier plastic membrane (Stego® wrap 15-mil or an approved equivalent) shouldl be placed in between the mat and the topping slab to be used as a moisture vapor barrier and a bond breaker.

7.06 Retaining Walls

Recommended lateral pressures are provided below for design of retaining walls in the permanent condition. Where possible, we recommend that retaining walls will be fully drained to prevent the build-up of hydrostatic pressure.

7.06.1 Wall Back-drainage

Back-drainage should consist of either: (a) prefabricated drainage material (Miradrain or an approved alternative) installed in accordance with the manufacturer's recommendations, or (b) a drain rock layer at least 12 inches wide. Prefabricated drainage material should drain to a perforated plastic pipe or an approved prefabricated drainage conduit. Back-drainage should drain into a perforated plastic pipe installed (with perforations down) along the base of the walls on a 2-inch-thick bed of drain rock. Plastic pipe should be sloped to drain by gravity to a sump, relief wells or other suitable discharge and a cleanout should be provided at the pipe's upslope end. Perforated and non-perforated plastic pipe used in the drainage system should consist of 4-

inch diameter Schedule 40 PVC or an approved equivalent. Drain rock should conform to Caltrans specifications for Class 2 permeable material. Alternatively, locally available, clean, ½- to ¾-inch maximum size crushed rock or gravel could be used, provided it is encapsulated in a non-woven geotextile filter fabric, such as Mirafi 140N or an approved alternative. The upper 2 feet of retaining wall backfill (above back-drainage) should be comprised of low-permeability soil to limit surface water infiltration into the retaining wall back-drainage system.

7.06.2 Design Earth Pressures

Walls that are not free to rotate at their tops (including building walls) should be evaluated using an "at-rest" earth lateral pressure distribution for restrained walls. Retaining walls that are not restrained at the top (i.e., cantilever) can be evaluated using "active" lateral earth pressures. The equivalent fluid pressure (triangular distribution) values in Table 12 can be used for design.

Table 12 - Retaining Wall Lateral Earth Pressures Distribution

Load Condition	At-Rest (Restrained) Lateral Pressure[1]	Active (Cantilever) Lateral Pressure[1]	Water Lateral Pressure[1,2]
Static Lateral Pressure, Level Backfill	60 pcf	40 pcf	45 pcf
Surcharge (general)	0.5 times anticipated surcharge load (uniform) – acting on the back side of the wall, applied over the full height of the wall.	0.33 times anticipated surcharge load (uniform) – acting on the back side of the wall, applied over the full height of the wall.	---
Seismic Surcharge (earthquake)	0	20 pcf	---

Notes

[1] Pressures are triangular equivalent fluid pressure unless otherwise noted.
[2] Water pressure starts at portion of walls without a backdrain.

7.07 Earthwork

7.07.1 Subgrade Preparation, Overexcavation and Replacement of Unsuitable Materials

From a geotechnical standpoint, it will be necessary to remove all existing footings, slabs, walls, pavements, and buried utilities from within and below the footprint of the planned building. Excavations should be backfilled with engineered fill per the recommendations in this report. Where existing deep foundations (e.g., drilled piers or drilled/belled caissons) exist, we recommend removal of the upper 5 feet of these elements so that they do not interfere with planned construction or create localized "hard spots" beneath new foundations or slabs-on-grade.

Unsuitable materials include, but may not be limited to dry, loose, soft, wet, expansive, organic, or compressible natural soil, and undocumented or otherwise deleterious fill materials. Based on the site history and materials encountered in our subsurface exploration, undocumented fill should be anticipated to depths of about 3 feet. Excavations of unsuitable materials should be backfilled with engineered fill or controlled low strength material (CLSM).

If unsuitable materials are encountered during construction, we recommend that all unsuitable soils be removed from within the bearing zone below and surrounding, where feasible, planned foundations. We recommend that the bearing zone be defined by imaginary planes inclined at 1:1 (horizontal to vertical) extending downwards and outwards from the outer edge of the foundations. The minimum vertical extent of overexcavation will depend upon the depth of unsuitable material requiring removal, which A3GEO will determine in the field during over-excavation.

Mat and footing excavations should be checked by A3GEO for proper depth, bearing, and cleanout prior to the placement of fill or reinforcing steel. Any wet, weak, soft, or otherwise unsuitable soils found to be present at that time should be excavated and replaced in accordance with A3GEO's recommendations. Foundation excavations should be kept moist and free of loose material and standing water prior to concrete placement.

7.07.2 Fill Materials

Geotechnical requirements for fill materials are provided below:

> ***General Fill*** – General Fill material should have an organic content of less than 3 percent by volume and should not contain environmental contaminants or rocks or lumps larger than 6 inches in greatest dimension.
>
> ***Non-Expansive Fill*** – Non-Expansive material should conform to the requirements for General Fill, have a PI no greater than 12, and a Liquid Limit (LL) no greater than 40.
>
> ***Caltrans Class 2 Aggregate Base*** – Aggregate Base (AB) should conform to the requirements of Caltrans Class 2 Aggregate Base, ¾-inch maximum (Caltrans, 2018). Note that Caltrans Class 2 AB meets the requirements for Non-Expansive Fill.

All proposed fill materials should be approved by A3GEO and the project environmental consultant prior to their importation to the site or use. Materials from the site may be suitable for re-use as fill, from a geotechnical standpoint, if they can be processed (i.e., by crushing or blending) to meet the above requirements.

7.07.3 Fill Placement

Fill should be placed on nearly-level, non-yielding subgrades that have been checked and approved by A3GEO. Fill materials should be placed in a manner that minimizes lenses, pockets, and/or layers of materials differing substantially in texture or gradation from the surrounding fill materials. The soils should be spread in uniform layers not exceeding 8 inches in loose thickness prior to compaction. Each layer should be compacted using mechanical means in a uniform and systematic manner. The fill should be constructed in layers such that the surface of each layer is nearly level. Fill should be placed and compacted based on the following requirements (per ASTM D-1557 Test Methods):

- General Fill that is predominantly cohesive (>15 percent passing the No. 200 sieve) should be moisture conditioned, as necessary, to between 2 and 5 percent over optimum moisture content, and compacted to at least 90 percent relative compaction;
- General Fill that is predominantly granular (<15 percent passing the No. 200 sieve) should be moisture conditioned, as necessary, to near or above optimum moisture content and compacted to at least 95 percent relative compaction; and
- Non-Expansive Fill should be moisture conditioned, as necessary, to near or above optimum moisture content and compacted to at least 95 percent relative compaction.

It is possible that the soil to be compacted may be excessively wet or dry depending on the moisture content at the time of construction. If the soils are too wet, they may be dried by aeration or by mixing with drier materials. If the soils are too dry, they may be wetted by the addition of water or by mixing with wetter materials.

7.07.4 Utility Trenches

Utility trenches should be backfilled with fill placed in lifts not exceeding 8 inches in uncompacted thickness. Trenches should be filled by placing a granular layer (shading) beneath and around the pipe, and then 6 to 12 inches of shading should be carefully placed and tamped above the pipe. The remaining portion of the trench

should be backfilled with onsite or import soil. The backfill (above shading layers) should be placed and compacted to a minimum relative degree of compaction of 90 percent based on ASTM D-1557. The compaction requirements given above should be considered minimum recommended requirements. If the City of Berkeley and/or utility company specifications require more stringent backfill requirements, those specifications should be followed.

If imported granular soil is used, sufficient water should be added during the trench backfilling operations to prevent the soil from "bulking" during compaction. All compaction operations should be performed by mechanical means only. We recommend against jetting.

Where granular backfill is used in utility trenches, we recommend an impermeable plug or mastic sealant be used where utilities pass beneath shallow improvements (e.g., pavements, slabs, shallow foundations) to minimize the potential for free water or moisture to affect any underlying or adjacent expansive soil materials. Finally, because of the potential for collapse of trench walls, we recommend the contractor carefully evaluate the stability of all trenches and use temporary shoring, where appropriate. The design and installation of the temporary shoring should be wholly the responsibility of the contractor. In addition, all state and local regulations governing safety around such excavations should be carefully followed.

7.08 Exterior Flatwork

7.08.1 Subgrade Preparation

We recommend exterior flatwork (including exterior slabs-on-grade, sidewalks, and flexible and rigid pavements) be supported directly upon subgrade materials that are firm, non-yielding, and predominantly non-expansive (per the requirements of Non-Expansive Fill presented in Section 7.07.27.07.2). The upper 6-inches of soil subgrade below exterior slabs-on-grade and pavement sections should consist of either: 1) Non-Expansive Fill placed and compacted in accordance with the requirements of this report; or 2) onsite soil that is checked and confirmed to be non-expansive and suitable by A3GEO. Subgrades beneath exterior slabs-on-grade should be proof-rolled under our observation and confirmed to be uniform and non-yielding prior to the placement of slab reinforcement.

7.08.2 Exterior Slabs-on-Grade

Slab reinforcement should be provided in accordance with the anticipated use and loading of the slab. We recommend that exterior slabs-on-grade be structurally independent from buildings. Concrete slabs that may be subject to vehicle loadings should be designed in accordance with recommendations for rigid pavements.

7.09 Drainage and Site Maintenance

Positive surface drainage should be provided to direct surface water away from the foundations of the buildings into closed pipes that discharge downslope of the proposed improvements. We recommend the rainwater collected on the roof of the buildings be transmitted through gutters and downspouts to closed pipes that drain by gravity to an appropriate discharge. Drainage structures should be periodically cleaned out and repaired, as needed, to maintain appropriate site drainage patterns. Where feasible, and not in conflict with accessibility design requirements, drainage gradients should be 2 percent or more a distance of 5 feet or more from the structure for impervious surfaces and 5 percent or more a distance of 10 feet or more from the structure for pervious surfaces.

If onsite disposal of water is desired, we recommend that water discharge in areas as far away from the new building as possible. Based on the cohesive nature of the onsite soils, bioswale systems should be designed assuming that the bottom of the bioswale will be underlain by clayey materials which generally will have low permeability and slow infiltration rates.

Landscaping adjacent to foundations should include vegetation with low water demands, and irrigation should be limited to that which is needed to sustain the plants. Trees should be restricted from the areas adjacent to foundations a distance equivalent to the canopy radius of the mature tree. Where feasible, bioretention areas should not be located within a distance of 20 feet from structure foundations.

7.10 Construction Monitoring and Instrumentation

An instrumentation program can be implemented to evaluate design assumptions, and monitor vibrations at adjacent structures, deformations of the excavations, and ground surface settlement. The monitoring program would include seismographs and an array of surface control points. The data obtained should be distributed to appropriate parties during the course of construction. To reduce the potential for damage claims from nearby property owners, an instrumentation and monitoring program should be implemented, consisting of the components presented in the following sections.

7.10.1 Preconstruction Conditions Surveys

We recommend preconstruction conditions surveys be completed before the beginning of construction on structures within approximately 50 feet of proposed construction activities. Preconstruction condition surveys should include the exterior and interior of the adjacent neighboring structures. Surveys should include photographs and measurements of relevant site features and hardscape features, including distress features, such as cracks and/or separations that may be present. Consideration may be given to videotaping the survey.

7.10.2 Survey Reference Points

Survey reference points should be installed on the faces of existing adjacent building walls to monitor for potential movement. Additional survey reference points should be placed on adjacent streets, sidewalks, and at other locations determined by the design team. A survey monitoring plan should be developed by the design team prior to construction, and monitoring program threshold and limiting criteria should be incorporated into the Contract Documents. The survey targets should be installed near the excavations at approximately 20-foot spacings. We recommend that the contractor be responsible for maintaining total settlement or horizontal displacement at any survey point to less than ½ inch. If the settlements reach this limit, we recommend that a further review of construction methodologies be performed, and appropriate changes be made.

7.10.3 Construction Vibration Monitoring

Humans can detect vibrations at very low levels which may result in complaints and damage claims. Published data indicate that transient vibrations from construction activities, such as pile driving, are noticeable at peak particle velocities as low as 0.02 to 0.06 inches per second (ips). At peak particle velocities as low as 0.2 to 0.4 ips, the vibrations are disturbing and may result in complaints and damage claims. However, these vibration levels are typically below the peak particle velocity threshold considered to cause cosmetic damage to modern commercial/residential construction.

An additional concern is the possibility of settlement of the sand, silty sand, and sandy silt underlying structures during construction activities. This settlement may result in damage to the structures. Based on our experience with past projects in similar conditions, if the construction vibrations can be maintained below a peak particle velocity of 0.2 ips, the settlement can likely be limited to acceptable levels.

We recommend that vibration caused by construction activities be monitored in terms of peak particle velocity during construction with seismographs positioned near the adjacent structures and monitored during construction. Based on the type and condition of adjacent structures, an appropriate peak particle velocity threshold should be selected by the vibration monitoring specialist. If peak particle velocities exceed this threshold, construction activity should stop, and construction procedures should be re-evaluated to reduce the potential for excessive vibration. Of greater concern is the possibility of settlement of the sand, silty sand, and

sandy silt underlying structures during construction activities. This settlement may result in damage to the structures. Based on our experience with past projects in similar conditions, if the construction vibrations can be maintained below a peak particle velocity of 0.2 ips, the settlement can likely be limited to acceptable levels.

7.11 Future Geotechnical Services

7.11.1 Design Consultation and Plan Reviews

We recommend that we provide geotechnical consultation to the project team during the design phase in order to: 1) check that the design recommendations presented in this report are appropriately incorporated into the project plans and specifications; and 2) provide supplemental geotechnical recommendations, as needed. We recommend that we review the project plans and specifications as they are being developed so that we may provide timely input. We should also perform a general review of the geotechnical aspects of the final plans and specifications, the results of which we should document in a formal plan review letter.

7.11.2 Review of Contractor Requests and Submittals

During the bidding and construction phases, we should review all Requests for Clarification (RFCs) and Requests for Information (RFIs) that are geotechnical in nature. We recommend that we also review all geotechnical submittals from the contractor, including (but not necessarily limited to) those pertaining to excavations, backfilling, subgrade preparation, and geotechnical materials.

7.11.3 Construction Observation

As Geotechnical Engineer of Record, it is essential that A3GEO provide geotechnical services during construction to check whether geotechnical conditions are as anticipated, provide supplemental recommendations where necessary, and document that the geotechnical aspects of the work substantially conform to the approved Contract Documents and the intent of our geotechnical recommendations. Critical aspects of construction that A3GEO should observe and/or test include excavations, backfilling, and subgrade preparation.

8. LIMITATIONS

This report has been prepared for the exclusive use of XL Construction and their consultants for specific application to the proposed Berkeley City College project described herein. The opinions presented in this report were developed in accordance with generally accepted geotechnical and engineering geologic principles and practices. No other warranty, expressed or implied, is made. In the event that any changes in the nature or design of the project are planned, the conclusions and recommendations contained in this report should not be considered valid unless the changes are reviewed, and the conclusions of this report are modified or verified in writing.

The findings of this report are valid as of the present date. However, the passing of time will likely change the conditions of the existing property due to natural processes or the works of man. In addition, due to legislation or the broadening of knowledge, changes in applicable or appropriate standards may occur. Accordingly, the findings of this report may be invalidated, wholly or partly, by changes beyond our control. Therefore, this report should not be relied upon after a period of three years without being reviewed by this office.

9. REFERENCES

1. A3GEO, 2020, Geotechnical Investigation Report, Berkley Community Theater, Berkeley High School, Berkeley, California, June 17.
2. Alan Kropp & Associates, Inc., 2013, Geotechnical Investigation Stonefire Mixed-Use Retail & Residential Building, 1974 University Avenue, Berkeley, California, September 10.
3. Aqua Resources Inc., 1987, Results of Groundwater Monitoring at California School of Professional Psychology, 1900 Addison Street, Berkeley, November 13.
4. Bakun, W.H., 1999, Seismic Activity of the San Francisco Bay Region, Bulletin of the Seismological Society of America, June, v. 89, no. 3, p. 764-784.
5. Boulanger, R.W., and Idriss, I.M., 2014, CPT and SPT Based Liquefaction Triggering Procedures, Center for Geotechnical Modeling, Department of Civil and Environmental Engineering, University of California, Davis, California, Report No. UCD/CGM-14/-1, dated April.
6. Bray, Jonathan D., and Sancio, Rodolfo B., 2006, Assessment of the Liquefaction Susceptibility of Fine-Grained Soils, *in* ASCE Journal of Geotechnical and Geoenvironmental Engineering, Vol. 132, No. 9, September 1, 2006.
7. California Building Standards Commission, 2019, California Building Code (CBC): California Code of Regulations, Title 24, Part 2, Volumes 1 and 2.
8. California Department of Transportation (Caltrans), 2016, Highway Design Manual, http://www.dot.ca.gov/hq/oppd/hdm/hdmtoc.htm, dated December 16
9. California Department of Transportation (Caltrans), 2018a, Corrosion Guidelines, Version 3.0, Division of Engineering Services, Materials Engineering and Testing Services, Corrosion Branch: dated March
10. California Department of Transportation (Caltrans), 2018b, Standard Specifications.
11. California Department Water Resources (DWR), Division of Safety of Dams (DSOD), 2021, 'California Dam Breach Inundation Maps' visited 31 August 2021, https://fmds.water.ca.gov/maps/damim/
12. California Geological Survey (CGS), 2021, CGS Information Warehouse: Tsunami Hazard Area Map Application, visited 31 August 2021, https://maps.conservation.ca.gov/cgs/informationwarehouse/ts_evacuation/
13. California Geological Survey (CGS), 2019, "Note 48 Checklist for the Review of Engineering Geology and Seismology Reports for California Public Schools, Hospitals, and Essential Services Buildings," version dated November 2019.
14. California Geological Survey (CGS), 2003a, Earthquake Zones of Required Investigation, Oakland West Quadrangle, 14 February.
15. California Geological Survey (CGS), 2003b, Seismic Hazard Zone Report for Oakland West 7.5-Minute Quadrangle, Alameda County, California, Seismic Hazard Zone Report 080.
16. Clahan, K.B., Mattison, E., and Knudsen, K.L., 2000, Liquefaction Zones in the San Jose East 7.5-Minute Quadrangle, Santa Clara County, California, *in* Seismic Hazard Evaluation of the San Jose East 7.5-Minute Quadrangle: California Division of Mines and Geology Open-File Report 2000-010.
17. CSW/Stuber-Stroeh Engineering Group, Inc., 2015, Topographic and Utility Map, 2118 Milvia Street, Peralta Community College District, January 29.
18. Engeo, 2013, Geotechnical Feasibility Report, High Rise At The Shattuck Berkeley, California, January 25.
19. Federal Emergency Management Agency (FEMA), 2009, National Flood Insurance Program Flood Insurance Rate Map, Alameda County, California and Incorporated Areas, Panel 57 or 725, Map Number 06001C0057G, effective date 3 August 2009.
20. Freels, L.L., and Associates, 1966, Floor and Foundation Plan, Office Building, James Y. Smith, Inc., August 18.
21. Golden Gate Environmental, Inc., 2009, Additional Site Characterization Report, 1931, 1933 & 1935 Addison Street, Berkeley, California, July 27.
22. Graymer, R.W., et al., 2006, Geologic Map of the San Francisco Bay Region, U.S. Geological Survey Scientific Investigations Map 2918.
23. Graymer, R.W., 2000, Geologic Map and Map Database of the Oakland Metropolitan Area, Alameda, Contra Costa, and San Francisco Counties, California, U.S. Geological Survey Miscellaneous Field Study MR-2342.

24. Harza Kaldveer, 1992, Geotechnical Investigation for Proposed Mixed-Use Project, Six-Story Office/Retail Building and Berkeley YMCA Addition, Berkeley, California, January 25.
25. Idriss, I.M., and Boulanger, R.W., 2008, "Soil Liquefaction During Earthquakes," Earthquake Engineering Research Institute, MNO-12, Oakland, California.
26. Jennings, C.W., and Bryant, W.M., 2010, Fault Activity Map of California, California Geological Survey, Geologic Data Map No. 6.
27. Knudsen, K.L., et al., 2000, Description of Quaternary Deposits and Liquefaction Susceptibility, Nine-County San Francisco Bay Region, California, U.S. Geological Survey, Part 3 of Open-File Report 00-444.
28. Rockridge Geotechnical, 2015, Geotechnical Investigation Center Street Parking Garage, 2025 Center Street, Berkeley, California, March 30.
29. Sowers, J.M., 1993, Creek & Watershed Map of Oakland & Berkeley, Oakland Museum of California, Revised 2000.
30. Subsurface Consultants, Inc., 2000, Geotechnical Investigation, Seismic Upgrade, 2150 Shattuck Avenue, Berkeley, California, April 12.
31. Terraphase Engineering, 2015, Draft Phase I Environmental Site Assessment, 2118 Milvia Street, Berkeley California, January 30.
32. Terraphase Engineering, 2017, Geotechnical Investigation and Foundation Design, Berkeley City College, 2118 Milvia Street, Berkeley California, June 9.
33. United States Geological Survey (USGS) and California Geological Survey (CGS), 2006, Quaternary Fault and Fold Database for the United States, accessed 31 August 2021, from USGS website: http://earthquake.usgs.gov/hazards/qfaults/.
34. Witter, R.C., et al., 2006, Maps of Quaternary Deposits and Liquefaction Susceptibility in the Central San Francisco Bay Region, California, U.S. Geological Survey Open-File Report, 2006-1037.
35. Working Group on California Earthquake Probabilities (WGCEP), 2013, Uniform California Earthquake Rupture Forecast, Version 3 (UCERF3) – Time Independent Model, U.S. Geological Survey Open-File Report 2013-1165, 97 p., California Geological Survey Special Report 228, and Southern California Earthquake Center Publication 1792, http://pubs.usgs.gov/of/2013/1165/.
36. Working Group on California Earthquake Probabilities (WGCEP), 2008, The Uniform California Earthquake Rupture Forecast, Version 2 (UCERF 2): for 2007-2036, U.S. Geological Survey Open File Report 2007-1437, California Geological Survey Special Report 203; and Southern California Earthquake Center Contribution #1138.

FIGURES

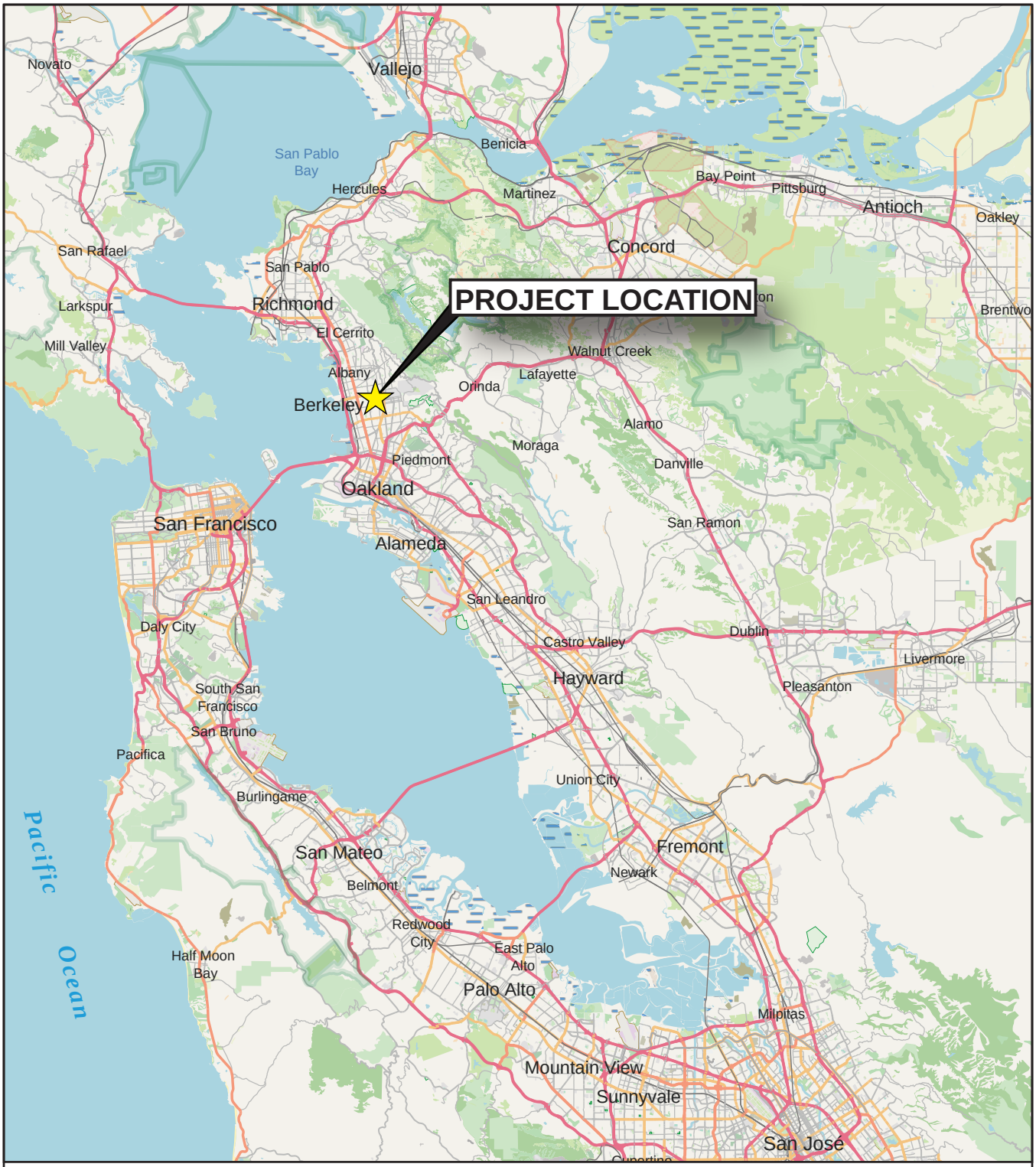

BERKELEY CITY COLLEGE
PERALTA COMMUNITY COLLEGE DISTRICT
BERKELEY, CALIFORNIA

Project No. 1185-1A

SITE LOCATION MAP

A3GEO

FIGURE 1

Date: 9/1/2021

Base: USGS 7.5 Minute Topographic Quadranges - Richmond, Briones Valley, Oakland West & Oakland East

(APPROX. SCALE IN FEET)

0 4,000 8,000

BERKELEY CITY COLLEGE
PERALTA COMMUNITY COLLEGE DISTRICT
BERKELEY, CALIFORNIA

Project No. 1185-1A

SITE VICINITY MAP

A3GEO

FIGURE 2

Date: 9/1/2021

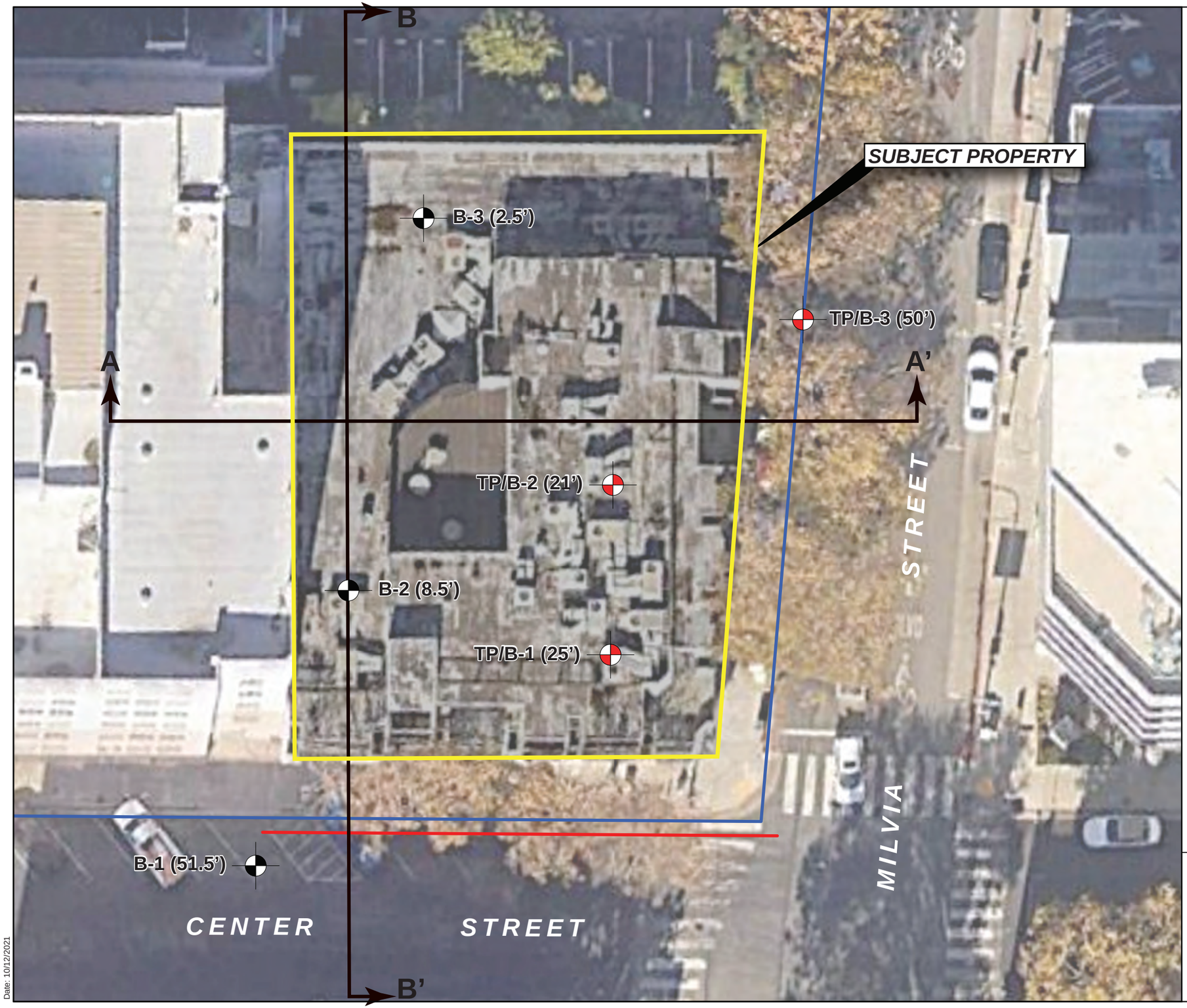

LEGEND:

GEOPHYSICAL SURVEY LOCATION: ACTIVE SURFACE WAVE (MASW) ARRAY

GEOPHYSICAL SURVEY LOCATION: PASSIVE SURFACE WAVE L-ARRAY

H/V SPECTRAL RATIO MEASUREMENT LOCATION

B-3

A3GEO EXPLORATORY BORING (2021) (WITH HOLE DEPTH INDICATED)

TP/B-3

TERRAPHASE ENGINEERING EXPLORATORY BORING (2017) (WITH HOLE DEPTH INDICATED)

B B'

LOCATION OF GEOLOGIC CROSS SECTION

N

(SCALE IN FEET)

0 20 40

BERKELEY CITY COLLEGE
PERALTA COMMUNITY COLLEGE DISTRICT
BERKELEY, CALIFORNIA

Project No. 1185-1A

SITE PLAN

A3GEO

FIGURE 3

Date: 10/12/2021

LEGEND:

- GEOPHYSICAL SURVEY LOCATION: ACTIVE SURFACE WAVE (MASW) ARRAY
- GEOPHYSICAL SURVEY LOCATION: PASSIVE SURFACE WAVE L-ARRAY
- H/V SPECTRAL RATIO MEASUREMENT LOCATION
- B-3 — A3GEO EXPLORATORY BORING (2021) (WITH HOLE DEPTH INDICATED)
- TP/B-3 — TERRAPHASE ENGINEERING EXPLORATORY BORING (2017) (WITH HOLE DEPTH INDICATED)

(SCALE IN FEET)

0 100 200

BERKELEY CITY COLLEGE
PERALTA COMMUNITY COLLEGE DISTRICT
BERKELEY, CALIFORNIA

Project No. 1185-1A

GEOPHYSICAL SURVEY PLAN

A3GEO

FIGURE 4

Date: 10/12/2021

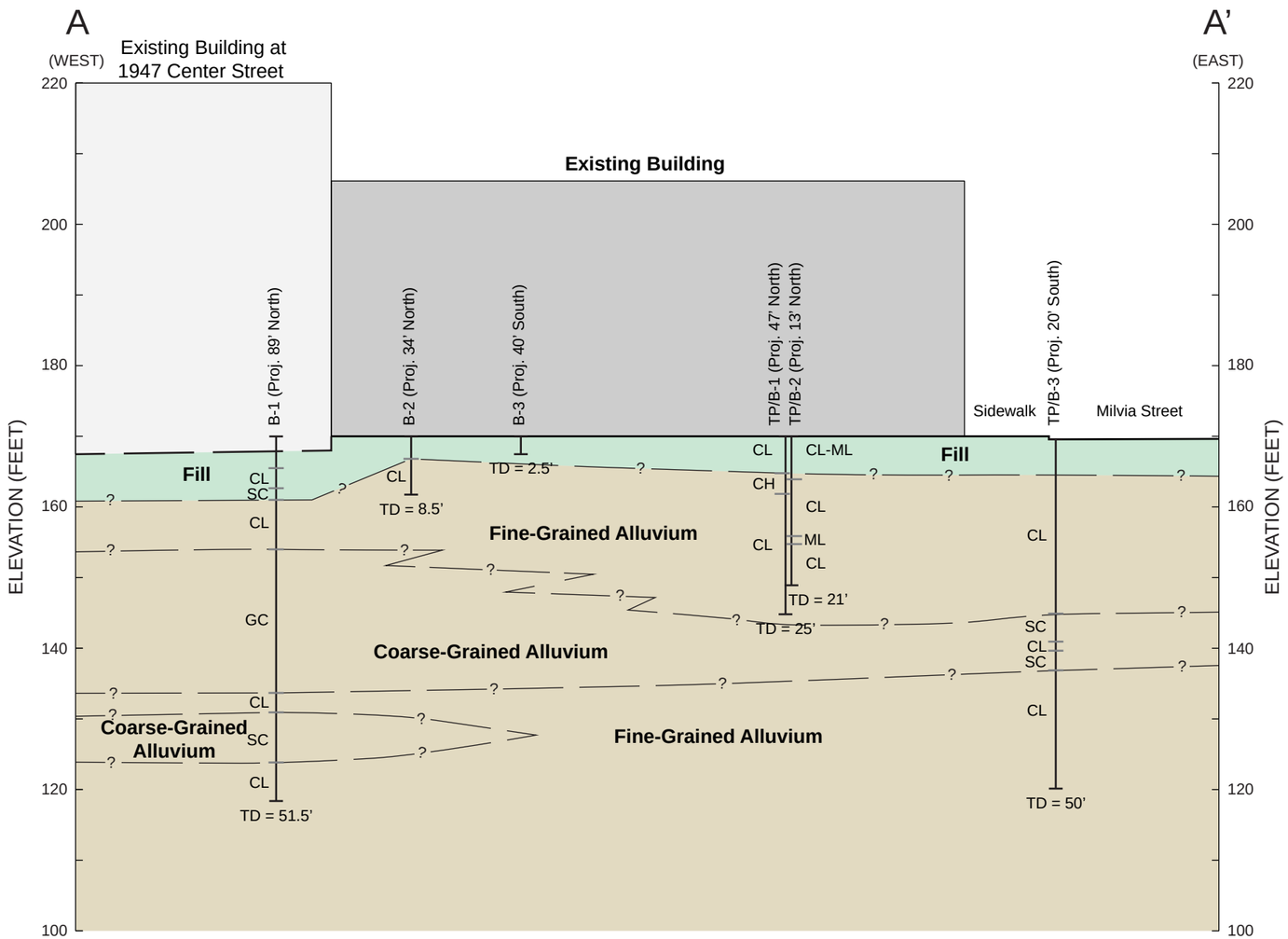

Note: Elevation based on NAVD88
Horizontal: 1” = 20’
Vertical: 1” = 20’

(SCALE IN FEET)

0 20 40

Date: 12/22/2021

BERKELEY CITY COLLEGE
PERALTA COMMUNITY COLLEGE DISTRICT
BERKELEY, CALIFORNIA

Project No. 1185-1A

GEOLOGIC CROSS SECTION A - A’

A3GEO

FIGURE 5

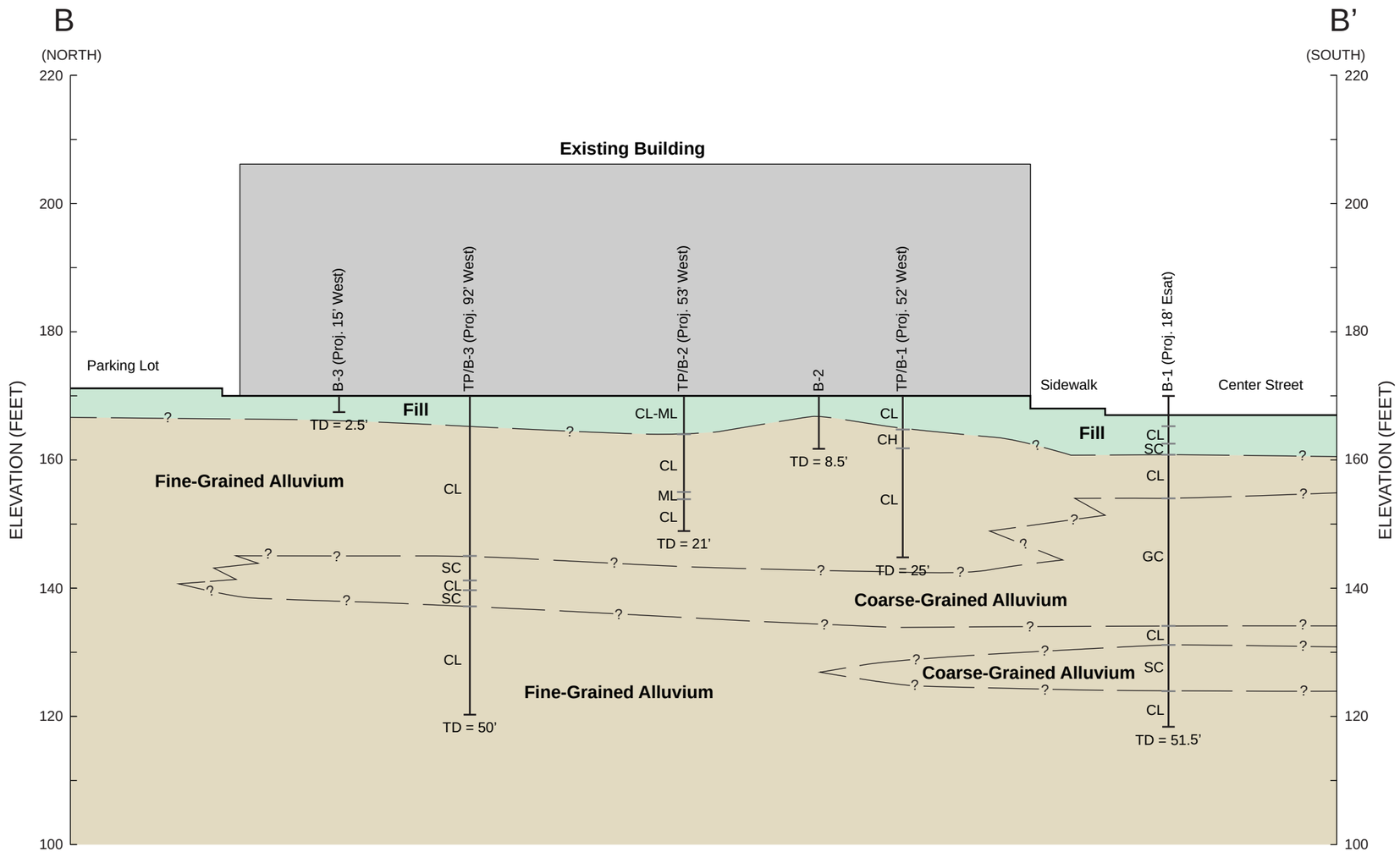

Note: Elevation based on NAVD88
Horizontal: 1” = 20’
Vertical: 1” = 20’

(SCALE IN FEET)

0 20 40

Date: 12/22/2021

BERKELEY CITY COLLEGE
PERALTA COMMUNITY COLLEGE DISTRICT
BERKELEY, CALIFORNIA

Project No. 1185-1A

GEOLOGIC CROSS SECTION B - B’

A3GEO

FIGURE 6

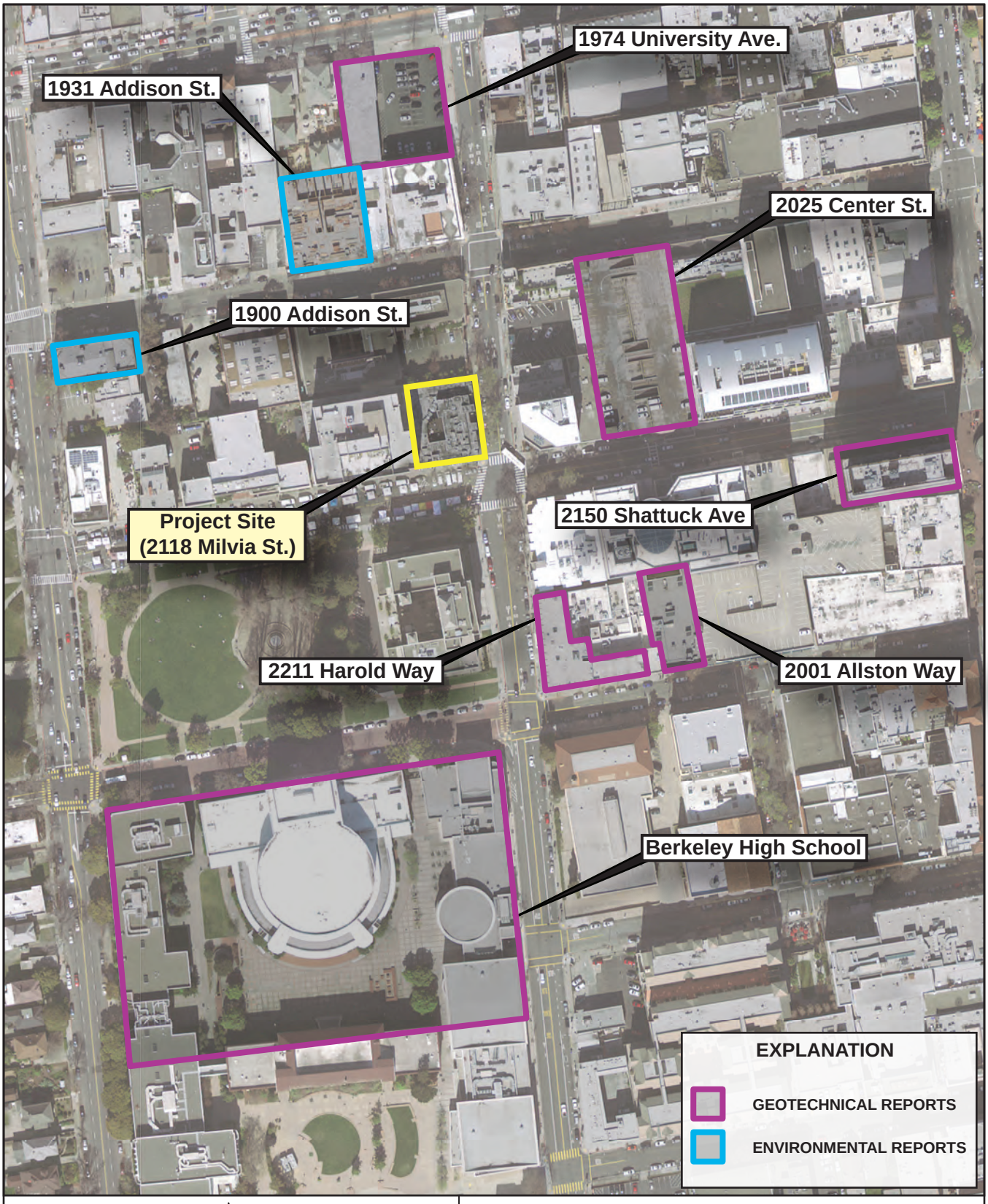

(SCALE IN FEET)

0 200 400

BERKELEY CITY COLLEGE
PERALTA COMMUNITY COLLEGE DISTRICT
BERKELEY, CALIFORNIA

Project No. 1185-1A

EXISTING GEOTECHNICAL DATA - NEARBY SITES

A3GEO

FIGURE 7

Date: 10/12/2021

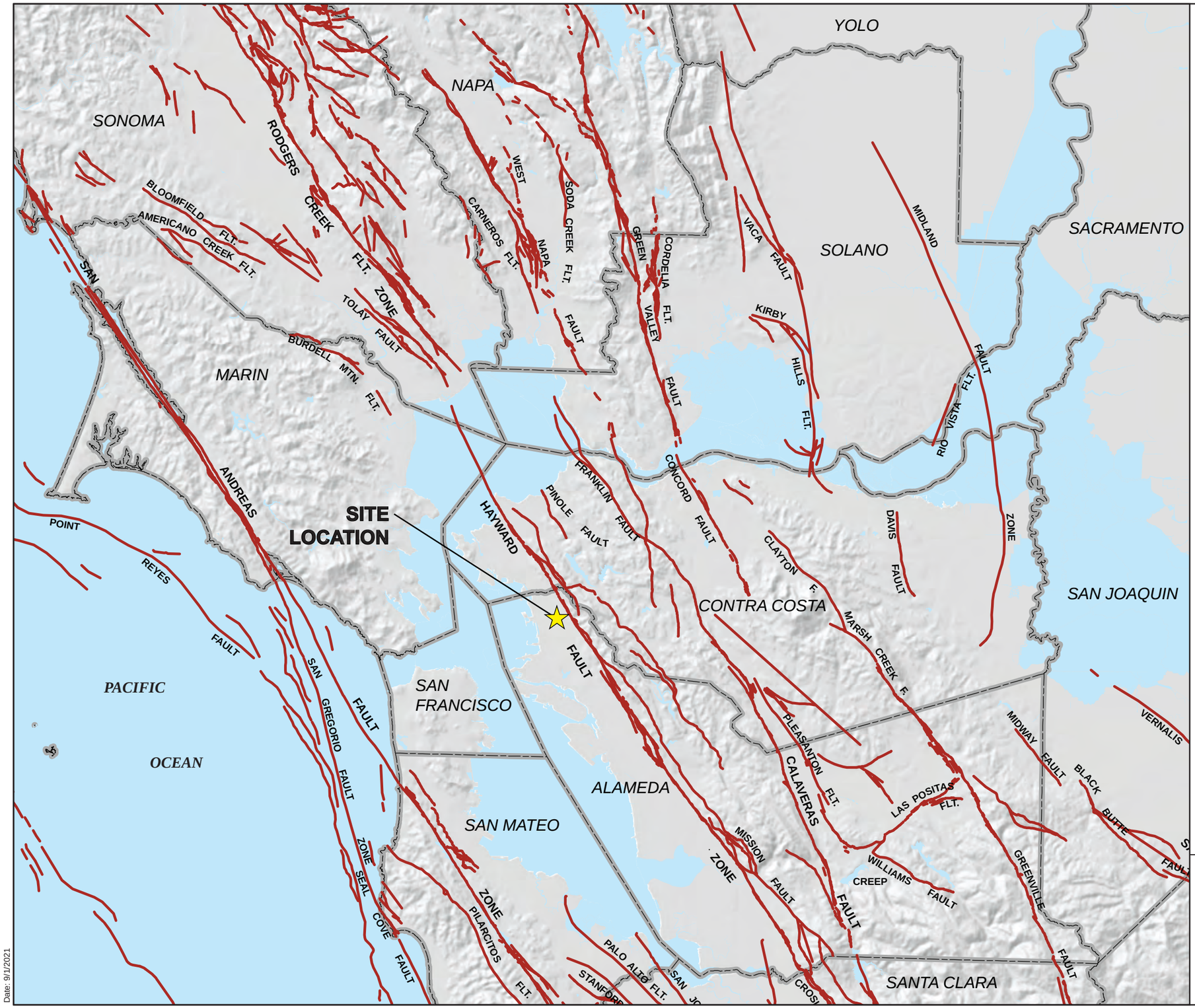

LEGEND:

QUATERNARY FAULT

COUNTY BOUNDARY

NOTES:

1. BASE MAP MODIFIED FROM USGS AND CALIFORNIA GEOLOGICAL SURVEY, 2006, QUATERNARY FAULT AND FOLD DATABASE FOR THE UNITED STATES, ACCESSED 25 JANUARY, 2018, FROM USGS WEBSITE: HTTP://EARTHQUAKE.USGS.GOV/HAZARDS/QFAULTS/

(SCALE IN MILES)

0 8 16

BERKELEY CITY COLLEGE
PERALTA COMMUNITY COLLEGE DISTRICT
BERKELEY, CALIFORNIA

Project No. 1185-1A

QUATERNARY FAULT MAP

A3GEO

FIGURE 8

Date: 9/1/2021

LEGEND:

SURFICIAL DEPOSITS

Qhaf	ALLUVIAL FAN AND FLUVIAL (HOLOCENE)
Qhl	NATURAL LEVEE (HOLOCENE)
Qpaf	ALLUVIAL FAN AND FLUVIAL (PLEISTOCENE)

BEDROCK

FRANCISCAN COMPLEX

KJfs	SANDSTONE (LATE CRETACEOUS TO LATE JURASSIC)
KJfm	MELANGE (CRETACEOUS TO LATE JURASSIC)

MAP SYMBOLS

- GEOLOGIC CONTACT
- FAULT APPROX. LOCATED
- FAULT INFERRED

Notes:

1. DATA TAKEN FROM GRAYMER, R.W., 2000, GEOLOGIC MAP AND MAP DATABASE OF THE OAKLAND METROPOLITAN AREA, ALAMEDA, CONTRA COSTA, AND SAN FRANCISCO COUNTIES, CALIFORNIA, USGS MISCELLANEOUS FIELD STUDY MR-2342.

N

(SCALE IN FEET)

0 600 1,200

BERKELEY CITY COLLEGE
PERALTA COMMUNITY COLLEGE DISTRICT
BERKELEY, CALIFORNIA

Project No. 1185-1A

REGIONAL GEOLOGIC MAP

A3GEO

FIGURE 9

Date: 9/1/2021

LEGEND:

QUATERNARY DEPOSITS

HISTORICAL

acf	ARTIFICIAL CHANNEL FILL
Qhc	HISTORICAL STREAM CHANNEL DEPOSITS

HOLOCENE

Qhf	ALLUVIAL FAN DEPOSITS

HOLOCENE TO LATEST PLEISTOCENE

Qf	ALLUVIAL FAN DEPOSITS

LATEST PLEISTOCENE

Qpf	ALLUVIAL FAN DEPOSITS

EARLY TO LATE PLEISTOCENE

Qop	PEDIMENT DEPOSITS

EARLY QUATERNARY AND OLDER

br	BEDROCK

Notes:

1. DATA TAKEN FROM WITTER, R.C., ET AL., 2006, MAPS OF QUATERNARY DEPOSITS AND LIQUEFACTION SUSCEPTIBILITY IN THE CENTRAL SAN FRANCISCO BAY REGION, USGS OFR 2006-1037

(SCALE IN FEET)

0 600 1,200

BERKELEY CITY COLLEGE
PERALTA COMMUNITY COLLEGE DISTRICT
BERKELEY, CALIFORNIA

Project No. 1185-1A

QUATERNARY DEPOSITS MAP

A3GEO

FIGURE 10

Date: 9/1/2021

LEGEND:

- CREEKS
- FORMER CREEKS, BURIED OR DRAINED, CIRCA 1850
- UNDERGROUND CULVERTS AND STORM DRAINS

Notes:

1. BASE MAP TAKEN FROM SOWERS, J.M., 1993, CREEK AND WATERSHED MAP OF OAKLAND AND BERKELEY, OAKLAND MUSEUM OF CALIFORNIA, REVISED 2000.

(SCALE IN FEET)

0 600 1,200

BERKELEY CITY COLLEGE
PERALTA COMMUNITY COLLEGE DISTRICT
BERKELEY, CALIFORNIA

Project No. 1185-1A

HISTORICAL CREEKS MAP

A3GEO

FIGURE 11

Date: 9/1/2021

LEGEND:

LIQUEFACTION ZONES

AREAS WHERE HISTORICAL OCCURRENCE OF LIQUEFACTION, OR LOCAL GEOLOGICAL, GEOTECHNICAL AND GROUND WATER CONDITIONS INDICATE A POTENTIAL FOR PERMANENT GROUND DISPLACEMENTS SUCH THAT MITIGATION AS DEFINED IN PUBLIC RESOURCES CODE SECTION 2693(C) WOULD BE REQUIRED

Notes:

1. ZONES OF REQUIRED INVESTIGATION TAKEN FROM CALIFORNIA (CGS), 2003A, EARTHQUAKE ZONE OF REQUIRED INVESTIGATION, OAKLAND WEST QUADRANGLE, 14 FEBRUARY.

N

(SCALE IN FEET)

0 600 1,200

BERKELEY CITY COLLEGE
PERALTA COMMUNITY COLLEGE DISTRICT
BERKELEY, CALIFORNIA

Project No. 1185-1A

ZONES OF REQUIRED INVESTIGATION

A3GEO

FIGURE 12

Date: 9/1/2021

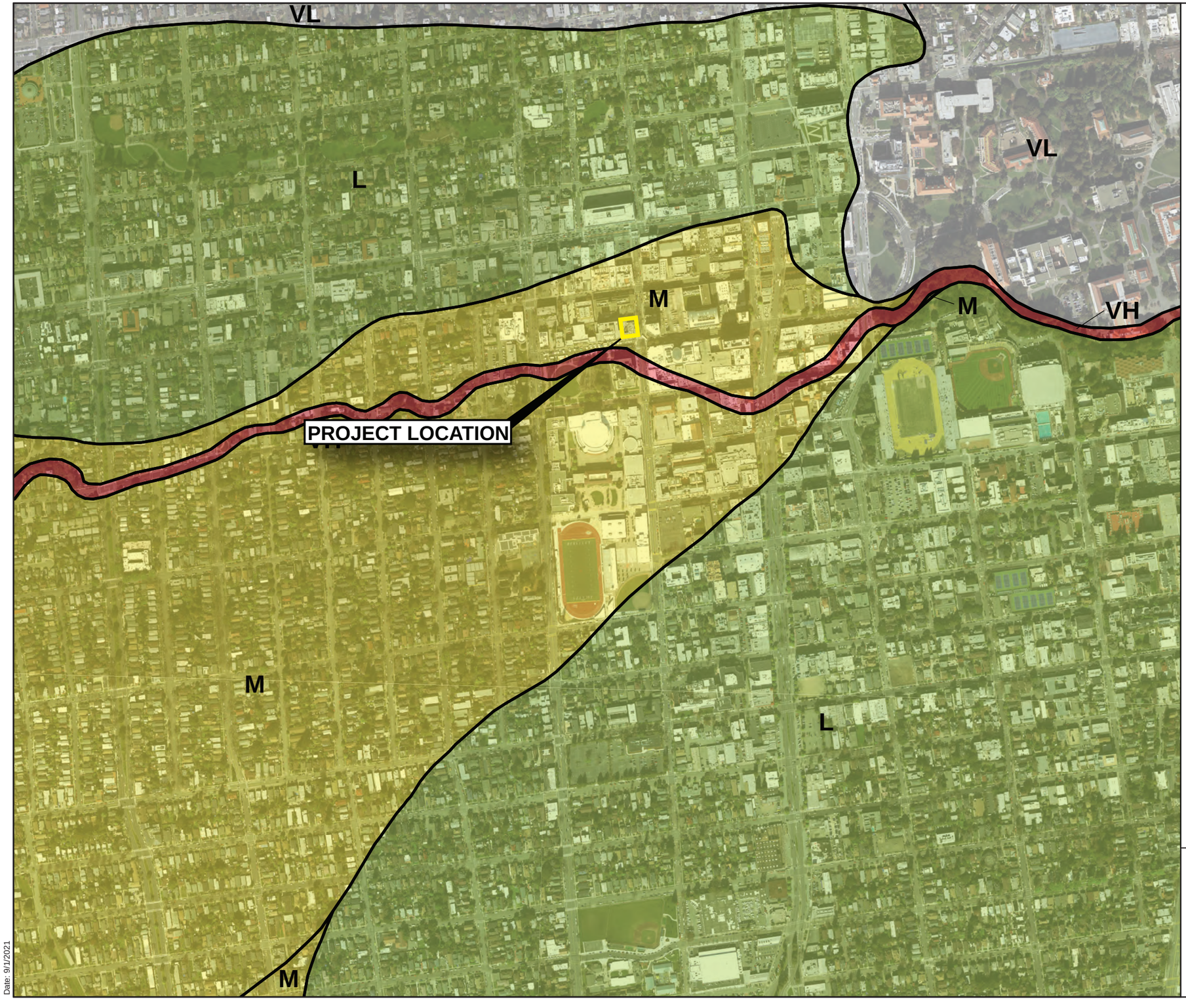

LEGEND:

LIQUEFACTION SUSCEPTIBILITY

VH	VERY HIGH
H	HIGH
M	MODERATE
L	LOW
VL	VERY LOW

Notes:

1. DATA TAKEN FROM WITTER, R.C., ET AL., 2006, MAPS OF QUATERNARY DEPOSITS AND LIQUEFACTION SUSCEPTIBILITY IN THE CENTRAL SAN FRANCISCO BAY REGION, USGS OFR 2006-1037

(SCALE IN FEET)

0 600 1,200

BERKELEY CITY COLLEGE
PERALTA COMMUNITY COLLEGE DISTRICT
BERKELEY, CALIFORNIA

Project No. 1185-1A

LIQUEFACTION SUSCEPTIBILITY MAP

A3GEO

FIGURE 13

Date: 9/1/2021

APPENDIX A

Exploratory Boring Logs

UNIFIED SOIL CLASSIFICATION CHART

MAJOR DIVISIONS				TYPICAL NAMES
COARSE GRAINED SOILS: more than 50% retained on No. 200 sieve	COARSE GRAINED SOILS: 50% or more of coarse fraction on No. 4 sieve	CLEAN GRAVELS	GW	Well graded gravels and gravel-sand mixtures, little or no fines
			GP	Poorly graded gravels and gravel-sand mixtures, little or no fines
		GRAVELS WITH SAND	GM	Silty gravels and gravel-sand-silt mixtures
			GC	Clayey gravels and gravel-sand-clay mixtures
	SANDS: more than 50% passing on No. 4 sieve	CLEAN SANDS	SW	Well graded sands and gravelly sand, little or no fines
			SP	Poorly graded sands and gravelly sand, little or no fines
		SANDS WITH FINES	SM	Silty sands, sand-silt mixtures
			SC	Clayey sands, sand-clay mixtures
FINE GRAINED SOILS: 50% or more passing No. 200 sieve	SILTS AND CLAY: Liquid Limit 50% or less		ML	Inorganic silts, very fine sands, rock flour, silty or clayey fine sands
			CL	Inorganic clays or low to medium plasticity, gravelly clays, sandy clays, silty clays, lean clays
			OL	Organic silts and organic silty clays of low plasticity
	SILTS AND CLAY: Liquid Limit 50% or greater		MH	Inorganic silts, micaceous or diatomaceous fine sands or silts, elastic clays
			CH	Inorganic clays of high plasticity, fat clays
			OH	Organic clays of medium to high plasticity
HIGHLY ORGANIC SOILS			PT	Peat, muck, and other highly organic soils

BOUNDARY CLASSIFICATION AND GRAIN SIZES

SILT OR CLAY	SAND			GRAVEL		COBBLES	BOULDERS
	FINE	MEDIUM	COARSE	FINE	COARSE		

U.S. Standard Sieve Sizes	No. 200	No. 40	No. 10	No. 4	3/4"	3"	12"
	0.075 mm	0.425 mm	2 mm	3/16"			

SYMBOLS

Modified California (MC) Sampler (3" O.D.)	ROCK CORE (RC)	Disturbed Sample
Standard Penetration Test: SPT (2" O.D.)	Shelby Tube, pushed or used Ostenberg Sampler	Water Levels At time of drilling At end of drilling After drilling

ABBREVIATIONS

Item	Meaning
LL	Liquid Limit (%) (ASTM D 4318)
PI	Plasticity Index (%) (ASTM D 4318)
-200	Passing No. 200 (%) (ASTM D 1140)
TXCU	Laboratory consolidated undrained triaxial test of undrained shear strength (psf) (ASTM D 4767)
TXUU	Laboratory unconsolidated, undrained triaxial test of undrained shear strength (psf) (ASTM D 2850)
psf/tsf	pounds per square foot / tons per square foot
psi	pounds per square inch
OD	Outside Diameter
ID	Inside Diameter

NOTES

1. Stratification lines represent the approximate boundaries between material types and the transitions may be gradual.
2. Modified California (MC) blow counts were adjusted by multiplying field blow counts by a factor of 0.63.
3. Recorded blow counts have not been adjusted for hammer energy.

A3GEO

KEY TO EXPLORATORY BORING LOGS

A3GEO, Inc.
821 Bancroft Way
Berkeley, CA 94710
Telephone: 510-705-1664

BORING NUMBER B-1

CLIENT XL Construction
PROJECT NAME 2118 Milvia
PROJECT NUMBER 1185-1A
PROJECT LOCATION Berkeley, CA
DATE STARTED 8/13/21 **COMPLETED** 8/13/21
GROUND ELEVATION 167 ft NAVD88 **HOLE SIZE** 4
DRILLING CONTRACTOR Taber Drilling Co.
GROUND WATER LEVELS:
DRILLING METHOD Mud Rotary
AT TIME OF DRILLING --- Not measured
LOGGED BY DB **CHECKED BY** TS
AT END OF DRILLING --- Not measured
NOTES
AFTER DRILLING --- Not measured

DEPTH (ft)	GRAPHIC LOG	MATERIAL DESCRIPTION	SAMPLE TYPE	ADJUSTED BLOW COUNTS (N VALUE)	DRY UNIT WT. (pcf)	POCKET PEN. (tsf)	MOISTURE CONTENT (%)	% RECOVERED	OTHER LAB TESTS / NOTES
0		12" Asphalt							Drill Auger 0' - 1'
		7" Concrete							Concrete Core 1' - 1.5'
		SANDY LEAN CLAY (CL) - stiff, dark gray, moist, mostly fine sand (Fill)							Hand Auger 1.5' - 5'
			GB 1				29		Gravel=1% Sand=32% -#200=67% LL=48, PI=28
5		CLAYEY SAND WITH GRAVEL (SC) - medium dense, dark brown and yellowish brown, moist, fine to coarse sand, gravel up to 1" diameter; mixed fill and top-soil (Fill)	MC 2	11	92	2.0 2.5	18	67	Gravel=34% Sand=37% -#200=29%
		SANDY LEAN CLAY (CL) - stiff to very stiff, very dark gray (10YR 3/1), moist, medium plasticity, mostly fine sand (Alluvium)							Switched to mud rotary
			ST 3		108	2.0	19	75	Gravel=11% Sand=31% -#200=58% LL=40, PI=23 TXUU = 2443 psf shear strength Consolidation Test
10		- dark brown (10YR 3/3) at 10 ft	MC 4	9		1.5		56	
		CLAYEY GRAVEL WITH SAND (GC) - dense, dark brown to grayish brown (10YR 3/3 to 10YR 4/2), wet, fine to coarse sand (Alluvium)							
15			MC 5	49	120		13	50	Gravel=51% Sand=33% -#200=16%
		- angular to subrounded gravel (fine grained sandstone) up to 2-inch diameter; clay skins on gravel at 16 ft							
20									

(Continued Next Page)

A3GEO, Inc.
821 Bancroft Way
Berkeley, CA 94710
Telephone: 510-705-1664

BORING NUMBER B-1

CLIENT XL Construction
PROJECT NAME 2118 Milvia
PROJECT NUMBER 1185-1A
PROJECT LOCATION Berkeley, CA
DATE STARTED 8/13/21 **COMPLETED** 8/13/21
GROUND ELEVATION 167 ft NAVD88 **HOLE SIZE** 4
DRILLING CONTRACTOR Taber Drilling Co.
GROUND WATER LEVELS:
DRILLING METHOD Mud Rotary
AT TIME OF DRILLING --- Not measured
LOGGED BY DB **CHECKED BY** TS
AT END OF DRILLING --- Not measured
NOTES
AFTER DRILLING --- Not measured

DEPTH (ft)	GRAPHIC LOG	MATERIAL DESCRIPTION	SAMPLE TYPE	ADJUSTED BLOW COUNTS (N VALUE)	DRY UNIT WT. (pcf)	POCKET PEN. (tsf)	MOISTURE CONTENT (%)	% RECOVERED	OTHER LAB TESTS / NOTES
20		CLAYEY GRAVEL WITH SAND (GC) - dense, dark brown to grayish brown (10YR 3/3 to 10YR 4/2), wet, fine to coarse sand (Alluvium)*(continued)* - less gravel content and increased clay content at 21 ft	SPT 6	34				67	
25		- gravel is angular, fresh to highly weathered; clay films common on gravel (volcanics, sandstone, meta-volcanics)	SPT 7	35			16	72	Gravel=46% Sand=38% -#200=16%
30		- at 30 ft, brown to dark yellowish brown (10YR 4/3 to 10YR 4/4), increased sand content and decreased clay content; clay films common on gravel; clasts fresh to highly weathered with ferrous staining	MC 8	50				67	
35		SANDY LEAN CLAY (CL) - soft, brown (10YR 5/3 to 10YR 4/3), moist, medium plasticity, mostly fine sand, trace coarse sand and fine gravel, some ferrous staining (Alluvium)	SPT 9	19			22	78	Gravel=2% Sand=46% -#200=52% LL=25, PI=14
40		CLAYEY SAND (SC) - medium dense, brown to dark brown (10YR 4/3), moist, fine to coarse sand, trace fine gravel (Alluvium)							

(Continued Next Page)

A3GEO, Inc.
821 Bancroft Way
Berkeley, CA 94710
Telephone: 510-705-1664

BORING NUMBER B-1

CLIENT XL Construction
PROJECT NAME 2118 Milvia
PROJECT NUMBER 1185-1A
PROJECT LOCATION Berkeley, CA
DATE STARTED 8/13/21 **COMPLETED** 8/13/21
GROUND ELEVATION 167 ft NAVD88 **HOLE SIZE** 4
DRILLING CONTRACTOR Taber Drilling Co.
GROUND WATER LEVELS:
DRILLING METHOD Mud Rotary
AT TIME OF DRILLING --- Not measured
LOGGED BY DB **CHECKED BY** TS
AT END OF DRILLING --- Not measured
NOTES
AFTER DRILLING --- Not measured

DEPTH (ft)	GRAPHIC LOG	MATERIAL DESCRIPTION	SAMPLE TYPE	ADJUSTED BLOW COUNTS (N VALUE)	DRY UNIT WT. (pcf)	POCKET PEN. (tsf)	MOISTURE CONTENT (%)	% RECOVERED	OTHER LAB TESTS / NOTES
40		CLAYEY SAND (SC) - medium dense, brown to dark brown (10YR 4/3), moist, fine to coarse sand, trace fine gravel (Alluvium)*(continued)* - brown to yellowish brown (10YR 5/3 to 10YR 5/4), decreased gravel content, mostly fine sand at 41 ft	MC 10	33	110	4.0 3.0	19	89	Gravel=7% Sand=57% -#200=36% LL=24, PI=10
45		SANDY LEAN CLAY (CL) - very stiff, yellowish brown (10YR 5/6), moist, medium plasticity, mostly fine sand, trace highly weathered sandstone clasts/gravel (Alluvium)	MC 11	23	95	2.0 3.0	29	78	Gravel=6% Sand=42% -#200=52%
50		- decreased gravel content at 50 ft; trace calcium carbonate filaments and ferrous staining	MC 12	29		4.0 3.5		94	

Bottom of borehole at 51.5 feet.
1. Stratification lines represent the approximate boundaries between material types and the transitions may be gradual.
2. Groundwater was not measured during drilling due to using mud rotary drilling techniques.
3. Elevations were estimated using the site Topographic and Utility Map (CSW/Stuber-Stroeh Engineering Group, 2015) and reference North American Vertica
4. The hole was backfilled with cement grout according to the permit requirements.

A3GEO, Inc.
821 Bancroft Way
Berkeley, CA 94710
Telephone: 510-705-1664

BORING NUMBER B-2

CLIENT XL Construction
PROJECT NAME 2118 Milvia
PROJECT NUMBER 1185-1A
PROJECT LOCATION Berkeley, CA
DATE STARTED 8/13/21 **COMPLETED** 8/13/21
GROUND ELEVATION 170 ft NAVD88 **HOLE SIZE** 4
DRILLING CONTRACTOR Taber Drilling Co.
GROUND WATER LEVELS:
DRILLING METHOD Hand Auger
AT TIME OF DRILLING --- Not encountered
LOGGED BY DB/AW **CHECKED BY** TS
AT END OF DRILLING --- Not encountered
NOTES
AFTER DRILLING --- Not encountered

DEPTH (ft)	GRAPHIC LOG	MATERIAL DESCRIPTION	SAMPLE TYPE	ADJUSTED BLOW COUNTS (N VALUE)	DRY UNIT WT. (pcf)	POCKET PEN. (tsf)	MOISTURE CONTENT (%)	% RECOVERED	OTHER LAB TESTS / NOTES
0		4" Concrete, Plastic Liner, and 3" Sand							Concrete Core 0 - 0.5'
		Drain Rock w/ Sand - light gray and brown	GB 1						Hand Auger below 0.5'
		CLAYEY SAND W/ GRAVEL (SC) - medium dense, black to very dark brown (10YR 2/1 to 10YR 2/2), moist, gravel up to 3" diameter (Fill) - Piece of steel and 3" diameter cobble at 2 ft	GB 2						DCP = 7,9,10 for 1.75" increments
		SANDY LEAN CLAY (CL) - medium stiff, very dark grayish brown (10YR 3/2), moist, medium plasticity, mostly fine sand, trace gravel (Alluvium)	GB 3						Corrosivity Test DCP = 8,8,8 for 1.75" increments
5		- dark brown and light brown at 6 ft	GB 4				22		Gravel=2% Sand=35% -#200=63% LL=51, PI=29 DCP = 8,8,10 for 1.75" increments
		SANDY LEAN CLAY (CL) - stiff, dark grayish brown to very dark grayish brown (10YR 4/2 to 10YR 3/2), moist, some gravel (Alluvium)	GB 5						DCP = 14,14,19 for 1.75" increments

Refusal at 8.5 feet.
Bottom of borehole at 8.5 feet.
1. Stratification lines represent the approximate boundaries between material types and the transitions may be gradual.
2. Elevations were estimated using the site Topographic and Utility Map (CSW/Stuber-Stroeh Engineering Group, 2015) and reference North American Vertica
3. The hole was backfilled with cement grout according to the permit requirements.

A3GEO, Inc.
821 Bancroft Way
Berkeley, CA 94710
Telephone: 510-705-1664

BORING NUMBER B-3

CLIENT XL Construction
PROJECT NAME 2118 Milvia
PROJECT NUMBER 1185-1A
PROJECT LOCATION Berkeley, CA
DATE STARTED 8/13/21 **COMPLETED** 8/13/21
GROUND ELEVATION 170 ft NAVD88 **HOLE SIZE** 4
DRILLING CONTRACTOR Taber Drilling Co.
GROUND WATER LEVELS:
DRILLING METHOD Hand Auger
AT TIME OF DRILLING --- Not encountered
LOGGED BY DB/AW **CHECKED BY** TS
AT END OF DRILLING --- Not encountered
NOTES
AFTER DRILLING --- Not encountered

DEPTH (ft)	GRAPHIC LOG	MATERIAL DESCRIPTION	SAMPLE TYPE	ADJUSTED BLOW COUNTS (N VALUE)	DRY UNIT WT. (pcf)	POCKET PEN. (tsf)	MOISTURE CONTENT (%)	% RECOVERED	OTHER LAB TESTS / NOTES
0		5" Concrete, Plastic Liner, and 3" Sand							Concrete Core 0 - 0.5'
		Drain Rock w/ Sand - light gray and brown							Hand Auger below 0.5'
		CLAYEY SAND W/ GRAVEL (SC) - medium dense, very dark brown (10YR 3/2), moist, gravel up to 2" diameter (Fill)	GB 1						
		- increased gravel content (refusal)	GB 2						DCP = 10, 30/1", Refusal on gravel

Refusal at 2.5 feet.
Bottom of borehole at 2.5 feet.
1. Stratification lines represent the approximate boundaries between material types and the transitions may be gradual.
2. Elevations were estimated using the site Topographic and Utility Map (CSW/Stuber-Stroeh Engineering Group, 2015) and reference North American Vertica
3. The hole was backfilled with cement grout according to the permit requirements.

APPENDIX B

Historical Boring Logs (Previous Consultants)

Project: **2118 Milvia Street, Berkeley California** Project Location: **Berkeley, California** Project Number: **0062.004.001**	Log of Boring 1 **Sheet 1 of 1**

Date(s) Drilled **March 21, 2017**	Logged By **ng**	Checked By **jr**
Drilling Method **Direct Push**	Drill Bit Size/Type **2 inch**	Total Depth of Borehole **25**
Drill Rig Type **Limited Access**	Drilling Contractor **Gregg Drilling**	Approximate Surface Elevation **170**
Groundwater Level and Date Measured **20**	Sampling Method(s) **Continuous**	Hammer Data **Not Applicable**
Borehole Backfill **Cement Grout**	Location	

Elevation (feet)	Depth (feet)	Material Type	MATERIAL DESCRIPTION	REMARKS AND OTHER TESTS
170	0	CL	Brown, clayey-silt (CL), trace gravel, stiff, pp=3.5 tsf	
165	5	CH	Dark brown fat clay (CH), LL=58, PL=20, PI=38; pp= 4.0 tsf	
		CL	Lighter brown color, ~10% sand, some gravel (<3%)	
160	10			
		CL	Same as above, wet, pp=1.0 tsf	
155	15			
150	20			
		CL	Same as above, pp=1.75 tsf	
145	25			
140	30			

Sample Type; Sample Number; Sampling Resistance, blows/ft; Graphic Log

C:\Users\Jeff\AppData\Local\Temp\borings_temp\tmpfile.bgs[terraphase.tpl]

terraphase engineering

Figure 1

Project: **2118 Milvia Street, Berkeley California** Project Location: **Berkeley, California** Project Number: **0062.004.001**	Log of Boring 2 **Sheet 1 of 1**

Date(s) Drilled **March 21, 2017**	Logged By **ng**	Checked By **jr**
Drilling Method **Direct Push/hand auger 0 to 10 feet**	Drill Bit Size/Type **2 inch**	Total Depth of Borehole **21**
Drill Rig Type **Limited Access**	Drilling Contractor **Gregg Drilling**	Approximate Surface Elevation **170**
Groundwater Level and Date Measured **none**	Sampling Method(s) **Continuous/hand auger where refusal**	Hammer Data **Not Applicable**
Borehole Backfill **Cement Grout**	Location	

Elevation (feet)	Depth (feet)	Material Type	MATERIAL DESCRIPTION	REMARKS AND OTHER TESTS
170	0	CL	Brown, clayey-silt (CL), trace gravel, stiff	
165	5	CL	Hand Auger - Light Brown Silty Clay (CL) pp = 1 tsf	
160	10			
		ML	Sandy silt, trace gravel, low recovery	
155	15	CL	Stiff silty clay, brown and dark brown, gravel 1 inch; turns lighter brown below 17 feet	
150	20	CL	Bottom of Boring	
145	25			
140	30			

J:\Projects\0034 Peralta\Berkeley City College Milvia Site\Technical\Boring Logs\Milvia Boring 1.bg4[(master 0 lab).tpl]

Figure 2

Project: **2118 Milvia Street, Berkeley California** Project Location: **Berkeley, California** Project Number: **0062.004.001**	Log of Boring 3 **Sheet 1 of 2**

Date(s) Drilled **March 21, 2017**	Logged By **ng**	Checked By **jr**
Drilling Method **Hollow Stem Auger**	Drill Bit Size/Type **8 inch**	Total Depth of Borehole **25**
Drill Rig Type	Drilling Contractor **Gregg Drilling**	Approximate Surface Elevation **170**
Groundwater Level and Date Measured **20**	Sampling Method(s) **SPT and Cal-Mod (all unlined)**	Hammer Data **Safety, 140# falling 30 inches**
Borehole Backfill **Cement Grout**	Location	

Elevation (feet)	Depth (feet)	Sample Type	Sample Number	Sampling Resistance, blows/ft	Material Type	Graphic Log	MATERIAL DESCRIPTION	REMARKS AND OTHER TESTS
170	0				GW		Road base	
					CL		Dark brown clay (CL), thin sand band at 57"	
165	5		1					
160	10		2	5 ,7, 8	CL		stiff, light brown clay, 8 inch gravel/sand band at 10'-4"	
155	15		3	3, 3, 4	CL		Same as above, softer between 15.5 and 16.5 ft	
150	20		4	9, 10, 19	CL		with gravel, water table at 20 feet bgs ▽	
145	25		5	11, 20, 18	SC		Clayey sand with gravel (19.8% gravel, 59% sand, 21.2% fines)	
					CL		Light brown stiff clay (CL) wet	
140	30							

J:\Projects\0034 Peralta\Berkeley City College Milvia Site\Technical\Boring Logs\Milvia Boring 3.bg4[(master 0 lab).tpl]

Figure 3

Project: **2118 Milvia Street, Berkeley California**

Project Location: **Berkeley, California**

Project Number: **0062.004.001**

Log of Boring 3

Sheet 2 of 2

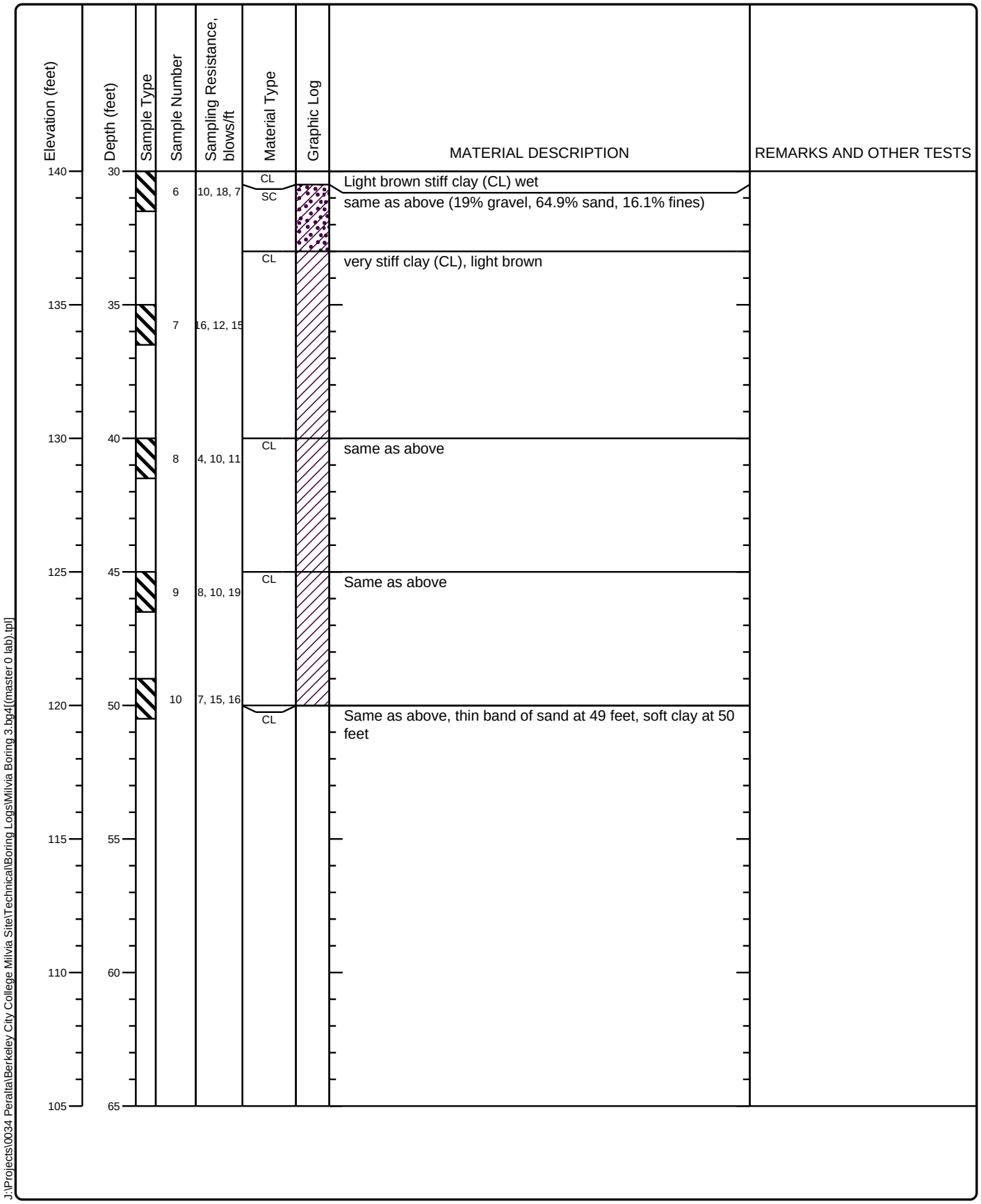

J:\Projects\0034 Peralta\Berkeley City College Milvia Site\Technical\Boring Logs\Milvia Boring 3.bg4[(master 0 lab).tpl]

Figure 3

Project: **2118 Milvia Street, Berkeley California**
Project Location: **Berkeley, California**
Project Number: **0062.004.001**

Key to Log of Boring
Sheet 1 of 1

Elevation (feet)	Depth (feet)	Sample Type	Sample Number	Sampling Resistance, blows/ft	Material Type	Graphic Log	MATERIAL DESCRIPTION	REMARKS AND OTHER TESTS
1	2	3	4	5	6	7	8	9

COLUMN DESCRIPTIONS

1 Elevation (feet): Elevation (MSL, feet).
2 Depth (feet): Depth in feet below the ground surface.
3 Sample Type: Type of soil sample collected at the depth interval shown.
4 Sample Number: Sample identification number.
5 Sampling Resistance, blows/ft: Number of blows to advance driven sampler one foot (or distance shown) beyond seating interval using the hammer identified on the boring log.
6 Material Type: Type of material encountered.
7 Graphic Log: Graphic depiction of the subsurface material encountered.
8 MATERIAL DESCRIPTION: Description of material encountered. May include consistency, moisture, color, and other descriptive text.
9 REMARKS AND OTHER TESTS: Comments and observations regarding drilling or sampling made by driller or field personnel.

FIELD AND LABORATORY TEST ABBREVIATIONS

CHEM: Chemical tests to assess corrosivity
COMP: Compaction test
CONS: One-dimensional consolidation test
LL: Liquid Limit, percent
PI: Plasticity Index, percent
SA: Sieve analysis (percent passing No. 200 Sieve)
UC: Unconfined compressive strength test, Qu, in ksf
WA: Wash sieve (percent passing No. 200 Sieve)

MATERIAL GRAPHIC SYMBOLS

Lean CLAY, CLAY w/SAND, SANDY CLAY (CL)
Well graded GRAVEL (GW)
Clayey SAND (SC)

TYPICAL SAMPLER GRAPHIC SYMBOLS

Auger sampler
Bulk Sample
3-inch-OD California w/ brass rings
CME Sampler
Grab Sample
2.5-inch-OD Modified California w/ brass liners
Pitcher Sample
2-inch-OD unlined split spoon (SPT)
Shelby Tube (Thin-walled, fixed head)

OTHER GRAPHIC SYMBOLS

Water level (at time of drilling, ATD)
Water level (after waiting)
Minor change in material properties within a stratum
Inferred/gradational contact between strata
Queried contact between strata

GENERAL NOTES

1: Soil classifications are based on the Unified Soil Classification System. Descriptions and stratum lines are interpretive, and actual lithologic changes may be gradual. Field descriptions may have been modified to reflect results of lab tests.
2: Descriptions on these logs apply only at the specific boring locations and at the time the borings were advanced. They are not warranted to be representative of subsurface conditions at other locations or times.

J:\Projects\0034 Peralta\Berkeley City College Milvia Site\Technical\Boring Logs\Milvia Boring 3.bg4f(master 0 lab).tpl

Figure B-1

APPENDIX C

Geotechnical Laboratory Testing Data

B. HILLEBRANDT SOILS TESTING, INC.

29 Sugarloaf Terrace, Alamo, CA 94507 - Tel: (510) 409-2816 - Fax: (925) 891-9267 - Email: soiltesting@aol.com

LAB RESULTS SUMMARY FORM

Project Number: 1185-1A **Project Name:** Berkeley City College **Results Due By:**
Requested By: DB **Request Date:** 8/17/21 **Throw Samples Out On:**

					Atterberg			-200			Compaction				
Boring #	Sample Depth (feet)	Dry Density (pcf)	Moisture Content (%)	TxUU Shear Strength (psf)	Liquid Limit	Plastic Limit	Plasicity Index	Passing #4 Sieve (%)	Passing #40 sieve (%)	Passing #200 sieve (%)	Maximum Dry Density (pcf)	Optimum Moisture (%)	Pocket Penetrometer (tsf)	Torvane (tsf)	Remarks
B-1	2.5 - 3.0		28.5		48	20	28	99	88	67					
B-1	5.5 - 6.0	92	18.0					66	47	29					
B-1	16.0 - 16.5	120	12.5					49	24	15					
B-1	25.0 - 26.5		15.5					54	30	16					
B-1	35.0 - 36.0		21.9		25	14	11	98	94	52					
B-1	41.0 - 41.5	110	18.7		24	14	10	94	85	36					
B-1	46.0 - 46.5	95	28.7					94	78	52					
B-2	5.75 - 6.25		21.7		51	22	29	98	89	64					

B. HILLEBRANDT SOILS TESTING, INC.

29 Sugarloaf Terrace, Alamo, CA 94507 - Tel: (510) 409-2916 - Fax: (925) 891-9267 - Email: soiltesting@aol.com

MOISTURE CONTENT/DRY DENSITY

Job #: 1185-1A
Job Name: Berkeley City College
Date: 8/17/21
Tested by: Brad Hillebrandt

Additional Tests:	FS	FS	PI, FS	FS		
Boring #:	B-1	B-1	B-1	B-1		
Depth:	5.5 - 6.0	16.0 - 16.5	41.0 - 41.5	46.0 - 46.5		
Sample Description:	Dark brown clayey SAND with gravel	Brown clayey GRAVEL with sand	Olive brown clayey SAND	Dark yellowish brown sandy CLAY		
Can #:	414	B-13	357	386		
Wet Sample + can	264.6	879.8	270.8	278.0		
Dry Sample + can	229.3	807.6	233.2	223.3		
Weight can	33.1	227.7	32.4	32.8		
Weight water	35.3	72.2	37.6	54.7		
Weight Dry Sample	196.2	579.9	200.8	190.5		
WATER CONTENT (%)	**18.0%**	**12.5%**	**18.7%**	**28.7%**		
Weight Sample + Liner	1024.1	1228.7	1188.1	1137.8		
Weight Liner	280.3	274.0	274.3	275.4		
Sample Length	5.8	6.0	5.95	6.0		
Sample Diameter	2.39	2.39	2.39	2.39		
DRY DENSITY (pcf)	**92.3**	**120.2**	**109.8**	**94.8**		

B. HILLEBRANDT SOILS TESTING, INC.

29 Sugarloaf Terrace, Alamo, CA 94507 - Tel: (510) 409-2916 - Fax: (925) 891-9267 - Email: soiltesting@aol.com

MOISTURE CONTENT WORKSHEET

Job #: 1185-1A
Job Name: Berkeley City College
Date: 8/17/21
Tested by: B. Hillebrandt

Additional Tests:	PI, FS	FS	PI, FS	PI, FS					
Boring #:	B-1	B-1	B-1	B-2					
Depth:	2.5 - 3.0	25.0 - 26.5	35.0 - 36.0	5.75 - 6.25					
Sample Description:	Black sandy lean CLAY	Brown clayey GRAVEL with sand	Olive brown sandy lean CLAY	Very dark brown sandy CLAY					
Can #:	424	311	390	427					
Wet Sample + can	231.0	422.2	267.0	226.0					
Dry Sample + can	187.0	370.8	224.9	191.6					
Weight can	32.8	39.5	32.5	32.8					
Weight water	44	51.4	42.1	34.4					
Weight Dry Sample	154.2	331.3	192.4	158.8					
WATER CONTENT (%)	**28.5%**	**15.5%**	**21.9%**	**21.7%**					

LIQUID AND PLASTIC LIMITS TEST REPORT

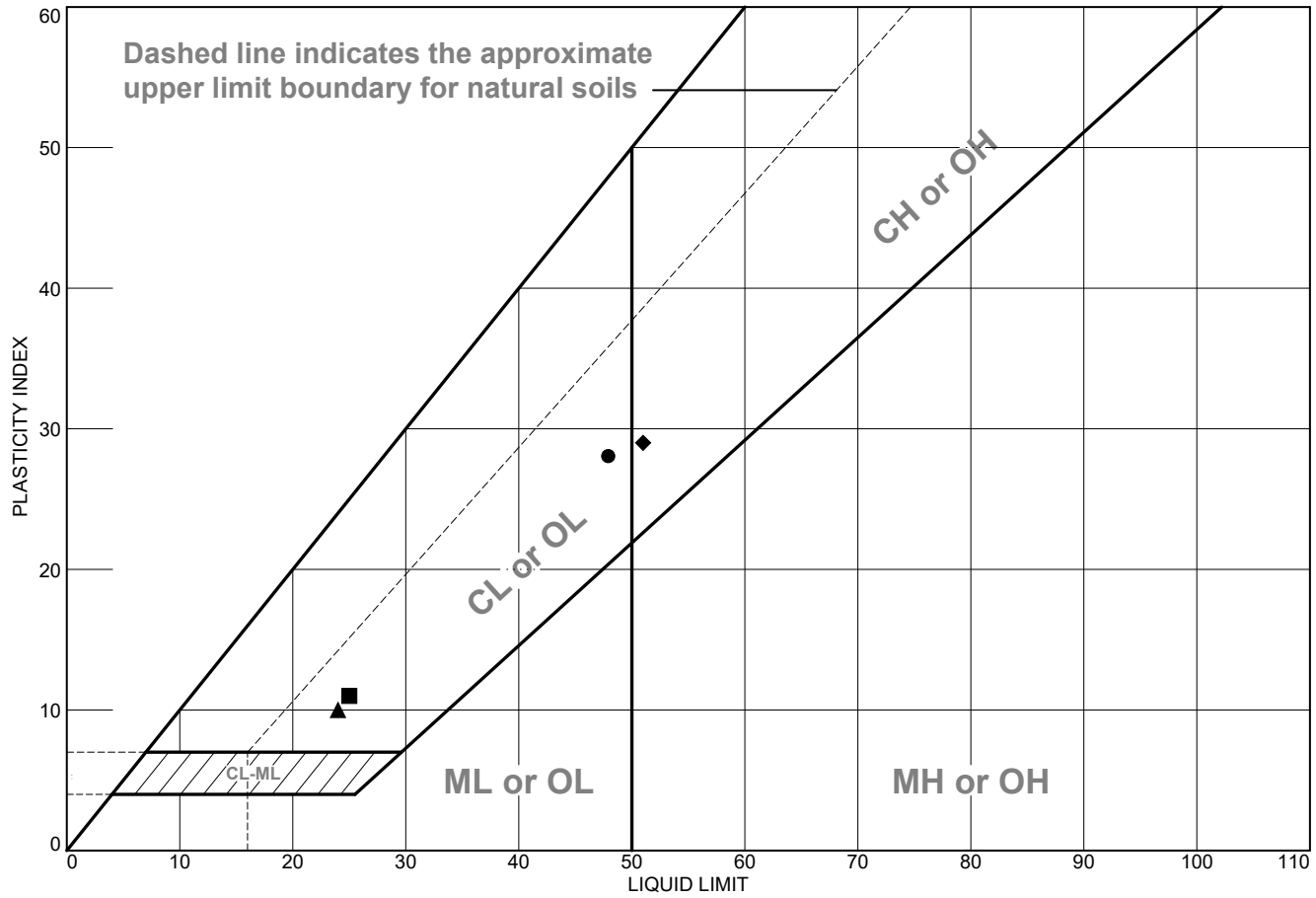

	MATERIAL DESCRIPTION	LL	PL	PI	%<#40	%<#200	USCS
●	Black sandy lean CLAY	48	20	28	88.3	67.4	CL
■	Olive brown sandy lean CLAY	25	14	11	93.6	51.8	CL
▲	Olive brown clayey SAND	24	14	10	84.5	36.2	SC
◆		51	22	29	88.5	63.6	CH

Project No. 1185-1A **Client:** A3Geo

Project: Berkeley City College

Remarks:

●**Source of Sample:** B-1 **Depth:** 2.5 - 3.0' **Sample Number:** 1

■**Source of Sample:** B-1 **Depth:** 35.0 - 36.0' **Sample Number:** 9A

▲**Source of Sample:** B-1 **Depth:** 41.0 - 41.5' **Sample Number:** 10C

◆**Source of Sample:** B-2 **Depth:** 5.75 - 6.25' **Sample Number:** 4

B. HILLEBRANDT SOILS TESTING, INC.
+1 510-409-2816
SoilTesting@aol.com

Figure

Tested By: BH

LIQUID AND PLASTIC LIMIT TEST DATA

9/3/2021

Client: A3Geo
Project: Berkeley City College
Project Number: 1185-1A
Location: B-1
Depth: 2.5 - 3.0' **Sample Number:** 1
Material Description: Black sandy lean CLAY
%<#40: 88.3 **%<#200:** 67.4 **USCS:** CL **AASHTO:** A-7-6(17)
Tested by: BH

Liquid Limit Data

Run No.	1	2	3	4	5	6
Wet+Tare	28.11	28.71	30.23			
Dry+Tare	22.78	23.04	23.84			
Tare	11.35	11.32	11.30			
# Blows	30	23	17			
Moisture	46.6	48.4	51.0			

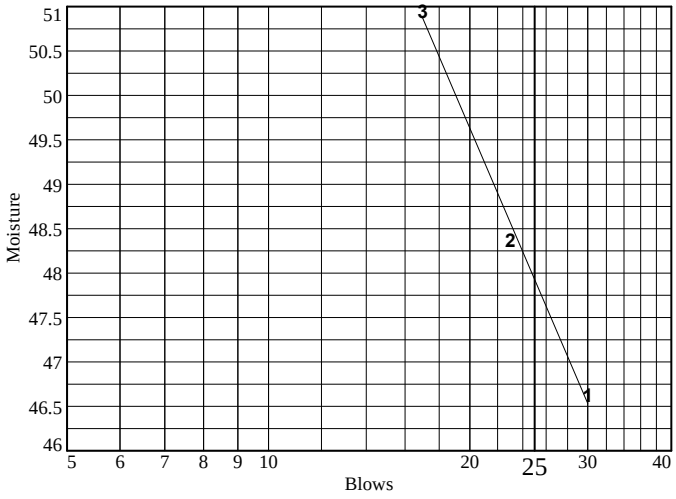

Liquid Limit= 48
Plastic Limit= 20
Plasticity Index= 28
Natural Moisture= 28.5
Liquidity Index= 0.3

Plastic Limit Data

Run No.	1	2	3	4	
Wet+Tare	18.06	17.74			
Dry+Tare	16.89	16.62			
Tare	11.23	11.10			
Moisture	20.7	20.3			

LIQUID AND PLASTIC LIMIT TEST DATA

9/3/2021

Client: A3Geo
Project: Berkeley City College
Project Number: 1185-1A
Location: B-1
Depth: 35.0 - 36.0' **Sample Number:** 9A
Material Description: Olive brown sandy lean CLAY
%<#40: 93.6 **%<#200:** 51.8 **USCS:** CL **AASHTO:** A-6(2)
Tested by: BH

Liquid Limit Data

Run No.	1	2	3	4	5	6
Wet+Tare	28.32	26.92	27.97			
Dry+Tare	24.98	23.76	24.50			
Tare	11.05	11.07	11.05			
# Blows	32	25	19			
Moisture	24.0	24.9	25.8			

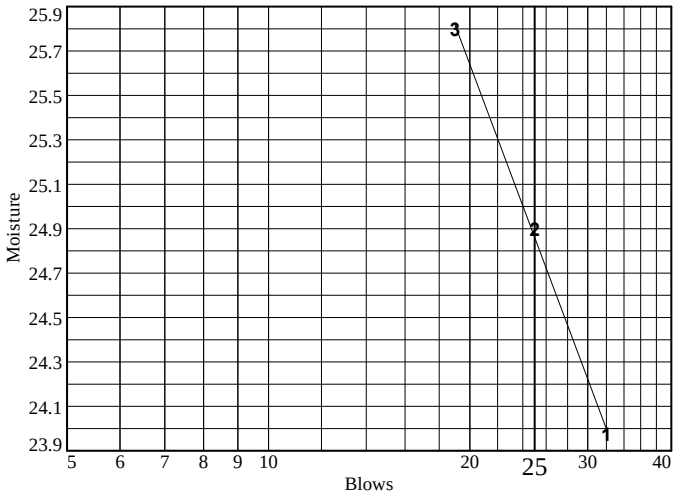

Liquid Limit= 25
Plastic Limit= 14
Plasticity Index= 11
Natural Moisture= 21.9
Liquidity Index= 0.7

Plastic Limit Data

Run No.	1	2	3	4	
Wet+Tare	18.99	17.58			
Dry+Tare	18.08	16.78			
Tare	11.38	11.09			
Moisture	13.6	14.1			

LIQUID AND PLASTIC LIMIT TEST DATA

9/3/2021

Client: A3Geo
Project: Berkeley City College
Project Number: 1185-1A
Location: B-1
Depth: 41.0 - 41.5' **Sample Number:** 10C
Material Description: Olive brown clayey SAND
%<#40: 84.5 **%<#200:** 36.2 **USCS:** SC **AASHTO:** A-4(0)
Tested by: BH

Liquid Limit Data

Run No.	1	2	3	4	5	6
Wet+Tare	26.21	28.18	25.40			
Dry+Tare	23.29	24.82	22.51			
Tare	11.11	11.16	11.15			
# Blows	27	21	16			
Moisture	24.0	24.6	25.4			

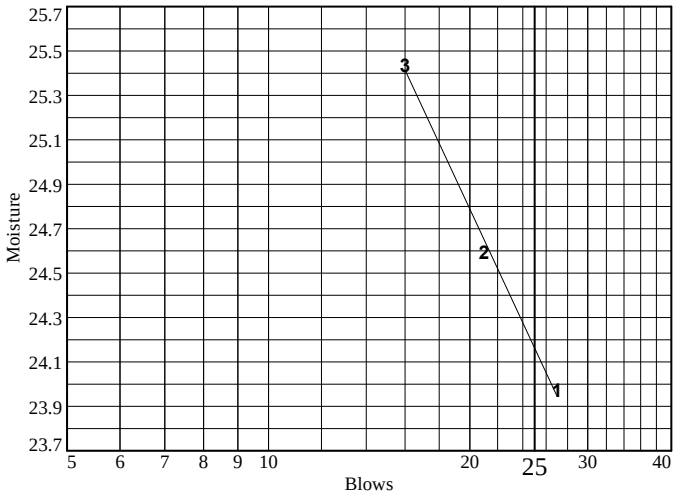

Liquid Limit= 24
Plastic Limit= 14
Plasticity Index= 10
Natural Moisture= 18.7
Liquidity Index= 0.5

Plastic Limit Data

Run No.	1	2	3	4	
Wet+Tare	20.53	19.46			
Dry+Tare	19.35	18.44			
Tare	11.42	11.03			
Moisture	14.9	13.8			

LIQUID AND PLASTIC LIMIT TEST DATA

9/3/2021

Client: A3Geo
Project: Berkeley City College
Project Number: 1185-1A
Location: B-2
Depth: 5.75 - 6.25'
Sample Number: 4
%<#40: 88.5
%<#200: 63.6
USCS: CH
AASHTO: A-7-6(17)
Tested by: BH

Liquid Limit Data

Run No.	1	2	3	4	5	6
Wet+Tare	26.94	28.31	27.07			
Dry+Tare	21.69	22.55	21.66			
Tare	11.12	11.25	11.36			
# Blows	31	26	20			
Moisture	49.7	51.0	52.5			

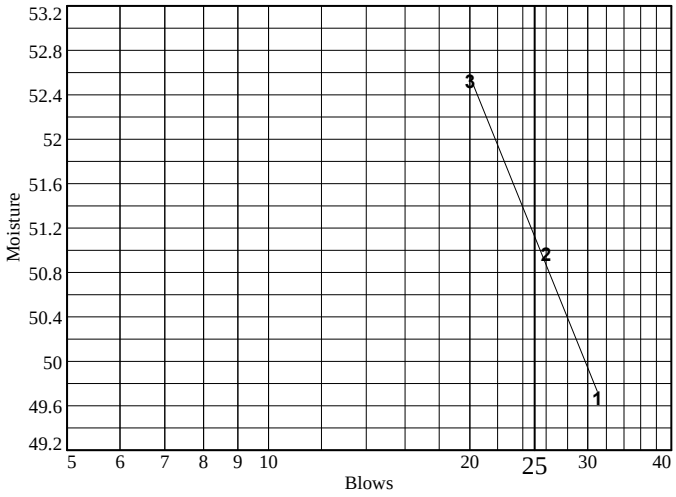

Liquid Limit= 51
Plastic Limit= 22
Plasticity Index= 29
Natural Moisture= 21.7
Liquidity Index= 0.0

Plastic Limit Data

Run No.	1	2	3	4	
Wet+Tare	17.98	17.41			
Dry+Tare	16.75	16.33			
Tare	11.11	11.24			
Moisture	21.8	21.2			

Particle Size Distribution Report

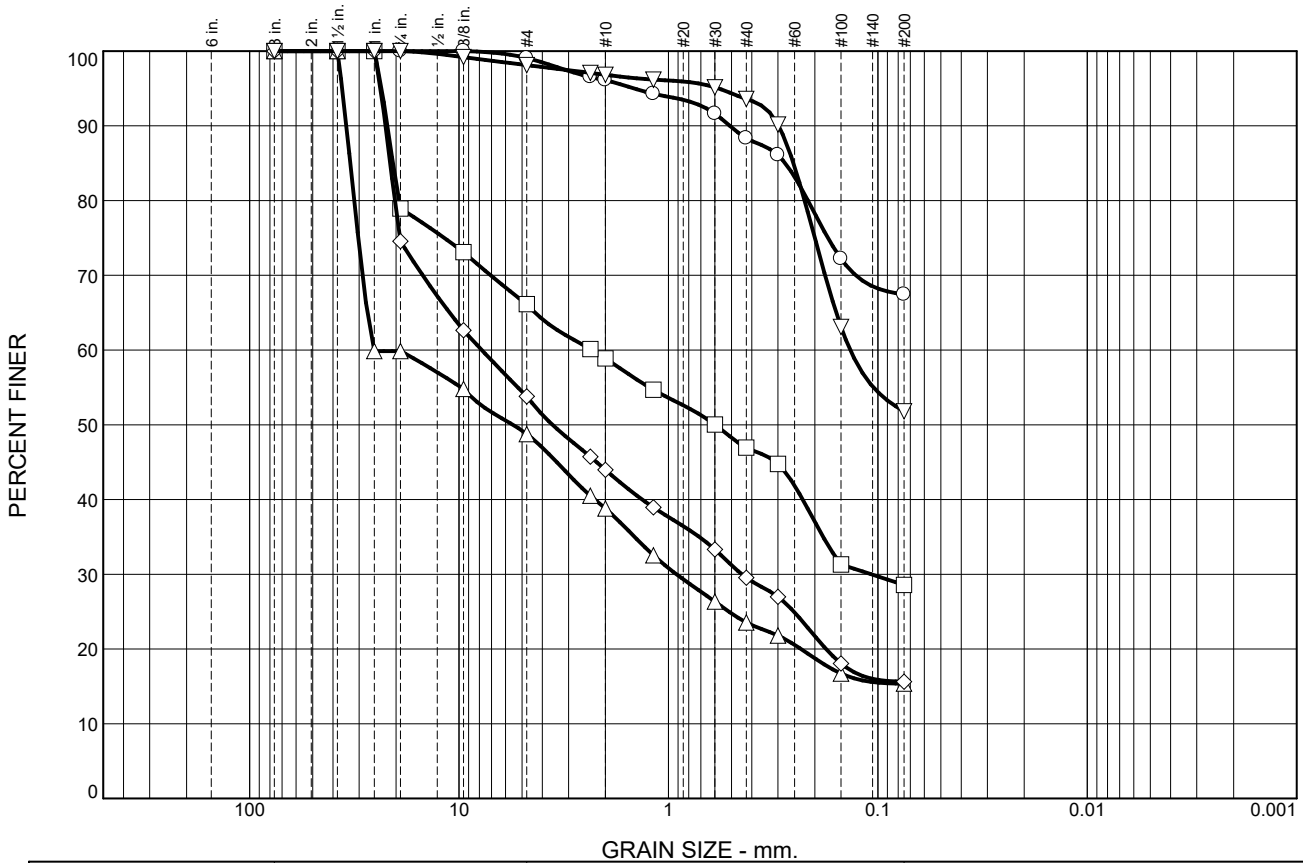

	% +3"	% Gravel		% Sand			% Fines	
		Coarse	Fine	Coarse	Medium	Fine	Silt	Clay
○	0.0	0.0	0.9	3.0	7.8	20.9	67.4	
□	0.0	21.1	12.8	7.2	11.9	18.4	28.6	
△	0.0	40.1	11.1	10.0	15.2	8.2	15.4	
◇	0.0	25.4	20.8	9.8	14.5	13.9	15.6	
▽	0.0	0.0	1.9	1.3	3.2	41.8	51.8	

SOIL DATA

SYMBOL	SOURCE	SAMPLE NO.	DEPTH (ft.)	Material Description	USCS
○	B-1	1	2.5 - 3.0'	Black sandy lean CLAY	CL
□	B-1	2A	5.5 - 6.0'	Dark brown clayey SAND with gravel	SC
△	B-1	5B	16.0 - 16.5'	Brown clayey GRAVEL with sand	GC
◇	B-1	7	25.0 - 26.5'	Brown clayey GRAVEL with sand	GC
▽	B-1	9A	35.0 - 36.0'	Olive brown sandy lean CLAY	CL

B. HILLEBRANDT SOILS TESTING, INC.
+1 510-409-2816
SoilTesting@aol.com

Client: A3Geo
Project: Berkeley City College
Project No.: 1185-1A **Figure**

Tested By: BH

Particle Size Distribution Report

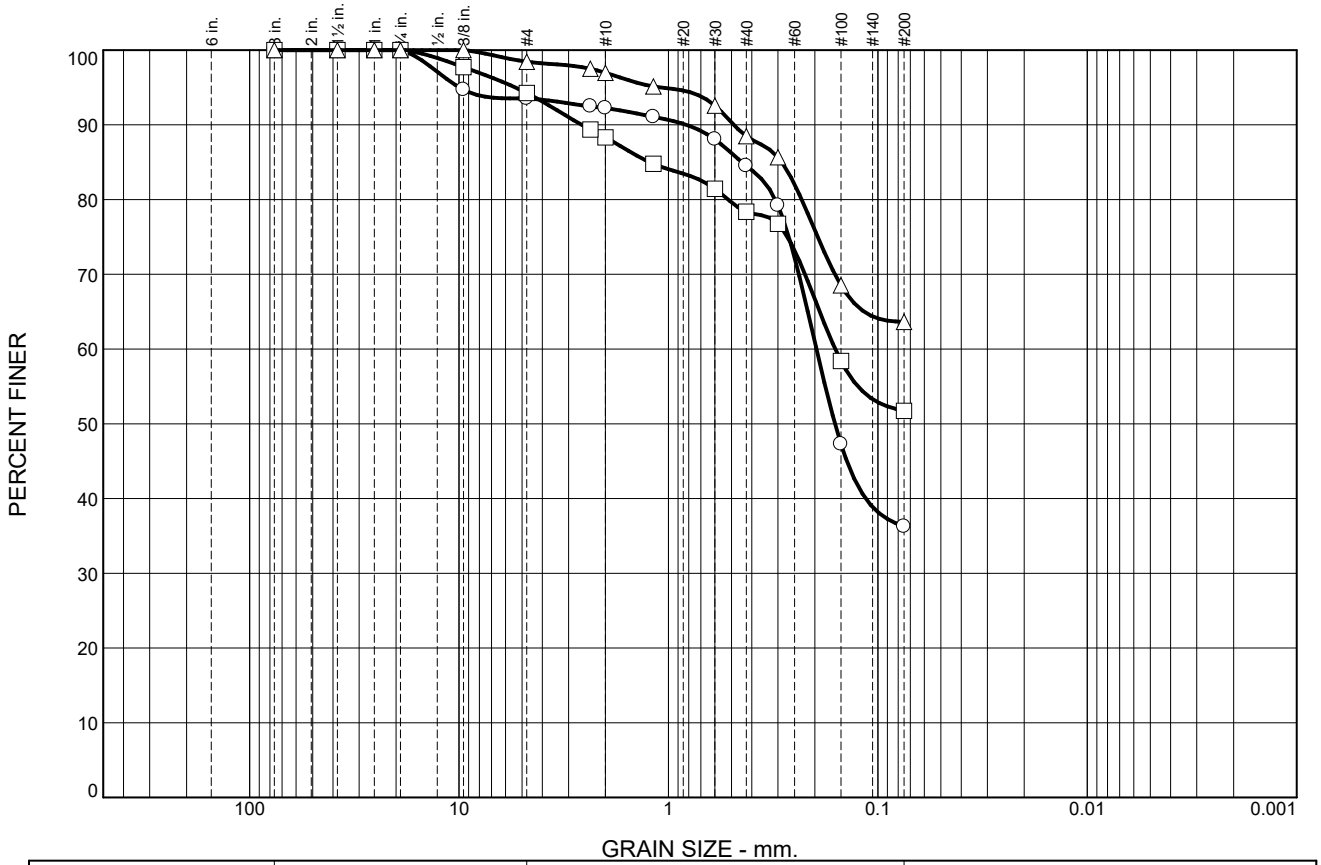

	% +3"	% Gravel		% Sand			% Fines	
		Coarse	Fine	Coarse	Medium	Fine	Silt	Clay
○	0.0	0.0	6.5	1.3	7.7	48.3	36.2	
□	0.0	0.0	5.7	6.0	9.9	26.7	51.7	
△	0.0	0.0	1.6	1.4	8.5	24.9	63.6	

SOIL DATA

SYMBOL	SOURCE	SAMPLE NO.	DEPTH (ft.)	Material Description	USCS
○	B-1	10C	41.0 - 41.5'	Olive brown clayey SAND	SC
□	B-1	11C	46.0 - 46.5'	Dark yellowish brown sandy CLAY	CL
△	B-2	4	5.75 - 6.25'		CH

B. HILLEBRANDT SOILS TESTING, INC.
+1 510-409-2816
SoilTesting@aol.com

Client: A3Geo
Project: Berkeley City College
Project No.: 1185-1A **Figure**

Tested By: BH

GRAIN SIZE DISTRIBUTION TEST DATA

9/3/2021

Client: A3Geo
Project: Berkeley City College
Project Number: 1185-1A
Location: B-1
Depth: 2.5 - 3.0' **Sample Number:** 1
Material Description: Black sandy lean CLAY
USCS: CL
Tested by: BH

Sieve Test Data

Dry Sample and Tare (grams)	Tare (grams)	Cumulative Pan Tare Weight (grams)	Sieve Opening Size	Cumulative Weight Retained (grams)	Percent Finer
187.00	32.80	0.00	3"	0.00	100.0
			1.5"	0.00	100.0
			1.0"	0.00	100.0
			3/4"	0.00	100.0
			3/8"	0.00	100.0
			#4	1.44	99.1
			#8	5.34	96.5
			#10	6.00	96.1
			#16	8.81	94.3
			#30	12.91	91.6
			#40	17.97	88.3
			#50	21.46	86.1
			#100	42.85	72.2
			#200	50.23	67.4

Fractional Components

Cobbles	Gravel			Sand				Fines		
	Coarse	Fine	Total	Coarse	Medium	Fine	Total	Silt	Clay	Total
0.0	0.0	0.9	0.9	3.0	7.8	20.9	31.7			67.4

D_5	D_{10}	D_{15}	D_{20}	D_{30}	D_{40}	D_{50}	D_{60}	D_{80}	D_{85}	D_{90}	D_{95}
								0.2157	0.2770	0.5090	1.4574

Fineness Modulus
0.60

GRAIN SIZE DISTRIBUTION TEST DATA

9/3/2021

Client: A3Geo
Project: Berkeley City College
Project Number: 1185-1A
Location: B-1
Depth: 5.5 - 6.0' **Sample Number:** 2A
Material Description: Dark brown clayey SAND with gravel
USCS: SC
Tested by: BH

Sieve Test Data

Dry Sample and Tare (grams)	Tare (grams)	Cumulative Pan Tare Weight (grams)	Sieve Opening Size	Cumulative Weight Retained (grams)	Percent Finer
229.30	33.10	0.00	3"	0.00	100.0
			1.5"	0.00	100.0
			1.0"	0.00	100.0
			3/4"	41.33	78.9
			3/8"	52.76	73.1
			#4	66.43	66.1
			#8	78.21	60.1
			#10	80.68	58.9
			#16	88.90	54.7
			#30	98.02	50.0
			#40	104.08	47.0
			#50	108.37	44.8
			#100	134.76	31.3
			#200	140.13	28.6

Fractional Components

Cobbles	Gravel			Sand				Fines		
	Coarse	Fine	Total	Coarse	Medium	Fine	Total	Silt	Clay	Total
0.0	21.1	12.8	33.9	7.2	11.9	18.4	37.5			28.6

D_5	D_{10}	D_{15}	D_{20}	D_{30}	D_{40}	D_{50}	D_{60}	D_{80}	D_{85}	D_{90}	D_{95}
				0.1075	0.2284	0.5973	2.3155	19.3548	20.6778	21.9838	23.4380

Fineness Modulus
3.41

GRAIN SIZE DISTRIBUTION TEST DATA

9/3/2021

Client: A3Geo
Project: Berkeley City College
Project Number: 1185-1A
Location: B-1
Depth: 16.0 - 16.5'
Sample Number: 5B
Material Description: Brown clayey GRAVEL with sand
USCS: GC
Tested by: BH

Sieve Test Data

Dry Sample and Tare (grams)	Tare (grams)	Cumulative Pan Tare Weight (grams)	Sieve Opening Size	Cumulative Weight Retained (grams)	Percent Finer
807.60	227.70	0.00	3"	0.00	100.0
			1.5"	0.00	100.0
			1.0"	232.74	59.9
			3/4"	232.74	59.9
			3/8"	262.11	54.8
			#4	297.17	48.8
			#8	344.99	40.5
			#10	354.88	38.8
			#16	391.19	32.5
			#30	427.13	26.3
			#40	443.32	23.6
			#50	453.45	21.8
			#100	482.95	16.7
			#200	490.75	15.4

Fractional Components

Cobbles	Gravel			Sand				Fines		
	Coarse	Fine	Total	Coarse	Medium	Fine	Total	Silt	Clay	Total
0.0	40.1	11.1	51.2	10.0	15.2	8.2	33.4			15.4

D_5	D_{10}	D_{15}	D_{20}	D_{30}	D_{40}	D_{50}	D_{60}	D_{80}	D_{85}	D_{90}	D_{95}
			0.2327	0.9158	2.2478	5.5300	25.4697	31.6510	33.0388	34.5129	36.1499

Fineness Modulus
4.99

GRAIN SIZE DISTRIBUTION TEST DATA

9/3/2021

Client: A3Geo
Project: Berkeley City College
Project Number: 1185-1A
Location: B-1
Depth: 25.0 - 26.5' **Sample Number:** 7
Material Description: Brown clayey GRAVEL with sand
USCS: GC
Tested by: BH

Sieve Test Data

Dry Sample and Tare (grams)	Tare (grams)	Cumulative Pan Tare Weight (grams)	Sieve Opening Size	Cumulative Weight Retained (grams)	Percent Finer
370.80	39.50	0.00	3"	0.00	100.0
			1.5"	0.00	100.0
			1.0"	0.00	100.0
			3/4"	84.27	74.6
			3/8"	123.75	62.6
			#4	153.04	53.8
			#8	179.79	45.7
			#10	185.61	44.0
			#16	202.25	39.0
			#30	220.90	33.3
			#40	233.43	29.5
			#50	241.89	27.0
			#100	271.46	18.1
			#200	279.52	15.6

Fractional Components

Cobbles	Gravel			Sand				Fines		
	Coarse	Fine	Total	Coarse	Medium	Fine	Total	Silt	Clay	Total
0.0	25.4	20.8	46.2	9.8	14.5	13.9	38.2			15.6

D_5	D_{10}	D_{15}	D_{20}	D_{30}	D_{40}	D_{50}	D_{60}	D_{80}	D_{85}	D_{90}	D_{95}
			0.1768	0.4464	1.3346	3.5781	7.7845	20.2509	21.3147	22.4307	23.7018

Fineness Modulus
4.46

GRAIN SIZE DISTRIBUTION TEST DATA

9/3/2021

Client: A3Geo
Project: Berkeley City College
Project Number: 1185-1A
Location: B-1
Depth: 35.0 - 36.0' **Sample Number:** 9A
Material Description: Olive brown sandy lean CLAY
USCS: CL
Tested by: BH

Sieve Test Data

Dry Sample and Tare (grams)	Tare (grams)	Cumulative Pan Tare Weight (grams)	Sieve Opening Size	Cumulative Weight Retained (grams)	Percent Finer
224.90	32.50	0.00	3"	0.00	100.0
			1.5"	0.00	100.0
			1.0"	0.00	100.0
			3/4"	0.00	100.0
			3/8"	1.54	99.2
			#4	3.61	98.1
			#8	5.61	97.1
			#10	6.10	96.8
			#16	7.35	96.2
			#30	9.32	95.2
			#40	12.33	93.6
			#50	18.90	90.2
			#100	71.00	63.1
			#200	92.74	51.8

Fractional Components

Cobbles	Gravel			Sand				Fines		
	Coarse	Fine	Total	Coarse	Medium	Fine	Total	Silt	Clay	Total
0.0	0.0	1.9	1.9	1.3	3.2	41.8	46.3			51.8

D_5	D_{10}	D_{15}	D_{20}	D_{30}	D_{40}	D_{50}	D_{60}	D_{80}	D_{85}	D_{90}	D_{95}
							0.1355	0.2237	0.2531	0.2977	0.5767

Fineness Modulus
0.61

GRAIN SIZE DISTRIBUTION TEST DATA

9/3/2021

Client: A3Geo
Project: Berkeley City College
Project Number: 1185-1A
Location: B-1
Depth: 41.0 - 41.5'
Sample Number: 10C
Material Description: Olive brown clayey SAND
USCS: SC
Tested by: BH

Sieve Test Data

Dry Sample and Tare (grams)	Tare (grams)	Cumulative Pan Tare Weight (grams)	Sieve Opening Size	Cumulative Weight Retained (grams)	Percent Finer
233.20	32.40	0.00	3"	0.00	100.0
			1.5"	0.00	100.0
			1.0"	0.00	100.0
			3/4"	0.00	100.0
			3/8"	10.64	94.7
			#4	13.02	93.5
			#8	15.12	92.5
			#10	15.59	92.2
			#16	17.94	91.1
			#30	23.99	88.1
			#40	31.10	84.5
			#50	41.73	79.2
			#100	105.89	47.3
			#200	128.01	36.2

Fractional Components

Cobbles	Gravel			Sand				Fines		
	Coarse	Fine	Total	Coarse	Medium	Fine	Total	Silt	Clay	Total
0.0	0.0	6.5	6.5	1.3	7.7	48.3	57.3			36.2

D_5	D_{10}	D_{15}	D_{20}	D_{30}	D_{40}	D_{50}	D_{60}	D_{80}	D_{85}	D_{90}	D_{95}
					0.1143	0.1603	0.1964	0.3088	0.4462	0.8205	9.9605

Fineness Modulus
1.14

GRAIN SIZE DISTRIBUTION TEST DATA

9/3/2021

Client: A3Geo
Project: Berkeley City College
Project Number: 1185-1A
Location: B-1
Depth: 46.0 - 46.5' **Sample Number:** 11C
Material Description: Dark yellowish brown sandy CLAY
USCS: CL
Tested by: BH

Sieve Test Data

Dry Sample and Tare (grams)	Tare (grams)	Cumulative Pan Tare Weight (grams)	Sieve Opening Size	Cumulative Weight Retained (grams)	Percent Finer
223.30	32.80	0.00	3"	0.00	100.0
			1.5"	0.00	100.0
			1.0"	0.00	100.0
			3/4"	0.00	100.0
			3/8"	4.35	97.7
			#4	10.93	94.3
			#8	20.25	89.4
			#10	22.25	88.3
			#16	28.99	84.8
			#30	35.35	81.4
			#40	41.20	78.4
			#50	44.28	76.8
			#100	79.24	58.4
			#200	91.95	51.7

Fractional Components

Cobbles	Gravel			Sand				Fines		
	Coarse	Fine	Total	Coarse	Medium	Fine	Total	Silt	Clay	Total
0.0	0.0	5.7	5.7	6.0	9.9	26.7	42.6			51.7

D_5	D_{10}	D_{15}	D_{20}	D_{30}	D_{40}	D_{50}	D_{60}	D_{80}	D_{85}	D_{90}	D_{95}
							0.1599	0.5185	1.2291	2.5939	5.3806

Fineness Modulus
1.17

GRAIN SIZE DISTRIBUTION TEST DATA

9/3/2021

Client: A3Geo
Project: Berkeley City College
Project Number: 1185-1A
Location: B-2
Depth: 5.75 - 6.25'
Sample Number: 4
USCS: CH
Tested by: BH

Sieve Test Data

Dry Sample and Tare (grams)	Tare (grams)	Cumulative Pan Tare Weight (grams)	Sieve Opening Size	Cumulative Weight Retained (grams)	Percent Finer
191.60	32.80	0.00	3"	0.00	100.0
			1.5"	0.00	100.0
			1.0"	0.00	100.0
			3/4"	0.00	100.0
			3/8"	0.00	100.0
			#4	2.48	98.4
			#8	3.96	97.5
			#10	4.83	97.0
			#16	7.72	95.1
			#30	11.80	92.6
			#40	18.29	88.5
			#50	22.77	85.7
			#100	50.00	68.5
			#200	57.74	63.6

Fractional Components

Cobbles	Gravel			Sand				Fines		
	Coarse	Fine	Total	Coarse	Medium	Fine	Total	Silt	Clay	Total
0.0	0.0	1.6	1.6	1.4	8.5	24.9	34.8			63.6

D_5	D_{10}	D_{15}	D_{20}	D_{30}	D_{40}	D_{50}	D_{60}	D_{80}	D_{85}	D_{90}	D_{95}
								0.2311	0.2876	0.4873	1.0912

Fineness Modulus
0.62

Consolidation Test
ASTM D2435

Job No.:	748-049	**Boring:**	B-1	**Run By:**	MD
Client:	A3GEO	**Sample:**	3	**Reduced:**	PJ
Project:	1185-1A	**Depth, ft.:**	7-9(Tip-3")	**Checked:**	PJ/DC
Soil Type:	Brown Sandy Lean CLAY			**Date:**	9/8/2021

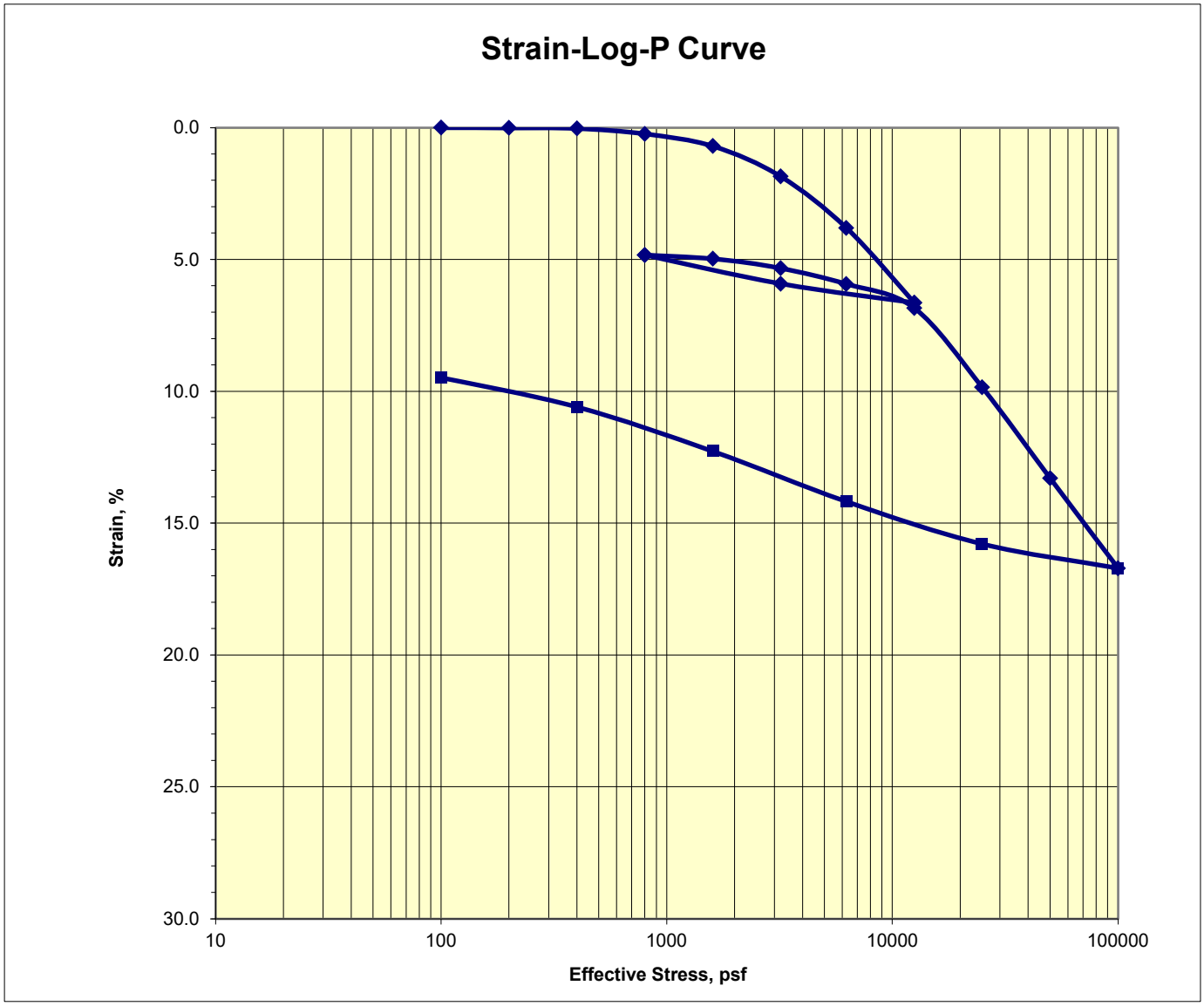

Assumed Gs 2.75	Initial	Final
Moisture %:	21.3	18.7
Dry Density, pcf:	103.3	113.4
Void Ratio:	0.661	0.514
% Saturation:	88.7	100.0

Remarks:

Cooper Testing Labs, Inc.
937 Commercial Street
Palo Alto, CA 94303

Unconsolidated-Undrained Triaxial Test
ASTM D2850

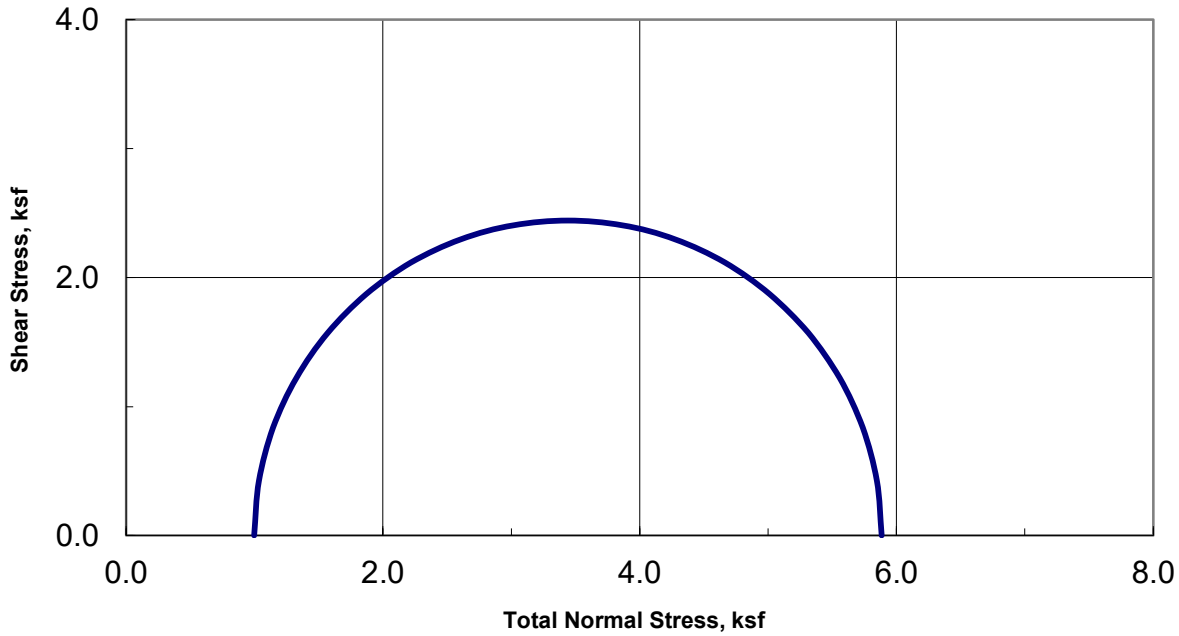

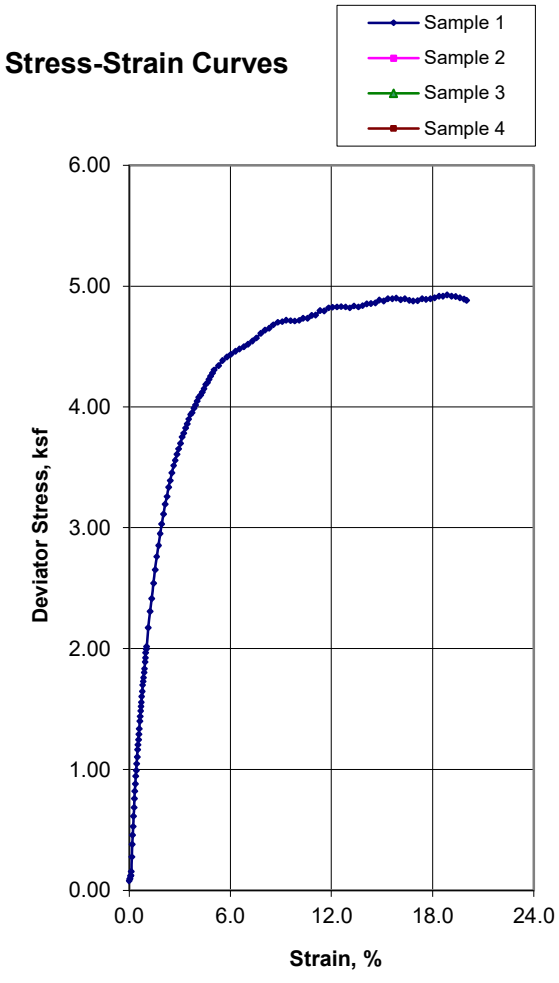

Sample Data	1	2	3	4
Moisture %	19.0			
Dry Den,pcf	107.8			
Void Ratio	0.563			
Saturation %	90.9			
Height in	5.99			
Diameter in	2.88			
Cell psi	6.9			
Strain %	15.00			
Deviator, ksf	4.886			
Rate %/min	1.00			
in/min	0.060			
Job No.:	748-049			
Client:	A3GEO			
Project:	1185-1A			
Boring:	B-1			
Sample:	3			
Depth ft:	7-9(Tip-4")			

Visual Soil Description	
Sample #	
1	Brown Sandy Lean CLAY
2	
3	
4	

Remarks:

Note: Strengths are picked at the peak deviator stress or 15% strain which ever occurs first per ASTM D2850.

Corrosivity Test Summary

CTL # 748-049 **Date:** 8/27/2021 **Tested By:** PJ **Checked:** PJ

Client: A3Geo **Project:** Berkeley City College **Proj. No:** 1185-1A

Remarks:

Sample Location or ID			Resistivity @ 15.5 °C (Ohm-cm)			Chloride	Sulfate		pH	ORP	Moisture	Soil Visual Description
Boring	Sample, No.	Depth, ft.	As Rec.	Minimum	Saturated	mg/kg	mg/kg	%		(Redox)	At Test	
						Dry Wt.	Dry Wt.	Dry Wt.		mv	%	
			ASTM G57	Cal 643	ASTM G57	Cal 422-mod.	Cal 417-mod.	Cal 417-mod.	Cal 643	SM 2580B	ASTM D2216	
B-2	3	3.75-4.25	-	940	-	10	278	0.0278	7.3	-	6.4	Black Sandy CLAY

APPENDIX D

Existing Building Foundation Plans

Typical E.W. for all 3¼ Std pipe columns in block walls
W 7.34 x 14.2
2 A.E. - 3¼ x 10

Provide 2 - #4 bars, full but welded to columns to match all band beam bars (TYPICAL)

14 x 14 tie beam (TYP)
4 - #4 bars
#2 ties @ 18 oc

S.A.D for depression

These footings 1'0 thick, bottom of footing 3'0 below floor elev. #4 w3.5x3.5 E.W. at bottom

Provide 3 #5 in each cell in these walls

Note: 8" conc. block wall across not on modulation this line. S.A.D.

FLOOR AND FOUNDATION PLAN

OFFICE BUILDING
JAMES Y. SMITH inc
BERKELEY

L. L. FREELS and associates
2711 TELEGRAPH AVE BERKELEY
841-8809

APPENDIX E

Geophysical Data Report

REPORT

SURFACE WAVE MEASUREMENTS

BERKELEY COMMUNITY COLLEGE PROJECT
2118 MILVIA STREET
BERKELEY, CALIFORNIA

GEO*Vision* Project No. 21283

Prepared for

A3GEO, Inc.
821 Bancroft Way
Berkeley, California 94710
(510) 705-1664

Prepared by

GEO*Vision*, Inc.
1124 Olympic Drive
Corona, California 92881
(951) 549-1234

Report 21283-01 Rev 1

September 5, 2021

TABLE OF CONTENTS

LIST OF TABLES

LIST OF FIGURES

1 INTRODUCTION

In-situ seismic measurements using active- and passive-source surface wave techniques were performed at the property located at 2118 Milvia Street, Berkeley, California on August 23, 2021. The purpose of this investigation was to provide a shear (S) wave velocity profile to a depth of 200 ft, or greater, and estimate the average S-wave velocity of the upper 30 m (V_{S30}) and 100 ft (V_{S100ft}). The active-source surface wave technique utilized during this investigation consisted of the multi-channel analysis of surface waves (MASW) method. The passive-source surface wave technique consisted of the array microtremor and H/V spectral ratio (HVSR) techniques. The locations of the active- and passive-source surface wave testing locations are shown on Figure 1. Array microtremor measurements were made using a L-shaped array (Arrays 1 and 3) and MASW measurements were made along a short linear array near one leg of Array 1 (Array 2). An HVSR measurement was made in a parking lot south of the project site after an attempted measurement near the corner of Array 1 was unsuccessful.

V_{S30} is used in the NEHRP provisions and the Uniform Building Code (UBC) to separate sites into classes for earthquake engineering design (BSSC, 2009). V_{S100ft} is used in the International Building Code (IBC) for site classification. These site classes are as follows:

Class A – hard rock – $V_{S30} > 1500$ m/s (UBC) or $V_{S100ft} > 5{,}000$ ft/s (IBC)
Class B – rock – $760 < V_{S30} \leq 1500$ m/s (UBC) or $2{,}500 < V_{S100ft} \leq 5{,}000$ ft/s (IBC)
Class C – very dense soil and soft rock – $360 < V_{S30} \leq 760$ m/s (UBC)
or $1{,}200 < V_{S100ft} \leq 2{,}500$ ft/s (IBC)
Class D – stiff soil – $180 < V_{S30} \leq 360$ m/s (UBC) or $600 < V_{S100ft} \leq 1{,}200$ ft/s (IBC)
Class E – soft soil – $V_{S30} < 180$ m/s (UBC) or $V_{S100ft} < 600$ ft/s (IBC)
Class F – soils requiring site-specific evaluation

At many sites, active surface wave techniques (MASW) with the utilization of portable energy sources, such as hammers and weight drops, are sufficient to obtain S-wave velocity sounding to 30 m (100 ft) depth. At sites with high ambient noise levels and/or very soft soils, these energy sources may not be sufficient to image to this depth and a larger energy source, such as a bulldozer, is necessary. Alternatively, passive surface wave techniques, such as the array microtremor technique can be used to extend the depth of investigation at sites that have adequate ambient noise conditions. It should be noted that two-dimensional passive-source surface wave arrays (e.g., triangular, circular, or L-shaped arrays) are expected to perform better than linear arrays.

This report contains the results of the active and passive surface wave measurements conducted at the site. An overview of the surface wave methods is given in Section 2. Field and data reduction procedures are discussed in Sections 3 and 4, respectively. Data modeling is presented in Section 5 and interpretation and results are presented in Section 6. References and our professional certification are presented in Sections 7 and 8, respectively.

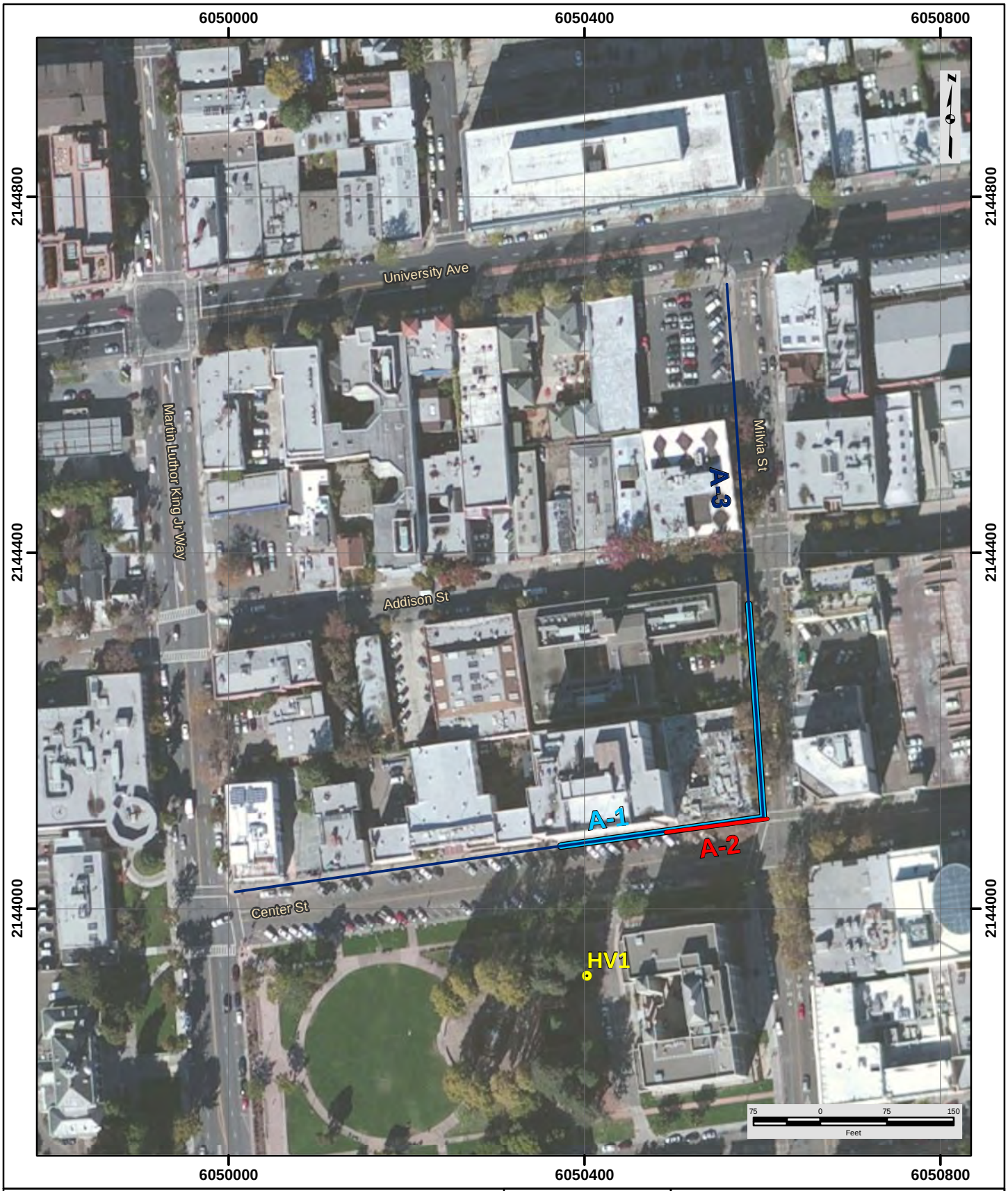

- Active Surface Wave Array (MASW)
- Passive Surface Wave Array (L-Array)
- Passive Surface Wave Array (L-Array)
- H/V Spectral Ratio Measurement Location

NOTES:
1. Coordinate System: California State Plane, NAD83, Zone III (0403), US Survey Feet
2. Base map source: Esri, DigitalGlobe, GeoEye, Earthstar Geographics, CNES/Airbus DS, USDA, USGS, AeroGRID, IGN, and the GIS User Community

GEOVision geophysical services

Date:	9/2/2021
GV Project:	21283
Developed by:	A Martin
Drawn by:	T Rodriguez
Approved by:	A Martin
File Name:	21283-1.MXD

FIGURE 1
SITE MAP

BERKELEY COMMUNITY COLLEGE PROJECT
2118 MILVIA STREET
BERKELEY, CALIFORNIA

PREPARED FOR
A3GEO, INC.

2 Overview of Surface Wave Techniques

2.1 Introduction

Active- and passive-source (ambient vibration) surface wave techniques are routinely utilized for site characterization. Active surface wave techniques include the spectral analysis of surface waves (SASW) and multi-channel array surface wave (MASW) methods. Passive surface wave techniques include the horizontal over vertical spectral ratio (HVSR) technique and the array refraction microtremor methods.

The basis of surface wave methods is the dispersive characteristic of Rayleigh and Love waves when propagating in a layered medium. Surface waves of different wavelengths (λ) or frequencies (f) sample different depth. As a result of the variance in the shear stiffness of the distinct layers, waves with different wavelengths propagate at different phase velocities; hence, dispersion. A surface wave dispersion curve is the variation of V_R or V_L with λ or f. The Rayleigh wave phase velocity (V_R) depends primarily on the material properties (V_S, mass density, and Poisson's ratio or compression wave velocity) over a depth of approximately one wavelength. The Love wave phase velocity (V_L) depends primarily on V_S and mass density. Rayleigh and Love wave propagation is also affected by damping or seismic quality factor (Q). Rayleigh wave techniques are utilized to measure vertically polarized S-waves (S_V-wave); whereas Love wave techniques are utilized to measure horizontally polarized S-waves (S_H-wave).

2.2 Surface Wave Techniques

The MASW and array microtremor techniques were utilized during this investigation and are discussed below. The MASW and array microtremor surveys were designed to measure Rayleigh wave propagation.

2.2.1 MASW Technique

A description of the MASW method is given by Park, 1999a and 1999b and Foti, 2000. Ground motions are typically recorded by 24, or more, geophones typically spaced 1 to 3 m apart along a linear array and connected to a seismograph. Energy sources for shallow investigations include various sized hammers and vehicle mounted weight drops. When applying the MASW technique to develop a one-dimensional (1-D) V_S model, the surface-wave data, preferably, are acquired using multiple-source offsets at both ends of the array. The most commonly applied MASW technique is the Rayleigh-wave based MASW method, which we refer to as MAS_RW to distinguish from Love-wave based MASW (MAS_LW). MAS_RW and MAS_LW acquisition can easily be combined with P- and S-wave seismic refraction acquisition, respectively. MAS_RW data are generally recorded using a vertical source and vertical geophone but may also be recorded using a horizontal geophone with radial (in-line) orientation. MAS_LW data are recorded using transversely orientated horizontal source and transverse horizontal geophone.

A wavefield transform is applied to the time-history data to convert the seismic record from time-offset space to frequency-wavenumber (f-k) space in which the fundamental or higher surface-wave modes can be easily identified as energy maxima and picked. Frequency and/or wavenumber can easily be mapped to phase velocity, slowness, or wavelength using the following properties: $k = 2\pi/\lambda$, $\lambda = v/f$. Common wave-field transforms include: the f-k

transform (a 2D fast Fourier transform), slant-stack transform (also referred to as intercept-slowness or τ-p transform and equivalent to linear Radon transform), frequency domain beamformer, and phase-shift transform. The minimum wavelength that can be recovered from an MASW data set without spatial aliasing is equal to the minimum receiver spacing. Occasionally, SASW analysis procedures are used to extract surface wave dispersion data, from fixed receiver pairs, at smaller wavelengths than can be recovered by wavefield transformation. Construction of a dispersion curve over the wide frequency/wavelength range necessary to develop a robust V_S model while also limiting the maximum wavelength based on an established near-field criterion (e.g. Yoon and Rix, 2009; Li and Rosenblad, 2011), generally requires multiple source offsets.

Although the clear majority of MASW surveys record Rayleigh waves, it has been shown that Love wave techniques can be more effective in some environments, particularly shallow rock sites and sites with a highly attenuative, low velocity surface layer (Xia, et al., 2012; **GEO***Vision*, 2012; Yong, et al., 2013; Martin, et al., 2014). Rayleigh wave techniques, however, are generally more effective at sites where velocity gradually increases with depth because larger energy sources are readily available for the generation of Rayleigh waves. Rayleigh wave techniques are also more applicable to sites with high velocity layers and/or velocity inversions because the presence of such structures is more apparent in the Rayleigh wave dispersion curves than in Love wave dispersion curves. Rayleigh wave techniques are preferable at sites with a high velocity surface layer because Love waves do not theoretically exist in such environments. Occasionally, the horizontal radial component of a Rayleigh wave may yield higher quality dispersion data than the vertical component because different modes of propagation may have more energy in one component than the other. Recording both the vertical and horizontal components of the Rayleigh wave is particularly useful at sites with complex modes of propagation or when attempting to recover multiple Rayleigh wave modes for multi-mode modeling as demonstrated in Dal Moro, et al, 2015. Joint inversion of Rayleigh and Love wave data may yield more accurate V_S models and also offer a means to investigate anisotropy, where S_V- and S_H-wave velocity are not equal, as shown in Dal Moro and Ferigo, 2011.

2.2.2 Array Microtremor Technique

A detailed discussion of the array microtremor method can be found in Okada, 2003. Unlike active source techniques which use an active energy source (i.e., hammer), the array microtremor technique (also referred to as passive surface wave or array ambient vibration method) records background noise (ambient vibrations) emanating from ocean wave activity, wind noise, traffic, industrial activity, construction, etc. The technique uses 4, or more, receivers aligned in a 2-dimensional array. Triangle, circle, semi-circle, and "L" shaped arrays are commonly used, although any 2-dimensional arrangement of receivers can be used. For the investigation of the upper 100 m, receivers typically consist of 1 to 4.5 Hz geophones. For deeper investigations, 5 to 120 s seismometers are generally utilized. The nested triangle array, which consists of several embedded equilateral triangles, is popular as it provides accurate dispersion curves with a relatively small number of geophones. The "L" array is useful at sites located at the corner of intersecting streets. The maximum receiver separation in an array should be at a minimum equal to the desired depth of investigation. Typically, 15 to 60 minutes of ambient vibration data is recorded depending on the size of the array, desired depth of investigation, and noise conditions. Investigations to depths on the order of 1 km may require that ambient vibrations are recorded for a much longer duration. The surface wave dispersion curve is typically estimated from array

microtremor data using various f-k methods such as beamforming (Lacoss, et al., 1969), and maximum-likelihood (Capon, 1969), and the spatial-autocorrelation (SPAC) method. The beam-forming and maximum-likelihood methods are generally referred to as the frequency wavenumber (FK) and high-resolution frequency wavenumber (HRFK or HFK) methods. The SPAC method was originally based on work by Aki, 1957 and has since been extended and modified (Ling and Okada, 1993 and Ohori *et al*., 2002) to permit the use of noncircular arrays, and is now collectively referred to as extended spatial autocorrelation (ESPAC or ESAC). Further modifications to the SPAC method permit the use of irregular or random arrays (Bettig *et al*., 2001). Although it is common to apply SPAC methods to obtain a surface wave dispersion curve for modeling, other approaches involve direct modeling of the coherency data, also referred to as SPAC coefficients (Asten, 2006 and Asten, *et al*., 2015).

FK and HRFK methods are generally expected to perform better when ambient vibration sources are not azimuthally well-distributed (e.g., rural area where the primary noise source is a large industrial facility). SPAC methods are expected to perform better when noise sources are azimuthally well-distributed (e.g., in a large, urbanized area).

The minimum and maximum wavelength surface wave that can be extracted from an array microtremor dataset acquired utilizing a symmetric array is typically set equal to the minimum and twice the maximum receiver spacings, respectively.

2.2.3 H/V Spectral Ratio Technique

The horizontal-to-vertical spectral ratio (HVSR) technique was first introduced by Nogoshi and Igarashi (1971) and popularized by Nakamura (1989). This technique utilizes single-station recordings of ambient vibrations (also referred to as microtremors and ambient noise) made with a three-component seismometer. In this method, the ratio of the Fourier amplitude spectra of the horizontal and vertical components is calculated to determine the frequency of the maximum HVSR response (HVSR peak frequency), commonly accepted as an approximation of the fundamental frequency (f_0) of the sediment column overlying bedrock. The HVSR peak frequency associated with bedrock is a function of the bedrock depth and S-wave velocity of the sediments overlying bedrock. The theoretical HVSR response can be calculated for an S-wave velocity model using modeling schemes based on surface wave ellipticity, vertically propagating body waves, or diffuse wavefields containing body and surface waves. The HVSR frequency peak can also be estimated using the quarter-wavelength approximation:

$$f_0 = \frac{\overline{V}_S}{4z}$$

where f_0 is the site fundamental frequency and $\overline{V}_S$ is the average shear-wave velocity of the soil column overlying bedrock at depth z.

2.3 Surface Wave Dispersion Curve Modeling

The dispersion curves generated from the active and passive surface wave soundings are generally combined and modeled using iterative forward and inverse modeling routines. The final model profile is assumed to represent actual site conditions. The theoretical model used to interpret the dispersion curve assumes horizontally layered, laterally invariant, homogeneous-isotropic material. Although these conditions are seldom strictly met at a site, the results of

active and/or passive surface wave testing provide a good "global" estimate of the material properties along the array. The results may be more representative of the site than a borehole "point" estimate.

The surface wave forward problem is typically solved using the Thomson-Haskell transfer-matrix (Thomson, 1950; Haskell, 1953) later modified by Dunkin (1965) and Knopoff (1964), dynamic stiffness matrix (Kausel and Roësset, 1981), or reflection and transmission coefficient (Kennett, 1974) methods. All of these methods can determine fundamental- and higher-mode phase velocities, which correspond to plane waves in 2-D space. The transfer-matrix method is often used in MASW and passive surface-wave software packages, whereas the dynamic stiffness matrix is utilized in many SASW software packages. MAS_RW and/or passive surface-wave modeling may involve modeling of the fundamental mode, some form of effective mode, or multiple individual modes (multi-mode). As outlined in Roësset et al. (1991), several options exist for the forward modeling of Rayleigh wave SASW data. One formulation considers only fundamental mode plane Rayleigh-wave motion (called the 2-D solution), whereas another includes all stress waves (e.g., body, fundamental, and higher mode surface waves) and incorporates a generalized receiver geometry (3-D global solution) or actual receiver geometry (3-D array solution).

The fundamental mode assumption is generally applicable to modeling Rayleigh-wave dispersion data collected at normally dispersive sites, providing there are not abrupt increases in velocity or steep velocity gradients. Effective-mode or multi-mode approaches are often required for irregularly dispersive sites and sites with steep velocity gradients at shallow depth. If active and passive surface wave data are combined or MAS_RW data are combined from multiple seismic records with different source offsets and receiver gathers, then effective-mode computations are limited to algorithms that assume far-field plane Rayleigh wave propagation. Local search (e.g., linearized matrix inversion methods) or global search methods (e.g., Monte Carlo approaches such as simulated annealing, generic algorithms, and neighborhood algorithm) are typically used to solve the inverse problem.

The maximum wavelength (λ_{max}) recovered from a surface wave data set is typically used to estimate the depth of investigation although a sensitivity analysis of the V_S models would be a more robust method. For normally dispersive velocity profiles with a gradual increase in V_S with depth, the maximum depth of investigation is on the order of $\lambda_{max}/2$ for both Rayleigh and Love wave dispersion data. Velocity profiles with an abrupt increase in V_S at depth, maximum depth of investigation is on the order of $\lambda_{max}/3$ for Rayleigh wave dispersion data but less than $\lambda_{max}/3$ for Love wave dispersion data. Depth of investigation can be highly variable for sites with complex velocity structure (e.g., high velocity layers).

As with all surface geophysical methods, inversion of surface wave dispersion data does not yield a unique V_S model and multiple possible solutions may equally well fit the experimental data. Based on our experience at other sites, the shear wave velocity models (V_S and layer thicknesses) determined by surface wave testing are within 20% of the velocities and layer thicknesses that would be determined by other seismic methods (Brown, 1998). The average velocity of the upper 30 m or 100 ft, however, is much more accurate, often to better than 5%, because it is not sensitive to the layering in the model. V_{S30} does not appear to suffer from the

non-uniqueness inherent in V_S models derived from surface wave dispersion curves (Martin et al., 2006, Comina et al., 2011). Therefore, V_{S30} can be accurately estimated from a single V_S model developed from inversion of the surface wave dispersion data.

It may not always be possible to develop a coherent, fundamental mode dispersion curve over sufficient frequency range for modeling due to dominant higher modes with the higher modes not identifiable for multi-mode modeling. It may, however, be possible to identify the Rayleigh wave phase velocity of the fundamental mode at 40 m wavelength (V_{R40}) in which case V_{S30} can at least be estimated using the Brown et al., 2000 relationship:

$$V_{S30} = 1.045V_{R40}$$

This relationship was established based on a statistical analysis of many surface wave data sets from sites with control by velocities measured in nearby boreholes and has been further evaluated by Martin and Diehl, 2004, and Albarello and Gargani, 2010. Further investigation of this approach has revealed that V_{S30} is generally between V_{R40} and V_{R45} with V_{R40} often being most appropriate for shallow groundwater sites and V_{R45} for deep ground water sites. A detailed study of such an approach for Love wave dispersion data has not been conducted; however, preliminary analysis demonstrates that V_{S30} is generally between V_{L50} and V_{L55}. Although we do not recommend that these empirical V_{S30} estimates replace modeling of surface wave dispersion data, they do offer a means of cost effectively evaluating V_{S30} over a large area. V_{R40} or V_{L55} can also be used to quantify the error in V_{S30} by evaluating the scatter in the dispersion data at these wavelengths.

3 FIELD PROCEDURES

The active- and passive-source surface wave sounding locations were established by **GEO***Vision* and are shown in Figure 1. Four types of surface wave data were acquired at the site: an active-source surface wave survey to characterize near-surface velocity structure, small aperture microtremor array to characterize intermediate depth velocity structure, a larger aperture microtremor array to characterize deeper velocity structure, and an HVSR measurement to potentially constrain data modeling. All array/sensor locations were surveyed using a Trimble R10 GPS with Centerpoint RTX differential corrections.

Active surface wave data were acquired along Array 2 using the MASW technique. MASW equipment used during this investigation consisted of a Geometrics Geode signal enhancement seismograph, 4.5 Hz vertical geophones, seismic cable, a 4 lb hammer and 10 lb sledgehammer. MASW data were acquired using a linear array of 48 geophones spaced 5 ft apart for an array length of 235 ft. Shot points were located 5 ft from the end geophone locations and at 30 ft intervals along the interior of the array. Both the 4 lb hammer and 10 lb sledgehammer were used at all source locations. Data from the transient impacts (hammers) were typically averaged 5 to 10 times to improve the signal-to-noise ratio. All field data were saved to hard disk and documented on field data acquisition forms.

Passive surface wave data were acquired on two (2) arrays; a small aperture L-shaped array (Array 1), and a larger aperture L-shaped (Array 3) using the array microtremor method. Array 1 was acquired using Geometrics Geode signal enhancement seismographs and 48, 4.5 Hz vertical geophones spaced 10 ft apart with the legs of the array having lengths of 230 and 240 ft, respectively. Ambient noise measurements were made for about one hour on the array. The large aperture microtremor array (Array 3) data were collected using three (3), 11-sensor L-shaped subarrays with the maximum length of each leg of the L-shaped array of 600 ft. These subarrays consisted of 11, 2 Hz vertical geophones connected to Geometrics Atom wireless seismographs with a sensor at the corner of the array and five sensors distributed along each leg of the subarrays. Passive surface wave measurements were made for about 1 hour on each subarray. Seismic data stored on the Atom seismographs were downloaded to a laptop computer at the end of the survey. All passive surface wave data were stored on a laptop computer for later processing. The field geometry and associated file names were documented in field data acquisition forms.

HVSR data were acquired at a single location (HV1), as shown on Figure 1, using a Nanometrics Trillium Compact 120 second seismometer coupled to a Nanometrics Centaur data acquisition unit (referred to herein as Trillium). One hour of ambient vibration data were acquired at the measurement location at a 200 Hz sample rate. Microtremor data were stored in the Centaur data acquisition system and downloaded as miniseed format files at the end of data acquisition. An attempt was also made to acquire HVSR data near the corner of Array 1, but the dataset was not useful.

4 DATA REDUCTION

4.1 HVSR Data Reduction

HVSR data were reduced using the Geopsy software package (http://www.geopsy.org) developed by Marc Wathelet, ISTerre, Grenoble, France with the help of many other researchers. Microtremor data recorded by the Trillium were exported to miniseed format. Data files were then loaded into the Geopsy software package, where data file columns containing the vertical and horizontal (north and east) components and the sample rate were specified. After applying a demean and detrend filter, the H/V spectral ratio was calculated over the 0.2 to 15 Hz frequency range using a time window length of 200 s. Fourier amplitude spectra were calculated after applying a 5% cosine taper and smoothed by the Konno and Ohmachi filter with a smoothing coefficient value of 30. The vertical amplitude spectra were divided by the root-mean-square (RMS) of the horizontal amplitude spectra to calculate the HVSR for each time window and the average HVSR. Time windows containing clear transients (high amplitude near-field signals caused by nearby foot or vehicular traffic, etc.) or yielding poor quality results were then deleted and the computations repeated. The average HVSR peak frequency and its standard deviation from all time windows used for analysis is computed and presented along with the standard deviation of the HVSR amplitudes for all time windows. A similar process was also utilized to compute the HVSR as a function of azimuth although in this case the horizontal components are rotated to the azimuth of interest. The observed HVSR and azimuthal HVSR data for measurement station HV1 are presented as Figure 2.

4.2 MASW Data Reduction

The MASW data collected along Array 2 were reduced using the software Seismic Pro Surface V9.1 developed by Geogiga and multiple in-house scripts for various data extraction and formatting tasks, with all data reduction documented in a Microsoft Excel spreadsheet.

The following steps were used for the data reduction of Array 2:

- Input seismic records to be used for analysis into the software package.
- Check and correct source and receiver geometry as necessary.
- Select the offset range used for analysis (multiple offset ranges utilized for each seismic record as discussed below) and document in the spreadsheet.
- Apply phase shift transform to seismic record to convert the data from time – offset to frequency – phase velocity space.
- Identify, pick, save, and document dispersion curve.
- Change the receiver offset range and repeat process.
- Repeat process for all seismic records.
- Use an in-house script to apply near-field criteria with maximum wavelength set equal to lesser of 100 ft (source frequency limitation) or 1 to 1.3 times the source to midpoint of receiver array distance.
- Use an in-house script to merge multiple dispersion curves extracted from the MASW data collected along each seismic line for a specific source type (different source locations, different receiver offset ranges, etc.).
- Edit dispersion data, as necessary (e.g., delete poor quality curves and outliers).

- Calculate a representative dispersion curve at equal log-frequency or log-wavelength spacing for each array of MASW dispersion data using a moving average, polynomial curve fitting routine.

This unique data reduction strategy, which can involve the combination of over 100 dispersion curves for a 1D sounding, is designed for characterizing sites with complex velocity structure that does not yield surface wave dispersion data over a wide frequency range from a single source type or source location. The data reduction strategy ensures that the dispersion curve selected for modeling is representative of average conditions beneath the array and spans as broad a frequency/wavelength range as possible while considering near field effects.

The MASW data collected along Array 2 yielded Rayleigh wave dispersion data over the 8 to 80 ft wavelength range with minor scatter associated with near-surface velocity variability beneath the array.

4.3 Array Microtremor Data Reduction

The array microtremor data for Arrays 1 and 3 were reduced using the ESAC method in the Seisimager software package developed by Oyo Corporation/Geometrics, Inc. The processing sequence for implementation is as follows:

- Input all seismic records for a dataset into the software.
- Load receiver geometry (x and y positions) for each channel in seismic record.
- Apply time-segmentation routine, as necessary, to break data file into multiple seismic records. Time segmentation was not necessary for smaller arrays where data acquired as 30 s records. For the large array, data were divided into multiple approximate 80 s time windows for analysis.
- Calculate the SPAC coefficients for each seismic record and average.
- Optionally, combine SPAC coefficients from different arrays (e.g. multiple double circle arrays from the large array).
- For each frequency calculate the RMS error between the SPAC coefficients and a Bessel function of the first kind and order zero over a user defined phase velocity range and velocity step.
- Plot an image of RMS error as a function for frequency (f) and phase velocity (v).
- Identify and pick the dispersion curve as the continuous trend on the f-v image with the lowest RMS error.
- Repeat process for all arrays and/or time blocks.
- Use an in-house script to convert dispersion curves to the appropriate format for editing.
- Edit dispersion data, as necessary, and use an in-house script to combine all dispersion data after setting maximum wavelength to about 2 times the maximum receiver spacing (2 times maximum receiver spacing approximately equivalent to $k_{min}/2$ for a symmetrical array).
- Calculate a representative dispersion curve for the passive dispersion data from each array using a moving average polynomial curve fitting routine.

The array microtremor data collected along Arrays 1 and 3 yielded Rayleigh wave dispersion data over the 26 to 330 ft and 90 to 765 ft wavelength ranges, respectively.

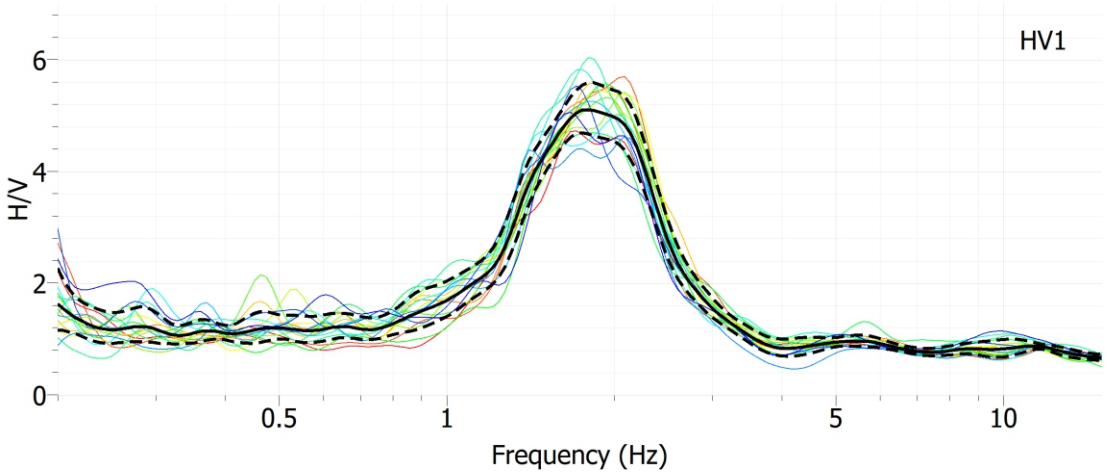

H/V Spectral Ratio

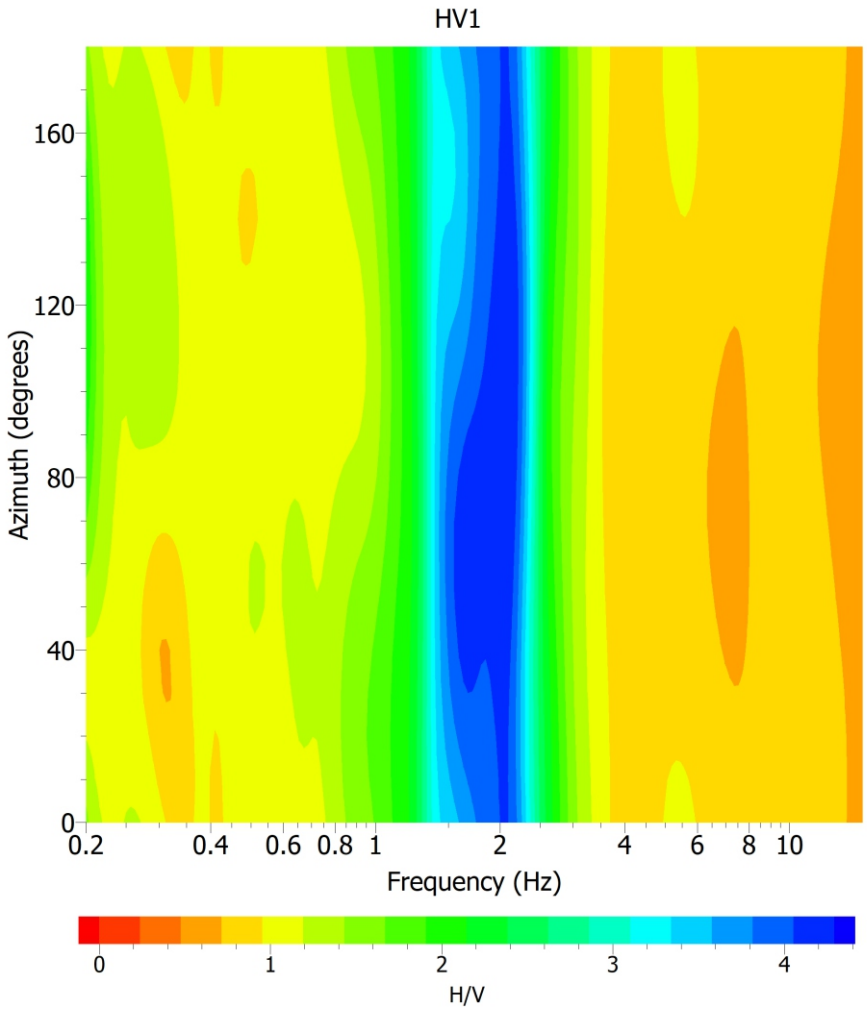

Azimuthal H/V Spectral Ratio

GEOVision geophysical services	FIGURE 2 H/V SPECTRAL RATIO - STATION HV1
Project No: 21283 Date: Sept 1, 2021 Drawn By: A. Martin Approved By: Antony J Martin R:\GVProjects\2021\21283A3GEO\Report\Figure 2.cdr	2118 MILVIA STREET BERKELEY, CALIFORNIA
	PREPARED FOR A3GEO, INC.

5 DATA MODELING

Prior to data modeling, the representative dispersion curves from the active and passive surface wave data were combined and the moving average polynomial curve fitting routine in WinSASW V3 was used to generate a composite representative dispersion curve for modeling. During this process the active and passive surface wave dispersion data were given equal weights. An equal logarithm wavelength sample rate was used for the representative dispersion curve to reflect the gradual loss in model resolution with depth.

Surface wave data were modeled using the effective mode routine in WinSASW V3 software package. During this process, an initial velocity model was generated based on general characteristics of the dispersion curve and the inverse modeling routine utilized to adjust the layer V_S until an acceptable agreement with the observed data was obtained. Layer thicknesses were adjusted, and the inversion process repeated until a V_S model was developed with low RMS error between the observed and calculated dispersion curves. Data inputs into the modeling software include layer thickness, S-wave velocity, P-wave velocity or Poisson's ratio, and mass density. P-wave velocity and mass density only have a very small influence (i.e., less than 10%) on the S-wave velocity model generated from a surface wave dispersion curve. However, realistic assumptions for P-wave velocity, which is significantly impacted by the location of the saturated zone, and mass density will slightly improve the accuracy of the S-wave velocity model.

Constant mass density values of 112 to 137 lb/ft^3 were used in the velocity profiles for subsurface soils/rock depending on P- and S-wave velocity. Within the normal range encountered in geotechnical engineering, variation in mass density has a negligible (±2%) effect on the estimated V_S from surface wave dispersion data. During modeling of Rayleigh wave dispersion data, the compression wave velocity, V_P, for unsaturated sediments was estimated using a Poisson's ratio, ν, of 0.3 and the relationship:

$$V_P = V_S \left[(2(1-\nu))/(1-2\nu)\right]^{0.5}$$

Poisson's ratio has a larger effect than density on the estimated V_S from Rayleigh wave dispersion data. Achenbach (1973) provides approximate relationship between Rayleigh wave velocity (V_R), V_S and ν:

$$V_R = V_S \left[(0.862 + 1.14\,\nu)/(1+\nu)\right]$$

Using this relationship, it can be shown that V_S derived from V_R only varies by about 10% over possible 0 to 0.5 range for Poisson's ratio where:

$$V_S = 1.16V_R \text{ for } \nu = 0$$
$$V_S = 1.05V_R \text{ for } \nu = 0.5$$

The realistic range of the Poisson's ratio for typical unsaturated sediments is about 0.25 to 0.35. Over this range, V_S derived from modeling of Rayleigh wave dispersion data will vary by about 5%. An intermediate Poisson's ratio of 0.3 was selected for modeling to minimize any error associated with the assumed Poisson's ratio.

High Poisson's ratio saturated sediments with V_P > 5,000 ft/s were constrained at an approximate depth of 20 ft based on interactive analysis of seismic refraction first arrival data and borehole information provided by A3GEO, Inc.

Multiple V_S models were developed with variable depths to variable depth to rock and rock properties to assess model non-uniqueness and uncertainty. The theoretical HVSR response was computed for these V_S models and compared to the observed HVSR data. The software package *HV-Inv* Release 2.5, which is based on the diffuse field assumption and is summarized in García-Jerez, et al., 2016, was used to compute the theoretical HVSR response with the assumption that the microtremor wavefield consists of both Rayleigh and Love waves.

6 INTERPRETATION AND RESULTS

The observed HVSR and azimuthal HVSR for measurement station HV1 is presented as Figure 2. There is a high amplitude HVSR peak at about 1.9 Hz that is expected to be associated with Franciscan bedrock. There is some azimuthal dependence of HVSR peak frequency, which may be indicative of a dipping bedrock surface in the site vicinity.

The Rayleigh wave phase velocities from the passive surface wave array are in excellent agreement with those from the MASW data in the region of overlapping wavelength (Figure 3). Scatter in the dispersion data from each technique is expected to be primarily associated with lateral velocity variability beneath the respective arrays.

A small ensemble of V_S models was developed from the surface wave dispersion data derived from MASW (Array 2) and array microtremor (Arrays 1 and 3) data to evaluate model non-uniqueness and uncertainty. The fit of the calculated effective mode dispersion curve to the experimental data collected at the site and the associated V_S models are presented as Figure 3. The resolution decreases gradually with depth due to the loss of sensitivity of the dispersion curve to changes in V_S at greater depth. A V_S model having calculated HVSR peak frequency in good agreement with the observed HVSR data was selected for purpose of site characterization and is presented in tabular form as Table 1. The other V_S models can be provided in digital form. The comparison of the observed and the calculated HVSR response for the V_S models presented in Figure 3 are presented in Figure 4. In this figure, the V_S models and respective calculated HVSR are presented using the same color lines and line type for purpose of correlation. Typically, calculated HVSR peak frequency decreases as the depth to the half space increases and calculated HVSR peak amplitude increases as half space V_S increases. Although some of the V_S models with greater depths to the half space have calculated HVSR peaks at lower frequency than the observed, these models should still be considered valid for uncertainty analysis because the HVSR measurement location is not near the center of the surface wave arrays (Figure 1).

The estimated depth of investigation for the combined active and passive surface wave sounding is about 250 to 300 ft. Except for a stiff surface layer associated with asphalt and road base at the surface, the V_S model presented as Table 1 indicates that V_S gradually increases with depth from about 600 ft/s at a depth of 3.5 ft to 3,150 ft/s at a depth of 265 ft. A possible weathered Franciscan rock unit with V_S of about 2,000 ft/s is modeled at a depth of 135 ft with a higher velocity 3,1250 ft/s rock unit modeled at a depth of 265 ft. The half-space velocity is not well resolved and varies from about 2,900 to 4,400 ft/s in the models presented in Figure 3. Typically, the half space rock velocity increases as depth increases, although the modeled velocity of the overlying unit also impacts the velocity of the half space.

The average shear wave velocity to a depth of 30 m (V_{S30}) and 100 ft (V_{S100ft}) are 324 m/s and 1,067 ft/s for the V_S model presented as Table 1. V_{S30} is not sensitive to model non-uniqueness and only varies from 319 to 325 m/s for the models presented in Figure 3. According to the NEHRP provisions of the Uniform Building Code, the area in the vicinity of Arrays 1 to 3 is classified as Site Class D, stiff soil.

Table 1 Sample V_S Model

Depth to Top of Layer (ft)	Layer Thickness (ft)	S-Wave Velocity (ft/s)	Inferred P-Wave Velocity (ft/s)	Inferred Poisson's Ratio	Inferred Unit Weight (lb/ft^3)
0	1.5	1966	3679	0.300	128
1.5	2	691	1292	0.300	115
3.5	4.5	601	1125	0.300	112
8	5	723	1353	0.300	115
13	7	1023	1913	0.300	120
20	20	1033	5500	0.482	120
40	25	1076	5500	0.480	121
65	30	1320	5750	0.472	123
95	40	1448	6000	0.469	124
135	130	2005	7000	0.455	129
265	Half Space	3153	8000	0.408	137

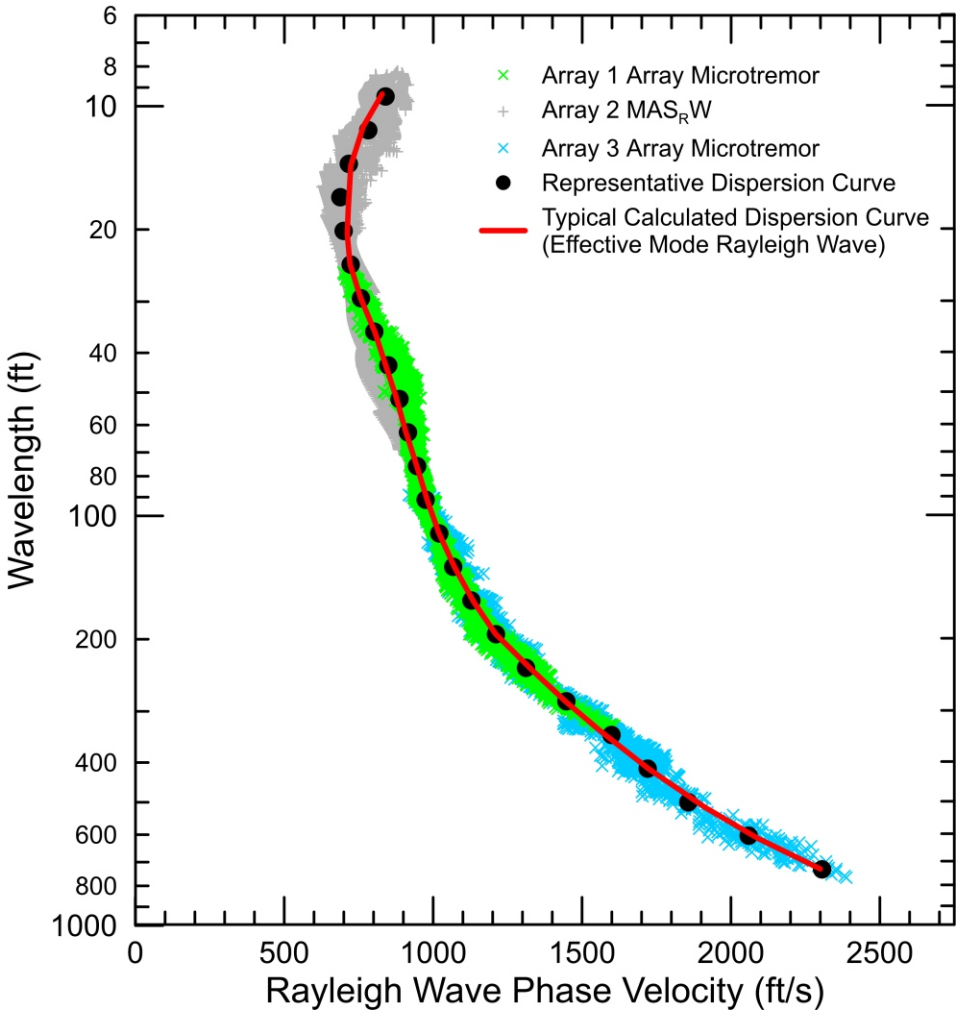

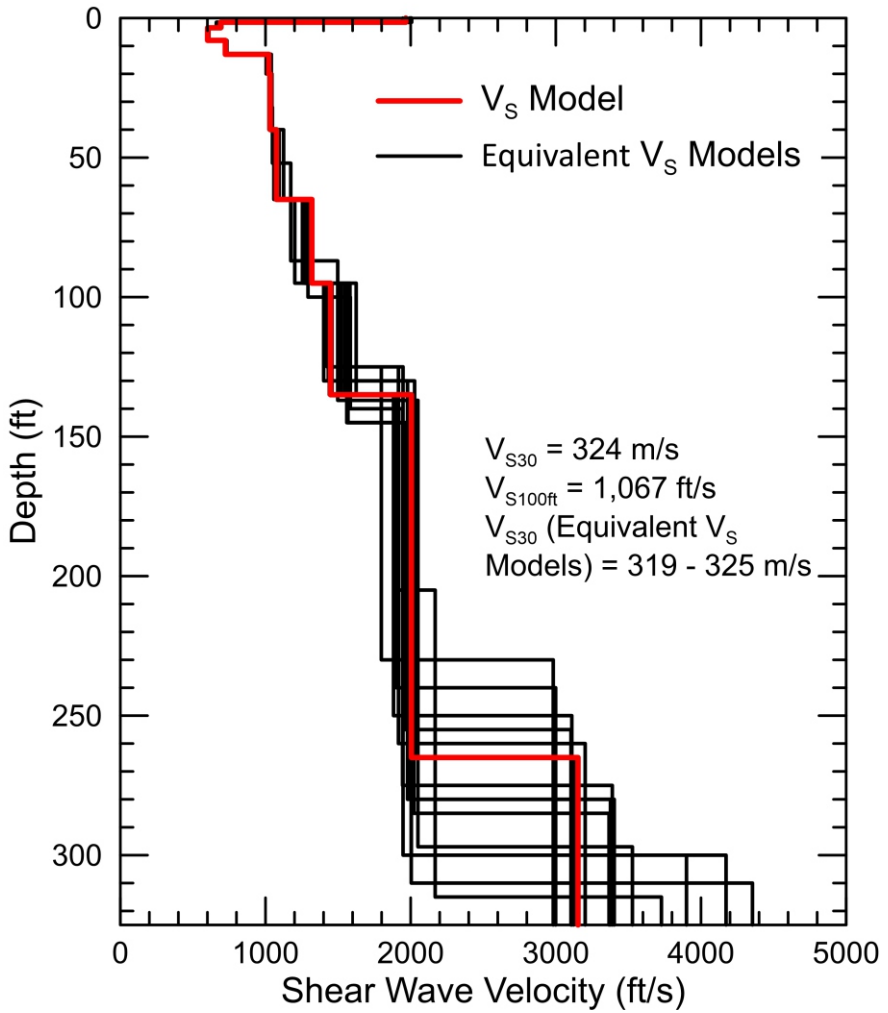

GEOVision geophysical services

Project No: 21283	FIGURE 3 SURFACE WAVE MODEL
Date: Sept 5, 2021	2118 MILVIA STREET BERKELEY, CALIFORNIA
Drawn By: A MARTIN	
Approved By: Antony J Martin	PREPARED FOR A3GEO, INC.
R:\GVProjects\2021\21283A3GEO\Report\Figure 3.cdr	

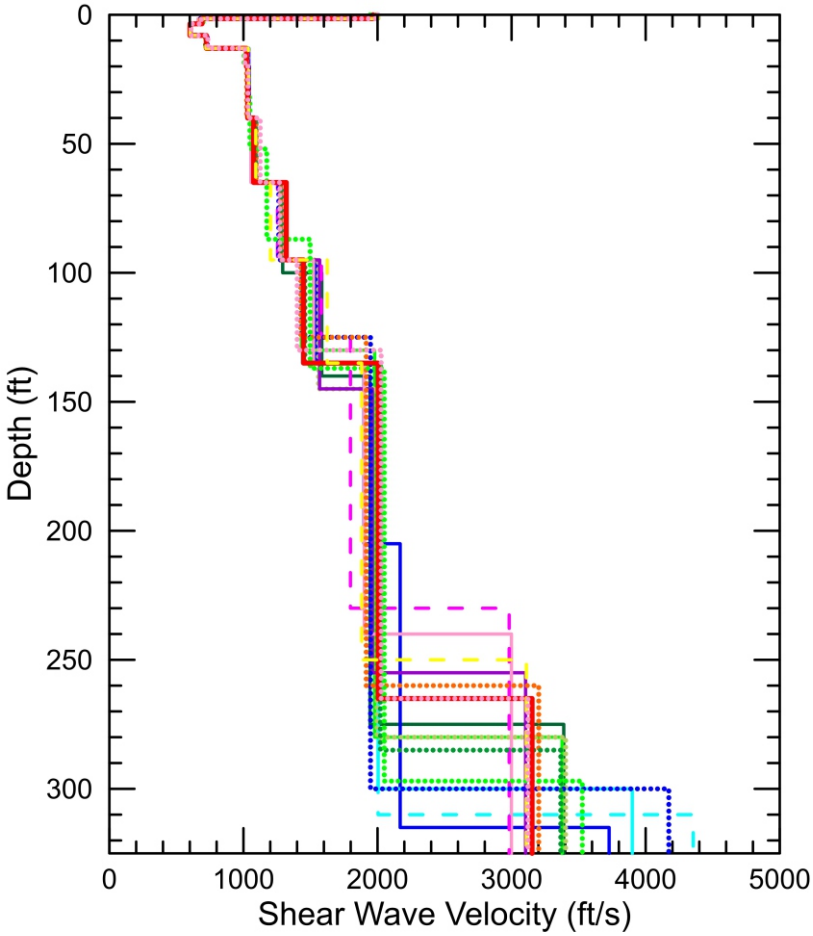

S-Wave Velocity Model

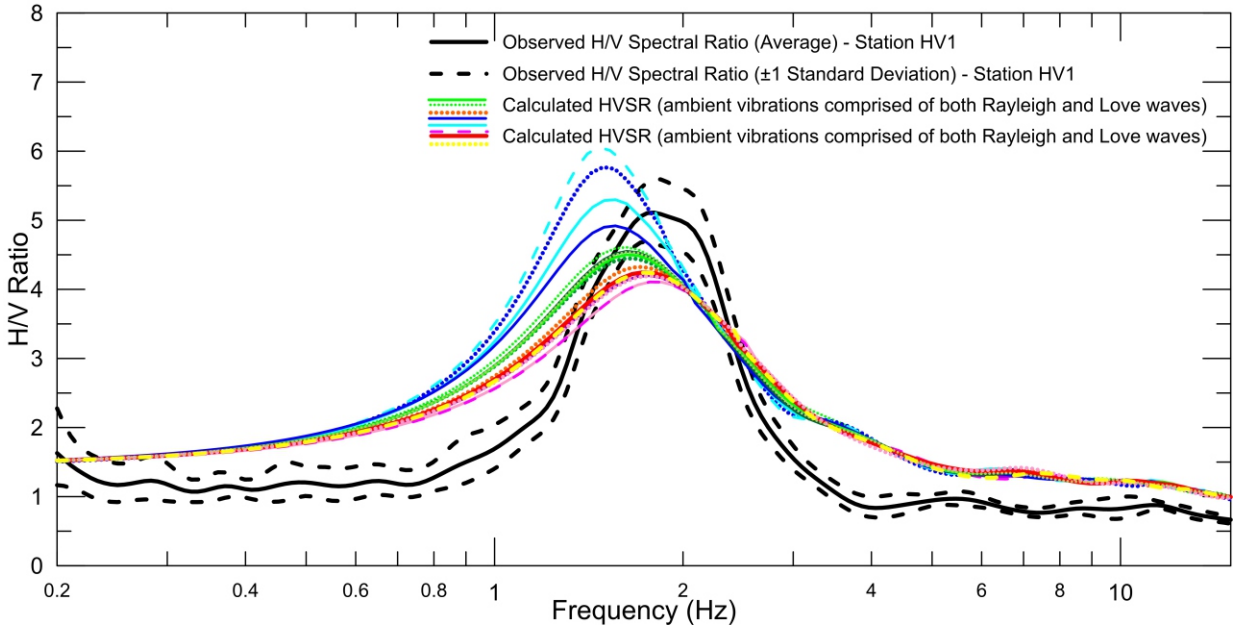

Calculated HVSR Response

GEOVision geophysical services	FIGURE 4 CALCULATED HVSR RESPONSE
Project No: 21283	2118 MILVIA STREET BERKELEY, CALIFORNIA
Date: Sept 5, 2021	
Drawn By: A. Martin	
Approved By: Antony J. Martin	PREPARED FOR A3GEO, INC.
R:\GVProjects\2021\21283A3GEO\Report\Figure 4.cdr	

7 REFERENCES

Achenbach J, 1973, Wave Propagation in Elastic Solids, Elsevier, Amsterdam, Netherlands.

Aki K, 1957, Space and time spectra of stationary stochastic waves, with special reference to microtremors. *Bull. Earthq. Inst. Univ. Tokyo*, Vol. 35, p 415–457.

Albarello D and Gargani G, 2010, "Providing NEHRP soil classification from the direct interpretation of effective Rayleigh-wave dispersion curves", *Bulletin of the Seismological Society of America*, Vol. 100, No. 6, p 3284-3294.

Asten M, 2006, Site shear velocity profile interpretation from microtremor array data by direct fitting of SPAC curves, in *Proceedings of the Third Int. Symp. Effects of Surface Geol. Seismic Motion*, Vol. 2, LCPC Edition, Grenoble, France, August 30–September 01, Paper No. 99, p 1069-1080.

Asten M, Stephenson WJ and Hartzell, S, 2015, The use of wavenumber normalization in computing spatially averaged coherencies (krSPAC) of microtremor data from asymmetric arrays, *Proceedings 6th International Conference on Earthquake Geotechnical Engineering*, Christchurch, New Zealand, 9 p.

Bettig B, Bard PY, Scherbaum F, Riepl J, Cotton F, Cornou C and Hatzfeld D, 2001, Analysis of dense array noise measurements using the modified spatial auto-correlation method (SPAC): application to the Grenoble area, *Bollettino di Geofisica Teoricaed Applicata*, Vol 42, p 281–304.

Brown L, 1998, Comparison of V_S profiles from SASW and borehole measurements at strong motion sites in Southern California, Master's thesis, University of Texas, Austin.

Brown L, Diehl J and Nigbor R, 2000, A simplified method to measure average shear-wave velocity in the top 30 m (V_s30), *Proc. 6th International Conference on Seismic Zonation*, p 1–6.

BSSC, 2003, *NEHRP recommended provisions for seismic regulations for new buildings and other structure (FEMA 450), Part I: Provisions*, Building Seismic Safety Council, Federal Emergency Management Agency, Washington D.C.

Capon J, 1969, High-resolution frequency-wavenumber spectrum analysis, *Proc. Institute of Electrical and Electronics Engineers (IEEE)*, Vol. 57, no. 8, p 1408–1418.

Comina C, Foti S, Boiero D, and Socco LV, 2011, Reliability of $V_{S,30}$ evaluation from surface-wave tests, *J. Geotech. Geoenviron. Eng.*, p 579–586.

Cox, B R and Teague D, 2016, Layering Ratios: A Systematic Approach to the Inversion of Surface Wave Data in the Absence of A-priori Information, *Geophysical Journal International*, Vol. 207, no. 1, p. 422-438.

Dal Moro G, Moura R, Moustafa A, 2015, Multi-component joint analysis of surface waves, *Journal of Applied Geophysics*, Vol. 119, p 128-138.

Dal Moro G and Ferigo F, 2011, Joint Analysis of Rayleigh- and Love-wave dispersion curves: Issues, criteria and improvements, *Journal of Applied Geophysics*, Vol. 75, p 573-589.

Dunkin J W, 1965, Computation of modal solutions in layered, elastic media at high frequencies, *Bulletin of the Seismological Society of America*, Vol. 55, pp. 335–358.

Foti S, 2000, Multistation Methods for Geotechnical Characterization using Surface Waves, Ph.D. Dissertation, Politecnico di Torino, Italy.

GEOVision, Inc (2012): EPRI (2004, 2006) ground-motion model (GMM) review project: Shear wave velocity measurements at seismic recording stations, http://www.epri.com/abstracts/Pages/ProductAbstract. aspx?ProductId=000000003002000719.

Haskell N A, 1953, The dispersion of surface waves on multilayered media, *Bull. Seismol. Soc. Am.*, v. 43, pp. 17–34.

García-Jerez A, Piña-Flores J, Sánchez-Sesma F, Luzón, F, Perton, M, 2016, A computer code for forward computation and inversion of the H/V spectral ratio under the diffuse field assumption, Computers & Geosciences, In Press.

Kausel, E. and J. M. Röesset (1981). Stiffness matrices for layered soils, *Bulletin of the Seismological Society of America*, v. 71, no. 6, pp. 1743–1761.

Kennett, B.L.N (1974). Reflections, rays and reverberations, *Bulletin of the Seismological Society of America*, v. 64, no. 6, pp. 1685–1696.

Knopoff L. (1964). "A matrix method for elastic wave problems." *Bulletin of the Seismological Society of America*, Vol. 54, pp. 431–438.

Lacoss R, Kelly E and Toksöz M, 1969, Estimation of seismic noise structure using arrays, *Geophysics*, v. 34, pp. 21-38.

Li J and Rosenblad B, 2011, Experimental study of near-field effects in multichannel array-based surface wave velocity measurements, *Near Surface Geophysics*, Vol. 9, 357-366.

Ling S and Okada H, 1993, An extended use of the spatial correlation technique for the estimation of geological structure using microtremors, *Proc. the 89th Conference Society of Exploration Geophysicists Japan (SEGJ)*, pp. 44–48 (in Japanese).

Martin A and Diehl J, 2004, Practical experience using a simplified procedure to measure average shear-wave velocity to a depth of 30 meters (V_S30), *Proceedings of the 13th World Conference on Earthquake Engineering*, Vancouver, B.C., Canada, August 1-6, 2004, Paper No. 952.

Martin A, Shawver J and Diehl J, 2006, Combined use of Active and Passive Surface Wave Techniques for Cost Effective UBC/IBC Site Classification, *Proceedings of the 8th National Conference on Earthquake Engineering*, San Francisco, California, Paper No. 1013.

Martin A, Yong A and Salomone L, 2014, Advantages of active Love wave techniques in geophysical characterization of seismographic station sites – case studies in California and the Central and Eastern United States, Proceedings of the Tenth U.S. National Conference on Earthquake Engineering, Frontiers of Earthquake Engineering, July 21-25, Anchorage, Alaska.

Nakamura Y, 1989, A method for dynamic characteristics estimation of subsurface using microtremor on the ground surface, *Quart. Reprt Rail. Tech. Res. Inst.*, Vol. 30, no. 1, p 25–33.

Nogoshi M and Igarashi T, 1971, On the amplitude characteristics of microtremor (part 2), *J. Seismol. Soc. Japan*, Vol. 24, p 26–40 (in Japanese).

Ohori M, Nobata A, and Wakamatsu K, 2002, A comparison of ESAC and FK methods of estimating phase velocity using arbitrarily shaped microtremor arrays, *Bull. Seismol. Soc. Am.*, v. 92, no. 6, p. 2323–2332.

Okada H, 2003, The Microtremor Survey Method, *Society of Exploration Geophysics Geophysical Monograph Series*, Number 12, 135p.

Park C, Miller R and Xia J, 1999a, Multimodal analysis of high frequency surface waves, *Proceedings of the Symposium on the Application of Geophysics to Engineering and Environmental Problems '99*, 115-121.

Park C, Miller R and Xia, J, 1999b, Multichannel analysis of surface waves, *Geophysics*, Vol 64, No. 3, 800-808.

Roesset J, Chang D and Stokoe K, 1991, Comparison of 2-D and 3-D Models for Analysis of Surface Wave Tests, *Proceedings*, 5th *International Conference on Soil Dynamics and Earthquake Engineering*, Karlsruhe, Germany.

Thomson W T, 1950, Transmission of elastic waves through a stratified solid medium, *J. Applied Physics*, v. 21, no. 2, pp. 89–93.

Xia J, Xu Y, Luo Y, Miller R, Cakir R and Zeng C, 2012, Advantages of using Multichannel analysis of Love waves (MALW) to estimate near-surface shear-wave velocity, *Surveys in Geophysics*, 841–860.

Yong A, Martin A, Stokoe K and Diehl J, 2013, ARRA-funded V_{S30} measurements using multi-technique method approach at strong-motion stations in California and Central-Eastern United States, Open-File Report 2013-1102, United States Geological Survey, http://pubs.usgs.gov/of/2013/1102/.

Yoon S and Rix G, 2009, Near-field effects on Array-based surface wave methods with active sources, *Journal of Geotechnical and Geoenvironmental Engineering*, Vol. 135, no. 3, 399-406.

8 CERTIFICATION

All geophysical data, analysis, interpretations, conclusions, and recommendations in this document have been prepared under the supervision of and reviewed by a **GEO*Vision*** California Professional Geophysicist.

Reviewed and approved by,

09/05/2021

Antony J. Martin — Date
California Professional Geophysicist, P. Gp.
GEO*Vision* Geophysical Services

* This geophysical investigation was conducted under the supervision of a California Professional Geophysicist using industry standard methods and equipment. A high degree of professionalism was maintained during all aspects of the project from the field investigation and data acquisition, through data processing interpretation and reporting. All original field data files, field notes and observations, and other pertinent information are maintained in the project files and are available for the client to review for a period of at least one year.

  A professional geophysicist's certification of interpreted geophysical conditions comprises a declaration of his/her professional judgment. It does not constitute a warranty or guarantee, expressed or implied, nor does it relieve any other party of its responsibility to abide by contract documents, applicable codes, standards, regulations or ordinances.

APPENDIX F

Site-Specific Seismic Hazard Analysis

Draft Report

Site-Specific Seismic Hazard Analyses and Development of Seismic Design Ground Motions for Berkeley City College, Berkeley, California

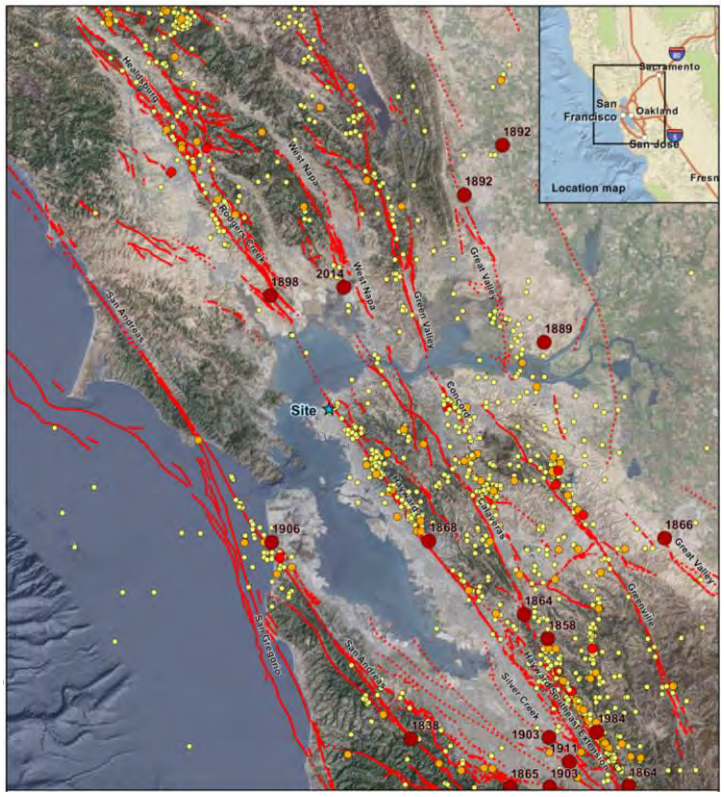

Prepared for:
A3GEO Inc.

Prepared by:
Ivan Wong and Qimin Wu
Lettis Consultants International, Inc. (LCI)
1000 Burnett Ave., Suite 350
Concord, CA 94520

Bob Darragh and Walt Silva
Pacific Engineering & Analysis (PE&A)
856 Sea View Drive, El Cerrito, CA 94530

15 October 2021

TABLE OF CONTENTS

LIST OF TABLES

LIST OF FIGURES

1.0 INTRODUCTION

At the request of A3GEO, we have performed site-specific seismic hazard analyses and developed seismic design ground motion spectra for the Berkeley City College located in Berkeley, California (Figure 1). The site is located in the seismically active San Francisco Bay region within the San Andreas fault system (Figure 1). The Hayward fault lies less than two km to the east of the school site (Figure 1).

The strong ground motion hazard at the site was estimated by performing a site-specific probabilistic seismic hazard analysis (PSHA), deterministic seismic hazard analysis (DSHA), and a site response analysis. The seismic hazard analyses and design ground motion parameters were developed in accordance with ASCE 7-16 *Minimum Design Loads and Associated Criteria for Buildings and Other Structures* as described in items 12 through 17 of California Geological Survey (CGS) Note 48. Two levels of ground motions were developed for the building following ASCE 7-16: (1) risk-adjusted Maximum Considered Earthquake (MCE_R); and (2) Design Earthquake (DE).

1.1 Scope of Work

As stated in our proposal, the scope of work was:

Task 1 – Review of Geotechnical and Geophysical Data and Development of Basecase V_S Profiles

We reviewed the available geotechnical and geophysical data and the shear-wave velocity (V_S) data collected as part of the scope of work to develop site-specific basecase V_S profiles to use in the site response analysis (Task 4). Our database of V_S profiles based on our seismic design studies of the UC Berkeley campus and other building sites in Berkeley was used to assist in the V_S profile development.

Task 2 – Deterministic Seismic Hazard Analysis (DSHA)

A DSHA was performed to calculate a rock 84th percentile horizontal deterministic spectrum for a **M** 7.6 earthquake on the Hayward-Rodgers Creek fault system and assuming a V_S30 of 960 m/sec. The spectrum was adjusted for forward rupture directivity. The 84th percentile deterministic spectrum was adjusted for maximum component following ASCE7-16 to arrive at the deterministic MCE.

Task 3 - Probabilistic Seismic Hazard Analysis (PSHA)

A PSHA was performed to calculate the probabilistic hazard curves for rock. Forward rupture directivity was accounted for in the PSHA. The 2,475-year return period UHS was adjusted for maximum component and risk factors were applied following ASCE7-16 (1% probability of collapse in 50 years) to arrive at the probabilistic MCE_R.

Task 4 – Site Response Analysis

A comparison was made between the deterministic MCE and probabilistic MCE_R and the code minimum spectrum as per ASCE 7-16 to calculate the MCE_R spectrum for rock. Five time histories were scaled to that spectrum and used in the site response analysis. The V_S profiles and dynamic material curves were the primary inputs. An equivalent-linear site response analysis was performed to calculate amplification factors. Randomized V_S profiles were calculated from the basecase V_S profiles and run in the analysis to account for aleatory uncertainty. The resulting amplification factors were applied to the site-specific MCE_R for rock to arrive at MCE_R spectrum at the ground surface. The site response analysis was performed by our subcontractor Pacific Engineering & Analysis (PE&A).

Task 5 – Development of MCE and DE Spectra

The site-specific MCE_R at the ground surface was compared to the code minimum spectrum to arrive at the final site-specific MCE_R spectrum at the ground surface. Based on this spectrum, the Design Earthquake (DE) spectrum was calculated also per ASCE7-16.

Task 6 – Reports and Meetings

This task consisted of preparing a report, participating in conference calls with the Project Team, and responding to CGS review of the final report.

1.2 Acknowledgements

Our thanks to Tim Sneddon and Dillon Braud of A3GEO for their project management support. Our appreciation to John Baldwin for project management effort as the project manager, and to Claire Unruh and Javier Chalini for their assistance in the preparation of this report.

2.0 HISTORICAL SEISMICITY

The earliest written accounts of earthquakes in California come from the logs of the Spanish missions established throughout California in the 1700's. The majority of the historical seismicity in the San Francisco Bay region is associated with the major faults of the San Andreas fault system. There have been 15 earthquakes of approximately **M** 6.0 or greater in the San Francisco Bay region in historical times. The most significant earthquakes to the site are discussed in detail below and shown on Figure 1.

It is likely that most of the significant historical earthquakes discussed below generated strong ground shaking at the school site with the strongest shaking in the 1868 Hayward earthquake at Modified Mercalli (MM) intensity VII (Toppazada *et al*., 1981).

10 June 1836 For several decades, this earthquake was thought to be associated with the Hayward fault. However, Toppozada and Borchardt (1998) reevaluated historical evidence and concluded that this 1836 earthquake probably occurred somewhere between Monterey and Santa Clara. Toppozada and Borchardt (1998) assigned this event a Richter local magnitude (M_L) 6.25 ± 0.5 based on felt reports. Recent trenching studies on the northern Hayward fault found little evidence for movement in the 1800's and corroborate this interpretation. Bakun (1999) supports a location east of Monterey Bay and assigns a magnitude of **M** 6.5.

June 1838 There are very few written records of the June 1838 earthquake, and the exact date is not known. No reports of this earthquake are available from north of San Francisco or south of Santa Clara, except from Monterey (Toppozada *et al*., 1981). Toppozada and Borchardt (1998) reviewed the historical records for this earthquake and found that reported shaking intensities suggest that this earthquake was the result of rupture of more than the 60-km long Peninsula segment of the San Andreas fault as was originally believed, and rather rupture may have extended a distance of 140 km from San Francisco to San Juan Bautista. In contrast, Bakun (1999) believes the 1838 earthquake was confined to the Peninsula segment and assigned a **M** 6.8 to the event.

21 October 1868 This **M** 6.8 earthquake occurred on the southern Hayward fault. It was one of the most destructive in California history. Heavy damage was sustained in towns along the Hayward fault in the eastern San Francisco Bay area, as well as in San Francisco and San Jose. The southern Hayward fault is thought to have ruptured from its southern end, in the eastern Santa Clara Valley, to northern Oakland or southern Berkeley.

31 March 1898 On 31 March 1898, the San Francisco Bay region was shaken by an earthquake that appears to have been centered near Mare Island in San Pablo Bay (north of area shown on Figure 1). The maximum intensity was MM VIII or greater and buildings were damaged in areas around the Bay Area. Toppozada *et al*. (1981) re-evaluated the magnitude of this event through comparisons with other historical earthquakes and assigned it a M_L 6.7. Bakun (1999) assigns a magnitude of only **M** 6.3 and suggests that the earthquake could have occurred on one of three

possible faults: the southern end of the Rodgers Creek fault, the southern end of the West Napa fault, or beneath the fold structures east of Mare Island.

18 April 1906 The **M** 7.8 Great San Francisco earthquake of 1906 was the most destructive earthquake to have occurred in northern California in historical times. The earthquake was felt from southern Oregon to south of Los Angeles, and as far east as central Nevada. It ruptured the northernmost 430 km of the San Andreas fault, from San Juan Bautista to the Mendocino Triple Junction. Damage was widespread in northern California and injury and loss of life was particularly severe. Ground shaking and fire caused the deaths of more than 3,000 people and injured approximately 225,000. Damage from shaking was most severe in areas of saturated or loose, young soils.

24 April 1984 The **M** 6.2 Morgan Hill earthquake occurred on the Calaveras fault about 18 km east of San Jose and 22 km north of Morgan Hill. This earthquake had a focal depth of 8 km and ruptured about 30 km of the fault. It was felt in California and Nevada over an area of 120,000 km^2 and caused damage estimated to be worth $7.5 million (1984 dollars). In San Jose, cracks formed in some walls and plaster fell, many items were thrown from store shelves and some chimneys cracked. This earthquake is thought to have been very similar to an earthquake that affected the area in 1911.

17 October 1989 The **M** 6.9 Loma Prieta earthquake occurred on a blind fault adjacent to the Santa Cruz segment of the San Andreas fault. The cities of Los Gatos, Watsonville, and Santa Cruz were severely damaged, and San Francisco and Oakland were also damaged. Shaking was felt throughout the San Francisco Bay area and as far away as San Diego and Nevada. While the Loma Prieta earthquake was one of the most expensive natural disasters in U.S. history, causing in excess of $6 billion damage (1989 dollars), the loss of life was significantly less than in 1906. Sixty-two people died and about 3,500 were injured. About 12,000 people were displaced from their homes. As in the 1906 earthquake, the worst damage from shaking occurred on unconsolidated or saturated soils, or with unreinforced masonry or inadequately designed structures.

24 August 2014 The **M** 6.0 South Napa earthquake occurred on the West Napa fault, which extends along the western margin of the basin underlying Napa Valley. Shaking was felt throughout the San Francisco Bay area and as far away as Reno, NV. The shaking caused damage to many homes and commercial buildings including significant damage to the 1870 courthouse in downtown Napa. The earthquake was unusual in that it had relatively long surface rupture for an event of its magnitude.

3.0 INPUTS TO SEISMIC HAZARD ANALYSES

The following section discusses the characterization of the seismic sources considered in the PSHA and DSHA, the geologic site conditions, and the empirical ground motion models (GMMs) selected and used. The PSHA was performed using our proprietary software APEX, which has been validated using the test cases in Pacific Earthquake Engineering Research Center (PEER)'s PSHA Computer Program Validation Project (Hale *et al*., 2018).

3.1 Seismic Source Model

Seismic source characterization for a PSHA is concerned with three fundamental elements: (1) the identification, location and geometry of significant sources of earthquakes; (2) the maximum size of the earthquakes associated with these sources; and (3) the rate at which the earthquakes occur. In the PSHA we estimated seismic source parameters for the significant faults in the site region, and used two approaches to represent background earthquakes, a uniform seismic source zone and gridded seismicity. These seismic sources and the associated input parameters for the PSHA are described in Sections 3.1.1 and 3.1.2.

In a DSHA, only scenario earthquakes specified by their maximum earthquake and the causative fault are considered. The scenario earthquakes are selected with no consideration of their frequency of occurrence other than they are "reasonably expected to occur" along a specific fault.

3.1.1 Faults

The fault model used in this study is adopted from a model originally developed as part of the California Department of Water Resources' Delta Risk Management Strategy Project (Wong *et al*., 2008, URS Corporation/Jack R. Benjamin & Associates, 2007). Each seismic source is characterized using the latest available geologic, seismological, and paleoseismic data and the currently accepted models of fault behavior developed by the Working Group on Northern California Earthquake Potential (WGNCEP, 1996) and the 2002 California Geological Survey's (CGS) seismic source model used in the USGS National Hazard Maps (Cao *et al.*, 2003). Characterizations of the major faults in the San Francisco Bay region, including the San Andreas, Hayward-Rodgers Creek, Concord-Green Valley, San Gregorio, Greenville, and Mt. Diablo thrust faults, are adopted from the 1999 and 2002 Working Groups on California Earthquake Probabilities (WGCEP, 2003). These characterizations were updated based on a review of the statewide rupture forecast projects, UCERF2 and UCERF3. Segmentation models for these faults remain based on the 2002 WGCEP (used in UCERF2). However, fault lengths, slip rates/recurrence intervals have been updated to be consistent with the lengths and geologic slip rates/recurrence intervals from UCERF3. For the Hayward-Rodgers Creek fault system, the Healdsburg fault and Hayward Southern Extension have been added, consistent with UCERF3. In addition, the characteristic magnitudes have been updated using the magnitude-area relations used in UCERF3.

Uncertainties in the seismic source parameters are incorporated into the PSHA using a logic tree approach. In this procedure, values of the source parameters are represented by the branches

of logic trees with weights that define the distribution of values. In general, three values for each parameter were weighted and used in the analysis. Statistical analyses by Keefer and Bodily (1983) indicate that a three-point distribution of 5th, 50th, and 95th percentiles weighted 0.185, 0.63, and 0.185 (rounded to 0.2, 0.6, and 0.2), respectively, is the best discrete approximation of a continuous distribution. Alternatively, they found that the 10th, 50th, and 90th percentiles weighted 0.3, 0.4, and 0.3, respectively, can be used when limited available data make it difficult to determine the extreme tails (i.e., the 5th and 95th percentiles) of a distribution. Note that the weights associated with the percentiles are not equivalent to probabilities for these values, but rather are weights assigned to define the distribution. We generally applied these guidelines in developing distributions for seismic source parameters with continuous distributions (e.g., Mmax, fault dip, slip rate or recurrence) unless the available data suggested otherwise. Details on the characterization of the Hayward-Rodgers Creek fault system is provided below.

Figure 1 shows the locations of Quaternary faults relative to the site. The faults included in the PSHA are judged to be at least potentially active and may contribute to the probabilistic hazard because of their maximum earthquakes and/or proximity to the site. The most significant fault to the site is the Hayward-Rodgers Creek fault system.

Hayward-Rodgers Creek Fault System

The characterization of the system of faults that included the originally defined Hayward and Rodgers Creek faults, and now the Healdsburg faults has evolved over time particularly in the past 30 years. The total length of the system is approximately 210 km long and includes what is called the Hayward Southern Extension. The addition of the Hayward Southern Extension and the Healdsburg fault to the fault system is relatively recent and this has added additional complexity to the potential rupture scenarios for the fault system. The Hayward fault extends approximately 108 km from the area of Mount Misery, east of San Jose, to north of San Pablo Bay (Figure 1). The fault has been divided into northern and southern segments by WGCEP (1999; 2003); however, this segmentation may not represent the general long-term behavior of the fault (Schwartz *et al*., 2014). There is uncertainty on whether the northern Hayward can rupture as an independent source because of the depth extent of creep along the fault (Schwartz *et al*., 2014).

With the addition of the Hayward Southern Extension, the Hayward fault now extends further south to Alum Rock adjacent to the Calaveras fault (Figure 1). Watt *et al*. (2016) based on high-resolution seismic reflection data have recognized a previously unidentified extension of the northern Hayward fault that extends across San Pablo Bay and onshore to join up with the Rodgers Creek fault.

Systematic right-lateral geomorphic offsets and creep offset of cultural features have been well documented along the entire length of the Hayward fault (Lienkaemper, 1992). In addition to undergoing displacement in earthquake ruptures, the Hayward fault also moves by aseismic creep. Measurements along the fault over the last two decades show that the mean creep rate is 4 to 7 mm/yr (Lienkaemper *et al*., 2012).

The last major earthquake on the Hayward fault in October 1868, occurred along the southern segment of the fault (Section 2.0). This **M** 6.8 event caused toppling of buildings in Hayward and other localities within about 5 km of the fault. The surface rupture associated with this earthquake is thought to have extended for approximately 30 km, from Warm Springs to San Leandro, with a maximum reported displacement of 1 m. Studies by Lienkaemper *et al.* (2010) indicate that there have been 11 earthquakes along the southern Hayward fault since about 136 A.D. resulting in an average recurrence interval of 161 years. There have been three ruptures of the southern Hayward fault since 1600 including the 1868 earthquake (Lienkaemper *et al.*, 2010). Paleoseismic trenching along the northern Hayward fault at the Mira Vista site indicates that the last surface rupturing earthquake along this part of the fault was sometime between 1635 and 1776 (Schwartz *et al.*, 2014). Lienkamper *et al.* (1999) also indicated at least four surface-rupturing earthquakes in the last 2,250 years.

The northern continuation of the fault system is the Rodgers Creek and Healdsburg faults. The Rodgers Creek fault is about 63 km (± 10 km) extending from San Pablo Bay to about 10 km south of Healdsburg (Figure 1) and its geomorphic expression is similar to that of the Hayward fault. At its northern end, the Rodgers Creek fault is separated from the Healdsburg fault by a 3-km-wide right-step, and separated from the Maacama fault by a 10-km-wide right-step (Wagner and Bortugno, 1982). Holocene activity along the Rodgers Creek is indicated by a series of fault scarps in Holocene deposits, side-hill benches, right-laterally offset streams, and closed linear depressions. Microseismicity is nearly absent along much of the length of the fault suggesting that it may be a seismic gap and the site of an impending earthquake (Budding *et al.*, 1991; Wong, 1991). Paleoseismic investigations by Schwartz *et al.* (1992) revealed three events in 925 to 1,000 years. This gives a preferred recurrence of 230 years for a maximum earthquake of **M** 7.0. Hecker *et al.* (2005) interpreted the most recent earthquake (MRE) on the Rodgers Creek fault occurred no earlier than 1690 and possibly sometime between 1715 and 1776. The elapsed time may have reached or exceeded the average recurrence interval of about 230 years. They also speculate that the Rodgers Creek and Hayward faults could have ruptured together in the MRE.

The Healdsburg fault is about 31 km long and is characterized by a high level of seismicity unlike the Rodgers Creek fault to the southwest and creep (Wong, 1991). The fault is not very well characterized and just a few paleoseismic investigations have been performed along the fault. Based on a trench at Shiloh Regional Park, three to four discrete events were interpreted since 560 A.D. (S. Hecker, USGS, personal communication, April 2020).

Given the limited paleoseismic data on the timing of large earthquakes along the Hayward-Rodgers-Creek fault system, there is considerable uncertainty on rupture scenarios and hence the potential characteristic earthquakes (terminology not used in UCERF3). The most recent analysis of statewide seismic hazard, UCERF3, utilized a different set of empirical relations between rupture geometry and earthquake magnitude to those of earlier working groups (Field *et al.*, 2013). They also used aseismic factors that are significantly smaller for the Hayward fault than used in UCERF2 and previous studies (see discussion below). These have resulted in magnitudes for specific rupture scenarios that are either the same or about 0.1 magnitude units larger than the WGCEP (2003, 2008) estimated magnitudes. In addition, the

Healdsburg fault was added to the Rodgers Creek fault in the Statewide Community Fault Model (SCFM) and UCERF3. As a result, the potential ruptures involving the Rodgers Creek fault increased in length by about 20 km. Furthermore, the segment boundary between the northern Hayward fault and Rodgers Creek fault was relocated farther north, which resulted in a lengthening of the northern Hayward segment from 35 to 53 km. Consequently, without the addition of the Healdsburg fault, the Rodgers Creek fault would have decreased in rupture length. Overall, these changes resulted in 0.1 to 0.2 magnitude unit increases in the Hayward-Rodgers Creek fault zone rupture scenarios.

UCERF3 has also expanded the range of conceivable ruptures for most faults in California by including the possibility of multi-fault ruptures, wherein fault ruptures can jump from one mapped fault to another in a single earthquake (Field *et al*., 2013). The result of this change is that considered earthquake magnitudes can be much larger than those in previous models like WGCEP (2003, 2008). The UCERF3 model permits the Hayward fault to rupture with other faults including the Calaveras fault, as well as a rupture scenario extending from the Rodgers Creek fault through the southern San Andreas fault to the Salton Sea, generating an **M** > 8 earthquake. The frequency of such an event is very low in the model, however, and unlikely to be relevant to the design purposes of most structures.

A key parameter in estimating characteristic earthquake magnitudes is the aseismic factor which was originally used in WGCEP (2003). These factors were developed to account for the effects of aseismic fault creep on magnitude since portions of a fault undergoing creep are unlikely to accumulate seismic moment to be released in earthquakes. Hence, the seismogenic areas of potential fault ruptures are the result of using the aseismic factors to reduce the total fault area. Based on UCERF3 magnitude scaling relationships and seismogenic area, the characteristic magnitude for rupture of the Hayward-Rodgers Creek system is a **M** 7.5 (includes the Healdsburg fault and Hayward Southern Extension). Without the Hayward Southern extension, the magnitude is still **M** 7.5 given its relatively short length and high aseismic factor. The characteristic magnitude for a Hayward-Rodgers Creek fault rupture is **M** 7.3 again based on the UCERF3 magnitude scaling relationships. Note the above magnitudes values are not necessarily those used in UCERF3 because as stated above, magnitudes for the faults within the San Andreas fault system including the Hayward-Rodgers Creek fault system cover a very wide range because of the large number of rupture scenarios due to their relaxation of fault segmentation.

Schwartz *et al*. (2014) computed mean magnitudes of a Hayward-Rodgers Creek fault rupture of **M** 7.25 (not including the Healdsburg fault or Hayward Southern Extension). For rupture of the Hayward and Rodgers Creek faults alone, they estimated a mean magnitude of **M** 7.0 for both scenarios. Separate northern and southern Hayward fault ruptures will result in a **M** 6.35 and 6.5, respectively.

As stated above, previous studies have adopted a scenario earthquake consisting of just the Hayward-Rodgers Creek faults with magnitudes closer to **M** 7.3. Potential rupture of both the Hayward-Rodgers Creek faults is permissive based on the ages of the most recent earthquake on the Rodgers Creek and northern Hayward faults and the penultimate event on the southern Hayward (Schwartz et al., 2014). However, this does not preclude the possibility that each segment

ruptures independently. Certainly the 1868 earthquake on the southern Hayward fault is evidence that at least that segment ruptures independent of the northern Hayward and Rodgers Creek faults. Also, there is no paleoseismic evidence that supports rupture of the Healdsburg or Hayward Southern Extension with the Hayward-Rodgers Creek faults. The small width of the stepover between the Rodgers Creek and Healdsburg faults would kinematically allow rupture together of the two faults but there is no paleoseismic evidence for such combined ruptures. The connectivity of rupture between the southern Hayward and Hayward Southern Extension is tenuous at best. The Hayward Southern Extension unlike the southern Hayward fault has been characterized as being dextral-oblique reverse faulting with the slip being distributed among several faults such as the Quimby, Mission, and Evergreen faults. Hence, we believe a combined rupture of the Hayward and Rodgers Creek fault resulting in a **M** 7.3 characteristic earthquake is sufficiently conservative to use in the DSHA. Longer ruptures beyond that of the Hayward-Rodgers Creek faults is due to relaxation of segmentation as in UCERF3 and is not supported by any paleoseismic evidence. As stated by Schwartz (2018), segmentation models that incorporate timing, dynamic, and rheological factors should be used in developing reasonable future rupture lengths.

For this project, which is under the DSA regulation, reviewed by California Geological Survey (CGS) and follows ASCE 7-16, we are using the BSSC **M** 7.6 rupture scenario. This selection is made to be solely to be consistent with the scenario defined by the Building Seismic Safety Commission (BSSC) and used as a deterministic cap in the design maps in ASCE 7-16. However, we disagree with the BSSC and USGS that this scenario should be used as a deterministic scenario. Using the magnitude-area scaling relationships and aseismic factors from UCERF3 results in a **M** 7.5 for the Hayward-Hayward South Extension-Rodgers Creek-Healdsburg rupture. BSSC chose to select the highest magnitude from the magnitude-area scaling relationships which is a **M** 7.6. In addition to this conservatism, we believe that the addition of both the Hayward South Extension fault and the Healdsburg fault to the deterministic scenario is overly conservative.

Note that the full range of rupture scenarios involving the Hayward-Rodgers Creek fault system was incorporated into the PSHA to address the epistemic uncertainty in rupture behavior of the four faults. The slip rates and recurrence intervals were consistent with the geologic slip rates and paleo observed recurrence intervals.

3.1.2 Background Seismicity

To account for the hazard from background (floating or random) earthquakes that are not associated with known or mapped faults, regional seismic source zones are used in the PSHA. In most of the western U.S., the maximum magnitude of earthquakes not associated with known faults usually ranges from **M** 6 to 6.5. Repeated events larger than these magnitudes generally produce recognizable fault-or-fold related features at the earth's surface (e.g., dePolo, 1994). An example of a background earthquake is the 1986 **M** 5.7 Mt. Lewis earthquake which occurred east of San Jose and resulted in no discernable surface rupture.

In this study, we model the hazard from background earthquakes through three seismic source zones that may contribute to the hazard because of their proximity to the site: 1) Coast Ranges-

Pacific (CRP); 2) Coast Ranges-Great Valley North (CRGVN); and 3) Coast Ranges-Great Valley South (CRGVS). The seismic source zones are delineated based on similar seismotectonic characteristics such as style of faulting, seismogenic thickness, maximum magnitude, and seismicity rate. Hazard from these zones is modeled through two different implementations: (1) a "gridded seismicity" model, in which locations of past seismicity are assumed to be likely locations of future seismicity (stationarity; captured by smoothing the catalog seismicity and having spatially variable rates defined over a grid of points); and (2) a "uniform" model, in which earthquakes are assumed to occur randomly and uniformly within each zone.

Earthquake recurrence estimates are required in order to assess the hazard from background earthquakes. The recurrence parameters for the source zones were developed using the historical seismicity record for the period of 1769 through July 2018, spanning almost 250 years. The seismicity catalog was assembled from the previous catalog compilations of the 2014 National Seismic Hazard Mapping Program (NSHMP; Petersen *et al.*, 2014) and the USGS Advanced National Seismic System (ANSS, USGS, 2018). The 2014 NSHMP compilation excluded duplicate events and anthropogenic events classified as mining-related and/or explosions. Similarly, only events reviewed and classified as earthquakes were included in the USGS ANSS compilation portion of the catalog (i.e., anthropogenic events were not considered). The majority of the earthquakes in the catalog had magnitudes reported either as duration magnitude (M_D), Richter local magnitude (M_L), or coda magnitude (M_C); other magnitude types in the catalog include moment magnitude (**M**), body wave magnitude (m_b), hand magnitude (M_h), or unknown magnitude type. The magnitudes of all events were converted to a uniform **M** using the same scaling relations applied in APS (2015).

The catalog was declustered using the Gardner and Knopoff (1974) algorithm to remove foreshocks and aftershocks. Additionally, fault-related crustal earthquakes were removed to avoid double-counting the resulting hazard. The completeness intervals for the catalog were estimated by considering the completeness intervals of URS (2012) and AMEC (2010), which were estimated based on settlement history, seismographic installation dates, and by using Stepp plot analyses (Stepp, 1972).

In this analysis, we considered the discrete five-point sampling method of Miller and Rice (1983) to model M_{max} ranges of **M** 7.2 ± 0.4, 7.0 ± 0.4, and 7.0 ± 0.4 for the seismic source zones CRP, CRGVN, and CRGVS, respectively. Recurrence parameters (b-values and rates) were calculated using the program ABSMOOTH (LCI proprietary software; EPRI/DOE/NRC, 2012). The ABSMOOTH program computes a b-value for the source zone and then divides the source zone into cells of a selected size (0.2-degree cells in this report) and calculates the rate in each cell using the likelihood function of the data in that cell along with penalty functions that smooth the cell-to-cell variation in the rate. The program outputs both mean values and eight alternative sets ("realizations") of the recurrence parameters in order to characterize epistemic uncertainty in the rates and b-values (EPRI/DOE/NRC, 2012). This approach is based on the Markov Chain Monte Carlo techniques to generate multiple realizations from a multi-dimensional probability distribution; in this case, the rate, b-value and uncertainty in those parameters. The equally-weighted eight alternative maps of rates and b-value represent the central tendency and statistical

uncertainty in the recurrence parameters and are selected using the Latin Hypercube sampling technique. Eight realizations are used to provide a good representation of the underlying distributions (EPRI/DOE/NRC, 2012).

Recurrence parameters for the uniform seismic source zone were adopted from the eight realizations generated for the gridded seismicity, such that the total rates generated for each realization were assumed to apply uniformly across each source zone. To incorporate uncertainty into the hazard analysis, we implemented the eight realizations (which include eight b-values and corresponding rates) generated by ABSMOOTH, with equal weight applied to each realization. Table 1 provides the mean rates of events of magnitude greater than **M** 5 for the corresponding b-values for use in the PSHA. We assign equal weights of [0.5] to the use of the uniform and gridded seismicity. Recent seismicity may be considered more likely representative of seismicity occurring in the next 100 years. Given the relatively short 250-year-long and incomplete historical record, the possibility exists that the catalog is not representative of the long-term record of seismicity; thus, the two approaches were implemented with equal weight.

3.2 Ground Motion Models

To estimate the ground motions for crustal earthquakes in the PSHA and DSHA, we have used recently developed GMMs appropriate for tectonically active crustal regions. The models, developed as part of the NGA-West2 Project sponsored by PEER Center Lifelines Program, were published in 2014.

The NGA-West2 models by Chiou and Youngs (2014), Campbell and Bozorgnia (2014), Abrahamson *et al*. (2014), and Boore *et al*. (2014) were used in the PSHA and DSHA. The models were weighted equally in the hazard analyses.

The NGA-West2 models use the V_S30 parameter as a proxy for site effects. Based on the site characterization (Section 3.3), a site-specific V_S30 value of 960 m/sec consistent with the rock beneath the site was used in the PSHA and DSHA (Sections 4 and 5).

Other input parameters for the NGA-West2 GMMs include $Z_{2.5}$, the depth to the V_S of 2.5 km/sec (a proxy for basin effects), which is only used in one model, Campbell and Bozorgnia (2014). In addition, Abrahamson *et al*. (2014), Boore *et al.* (2014) and Chiou and Youngs (2014) use $Z_{1.0}$, the depth to the V_S of 1.0 km/sec. In the absence of site-specific of site-specific information, the default $Z_{1.0}$ and $Z_{2.5}$ based on the equations provided by the NGA-West2 developers were used in the PSHA and DSHA. Other parameters such as depth to the top of rupture (zero for all faults with surficial expressions unless specified otherwise), dip angle, rupture width and aspect ratio were specified for each fault or calculated within the PSHA code.

Rupture directivity was incorporated using the model of Bayless and Somerville (2013) in the development of the seismic design ground motions. As described in Section 7, the predicted fault-normal ground motions were compared to the maximum direction factors applied in development of the seismic design spectra.

As noted by Al Atik and Youngs (2014) the development of the NGA-West2 models was a collaborative effort with many interactions and exchanges of ideas among the developers and the developers indicated that an additional epistemic uncertainty needs to be incorporated into the median ground motions in order to more fully represent an appropriate level of epistemic uncertainty. Hence, for each of the four NGA-West2 models an additional epistemic uncertainty on the median ground motion was included. The three-point distribution and model of Al Atik and Youngs (2014) was applied. The model is a function of magnitude, style of faulting, and spectral period.

3.3 Site Characterization

To characterize the V_S structure beneath the project site, GEOVision performed a MASW (multi-channel analysis of surface waves) survey (Array 2), passive-source surface wave array microtremor surveys (Arrays 1 and 3), and applied the horizontal-to-vertical spectral ratio (HVSR) technique.

Multiple V_S models were developed with variable depth to rock and rock properties to assess non-uniqueness and uncertainties. Figure 2 shows the final V_S profile beneath the site. The following is extracted from the GEOVision report.

The estimated depth of investigation for the combined active and passive surface wave sounding is about 250 to 300 ft. Except for a stiff surface layer associated with asphalt and road base at the surface, the V_S model indicates that V_S gradually increases with depth from about 600 ft/s at a depth of 3.5 ft to 3,150 ft/s at a depth of 265 ft. A possible weathered Franciscan rock unit with V_S of about 2,000 ft/s is modeled at a depth of 135 ft with a higher velocity 3,1250 ft/s rock unit modeled at a depth of 265 ft. The half-space velocity is not well resolved and varies from about 2,900 to 4,400 ft/s in the models presented in Figure 2. Typically, the half space rock velocity increases as depth increases, although the modeled velocity f the overlying unit also impacts the velocity of the half space.

The average shear wave velocity to a depth of 30 m (V_S30) and 100 ft (V_S100ft) are 324 m/s and 1,067 ft/s for the V_S model presented as Table 1. V_S30 is not sensitive to model non-uniqueness and only varies from 319 to 325 m/s for the models presented in Figure 2. According to the NEHRP provisions of the Uniform Building Code, the area in the vicinity of Arrays 1 to 3 is classified as Site Class D, stiff soil.

Based on the best-estimate V_S profile interpreted by GEOVision (red line in Figure 2), the hazard was calculated at the top of competent rock (265 ft [81 m]) with a V_S of 3153 ft/sec (960 m/sec). Given the uncertainty to the top of competent rock, the depth was varied in the site response analysis (Section 6.1).

4.0 PSHA RESULTS

The results of the PSHA at the site for a competent rock site condition with a V_S of 960 m/sec are presented in terms of ground motion as a function of annual frequency of exceedance (AFE). AFE is the reciprocal of the average return period. Figures 3 through 5 show the mean, median (50th percentile), 5th, 15th, 85th, and 95th percentile hazard curves for peak horizontal ground acceleration (PGA) and 0.2 and 1.0 sec horizontal spectral acceleration (SA). The fractiles indicate the range of uncertainties about the mean hazard. For a return period of 2,475 years, the range of uncertainty is about a factor of 2.0 between the 5th and 95th percentiles for PGA (Figure 3). This uncertainty is typical of Bay Area sites and is due in large part to the uncertainties in the GMMs.

The contributions of the various seismic sources to the mean PGA are shown on Figure 6. As expected, because of the proximity to the site, the Hayward-Rodgers Creek fault system is the dominant contributor to both the short-and long-period ground motion hazard. Figure 7 shows the fractional contributions of significant sources to the total mean PGA hazard. The source contributions for 0.2 and 1.0 sec SA hazard are shown on Figures 8 to 11. For all spectral periods, the Hayward-Rodgers Creek fault system dominates for all return periods.

Figures 12 to 14 illustrate deaggregation of the mean PGA and 0.2 and 1.0 sec horizontal SA hazard by magnitude, distance, and epsilon bins at the 2,475-year return period. Epsilon is the difference between the logarithm of the ground motion amplitude and the mean logarithm of ground motion (for that M and R) measured in units of the standard deviation (σ) of the logarithm of the ground motion. At a 2,475-year return period, the PGA hazard is dominated by events in the magnitude range of **M** 6.4 to 7.6 at distances less than 10 km corresponding to events on the Hayward fault (Figure 12). This is also the case for 0.2 and 1.0 sec SA (Figures 13 and 14.)

The UHS at a 2,475-year return period is shown on Figure 15. This UHS reflect the geometric mean of expected horizontal ground motions, as predicted by the NGA-West2 models.

5.0 DSHA RESULTS

5%-damped 84th percentile horizontal acceleration response spectra are calculated for the scenario characteristic earthquake on the Hayward-Rodgers Creek faults (**M** 7.6) using the same NGA-West2 models used in the PSHA and the V_S30 of 960 m/sec. As discussed in Section 3.1.1, we believe a **M** 7.6 scenario earthquake should not be used in seismic design but it is required by the California Building Code.

Figure 16 shows the lognormal average 84th percentile acceleration response spectrum along with the individual spectra from the four NGA-West2 GMMs for V_S30 960 m/sec. Input parameters are provided in Table 2. The range in spectra represent the epistemic uncertainty in the ground motion modeling. Figure 17 shows the lognormal average median and 84th percentile acceleration response spectra. These spectra are used in the development of rock MCE_R design spectra described in Section 6.1.1.

6.0 SITE RESPONSE ANALYSIS

A site response analysis was performed to model the effects of near-surface materials above competent rock (V_S30 960 m/sec) based on the site-specific velocity measurements provided in Section 3.3. This section describes the site response methodology, inputs and resulting ground motions.

6.1 Methodology and Inputs

The site response analysis was performed in accordance with ASCE 7-16, Chapter 21. The computational formulation that has been most widely employed to evaluate 1D site response assumes vertically-propagating plane S-waves. Departures of soil response from a linear constitutive relation are treated in an approximate manner through the use of the equivalent-linear formulation. The equivalent-linear formulation, in its present form, was introduced by Idriss and Seed (1968). A stepwise analysis approach was formalized into a 1D, vertically propagating S-wave code called SHAKE (Schnabel *et al*., 1972). Subsequently, this code has become the most widely used and validated analysis package for 1D site response calculations. The site response analysis for this study was performed using the computer program RASCALS (Silva and Lee, 1987), which, similar to SHAKE, propagates the input ground motions at the bedrock level up through the soil column using an equivalent-linear approach. Period-dependent amplification factors are computed as the ratio of surface response spectra to input bedrock response spectra.

Site response was performed using the rock MCE_R spectrum and corresponding V_S profiles. For the best-estimate basecase profile (P1), an upper (P2) and lower range profile (P3) was also computed to accommodate uncertainty in the soil V_S, as described in Section 6.1.2 below. The surface spectra from the three basecase V_S profiles are weighted 0.4, 0.3, and 0.3 for P1, P2, and P3, respectively to account for uncertainty and spatial variability.

6.1.1 Rock Ground Motions

In accordance with ASCE 7-16, Chapter 21.1.1, a MCE_R response spectrum was developed for rock. The horizontal MCE_R spectrum is defined in ASCE 7-16 Chapter 21 as the lesser of the deterministic MCE and probabilistic MCE_R ground motions. The deterministic MCE response spectrum is the 84th percentile response spectrum from the characteristic event on the controlling active fault. As per ASCE 7-16 (Supplement 1), the largest SA in the deterministic MCE must not be less than 1.5*Fa, where Fa for site class B is determined using Table 11.1.4 with the value of S_S taken as 1.5. Figure 18 shows the 84th percentile deterministic response spectrum for the **M** 7.6 event on the Hayward-Rodgers Creek faults at a distance of 1.7 km (V_S30 960 m/sec) and the adjustment from RotD50 (geometric mean) ground motions predicted by the NGA-West2 GMMs to maximum-direction ground motions using the factors of Shahi and Baker (2013). Note that the maximum direction adjustment factors of Shahi and Baker (2013) differ slightly from those in ASCE 7-16, Section 21.2, but are used in this study because they are recommended in the 2015 NEHRP provisions, the ATC 136-1 study, and are recommended for use in currently proposed changes for ASCE 7-22.

For comparison, the 84th percentile fault-normal spectrum was also computed using the directivity model of Bayless and Somerville (2013) for the deterministic scenario. In the directivity calculations, the hypocenter was uniformly distributed along the fault plane and the resulting weighted mean fault-normal scale factors were computed. Given the close distance to the **M** 7.6 rupture the directivity model predicts a strong increase in ground motions for periods greater than 0.75 sec. To account for directivity effects for such a near-field site, the envelope of the fault-normal and maximum direction spectra is used in developing the deterministic MCE spectrum. The peak of the resulting site-specific deterministic spectra far exceeds the minimum SA requirement of ASCE 7-16 (horizontal line on Figure 18) (Table 3).

The probabilistic MCE_R spectrum for a rock V_S30 of 960 m/sec was calculated using Method 1 in ASCE 7-16, Chapter 21 (Figure 19; Table 4). The 2,475-year return period rock UHS was adjusted to maximum-direction ground motions and compared to the fault-normal 2,475-year return period rock UHS. In the PSHA, the hypocenter of each rupture is uniformly distributed along strike on the rupture plane. The maximum-direction adjustment is greater than the fault-normal adjustment at all period. The envelope of fault-normal and maximum direction spectra is used to develop the probabilistic MCE_R. The enveloped spectrum is also adjusted using a risk coefficient to obtain a spectrum that is expected to achieve a 1% probability of collapse within a 50-year period. The risk coefficient, C_R is equal to C_{RS} at periods less than or equal to 0.2 sec and equal to CR1 at periods greater or equal to 1.0 sec. The values of C_{RS} and C_{R1} for this site, obtained from the USGS website (https://seismicmaps.org/ accessed October 2021) are 0.904 and 0.895, respectively.

Figure 20 compares the probabilistic rock MCE_R (risk-adjusted 2,475-year rock UHS) and the deterministic rock MCE spectra. The site-specific rock MCE_R is the lesser of these spectra, but not less than 80% of the general code MCE_R spectrum for Site Class B (S_S = 2.16 g, S_1 = 0.833 g, Fa = 0.9, Fv = 0.8). For this site and rock V_S30, the rock MCE_R is the deterministic MCE for periods less than 0.75 sec and the probabilistic MCE_R spectrum for all other periods (Table 5).

Five recorded horizontal time histories were selected from the NGA-West2 database (Ancheta *et al*., 2013) to scale the rock MCE_R spectra. Seed time histories were selected to match the spectral shape of the target spectrum. The input time histories are listed in Table 6.

6.1.2 Site Conditions

The near-surface material dynamic behavior is modeled using V_S profiles, shear modulus reduction and damping curves, and unit weights. Both epistemic uncertainty and aleatory variability in V_S and shear modulus and damping curves were accommodated in the site response analysis.

Epistemic uncertainty in the V_S profile was included by developing lower-range (P2) and upper-range (P3) basecase V_S profiles. These V_S profiles were computed from the best-estimate V_S profile using a factor of 1.377 (sigma ln of 0.25) for the bottom layer (960 m/sec) and a factor of 1.25 for the shallower layers (sigma ln of 0.17). In developing amplification factors the lower range, best-estimate and upper range basecase profiles are weighted 0.3, 0.4 and 0.3, respectively.

The uncertainty in depth to competent rock was also addressed by varying the depth from 220 to 320 ft (Figure 2). The rock V_S of 960 m/sec was also randomized.

For each of the basecase V_S profiles, 30 randomized V_S profiles were generated using a soil correlation model (Toro, 1996). These randomized V_S profiles accommodate aleatory variability in the soil properties.

For the dynamic material properties, the EPRI (1993) curves (Revision 1) and Peninsular Range curves for cohesionless soils (Silva *et al.*, 1997) were used to cover the possible range of nonlinear soil behavior at the site, which consists of alluvial materials (layered clays with some thin intermittent layers of sands). The EPRI (1993) model (M1) curves are depth-dependent. The Peninsular Range curves (M2), which are a subset of the EPRI (1993) curves, use the EPRI (1993) 51 to 120 ft curves for 0 to 50 ft and the 501 to 1,000 ft curves for deeper materials and reflect much more linear response than the EPRI curves. The two dynamic material models, were weighted equally when combining the site response analyses results obtained from the three basecase V_S models. As with the V_S profiles, a suite of 30 randomized curves about each of these basecase curves is generated.

6.2 Site Response Results

For the rock MCE_R spectrum, RASCALS was used to compute surface spectra using the five input time histories and the suites of randomized V_S profiles and dynamic material properties. For each combination of basecase V_S profile (e.g., P1, P2, and P3) and basecase material property curves (M1 and M2), an input time history is propagated through the 30 randomized soil columns and a surface spectrum is computed. Amplification factors are computed as the ratios of surface spectra to input spectra and average (mean) amplification factors for a total of 30 combinations using the five input time histories. Figure 21 shows an example of the period-dependent amplification factors for the 960 m/sec rock MCE_R input time histories. For each of the five input time histories, weighted average amplification factors are computed using the weights described in Section 6.1. The weighted average of these thirty amplification factors is applied to the rock MCE_R response spectrum to obtain the surface MCE_R response spectrum. Figure 22 compares the rock and surface MCE_R response spectra. At high ground motions the 1D equivalent linear method can overestimate damping in soils, which can result in unconservative surface ground motions. For this project, a minimum amplification factor of 0.5 was imposed. For spectral periods between 0.2 and 2 sec, there is significant amplification of the rock ground motions at this site.

7.0 SITE-SPECIFIC DESIGN SPECTRA

Design spectra were developed following the requirements of ASCE 7-16, as modified by the 2019 CBC for structures governed by the Division of the State Architect-Structural Safety (DSA-SS). As described in Section 6.0, the site-specific procedures of ASCE 7-16, Chapter 21 were used to develop rock MCE_R response spectrum.

In accordance with ASCE 7-16, Chapter 21, the average amplification factors are applied to the rock MCE_R response spectrum to develop the surface MCE_R response spectrum. This site-specific spectrum must not be less than 80% of the general ASCE 7-16 spectrum for the appropriate site class, which is Site Class D for this site (Section 3.3). The final site-specific MCE_R spectrum is the site-specific MCE_R spectrum from periods of 0.01 to 1.0 sec and the 80% code minimum at longer periods (Figure 23). The site-specific horizontal MCE_R spectrum is provided in Table 7.

Figure 24 and Table 7 provide the site-specific horizontal DE Spectra, which is defined as 2/3 the MCE_R response spectra, but not less than 80% of the general DE spectrum for Site Class D computed per ASCE 7-16 Chapter 11 (S_S = 2.164 g, S_1 = 0.835 g, F_a = 1.0, F_v = 2.5).

Site-specific spectral acceleration design parameters S_{DS} and S_{D1} were calculated in accordance with ASCE 7-16, Section 21.4 (Table 8). S_{DS} is defined as 90% of the maximum site-specific SA for spectral periods of 0.2 to 5 sec, but not less than 80% of the code S_{DS} for Site Class D. For this site, the site-specific S_{DS} is 1.62 g. S_{D1} is defined as the maximum of the site-specific SA times the spectral period for periods between 1 and 5 sec, but not less than 80% of the code S_{D1} for Site Class D. For this site, the site-specific S_{D1} is 1.11 g. S_{MS} and S_{M1}, defined as 1.5 times S_{DS} and S_{D1}, are 2.42 and 1.67 g, respectively.

8.0 REFERENCES CITED

Abrahamson, N.A., Silva, W.J., and Kamai, R., 2014, Summary of the ASK14 ground-motion relation for active crustal regions: Earthquake Spectra, v. 30, p. 1025-1055.

Al Atik, L. and Youngs, R., 2014, Epistemic uncertainty for NGA-West2 models: Earthquake Spectra, v. 30, p. 1301-1318.

AMEC, 2010, Seismic Hazard Assessment for Northern and Eastern Hydro Divisions, Southern Sierra Nevada, California: unpublished consulting report submitted to Southern California Edison.

American Society of Civil Engineers (ASCE)/Structural Engineering Institute (SEI), 2017, Minimum design loads and associated criteria for buildings and other structures, ASCE 7-16.

American Society of Civil Engineers (ASCE)/Structural Engineering Institute (SEI), 2013, Seismic evaluation and retrofit of existing buildings, ASCE 41-13.

Ancheta, T. D., Darragh, R.B., Stewart, J.P., Seyhan, E., Silva, W.J., Chiou, B.S-J., Wooddell, K.E., Graaves, R.W., Kottke, A.R, Boore, DM., Kishida, T., and Donahue, J.L., 2013, NGA-West2 Database: Earthquake Spectra, v.30, no.3, p. 989-1005.

Arizona Public Service (APS), 2015, Palo Verde Nuclear Generating Station Seismic Source Characterization, Technical Report prepared by Lettis Consultants International for Westinghouse Electric Company.

Bakun, W.H., 1999, Seismic activity of the San Francisco Bay region: Bulletin of the Seismological Society of America, v.89, p. 764-784.

Bayless, J. and Somerville, P. 2013. Bayless-Somerville Directivity Model, Chapter 3 of PEER Report No. 2013/09, P. Spudich (Editor), Pacific Earthquake Engineering Research Center, Berkeley, CA.

Bishop et al., 1973

Boore, D.M., Stewart, J.P., Seyhan, E., and Atkinson, G.M., 2014, NGA-West2 equations for predicting PGA, PGV, and 5%-damped PSA for shallow crustal earthquakes: Earthquake Spectra, v. 30, p. 1057-1085.

California Building Standards Commission, 2019, California Building Code (CBC), California Code of Regulations, Title 24, Vol. 1 and 2.

Campbell, K.W. and Bozorgnia, Y., 2014, NGA-West2 ground motion model for the average horizontal components of PGA, PGV, and 5%-damped linear acceleration response spectra: Earthquake Spectra, v. 30, p. 1087-1115.

Cao, T., Bryant, W.A, Rowshandel, B., Branum, D., Wills, C.J., 2003, The revised 2002 California probabilistic seismic hazard maps, June 2003: California Geological Survey, http://www.consrv.ca.gov/CGS/rghm/psha/fault_parameters/pdf/2002_CA_Hazard_Maps.pdf.

Chiou, B-S.J. and Youngs, R.R., 2014, Update of the Chiou and Youngs NGA ground motion model for average horizontal component of peak ground motion and response spectra: Earthquake Spectra, v. 30, p. 1117-1153.

ConeTec, 2020, Presentation of site investigation results, Lake Elementary School: unpublished report for Alan Kropp & Associates, 24 February 2020.

dePolo, C. M., 1994, The maximum background earthquake for the Basin and Range Province, western North America: Bulletin of the Seismological Society of America, v. 84, p. 466-472.

Electric Power Research Institute (EPRI), 1993, Guidelines for determining design basic ground motions, v. 1: Method and guidelines for estimating earthquakes ground motion in eastern North America: EPRI Report TR-102293.

EPRI/DOE/NRC, 2012, Technical Report: Central and Eastern United States Seismic Source Characterization for Nuclear Facilities: EPRI, Palo Alto, CA, U.S. DOE, and U.S. NRC: 2012.

Field, E.H., Biasi, G.P., Bird, P., Dawson, T.E., Felzer, K.R., Jackson, D.D., Johnson, K.M., Jordan, T.H., Madden, C., Michael, A.J., Milner, K.R., Page, M.T., Parsons, T., Powers, P.M., Shaw, B.E., Thatcher, W.R., Weldon, R.J., II, and Zeng, Y., 2013, Uniform California earthquake rupture forecast, version 3 (UCERF3)—The time-independent model: U.S. Geological Survey Open-File Report 2013–1165, 97 p., California Geological Survey Special Report 228, and Southern California Earthquake Center Publication 1792, http://pubs.usgs.gov/of/2013/1165/.

Gardner, J.K., and Knopoff, L., 1974, Is the sequence of earthquakes in southern California, with aftershocks removed, Poissonian?: Bulletin of the Seismological Society of America, v. 64, p. 1363–1367.

Hale, C., Abrahamson, N. and Bozorgnia, Y., 2018, Probabilistic seismic hazard analysis code verification: Pacific Earthquake Engineering Research Center, College of Engineering, University of California, Berkeley, PEER Report 2018/03, 105 p.

Hecker, S., Pantosti, D., Schwartz, D., Hamilton, J., Reidy, L., and Power, T., 2005, The most recent large earthquake on the Rodgers Creek fault, San Francisco Bay area: Bulletin of the Seismological Society of America, v. 95, p. 844-860.

Idriss, I.M. and Seed, H.B., 1968, Seismic response of horizontal soil layers: Journal of Soil Mechanics and Foundations Division, v. 94, p. 1003-1031.

Keefer, D.I. and Bodily, S.E., 1983, Three-point approximations for continuous random variables: Management Science, v. 26, p. 595-609.

Lienkaemper, J.J., 1992, Map of recently active traces of the Hayward fault, Alameda and Contra Costa counties, California: U.S. Geological Survey Miscellaneous Field Studies Map MF-2196, 1:24,000.

Lienkaemper, J.J., McFarland, F.S., Simpson, R.W., Bilham, R.G., Ponce, D.A., Boatwright, J.J. and Caskey, S.J., 2012, Long-term creep rates on the Hayward fault: Evidence for controls on the size and frequency of large earthquakes: Bulletin of the Seismological Society of America, v. 102, p. 31–41.

Lienkaemper, J.J. Schwartz, D.P., Kelson, K.I., Lettis, W.R., Simpson, G.D., Southon, J.R. Wanket, J.A., Williams, P.L., 1999, Timing of paleoearthquakes on the northern Hayward fault – preliminary evidence in El Cerrito, California: U.S. Geological Survey Open-File Report 99-318, 34 p.

Lienkaemper, J.J., Williams, P.L., and Guilderson, T.P., 2010, Evidence for a 12th large earthquake on the southern Hayward fault in the past 1900 years: Bulletin of the Seismological Society of America, v. 100, p. 2024-2034.

Miller, A.C., and Rice, T.R., 1983, Discrete approximations of probability distributions: Management Science, v. 29, p. 352-362.

Petersen, M.D., Frankel, A.D., Harmsen, S.C., Mueller, C.S., Haller, K.M., Wheeler, R.L., Wesson, R.L., Zeng, Y., Boyd, O.S., Perkins, D.M., Luco, N., Field, E.H., Wills, C.J., and Rukstales, K.S., 2014, Documentation for the 2014 update of the United States National Seismic Hazard Maps: U.S. Geological Survey Open-File Report 2014-1091, 243 p.

Schnabel, P.B., Lysmer, J., and Seed, H.B., 1972, SHAKE – A computer program for earthquake analysis of horizontally layered sites: Earthquake Engineering Research Center, University of California, Berkeley, Report No. EERC 72-12.

Schwartz, D.P., 2018, Review: Past and future fault rupture lengths in seismic source characterization – The long and short of it: Bulleting of the Seismological Society of America, v 108, p. 2493-2520.

Schwartz, D.P., Pantosti, D., Hecker, S., Okomura, K., Budding, K.E. and Powers, T., 1992, Late Holocene behavior and seismogenic potential of the Rodgers Creek fault zone, Sonoma County, California, in Proceedings of the Second Conference on Earthquake Hazards in the Eastern San Francisco Bay Area, Borchardt, G., Hirschfeld, S.E., Lienkaemper, J.J., McClellan, P., Williams, P.L. and Wong, I.G. (eds.), California Division of Mines and Geology Special Publication 113, p. 393-398.

Schwartz, D.P., Lienkaemper, J.J., Hecker, S., Kelson, K., Fumal, T.E., Baldwin, J.N., Seitz, G.G., and Niemi, T.M., 2014, The earthquake cycle in the San Francisco Bay region: A.D. 1600-2012; Bulletin of the Seismological Society of America, v. 104, p. 1299-1328.

Shahi, S.K. and Baker, J.W., 2013, NGA-West2 models for ground-motion directionality: Pacific Earthquake Engineering Research Center, PEER Report 2013/10, 73 p.

Silva, W.J., Abrahamson, N.A., Toro, G., and Constantino, C., 1997, Description and validation of the stochastic ground motion model: unpublished report prepared for the Brookhaven National Laboratory.

Silva, W.J. and Lee, K., 1987, WES RASCAL code for synthesizing earthquake ground motions: State-of-the-art for Assessing Earthquake Hazards in the United States, Report 24: U.S. Army Engineer Waterways Experiment Station Miscellaneous Paper S-73-1, 120 p.

Stepp, J.C., 1972, Analysis of completeness of the earthquake sample in the Puget Sound area and its effect on statistical estimates of earthquake hazard: Proceedings of the International Conference on Microzonation, v. 2, 897-910.

Toppozada, T.R. and Borchardt, G., 1998, Re-evaluation of the 1836 “Hayward Fault” earthquake and the 1838 San Andreas fault earthquake: Bulletin of the Seismological Society of America, v. 88, p. 140-159.

Toppozada, T.R., Real, C.R., and Parke, D.L., 1981, Preparation of isoseismal maps and summaries of reported effects for pre-1900 California earthquakes: California Division of Mines and Geology Open-File Report 81-11, 181 p.

Toro, G.R., 1996, Probabilistic models of site velocity profiles for generic and site-specific ground motion amplification studies. Appendix in Silva et al (1997).

URS Corporation/Jack R. Benjamin & Associates, Inc., 2007, Technical memorandum topical area: seismic hazard, Delta Risk Management Study (DRMS) Phase 1, unpublished report submitted to California Department of Water Resources.

URS Corporation, 2012, Update of the Probabilistic and Deterministic Seismic Hazard Analyses of Success Dam, California, unpublished report submitted to U.S. Army Corps of Engineers.

U.S. Geological Survey (USGS), 2018, Advanced National Seismic System (ANSS) Comprehensive Earthquake Catalog (ComCat): available at: https://earthquake.usgs.gov/earthquakes/search/.

Wagner, D.L. and Bortugno, E.J., 1982, Geologic map of the Santa Rosa quadrangle: California Division of Mines and Geology, Regional Geologic Map Series No. 2A, 1:250,000.

Watt, J., 2016, Missing link between the Hayward and Rodgers Creek faults: Science Advances: 19 October 2016, 8 p.

WGCEP (Working Group for California Earthquake Probabilities), 2008, The Uniform Earthquake Rupture Forecast, version 2 (UCERF2): U.S. Geological Survey Open-File Report 2007-1437.

WGCEP (Working Group on California Earthquake Probabilities), 2003, Earthquake probabilities in the San Francisco Bay region: 2002–2031: U.S. Geological Survey Open-File Report 03-214.

WGCEP (Working Group on California Earthquake Probabilities), 1999, Earthquake probabilities in the San Francisco Bay Region: 2000 to 2030 – A summary of findings: U.S. Geological Survey Open-File Report 99-517.

WGNCEP (Working Group On Northern California Earthquake Potential), 1996, Database of potential sources for earthquakes larger than magnitude 6 in Northern California: U.S. Geological Survey Open-File Report 96-705.

Wong, I.G., 1991, Contemporary seismicity, active faulting and seismic hazards of the Coast Ranges between San Francisco Bay and Healdsburg, California: Journal of Geophysical Research, v. 96, p. 19891-19904.

Wong, I.G., Thomas, P.A., Unruh, J., Hanson, K., and Youngs, R.R., 2008, characterizing the earthquake ground shaking hazard in the Sacramento-San Joaquin Delta, California: Geotechnical Engineering and Soil Dynamics IV Conference Proceedings, pp. 1-11.

Tables

Table 1. Recurrence Parameters for the Background Seismic Source Zones

REALIZATION	*b*-VALUE	N(M>5)	WEIGHT
CRP Zone			
1	0.95	0.17924	[0.125]
2	0.95	0.17339	[0.125]
3	1.01	0.14216	[0.125]
4	0.97	0.16091	[0.125]
5	0.95	0.17330	[0.125]
6	0.92	0.20408	[0.125]
7	0.91	0.20355	[0.125]
8	1.04	0.13930	[0.125]
CRGVN Zone			
1	0.64	0.01713	[0.125]
2	0.80	0.01359	[0.125]
3	1.01	0.00331	[0.125]
4	0.84	0.00792	[0.125]
5	0.90	0.00929	[0.125]
6	1.14	0.00318	[0.125]
7	0.75	0.00489	[0.125]
8	0.92	0.00531	[0.125]
CRGVS Zone			
1	0.96	0.03293	[0.125]
2	1.06	0.02008	[0.125]
3	0.87	0.04091	[0.125]
4	0.92	0.03597	[0.125]
5	1.02	0.02375	[0.125]
6	0.84	0.04821	[0.125]
7	0.93	0.03967	[0.125]
8	0.77	0.04810	[0.125]

Table 2. DSHA Input Parameters

INPUT PARAMETER	INPUT PARAMETER DEFINITION	HAYWARD SOUTH EXTENSION-HAYWARD-RODGERS CREEK-HEALDSBURG
M	Moment magnitude	7.6
R_{RUP}	Closest distance to coseismic rupture (km)	1.7
R_{JB}	Closest distance to surface projection of coseismic rupture (km)	1.7
R_X	Horizontal distance from top of rupture measured perpendicular to fault strike (km)	1.7
R_{y0}	The horizontal distance off the end of the rupture measured parallel to strike (km)	0
U	Unspecified-mechanism factor: 1 for unspecified; 0 otherwise	0
F_{RV}	Reverse-faulting factor: 0 for strike slip, normal, normal-oblique; 1 for reverse, reverse-oblique and thrust	0
F_N	Normal-faulting factor: 0 for strike slip, reverse, reverse-oblique, thrust and normal-oblique; 1 for normal	0
F_{HW}	Hanging-wall factor: 1 for site on down-dip side of top of rupture; 0 otherwise	0
Z_{TOR}	Depth to top of coseismic rupture (km)	0
Dip	Average dip of rupture plane (degrees)	90
V_{S30}	The average shear-wave velocity (m/s) over a subsurface depth of 30 m	960
$F_{Measured}$	0 = inferred, 1 = measured	0
Z_{HYP}	Hypocentral depth from the earthquake	Default
$Z_{1.0}$	Depth to Vs=1 km/sec	Default
$Z_{2.5}$	Depth to Vs=2.5 km/sec	Default
W	Fault rupture width (km)	Default
$Region$	Specific Regions considered in the models	California

Table 3. Calculation of Deterministic Rock MCE as per ASCE 7-16, Chapter 21

Period (sec)	84th deterministic Rock spectrum, Geomean[1] SA (g)	Maximum Direction Factor[2]	Fault Normal Factor[3]	Site-Specific Deterministic Rock MCE[4] SA (g)
0.01	0.846	1.19	1.00	1.006
0.02	0.876	1.19	1.00	1.042
0.03	1.000	1.19	1.00	1.190
0.05	1.341	1.19	1.00	1.596
0.075	1.729	1.19	1.00	2.058
0.1	1.922	1.19	1.00	2.287
0.15	2.018	1.20	1.00	2.422
0.2	1.864	1.21	1.00	2.255
0.25	1.685	1.22	1.00	2.056
0.3	1.528	1.22	1.00	1.865
0.4	1.292	1.23	1.00	1.589
0.5	1.112	1.23	1.00	1.368
0.75	0.824	1.24	1.14	1.022
1	0.634	1.24	1.22	0.786
1.5	0.410	1.24	1.24	0.509
2	0.298	1.24	1.33	0.398
3	0.205	1.25	1.41	0.290
4	0.152	1.26	1.49	0.226
5	0.119	1.26	1.52	0.181
7.5	0.066	1.28	1.53	0.101
10	0.043	1.29	1.56	0.066

[1] 84th deterministic spectrum, geomean using V_S30 = 960 m/sec (Section 5)
[2] Maximum-direction factors from Shahi and Baker (2013)
[3] Fault-normal spectrum computed using the model of Bayless and Somerville (2013)
[4] Minimum deterministic SA for Site Class B is 1.35 g (Fa=0.9)

Table 4. Calculation of Probabilistic Rock MCE_R as per ASCE 7-16, Chapter 21

Period (sec)	2,475-YR UHS, Geomean[1] SA (g)	Maximum Direction Factor[2]	2,475-YR UHS, Maximum Direction SA (g)	2,475-YR UHS, Fault-Normal[3] SA (g)	Risk coefficient[4]	Site-Specific Probabilistic MCE_R SA (g)
0.01	1.040	1.19	1.238	1.040	0.904	1.119
0.02	1.085	1.19	1.291	1.085	0.904	1.167
0.03	1.277	1.19	1.519	1.277	0.904	1.373
0.05	1.808	1.19	2.152	1.808	0.904	1.945
0.075	2.340	1.19	2.784	2.340	0.904	2.517
0.1	2.564	1.19	3.051	2.564	0.904	2.758
0.15	2.601	1.20	3.121	2.601	0.904	2.821
0.2	2.352	1.21	2.845	2.352	0.904	2.572
0.25	2.068	1.22	2.523	2.068	0.903	2.279
0.3	1.861	1.22	2.271	1.861	0.903	2.050
0.4	1.537	1.23	1.890	1.537	0.902	1.705
0.5	1.307	1.23	1.608	1.307	0.901	1.448
0.75	0.943	1.24	1.170	0.986	0.898	1.050
1	0.702	1.24	0.871	0.733	0.895	0.779
1.5	0.433	1.24	0.537	0.449	0.895	0.481
2	0.308	1.24	0.382	0.333	0.895	0.342
3	0.200	1.25	0.250	0.222	0.895	0.224
4	0.143	1.26	0.181	0.164	0.895	0.162
5	0.112	1.26	0.142	0.129	0.895	0.127
7.5	0.066	1.28	0.084	0.075	0.895	0.075
10	0.043	1.29	0.056	0.049	0.895	0.050

[1] 2,475-Yr UHS, geomean using V_S30 = 960 m/sec (Section 4)
[2] Maximum-direction factors from Shahi and Baker (2013)
[3] Fault-normal spectrum computed using the model of Bayless and Somerville (2013)
[4] Risk coefficients from https://seismicmaps.org/ accessed 1 October 2021

Table 5. Calculation of Site-Specific Rock MCE_R as per ASCE 7-16, Chapter 21

Period (sec)	Site-Specific Probabilistic MCE_R SA (g)	Site-Specific Deterministic MCE SA (g)	80% ASCE 7-16 MCE_R, Site Class B[1] SA (g)	Site-Specific MCE_R SA (g)
0.01	1.119	1.006	0.758	1.006
0.02	1.167	1.042	0.894	1.042
0.03	1.373	1.190	1.030	1.190
0.05	1.945	1.596	1.303	1.596
0.075	2.517	2.058	1.555	2.058
0.1	2.758	2.287	1.555	2.287
0.15	2.821	2.422	1.555	2.422
0.2	2.572	2.255	1.555	2.255
0.25	2.279	2.056	1.555	2.056
0.3	2.050	1.865	1.555	1.865
0.4	1.705	1.589	1.333	1.589
0.5	1.448	1.368	1.066	1.368
0.75	1.050	1.022	0.711	1.022
1	0.779	0.786	0.533	0.779
1.5	0.481	0.509	0.355	0.481
2	0.342	0.398	0.267	0.342
3	0.224	0.290	0.178	0.224
4	0.162	0.226	0.133	0.162
5	0.127	0.181	0.107	0.127
7.5	0.075	0.101	0.071	0.075
10	0.050	0.066	0.043	0.050

[1] S_S = 2.16 g, S_1 = 0.833 g, Site Class B, Fa = 0.9, Fv = 0.8

Table 6. Scaled Input Time Histories for Site Response Analysis

RSN	YEAR	EARTHQUAKE NAME	STATION NAME	MAG (M)	R_{RUP} (km)	V_{S30} (m/sec)	COMP	SCALE FACTOR	PGA (g)	PGV (cm/sec)	PGD (cm)	ARIAS INTENSITY (m/sec)	5-95% DURATION (sec)
143	1978	Tabas, Iran	Tabas	7.4	2.1	767	L1	0.99	0.85	98.2	37.3	11.7	16.5
801	1989	Loma Prieta	San Jose - Santa Teresa Hills	6.9	14.7	672	225	3.47	0.96	97.8	80.3	15.7	10.1
825	1992	Cape Mendocino	Cape Mendocino	7.0	7.0	568	000	0.92	1.37	112.5	30.0	5.0	6.2
1549	1999	Chi-Chi, Taiwan	TCU129	7.6	1.8	511	E	1.19	1.19	74.4	72.1	13.0	27.3
1633	1990	Manjil, Iran	Abbar	7.4	12.6	724	L	1.88	0.96	79.6	27.9	16.3	28.7

Table 7. Site-Specific Surface MCER and DE Spectra as per ASCE 7-16, Chapter 21

Period (sec)	Site-Specific Rock MCE_R * Site AFs [1] SA (g)	80% ASCE 7-16 MCE_R, Site Class D SA (g)	Site-Specific MCE_R SA (g)	2/3 MCE_R SA (g)	80% ASCE 7-10 DE, Site Class D[2] SA (g)	Site-Specific DE SA (g)
0.01	1.356	0.746	1.356	0.904	0.498	0.904
0.02	1.388	0.800	1.388	0.926	0.533	0.926
0.03	1.421	0.854	1.421	0.947	0.569	0.947
0.05	1.714	0.962	1.714	1.143	0.641	1.143
0.075	1.976	1.096	1.976	1.317	0.731	1.317
0.1	2.188	1.231	2.188	1.459	0.821	1.459
0.15	2.479	1.500	2.479	1.653	1.000	1.653
0.193	-	1.731	2.666	1.777	1.154	1.777
0.2	2.693	1.731	2.693	1.796	1.154	1.796
0.25	2.684	1.731	2.684	1.790	1.154	1.790
0.3	2.677	1.731	2.677	1.785	1.154	1.785
0.4	2.533	1.731	2.533	1.689	1.154	1.689
0.5	2.371	1.731	2.371	1.580	1.154	1.580
0.75	2.084	1.731	2.084	1.390	1.154	1.390
0.965	-	1.731	1.731	1.154	1.154	1.154
1	1.537	1.670	1.670	1.113	1.113	1.113
1.5	0.793	1.113	1.113	0.742	0.742	0.742
2	0.523	0.835	0.835	0.557	0.557	0.557
3	0.286	0.557	0.557	0.371	0.371	0.371
4	0.183	0.418	0.418	0.278	0.278	0.278
5	0.135	0.334	0.334	0.223	0.223	0.223
7.5	0.079	0.223	0.223	0.148	0.148	0.148
10	0.054	0.134	0.134	0.089	0.089	0.089

[1] AFs = Amplification factors
[2] S_S = 2.164, S_1 = 0.835, Fa = 1.0, Fv = 2.5

Table 8. Site-Specific Ground Motion Parameters as per ASCE 7-16, Chapter 21

PARAMETER	DESCRIPTION	VALUE
S_S	Mapped Short-Period (0.2 sec) Spectral Acceleration Value (Site Class B)	2.16 g
S_1	Mapped Long-Period (1.0 sec) Spectral Acceleration Value (Site Class B)	0.833 g
Seismic Design Category	Based on 1.0 sec mapped spectral acceleration, S1, as per 2019 CBC Section 1613A.3.5	E
Site Class	Site Class Based on ASCE 7-16 Chapter 20	D
F_a	Site Class D	1.0
F_v	Site Class D	2.5*
C_{RS}	Short-period risk coefficient	0.904
C_{R1}	Long-Period risk coefficient	0.895
S_{DS}, Site-Specific	90% of maximum SA for periods between 0.2 and 5 sec, but not less than 80% code S_{DS}	1.62 g
S_{D1}, Site-Specific	Maximum of SA*T for periods between 1 and 5 sec, but not less than 80% code S_{D1}	1.11 g
S_{MS}, Site-Specific	1.5*S_{DS}	2.42 g
S_{M1}, Site-Specific	1.5*S_{D1}	1.67 g
PGA_M	Site-Specific MCE_G peak ground acceleration	1.14 g
M	Magnitude for liquefaction analysis based on deterministic analysis	7.6
R	Distance for liquefaction analysis based on deterministic analysis	1.7 km

*Fv factor used for minimum site-specific spectrum as per ASCE 7-16, Section 21.3

Figures

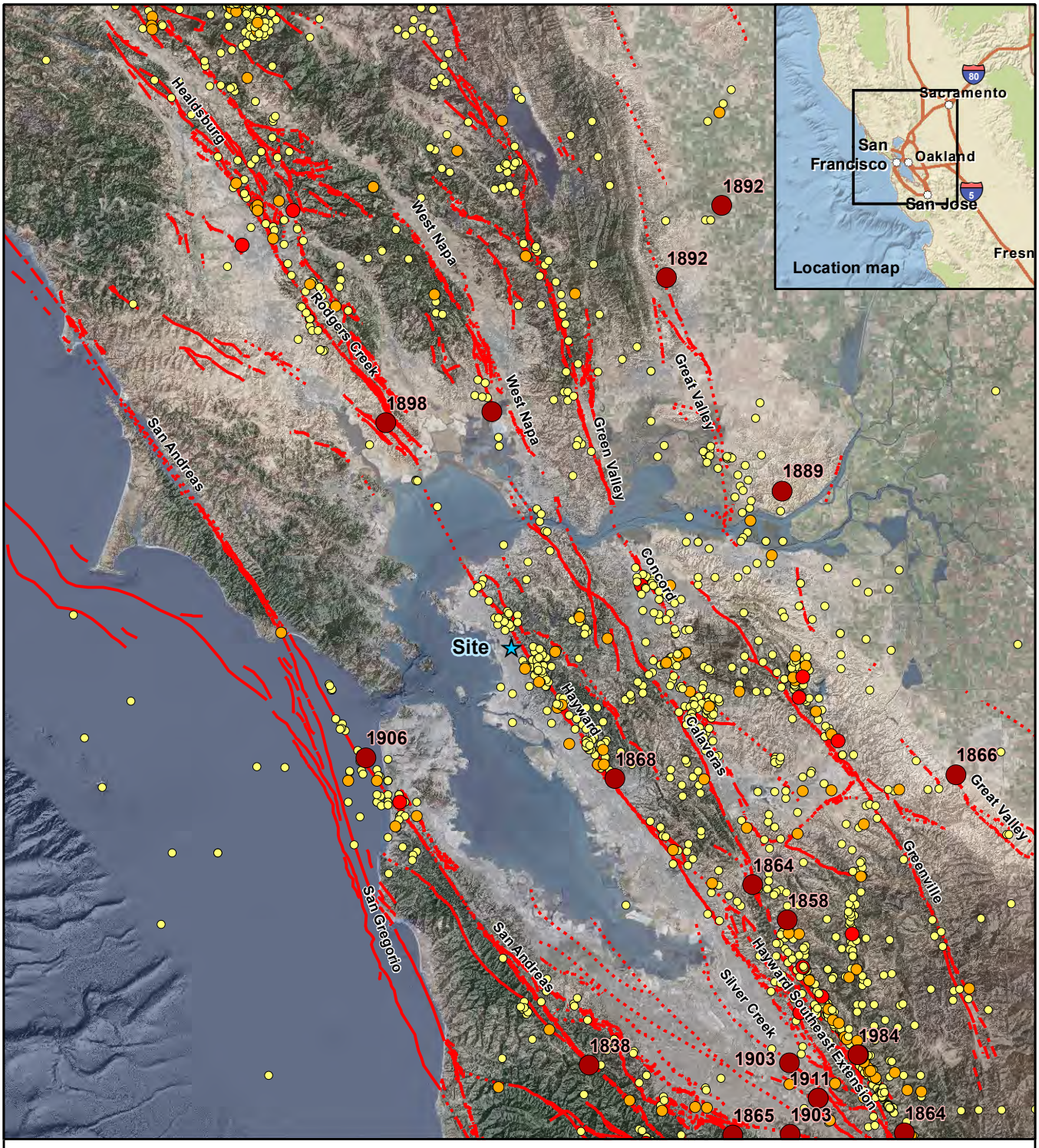

EXPLANATION

Site location

Fault; solid where well constrained, dashed where moderately constrained, dotted where inferred (USGS, 2018)

Magnitude

- 3.0 - 4.0
- 4.1 - 5.0
- 5.1 - 6.0
- 6.1 - 7.0

N W E S

0 10 20 mi

0 20 40 km

Map projection and scale: NAD 1983 UTM Zone 10N, 1:900,000

Historical Seismicity (M > 3.0, 1800 - 2019) and Quaternary Faults in the San Francisco Bay Region

BERKELEY CITY COLLEGE

LCI Lettis Consultants International, Inc.

Figure 1

File path: S:\2045\00_Figures\Figure_01_BCC.mxd; Date: 10/13/2021; User: Javier, LCI; Rev.1

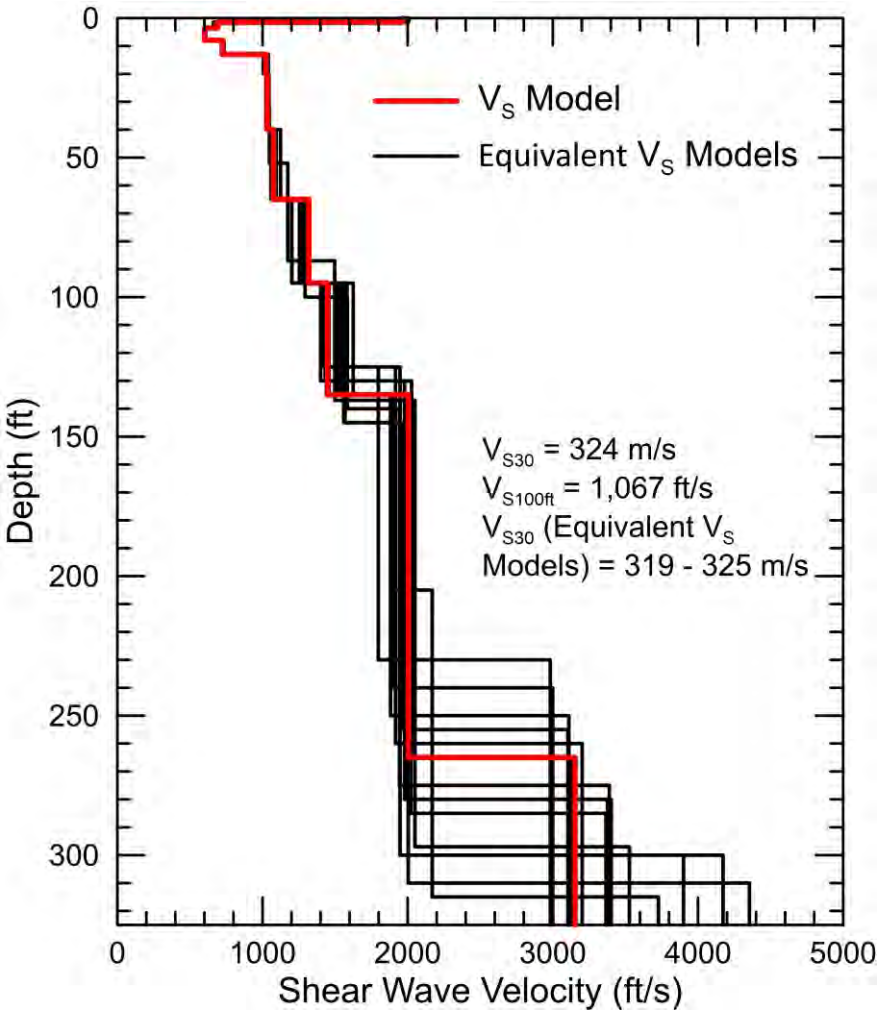

Vs Profiles from GEOVision

BERKELEY CITY COLLEGE

Lettis Consultants International, Inc. | Figure **2**

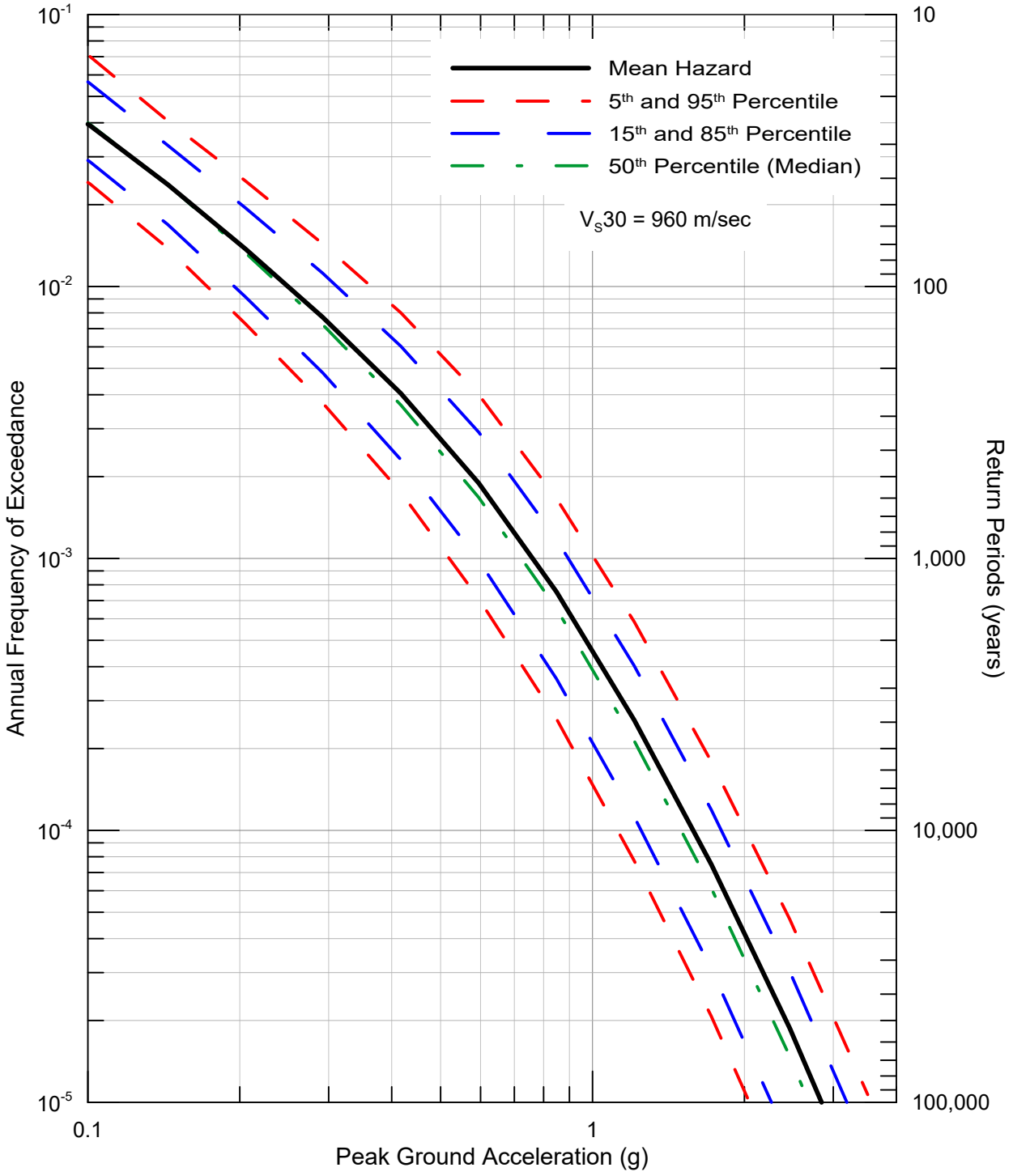

Seismic Hazard Curves for Peak Horizontal Acceleration for Rock

BERKELEY CITY COLLEGE, CA

Lettis Consultants International, Inc. | Figure 3

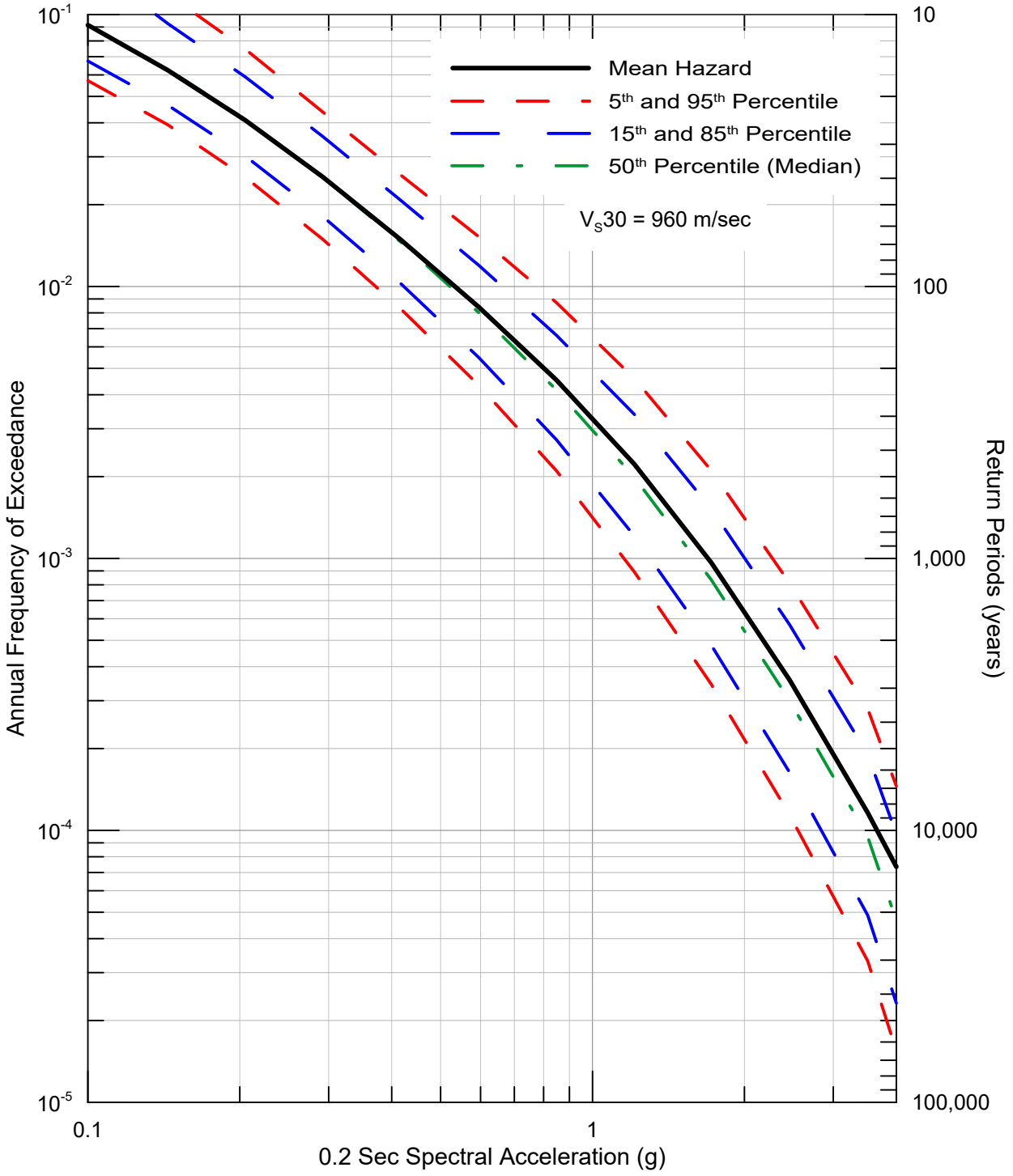

Seismic Hazard Curves for 0.2 Sec Horizontal Spectral Acceleration for Rock

BERKELEY CITY COLLEGE, CA

Lettis Consultants International, Inc. | Figure 4

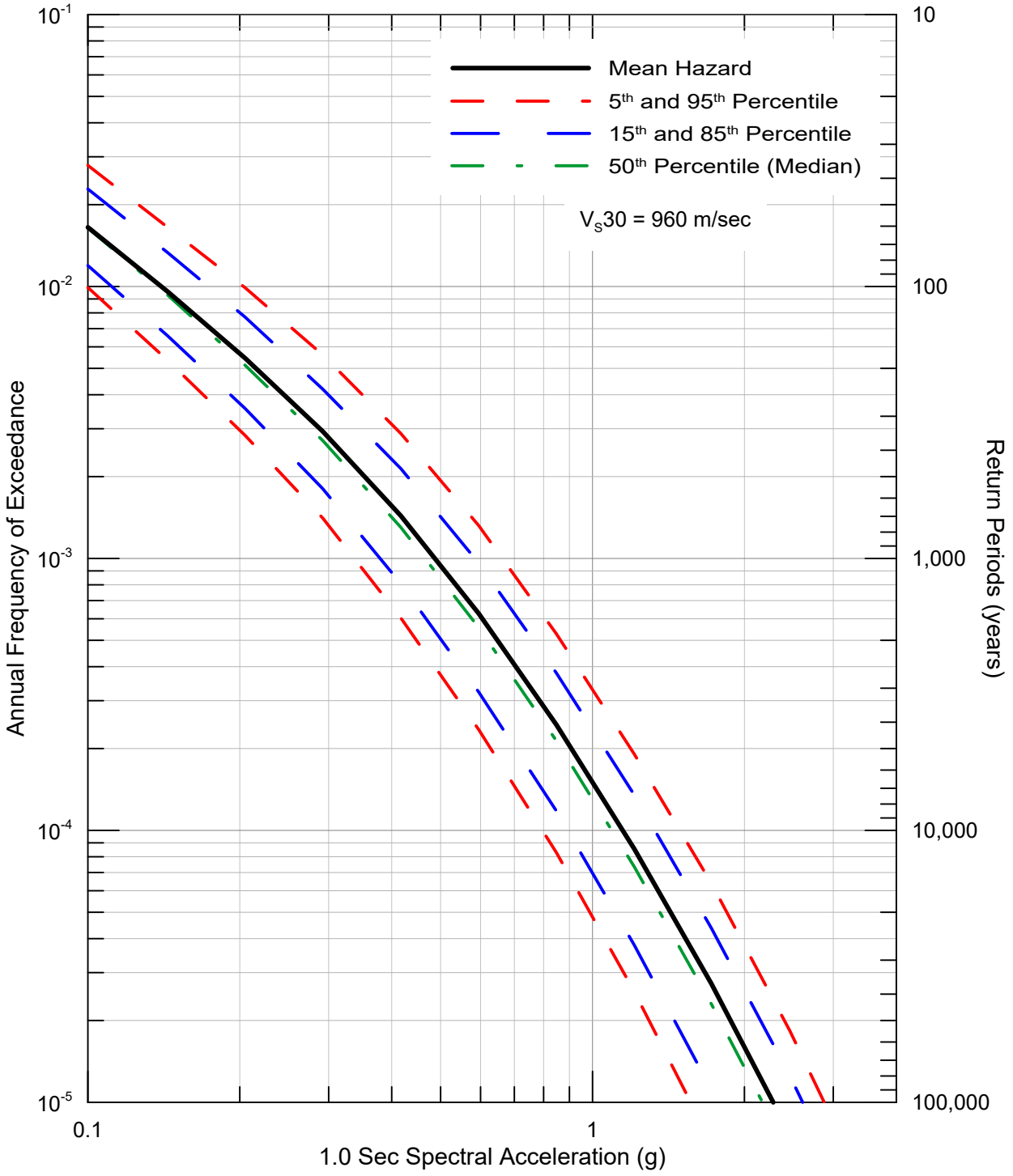

Seismic Hazard Curves for 1.0 Sec Horizontal Spectral Acceleration for Rock

BERKELEY CITY COLLEGE, CA

Lettis Consultants International, Inc. | Figure **5**

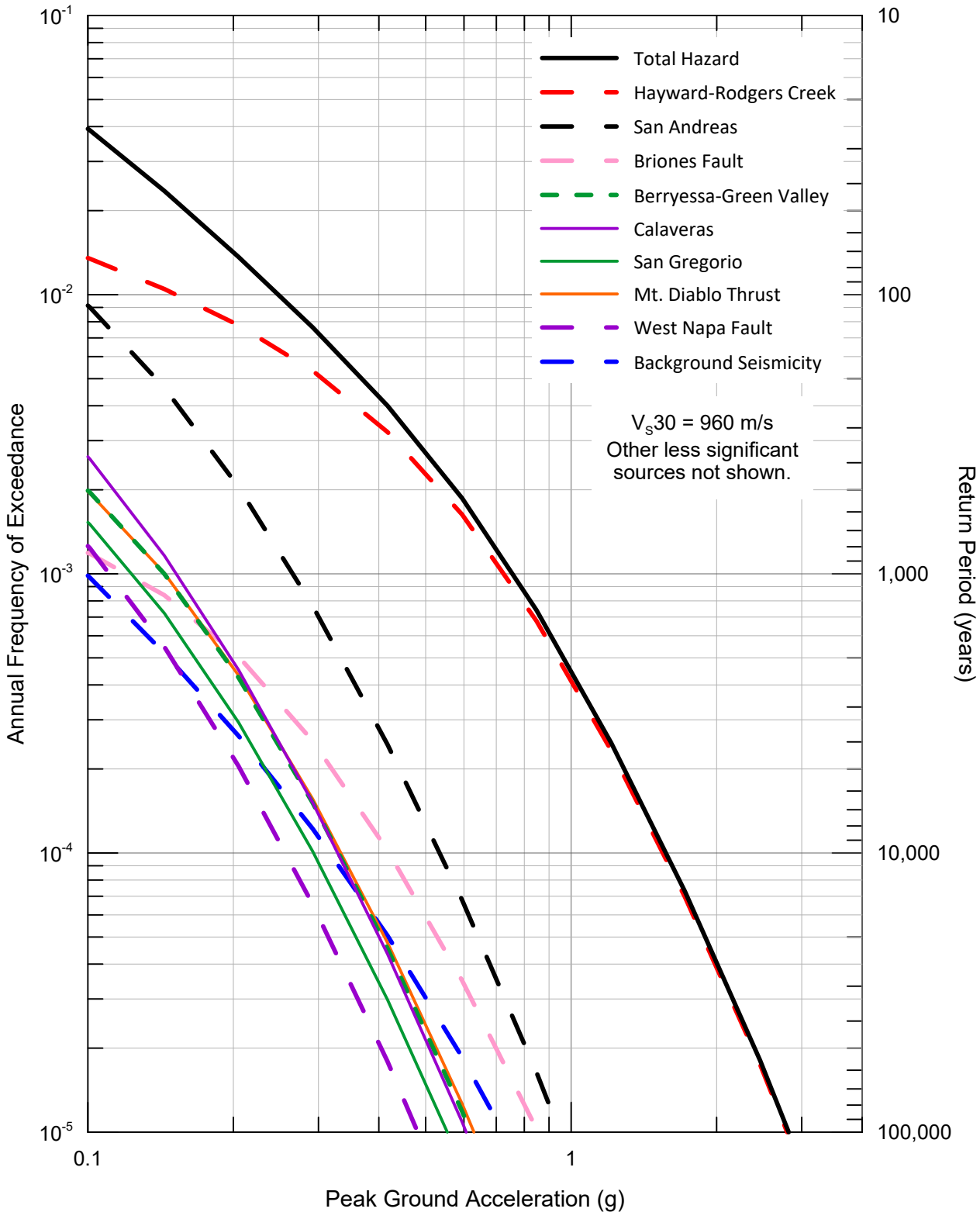

Seismic Source Contributions to Mean Peak Horizontal Acceleration Hazard for Rock

BERKELEY CITY COLLEGE, CA

Lettis Consultants International, Inc. | Figure **6**

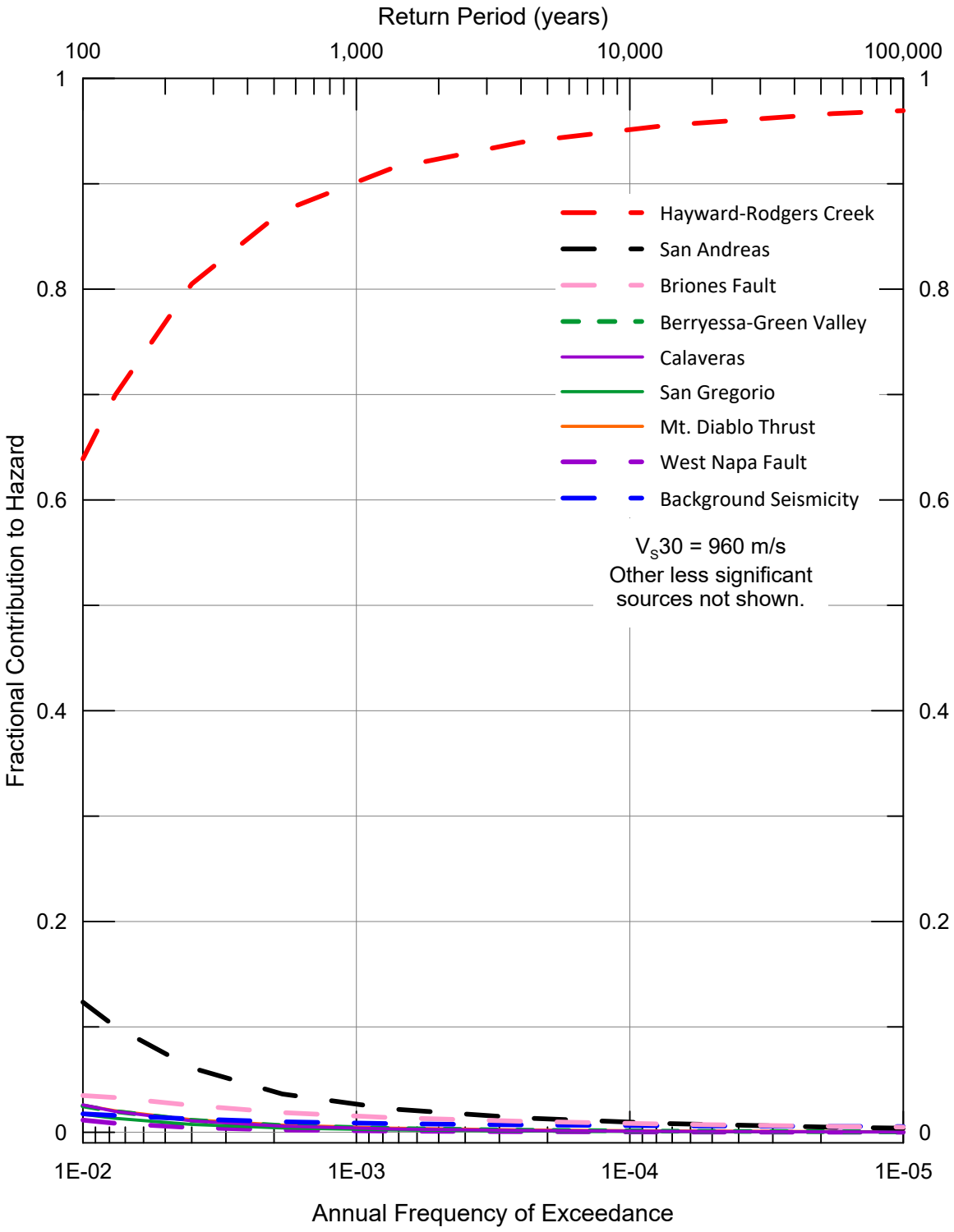

Seismic Source Fractional Contributions to Mean Peak Horizontal Acceleration Hazard for Rock

BERKELEY CITY COLLEGE, CA

LCI **Lettis Consultants International, Inc.** | Figure **7**

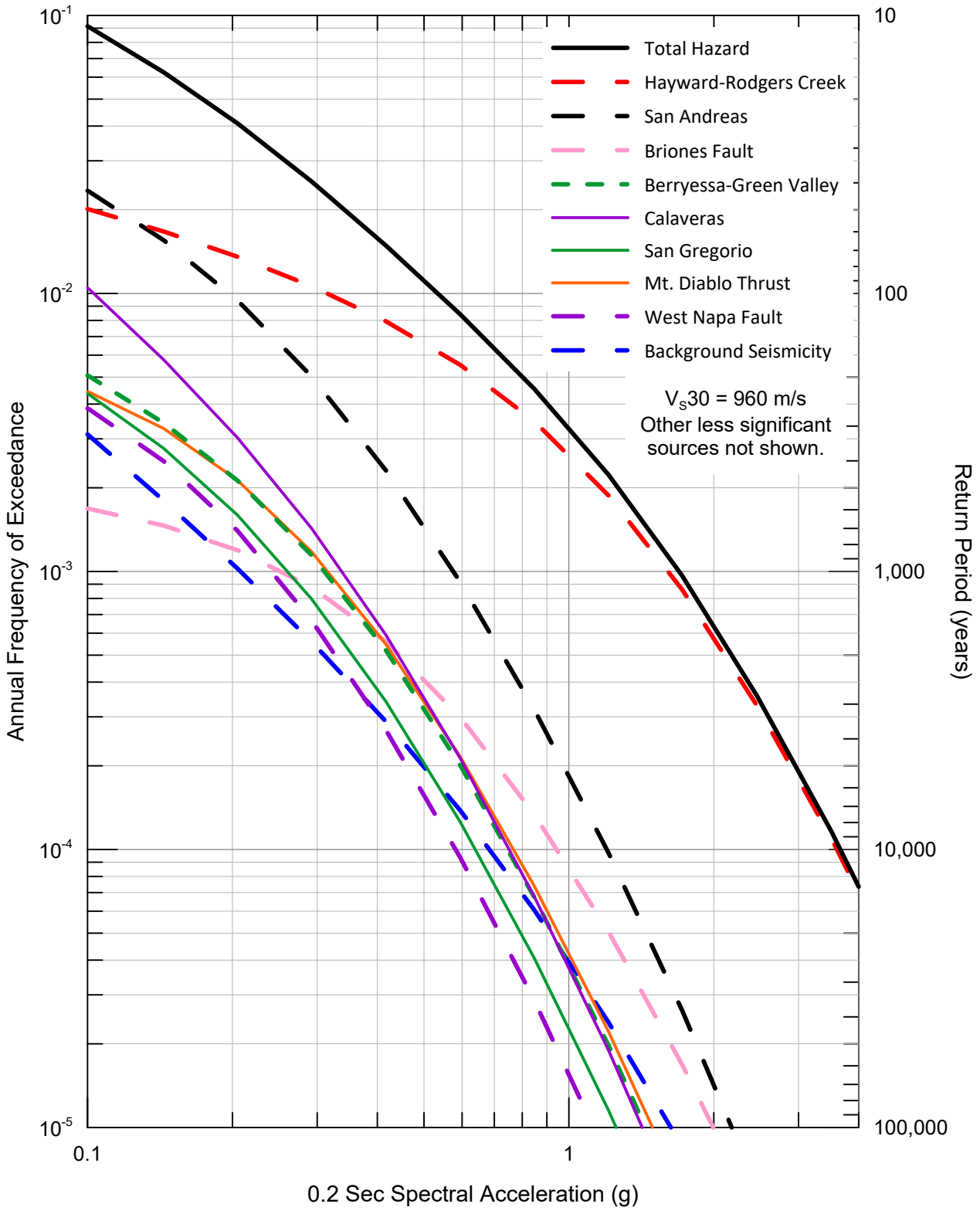

Seismic Source Contributions to Mean 0.2 Sec Horizontal Spectral Acceleration Hazard for Rock

BERKELEY CITY COLLEGE, CA

Lettis Consultants International, Inc. | Figure **8**

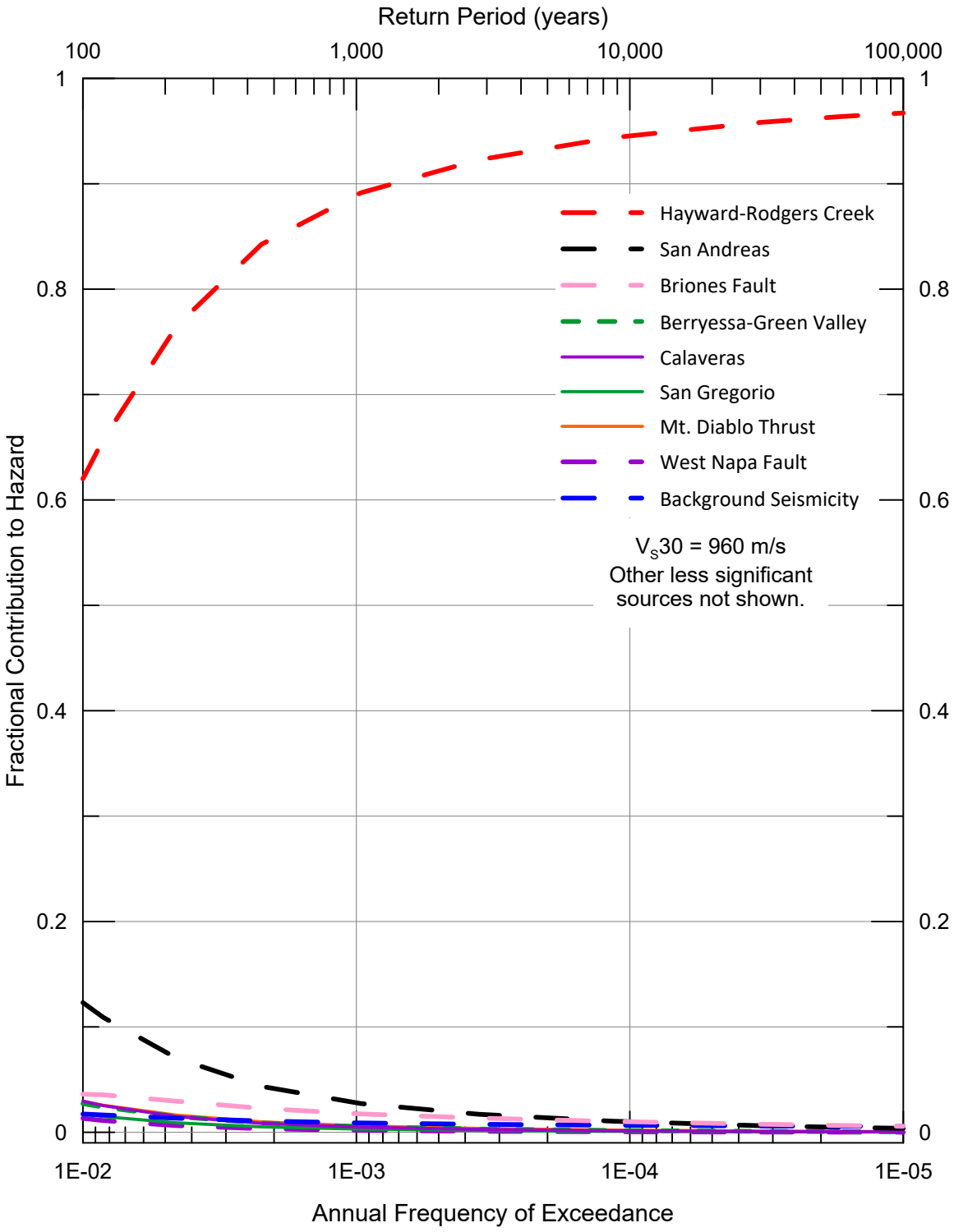

Seismic Source Fractional Contributions to Mean 0.2 Sec Horizontal Spectral Acceleration Hazard for Rock

BERKELEY CITY COLLEGE, CA

Lettis Consultants International, Inc.

Figure **9**

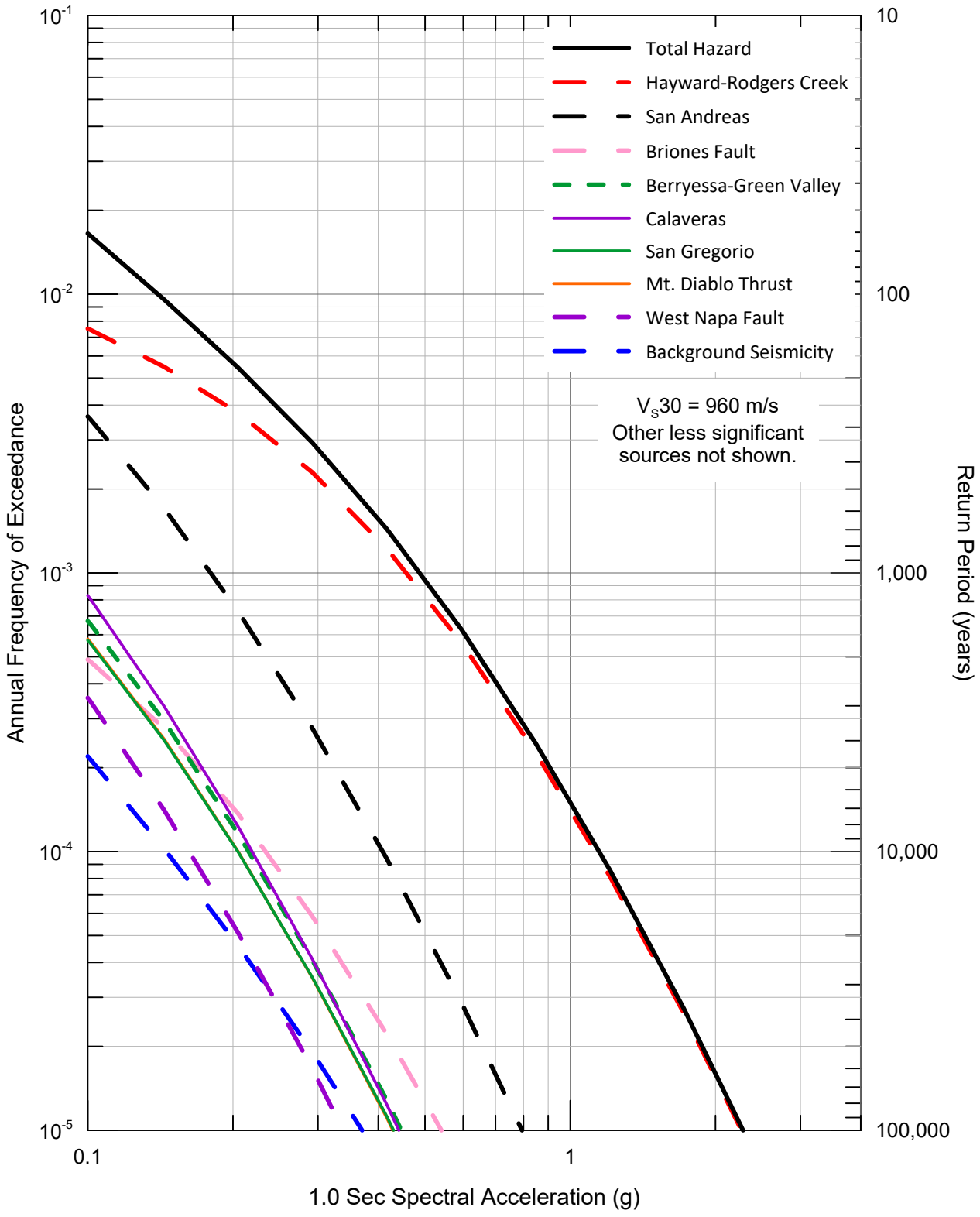

Seismic Source Contributions to Mean 1.0 Sec Horizontal Spectral Acceleration Hazard for Rock

BERKELEY CITY COLLEGE, CA

Lettis Consultants International, Inc. | Figure **10**

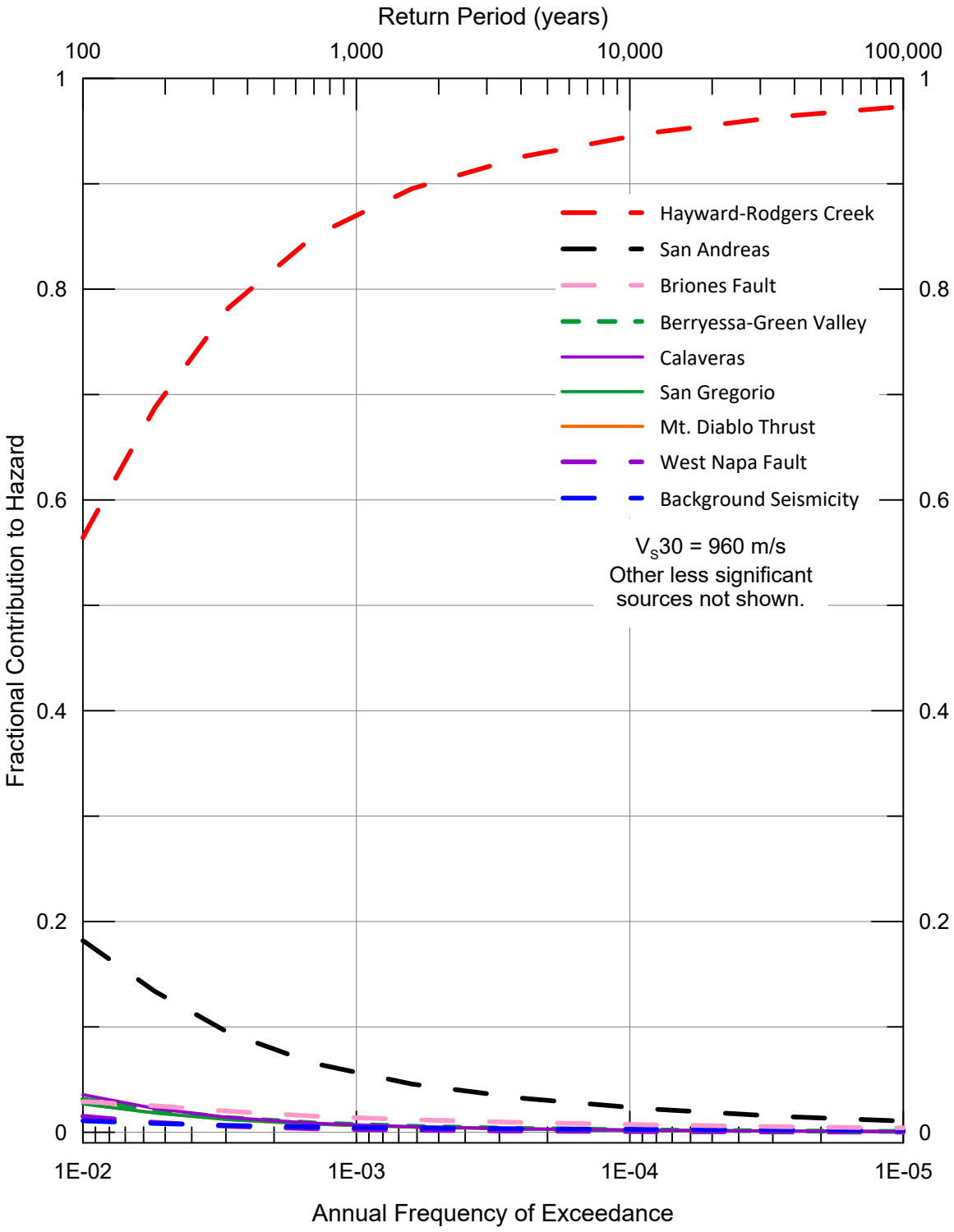

Seismic Source Fractional Contributions to Mean 1.0 Sec Horizontal Spectral Acceleration Hazard for Rock

BERKELEY CITY COLLEGE, CA

Lettis Consultants International, Inc. | Figure **11**

2,475-Year Return Period, PGA
Modal **M,** Rrup: 6.9, 2.5 km
Mean **M,** Rrup: 6.7, 3.6 km

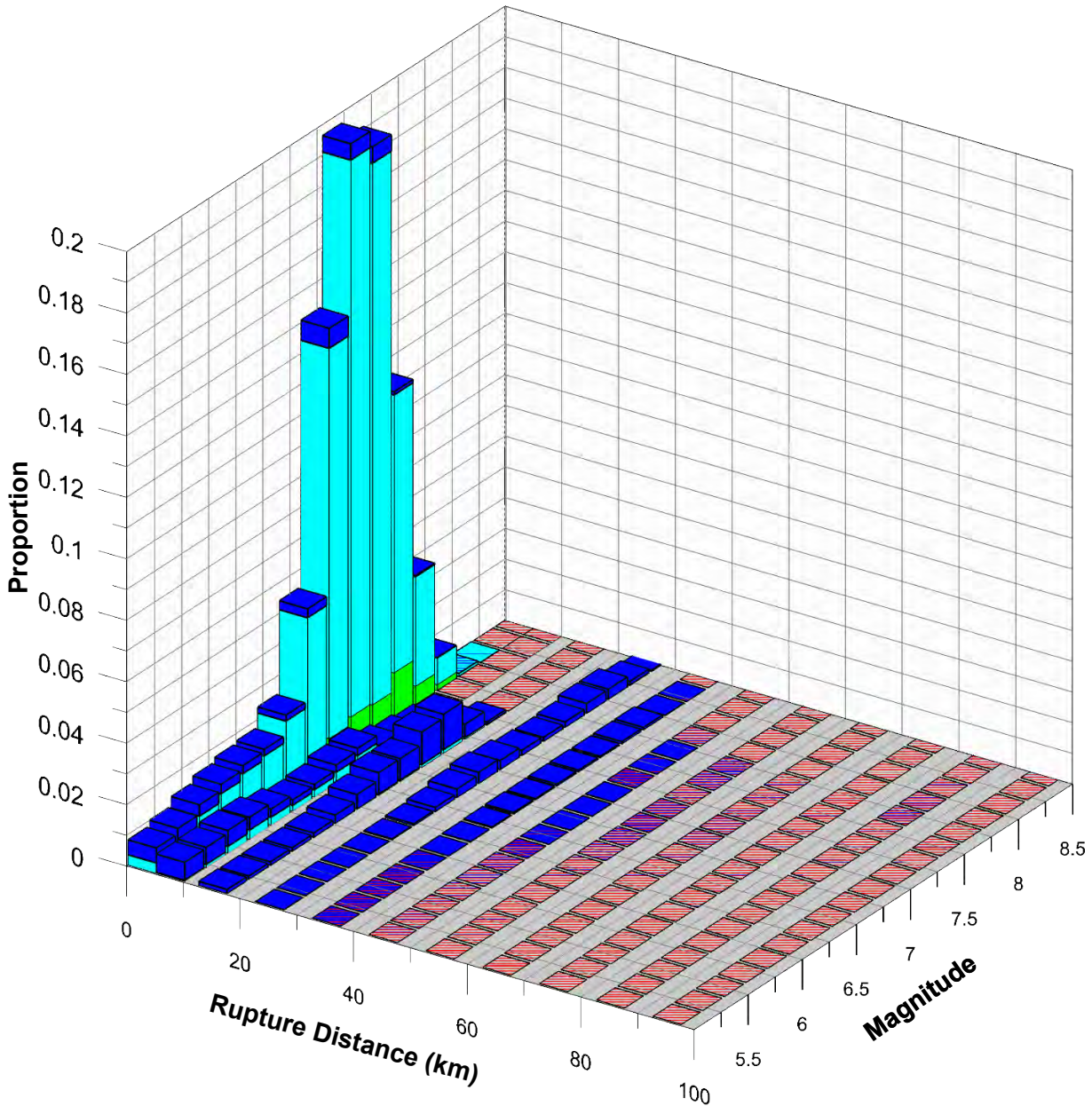

Epsilon
- >2
- 1 to 2
- 0 to 1
- -1 to 0
- -2 to -1
- <-2

Magnitude and Distance Contributions to the Mean Peak Horizontal Acceleration Hazard at 2,475-Year Return Period for Rock

BERKELEY CITY COLLEGE, CA

Lettis Consultants International, Inc. | Figure **12**

2,475-Year Return Period, 0.2 Sec
Modal **M,** Rrup: 6.9, 2.5 km
Mean **M,** Rrup: 6.0, 3.8 km

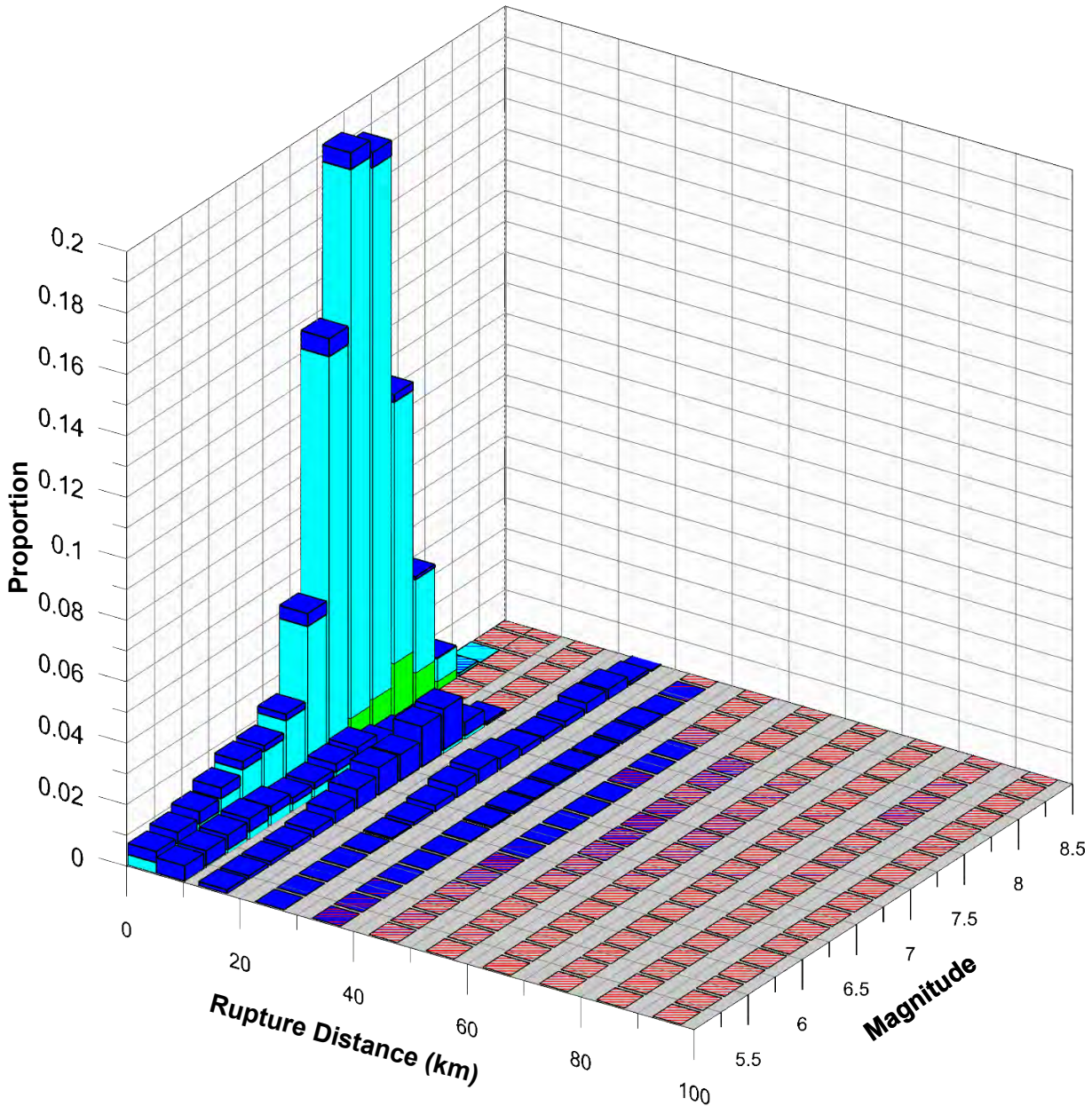

Epsilon
- >2
- 1 to 2
- 0 to 1
- -1 to 0
- -2 to -1
- <-2

Magnitude and Distance Contributions to the Mean 0.2 Sec Horizontal Spectral Acceleration Hazard at 2,475-Year Return Period for Rock

BERKELEY CITY COLLEGE, CA

LCI **Lettis Consultants International, Inc.** Figure **13**

2,475-Year Return Period, 1.0 Sec
Modal **M,** Rrup: 7.1, 2.5 km
Mean **M,** Rrup: 6.9, 4.4 km

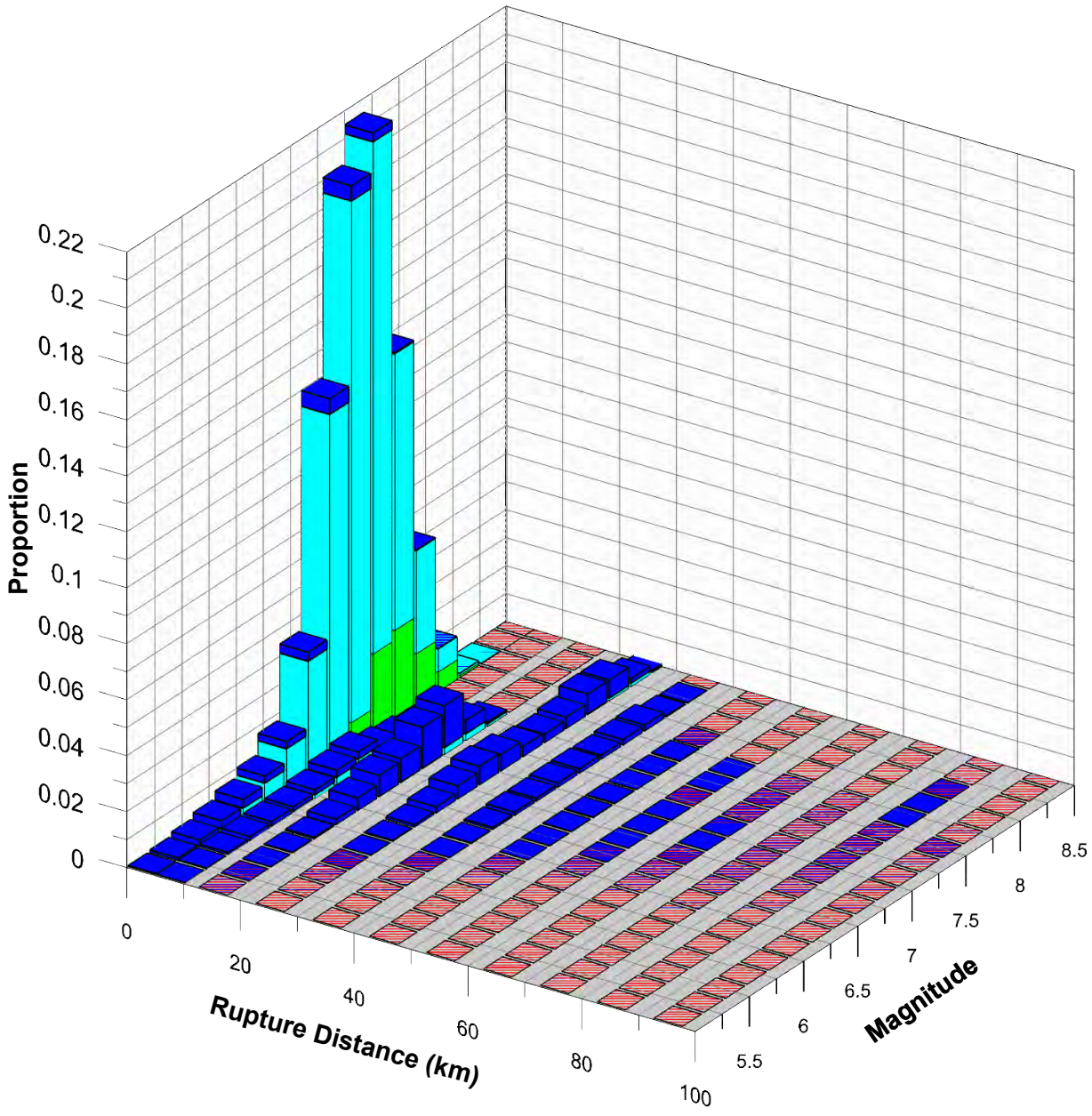

Epsilon
- >2
- 1 to 2
- 0 to 1
- -1 to 0
- -2 to -1
- <-2

Magnitude and Distance Contributions to the Mean 1.0 Sec Horizontal Spectral Acceleration Hazard at 2,475-Year Return Period for Rock

BERKELEY CITY COLLEGE, CA

Lettis Consultants International, Inc. | Figure **14**

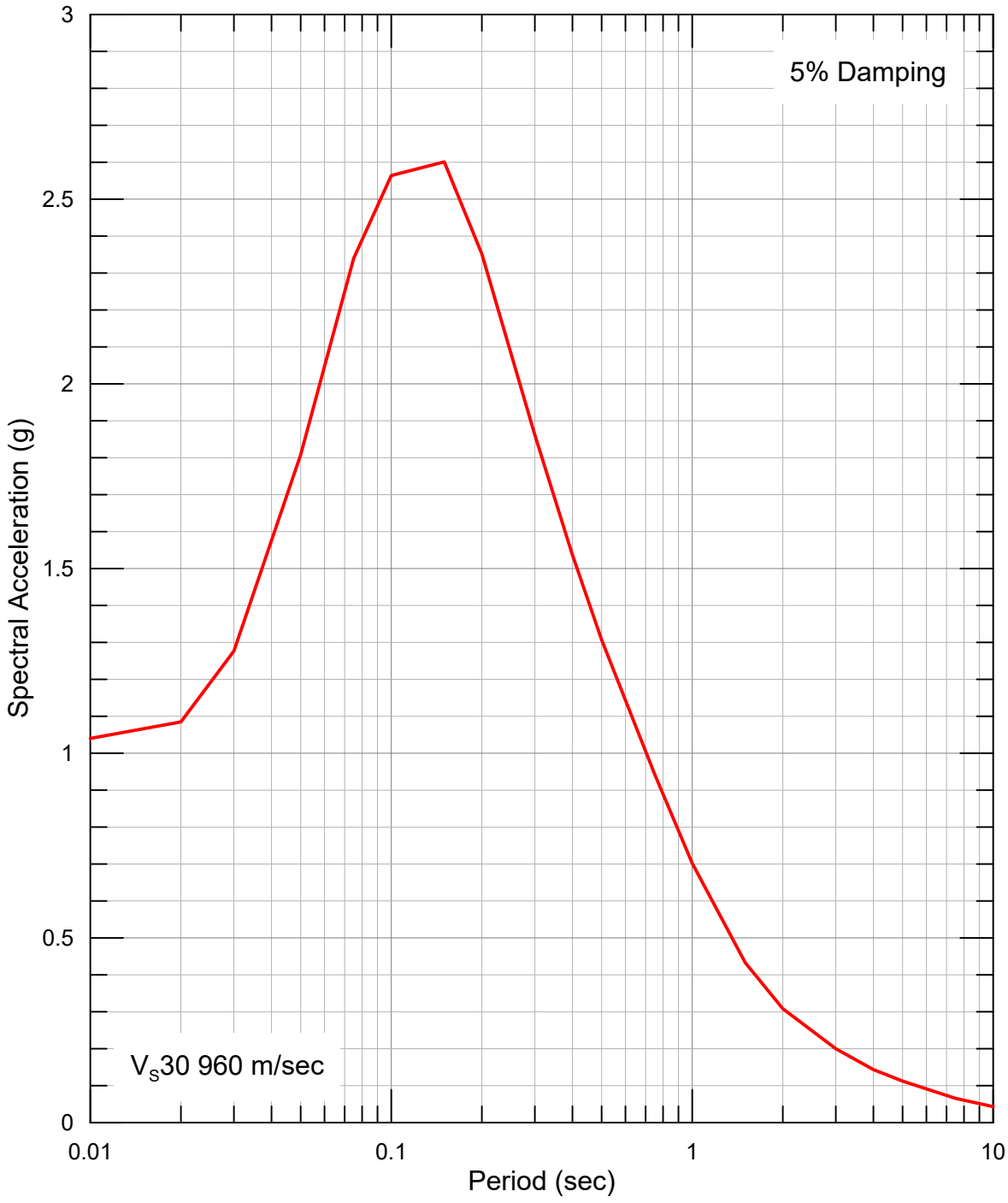

5%-Damped Uniform Hazard Spectrum at Return Period of 2,475 Years for Rock

BERKELEY CITY COLLEGE, CA

Lettis Consultants International, Inc. | Figure **15**

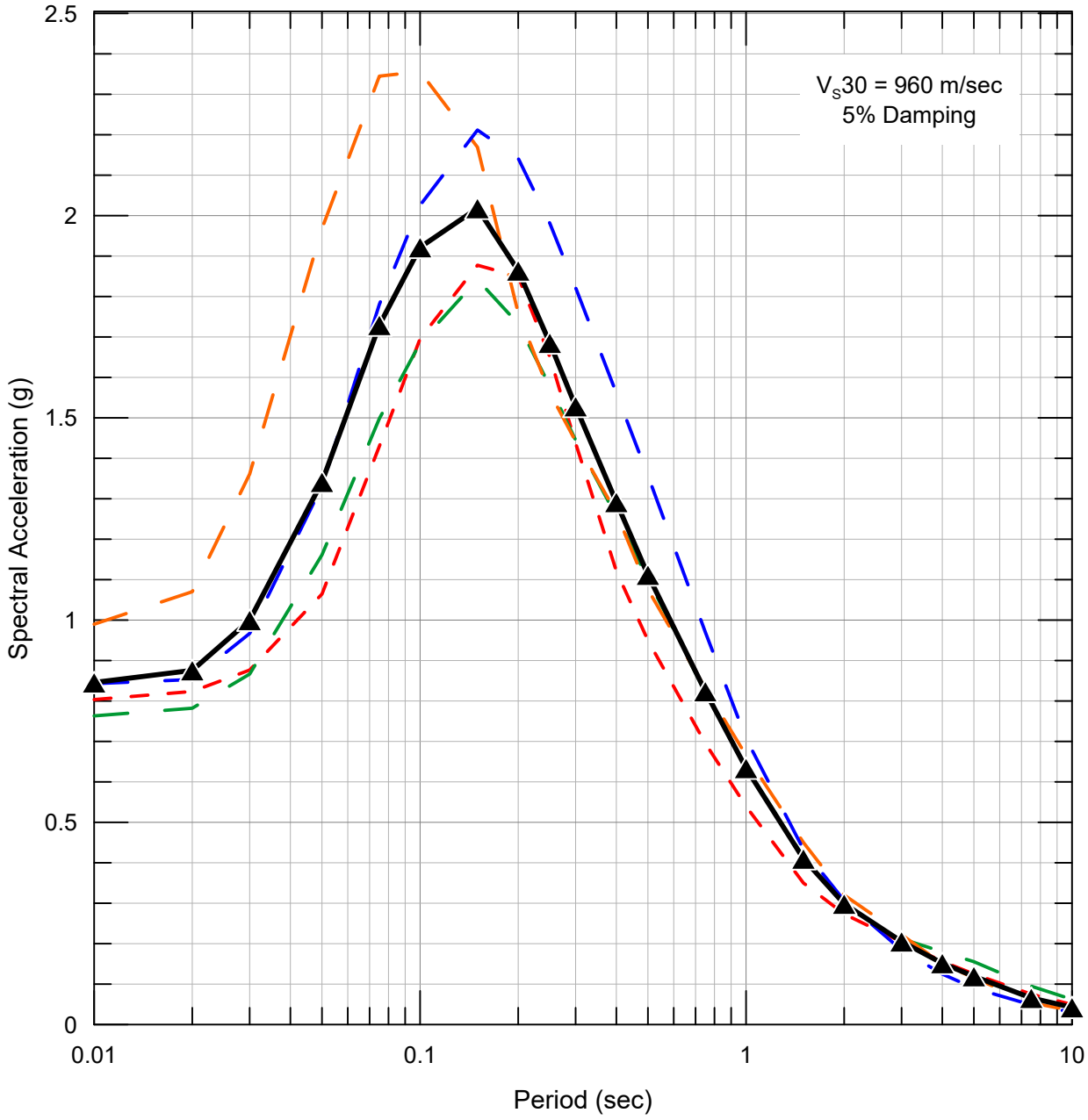

Abrahamson *et al*. (2014)
Boore *et al*. (2014)
Campbell and Bozorgnia (2014)
Chiou and Youngs (2014)
Geometric Mean

5%-Damped 84th Percentile Deterministic Horizontal Spectrum for the M 7.6 Hayward-Rodgers Creek Earthquake for Rock

BERKELEY CITY COLLEGE, CA

Lettis Consultants International, Inc.

Figure **16**

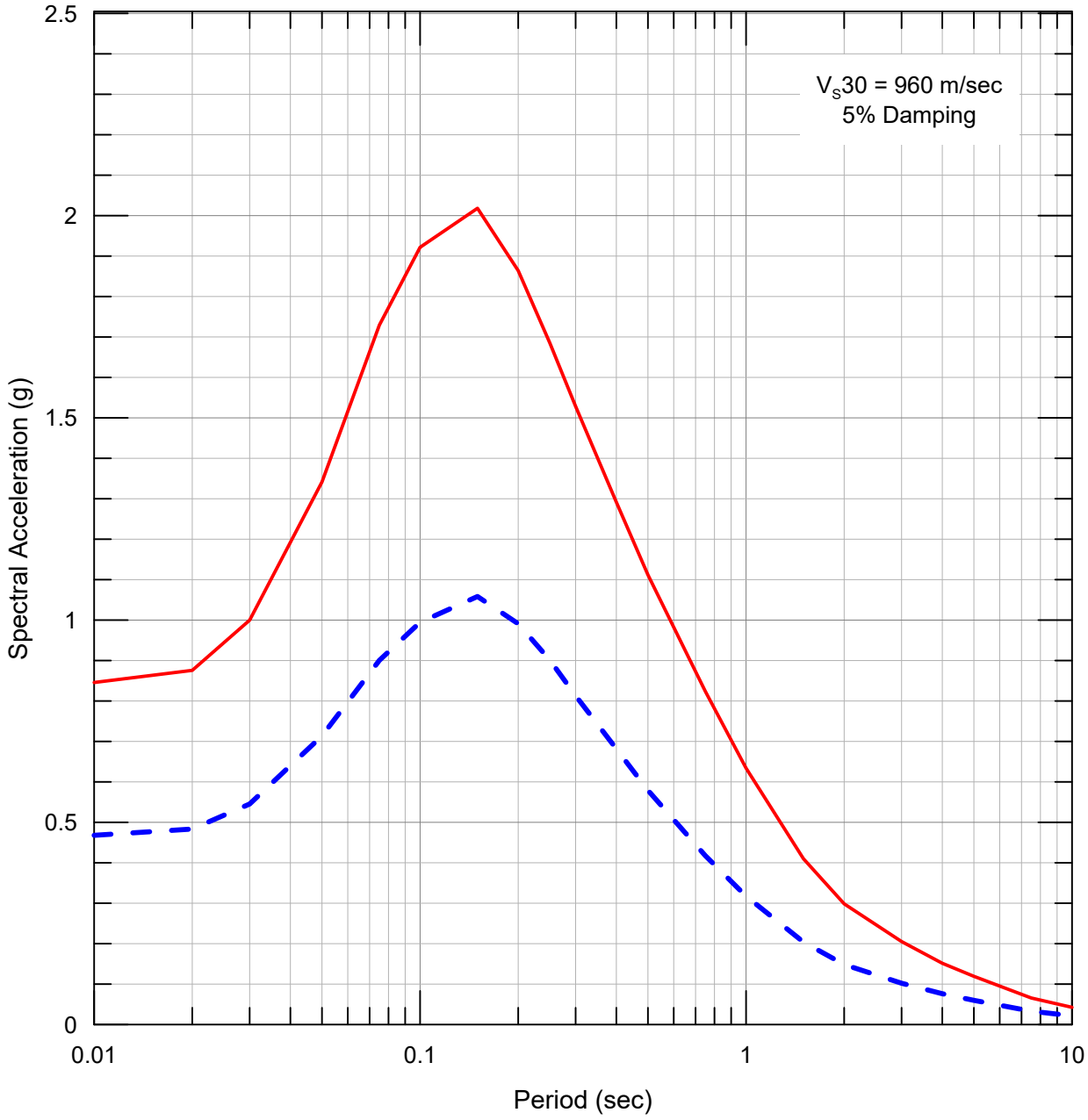

Median and 84th Percentile Deterministic Horizontal Spectrum for the M 7.6 Hayward-Rodgers Creek Earthquake for Rock

BERKELEY CITY COLLEGE, CA

Lettis Consultants International, Inc.

Figure **17**

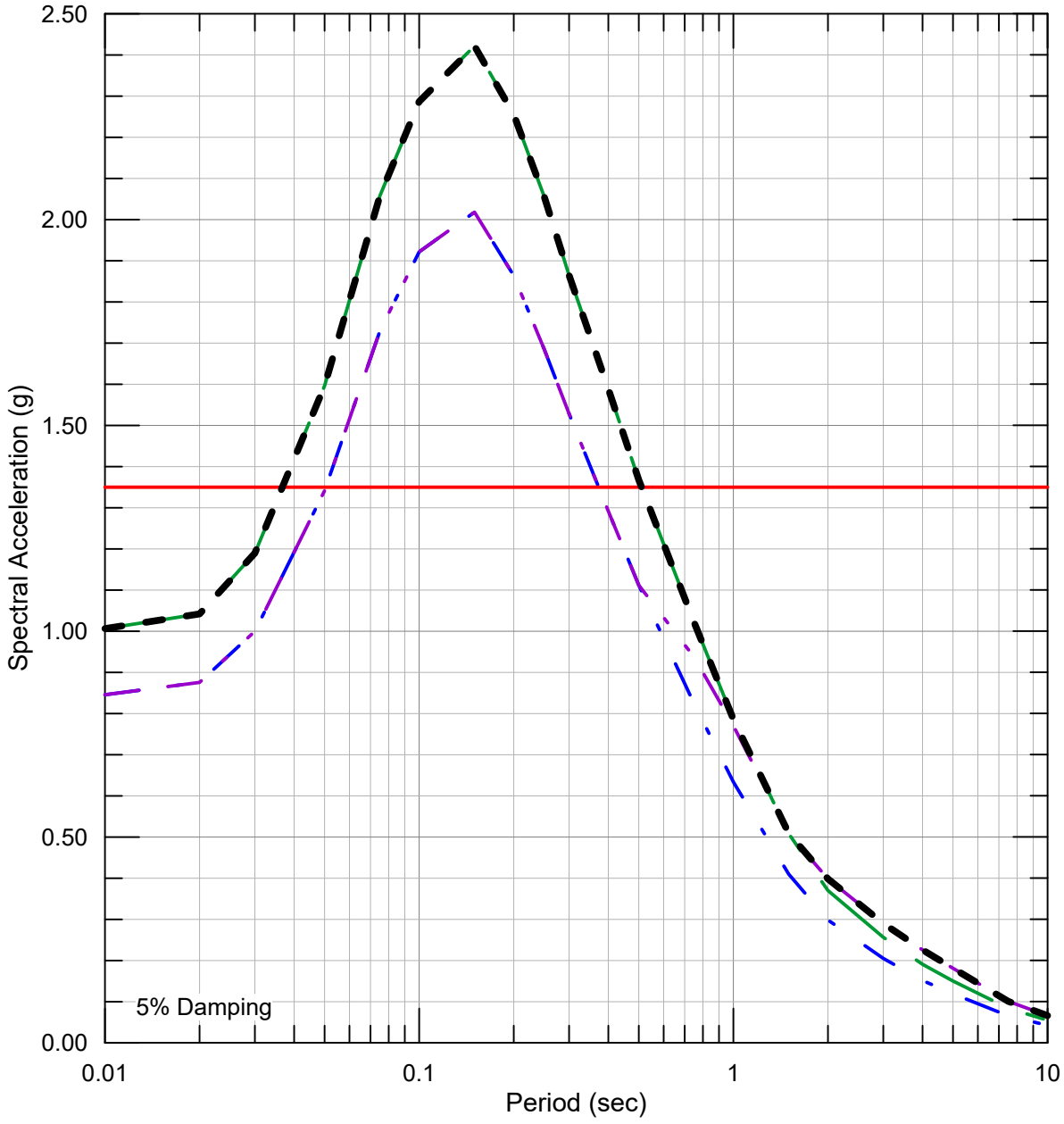

84th Percentile Deterministic - Geomean (RotD50)

84th Percentile Deterministic - Maximum Direction (RotD100)

84th Percentile Deterministic - Geomean (RotD50) adjusted to fault-normal

Minimum Deterministic Peak Spectral Acceleration, per ASCE 7-16, Supplement 1

Deterministic Rock MCE

Calculation of Site-Specific Deterministic Rock MCE Spectrum as per ASCE 7-16, Chapter 21 for Rock

Notes:
Maximum direction factors from Shahi and Baker (2014)
Fault directivity adjustement from
Bayless and Somerville (2013)

BERKELEY CITY COLLEGE, CA

Lettis Consultants International, Inc.

Figure **18**

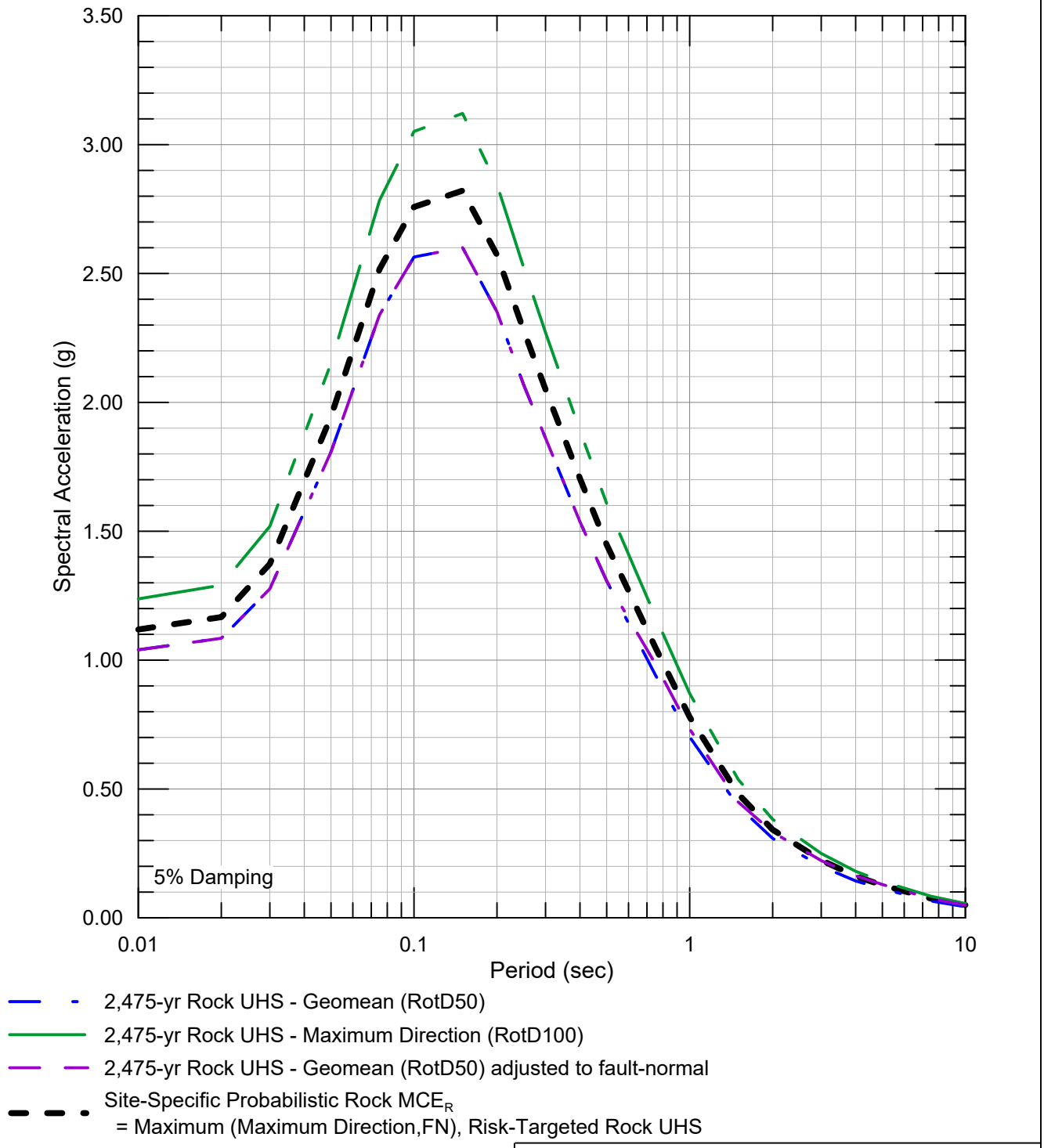

Calculation of Site-Specific Probabilistic Rock MCE$_R$ Spectrum as per ASCE 7-16, Chapter 21 for Rock

BERKELEY CITY COLLEGE, CA

Notes:
Maximum direction factors from Shahi and Baker (2013)
Risk coefficients C_{RS} = 0.904, C_{R1} = 0.895 from USGS Website

Lettis Consultants International, Inc.

Figure **19**

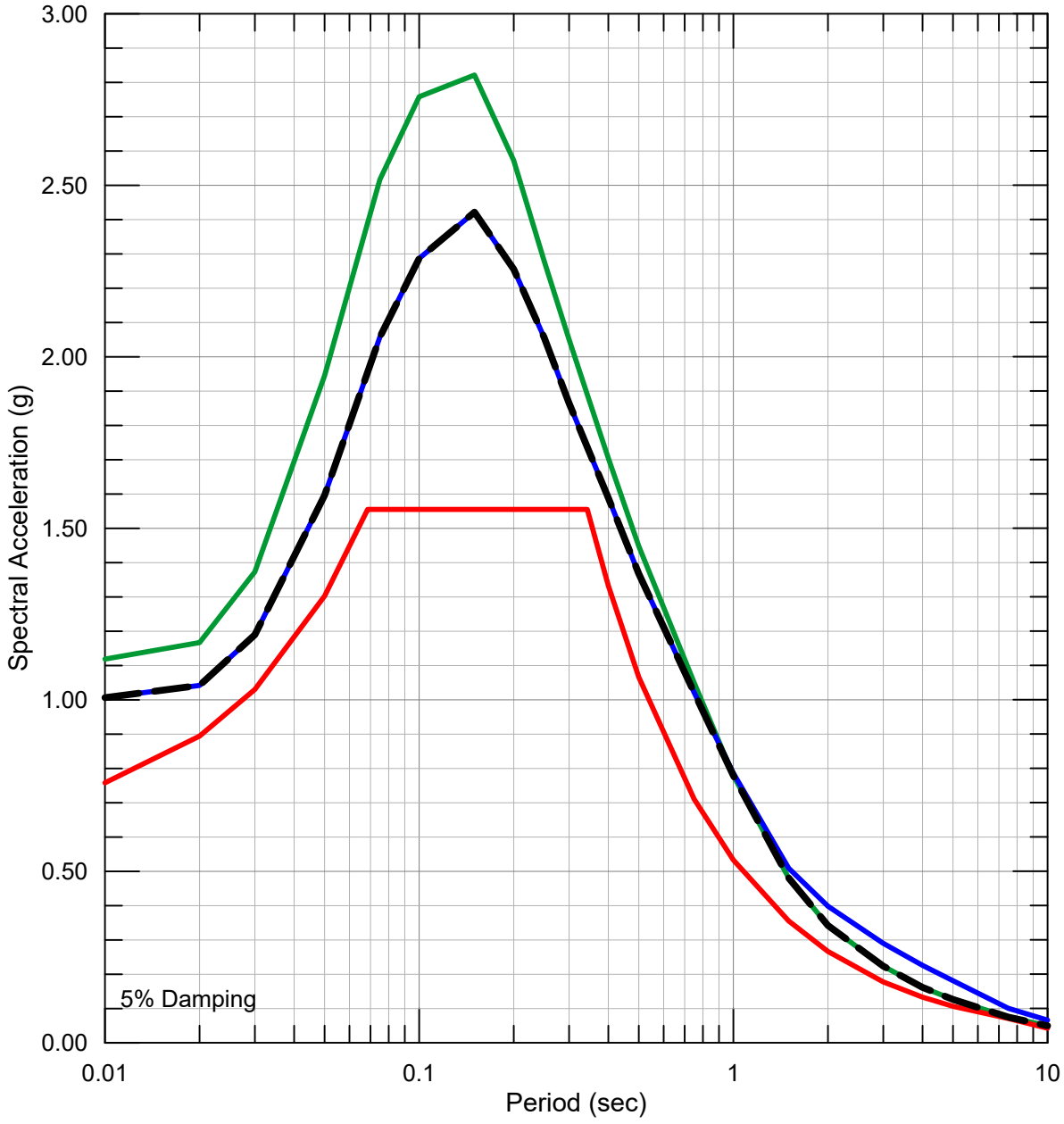

Probabilistic Rock MCE_R

Deterministic Rock MCE

80% ASCE 7-16 MCE_R, Site Class B

Site-Specific Rock MCE_R

Site-Specific Rock MCE_R Spectrum as per ASCE 7-16, Chapter 21 for Rock

BERKELEY CITY COLLEGE, CA

Lettis Consultants International, Inc.

Figure **20**

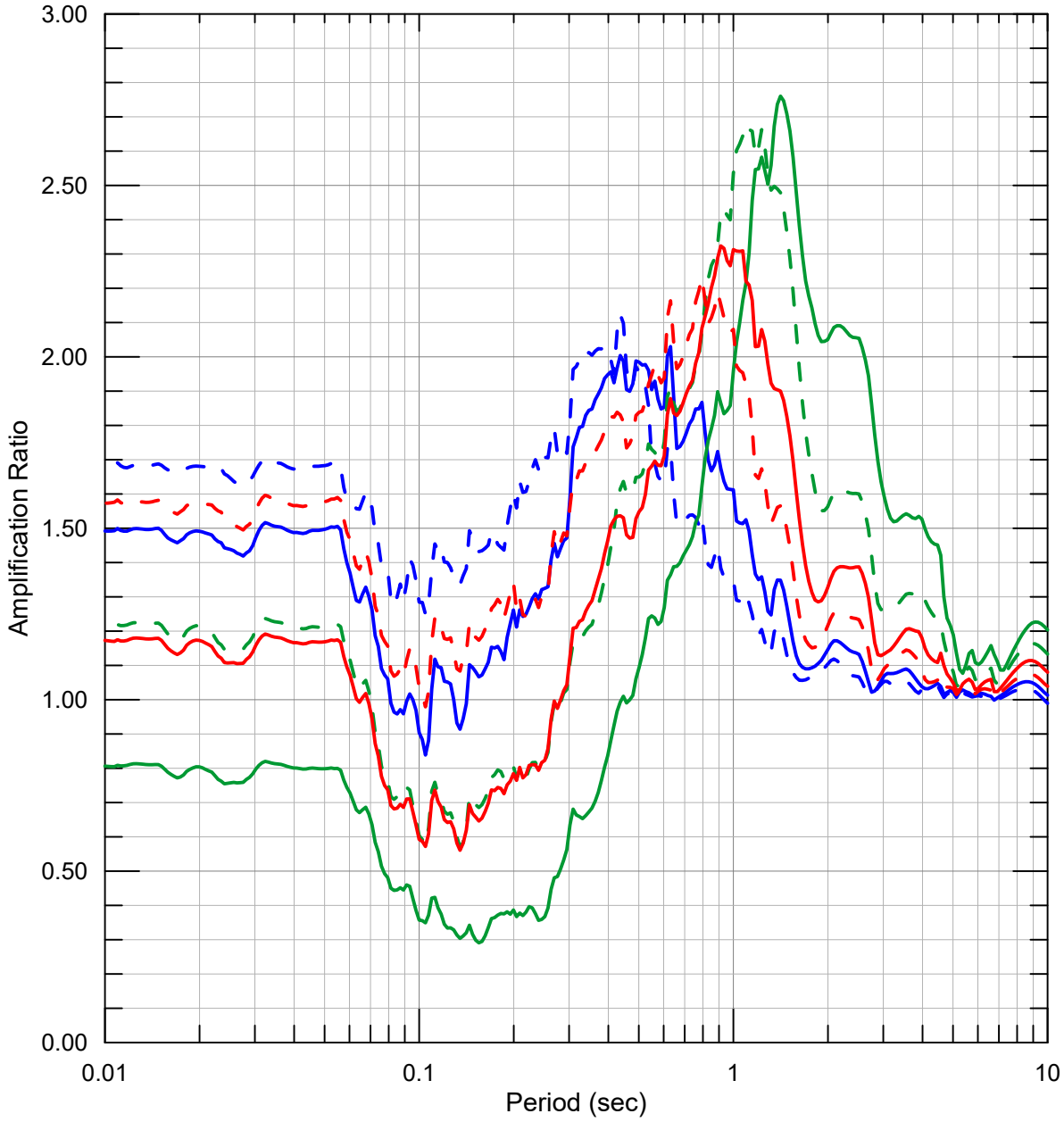

Median Amplification Factors (RSN143 Seed)

- M1P1
- M2P1
- M1P2
- M2P2
- M1P3
- M2P3

M1 = EPRI (1993) Curves
M2 = Peninsular Range Curves (Silva et al. 1996)
P1 = Best-estimate Vs Profile
P2 = Lower range Vs Profile
P3 = Upper range Vs Profile

Example of Amplification Factors

BERKELEY CITY COLLEGE, CA

Lettis Consultants International, Inc.

Figure **21**

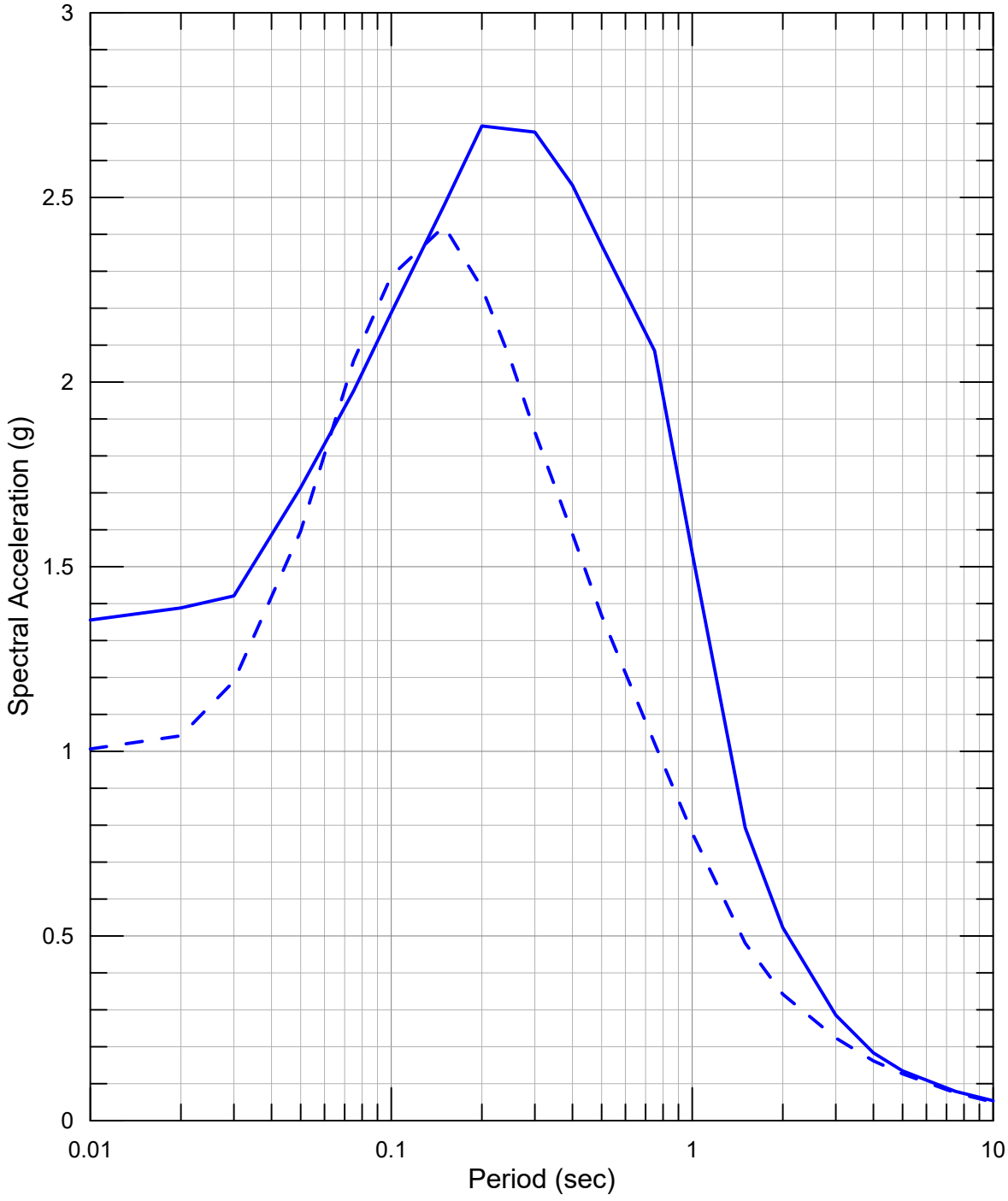

Site-Specific Rock MCE_R - (Rock V_S30 960 m/sec)

Site-Specific Surface MCE_R

Rock Versus Surface MCE_R Spectra

BERKELEY CITY COLLEGE, CA

Lettis Consultants International, Inc. Figure **22**

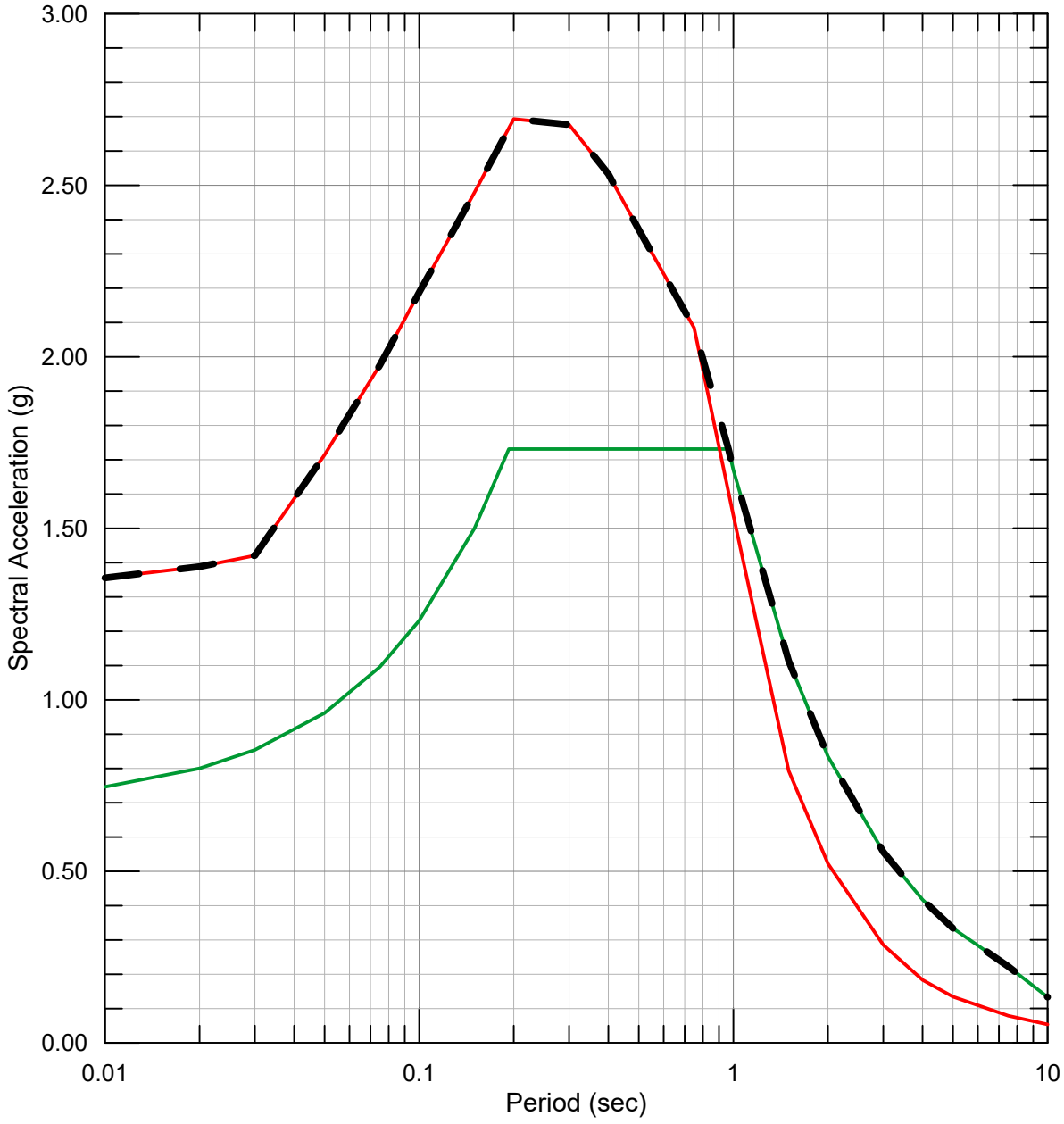

Site-Specific Surface MCE_R

80% ASCE 7-10 MCE_R - Site Class D
(S_S = 2.164, S_1 = 0.835, Fa = 1.0, Fv = 2.5)

Final Site-Specific MCE_R

Calculation of Site-Specific MCE_R Spectrum, as per ASCE 7-16, Chapter 21

BERKELEY CITY COLLEGE, CA

Lettis Consultants International, Inc.

Figure **23**

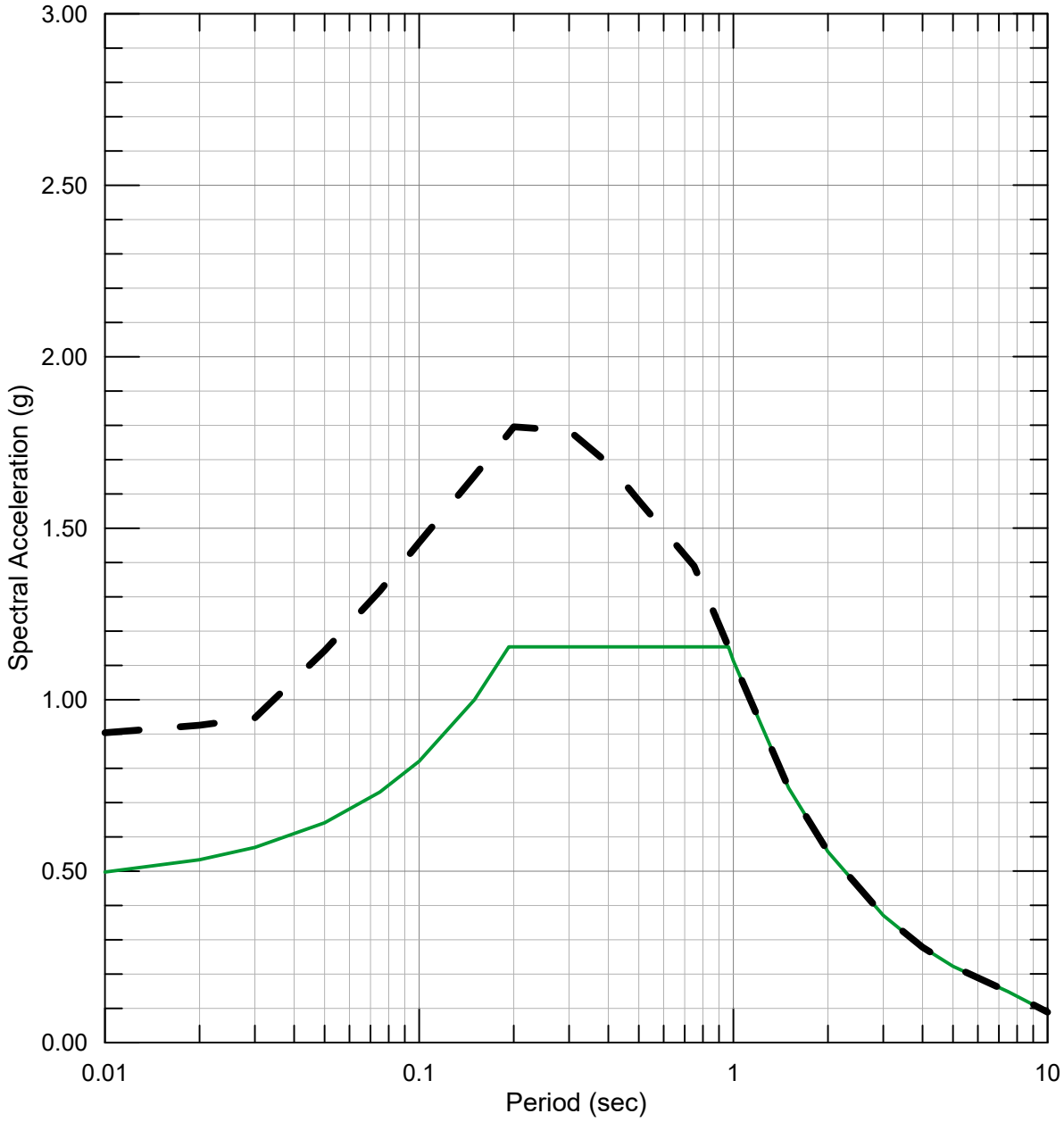

80% ASCE 7-10 DE - Site Class D
(S_S = 2.164, S_1 = 0.835, Fa = 1.0, Fv = 2.5)

Final Site-Specific DE

Calculation of Site-Specific DE Spectrum, as per ASCE 7-16, Chapter 21

BERKELEY CITY COLLEGE, CA

Lettis Consultants International, Inc.

Figure **24**

APPENDIX G

Liquefaction and Dynamic Settlement Analysis

LIQUEFACTION ANALYSIS

Peralta Community College District / XL Construction
Berkeley City College - 2118 Milvia Street, Berkeley, CA
A3GEO, Inc.
Project # 1185-1A

References:
Boulanger, R.W. and Idriss, I.M, 2014, "CPT and SPT based liquefaciont triggering procedures", Report No UCD/CGM-14/01, Center for Geotechnical Modeling, University of California at Davis, April.
Idriss, I.M., and Boulanger, R.W., 2008, "Soil Liquefaction During Earthquakes," Earthquake Engineering Research Institute, MNO-12, Oakland, California.

CR = Correction Factor for Rod Length; 0-10'=0.75; 10-13' = 0.80; 13-20' = 0.85; 20-33' = 0.95; 33-100' = 1.0
CS = Correction Factor for Sampling Method; SPT Sampler without liners = 1.2; Modified California Sampler = 0.63
CB = Correction Factor for Borehole Diameter; For Hollow Stem, use ID.; 2.5-4.5" = 1.0; 5.9" = 1.05; 7.9" = 1.15
CE - Correction Factor for Hammer Energy Ratio; Automatic Trip Hammer = 1.3, Rope and Cathead = 1.0, Wireline Downhole Hammer = 1.0
CN - Correction Factor for Overburden Pressure

Design Mw = 7.6
peak acceleration amax = 1.14
water table during investigation = 20 feet below ground surface
assumed water table during EQ = 10 feet below ground surface

Hammer Type = Automatic Trip Hammer (B-1)
Hammer Type = Wireline Downhole Hammer (TP/B-3)

Input Values										Correction Factors					Triggering Anlaysis (Boulanger and Idriss, 2014)											Vertical Settlement (Idriss & Boulanger 2008)				
															eq. 2.15c	eq. 2.15a	eq. 2.5	eq. 2.23	eq. 2.14a	eq. 2.2	eq. 2.16a, b	eq. 2.25	eq 2.7; eq 2.21							
Boring	Top of Layer (ft)	Bottom of Layer (ft)	Sample Depth (ft)	Sample Type	N (field value)	Unified Soil Class.	γ_m (pcf)	% Fines	Material Liquefiable?	C_R	C_S	C_B	C_E	N_{60}	m	C_N	$N_{1,60}$	$N_{1,60cs}$	R_d	$CSR_{,Mw}$	K_σ	$CRR_{,M=7.5}$	$CRR_{,M,\sigma v'}$	FS	FS <1.3?	Shear Strain Limit, γ_{lim}	Reference FS, F_α	Shear Strain Max, γ_{max}	ε (%)	Settlement (in)
B-1	0	4	3	MC	12	CL	100	67	No	0.75	0.63	1.00	1.3	7	0.46	1.70	12	18	1.002	0.743	1.1	0.180	0.277	--	--	0.208	0.64	0.00	0.00	--
	4	6	5.5	MC	15	SC	100	29	No	0.75	0.63	1.00	1.3	9	0.44	1.70	15	20	0.996	0.738	1.1	0.210	0.348	--	--	0.153	0.50	0.00	0.00	--
	13	18	15.5	MC	77	GC	120	16	Yes	0.85	0.63	1.00	1.3	54	0.19	1.05	56	60	0.967	0.902	1.1	2.000	2.000	2.22	no	0.000	-2.39	0.00	0.00	--
	18	23	20.5	SPT	34	GC	120	16	Yes	0.95	1.2	1.00	1.3	50	0.23	0.99	49	53	0.950	0.990	1.1	2.000	2.000	2.02	no	0.000	-1.80	0.00	0.00	--
	23	27	25.5	SPT	35	GC	120	16	Yes	0.95	1.2	1.00	1.3	52	0.23	0.96	49	53	0.934	1.038	1.0	2.000	2.000	1.93	no	0.000	-1.80	0.00	0.00	--
	27	33	30.5	MC	79	GC	120	16	Yes	0.95	0.63	1.00	1.3	61	0.18	0.95	58	62	0.915	1.069	1.0	2.000	2.000	1.87	no	0.000	-2.56	0.00	0.00	--
	33	36	35	SPT	6	CL	110	52	No	1.00	1.2	1.00	1.3	9	0.51	0.83	7	13	0.897	1.087	1.0	0.137	0.169	--	--	0.356	0.84	0.00	0.00	--
	36	38	36	SPT	19	SC	110	36	Yes	1.00	1.2	1.00	1.3	30	0.36	0.87	25	31	0.886	1.095	1.0	0.520	1.016	0.93	yes	0.043	-0.12	0.04	0.78	0.19
	38	43	40.5	MC	52	SC	110	36	Yes	1.00	0.63	1.00	1.3	43	0.28	0.88	37	43	0.872	1.103	0.9	2.000	2.000	1.81	no	0.005	-1.00	0.00	0.06	--
	43	47	45.5	MC	36	CL	100	52	No	1.00	0.63	1.00	1.3	29	0.37	0.83	24	30	0.852	1.110	0.9	0.462	0.855	--	--	0.049	-0.06	0.00	0.00	--
	47	51.5	50.5	MC	46	CL	100	52	No	1.00	0.63	1.00	1.3	38	0.32	0.84	31	37	0.834	1.115	0.9	1.592	2.000	--	--	0.017	-0.55	0.00	0.00	--
																												Total Settlement:		**0.2**
TP/B-3	0	10	5	MC	7	CL	100	67	No	0.75	0.63	1.00	1.00	3	0.53	1.70	5.00	10.58	1.00	0.74	1.10	0.12	0.16	--	--	0.44	0.90	0.00	0.00	--
	10	15	10	MC	15	CL	110	60	No	0.80	0.63	1.00	1.00	8	0.48	1.43	10.00	15.60	0.98	0.82	1.07	0.16	0.23	--	--	0.26	0.73	0.00	0.00	--
	15	20	15	MC	7	CL	110	60	No	0.85	0.63	1.00	1.00	4	0.55	1.19	4.00	9.60	0.96	0.96	1.04	0.12	0.14	--	--	0.49	0.92	0.00	0.00	--
	20	25	20	MC	29	CL	110	60	No	0.95	0.63	1.00	1.00	17	0.42	1.00	17.00	22.60	0.94	1.04	1.04	0.24	0.41	--	--	0.12	0.37	0.00	0.00	--
	25	29	25	SPT	38	SC	120	21	Yes	0.95	1.20	1.00	1.00	43	0.26	0.97	42.00	46.63	0.93	1.08	1.04	2.00	2.00	1.84	no	0.00	-1.32	0.00	0.02	--
	29	30.5	30	SPT	25	CL	120	55	No	0.95	1.20	1.00	1.00	29	0.35	0.93	26.00	31.61	0.92	1.10	1.01	0.61	1.29	--	--	0.04	-0.20	0.00	0.00	--
	30.5	33	31	SPT	25	SC	120	16	Yes	0.95	1.20	1.00	1.00	29	0.37	0.92	26.00	29.58	0.91	1.11	1.00	0.46	0.91	0.82	yes	0.05	-0.06	0.05	0.99	0.30
	33	40	35	SPT	27	CL	110	55	No	1.00	1.20	1.00	1.00	32	0.33	0.90	29.00	34.61	0.89	1.12	0.97	1.02	2.00	--	--	0.02	-0.41	0.00	0.00	--
	40	45	40	SPT	21	CL	110	55	No	1.00	1.20	1.00	1.00	25	0.39	0.86	21.00	26.61	0.86	1.13	0.96	0.33	0.58	--	--	0.07	0.13	0.00	0.00	--
	45	49	45	SPT	29	CL	110	55	No	1.00	1.20	1.00	1.00	35	0.33	0.86	29.00	34.61	0.84	1.13	0.92	1.02	2.00	--	--	0.02	-0.41	0.00	0.00	--
	49	50.5	49	SPT	31	CL	110	55	No	1.00	1.20	1.00	1.00	37	0.32	0.85	31.00	36.61	0.83	1.13	0.90	1.59	2.00	--	--	0.02	-0.55	0.00	0.00	--
																												Total Settlement:		**0.3**

APPENDIX H

Vertical and Lateral Pile Analysis

West Side
Axial Capacity
18-Inch Pile

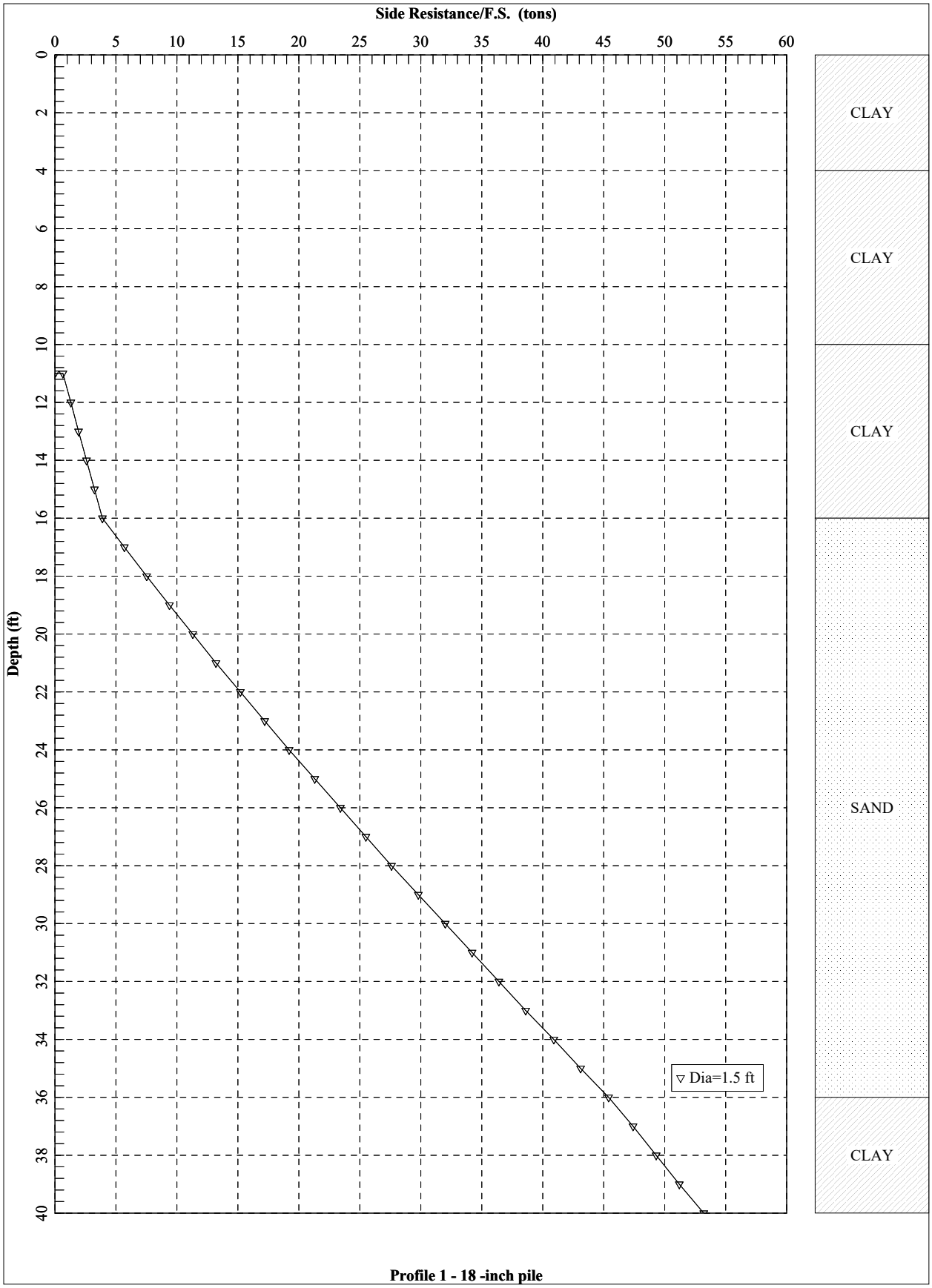

Profile 1 - 18 -inch pile

West Side
Axial Capacity
30-Inch Pile

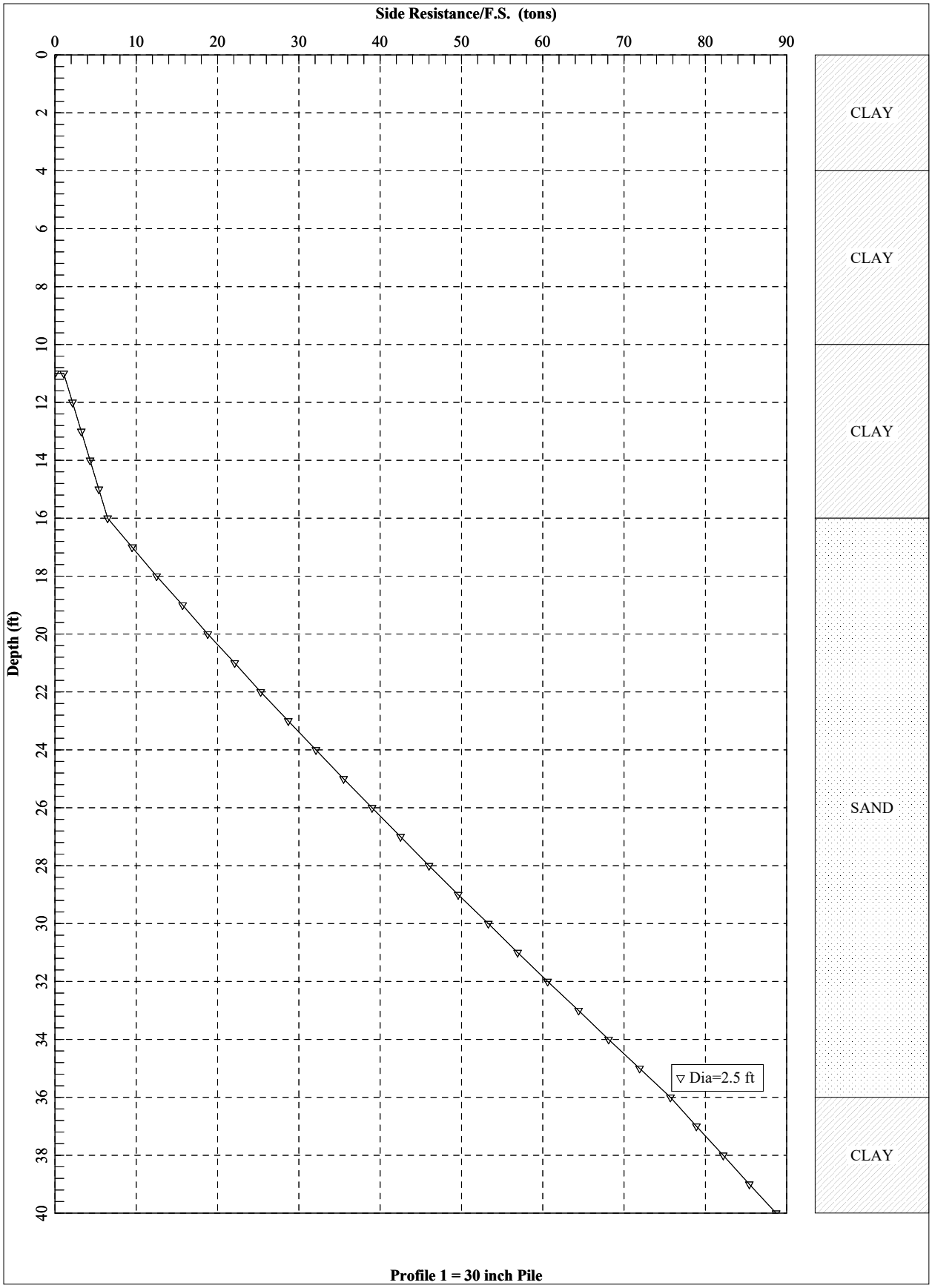

West Side
Lateral Response - Bending Moment
18-Inch Pile

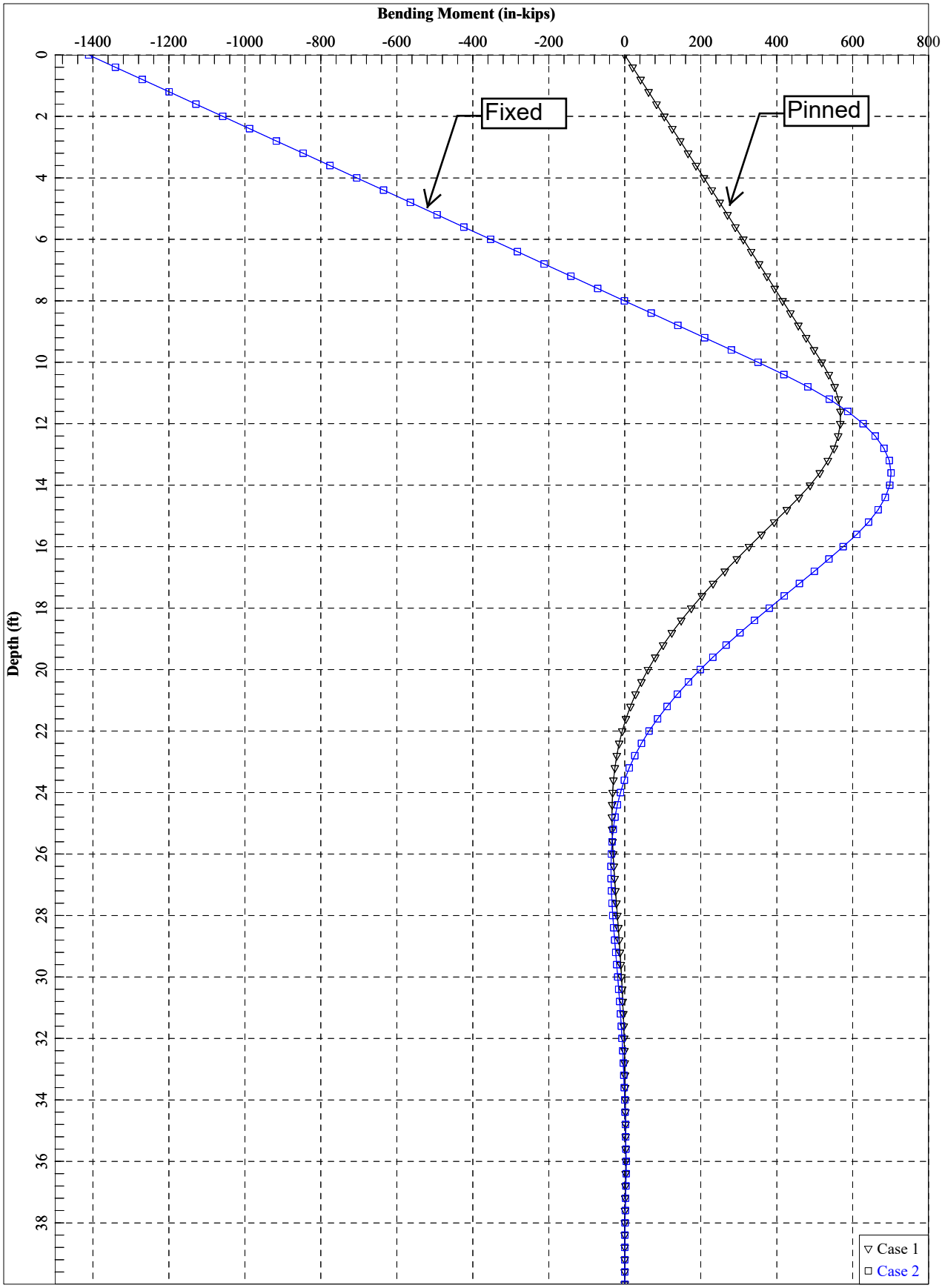

West Side
Lateral Response - Shear Force
18-Inch Pile

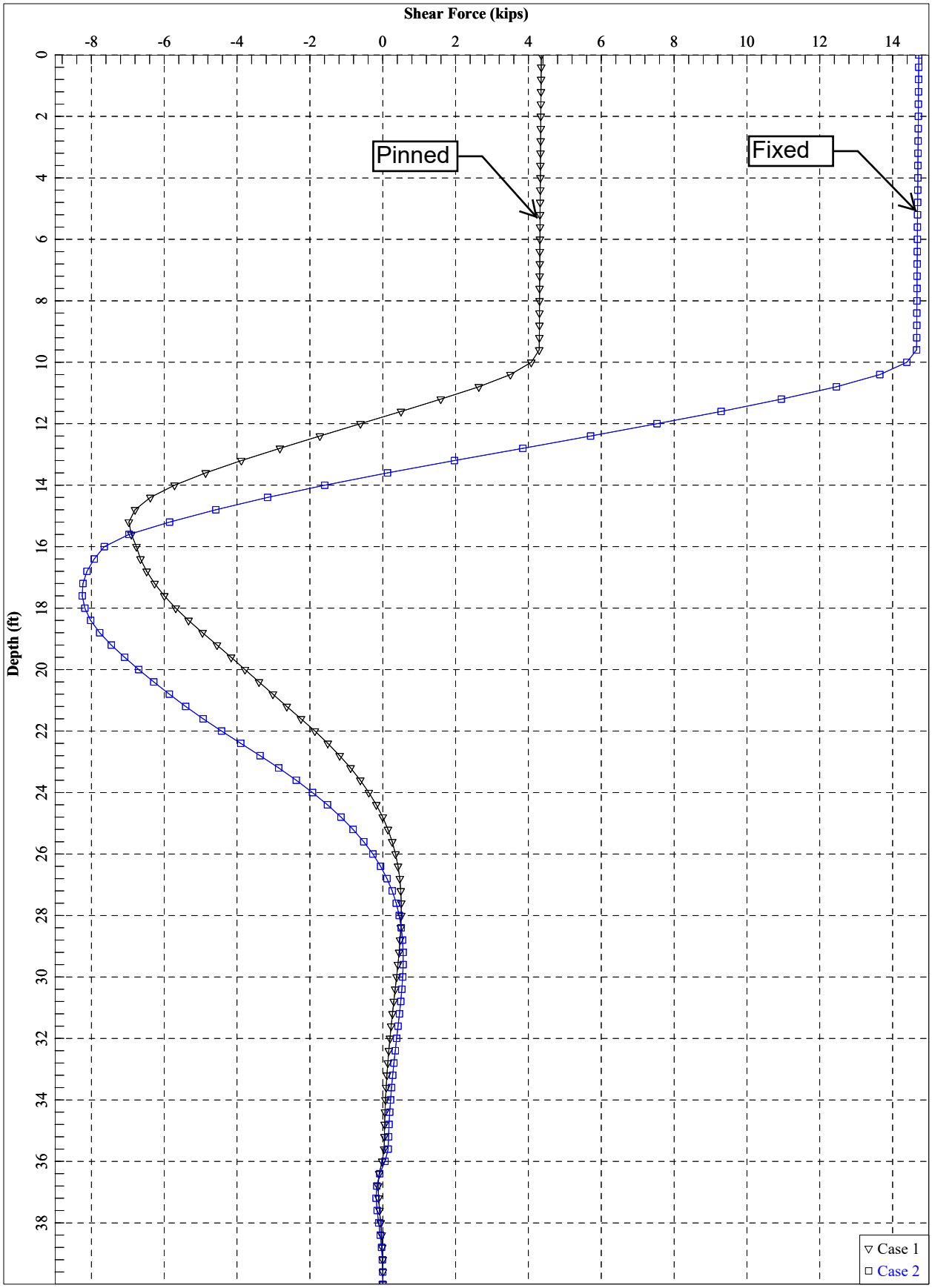

West Side
Mobilized Soil Reaction vs. Depth
18-Inch Pile

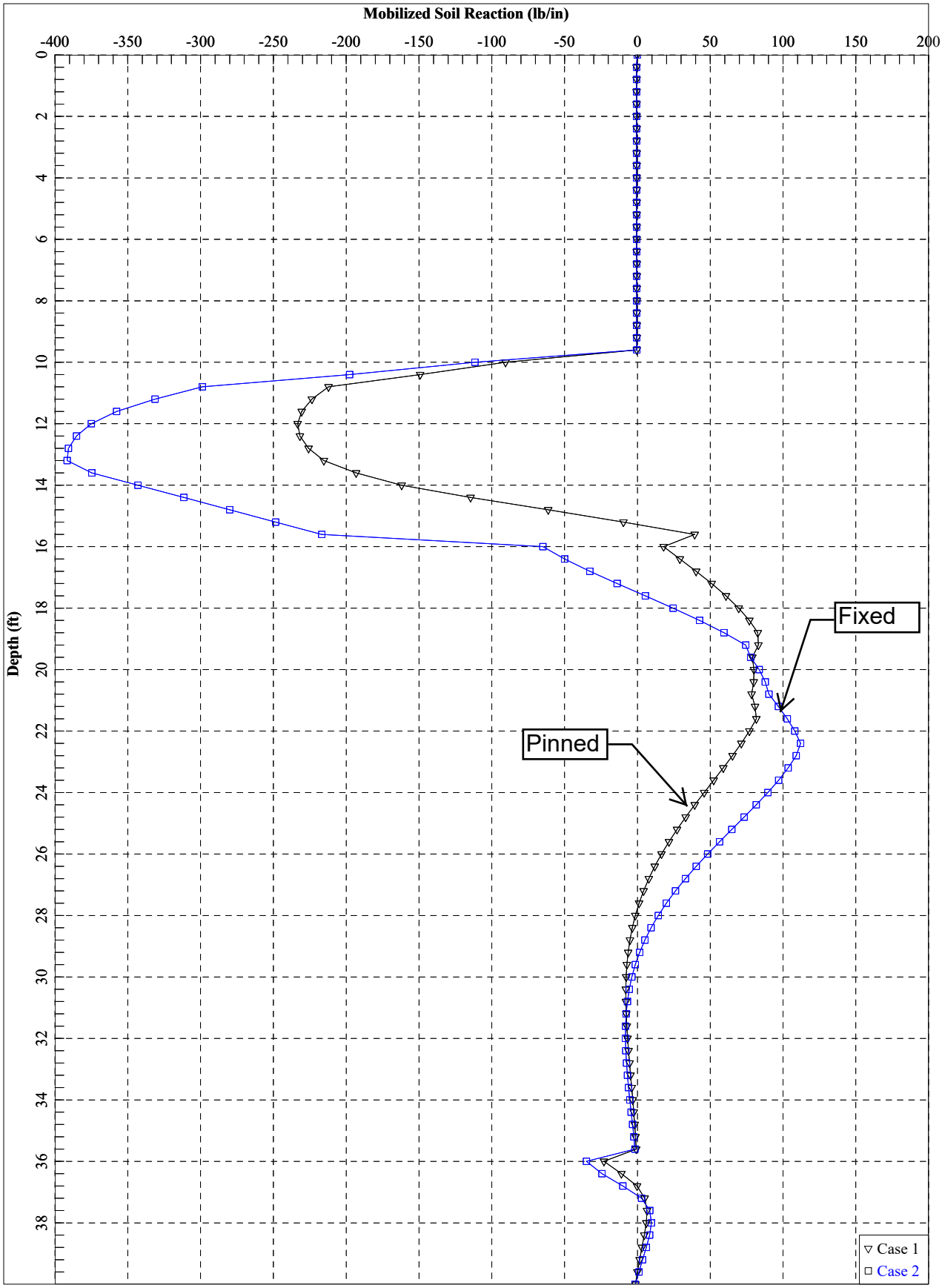

West Side
Lateral Response - Bending Moment
30-Inch Pile

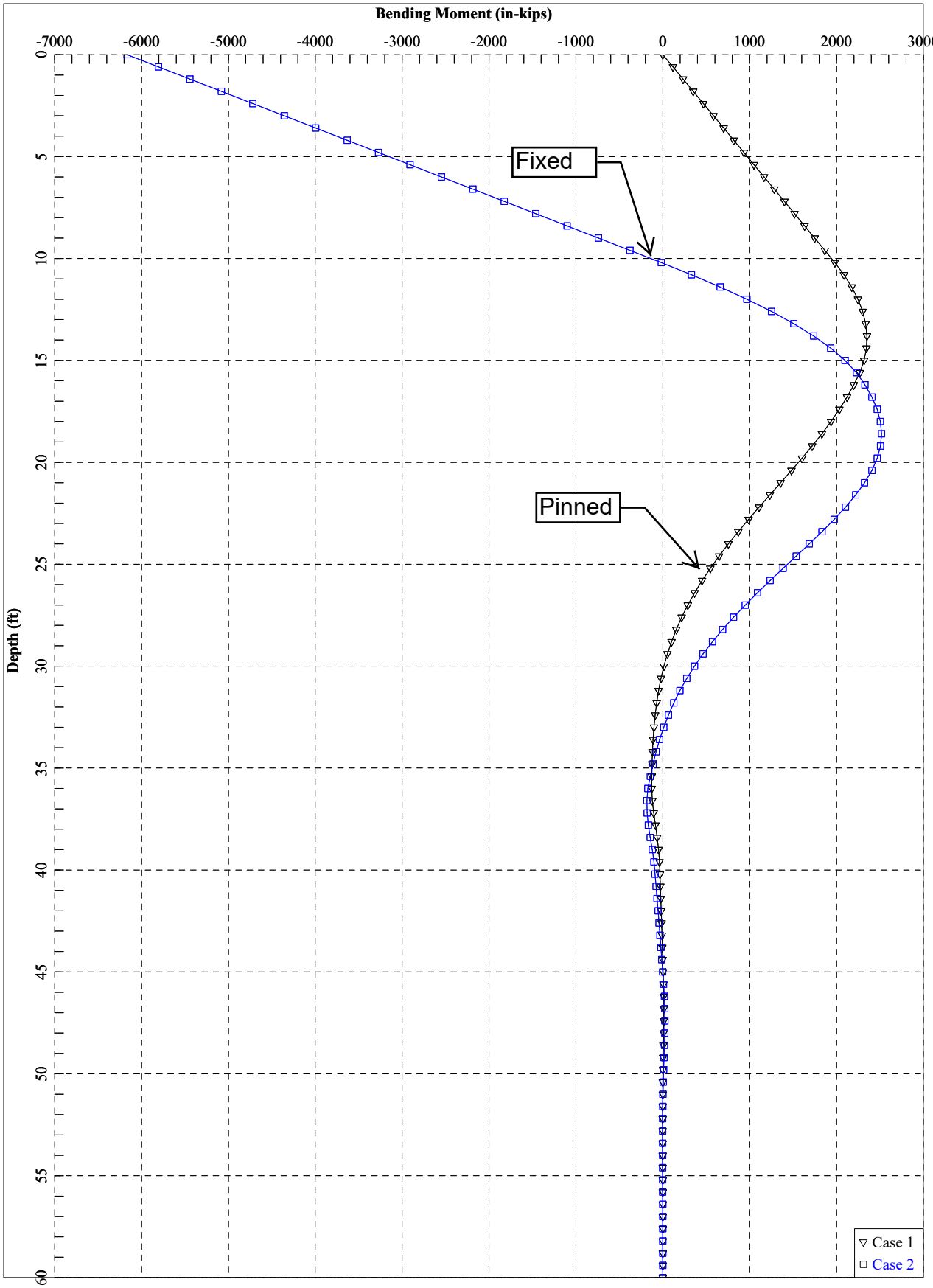

West Side
Lateral Response - Shear Force
30-Inch Pile

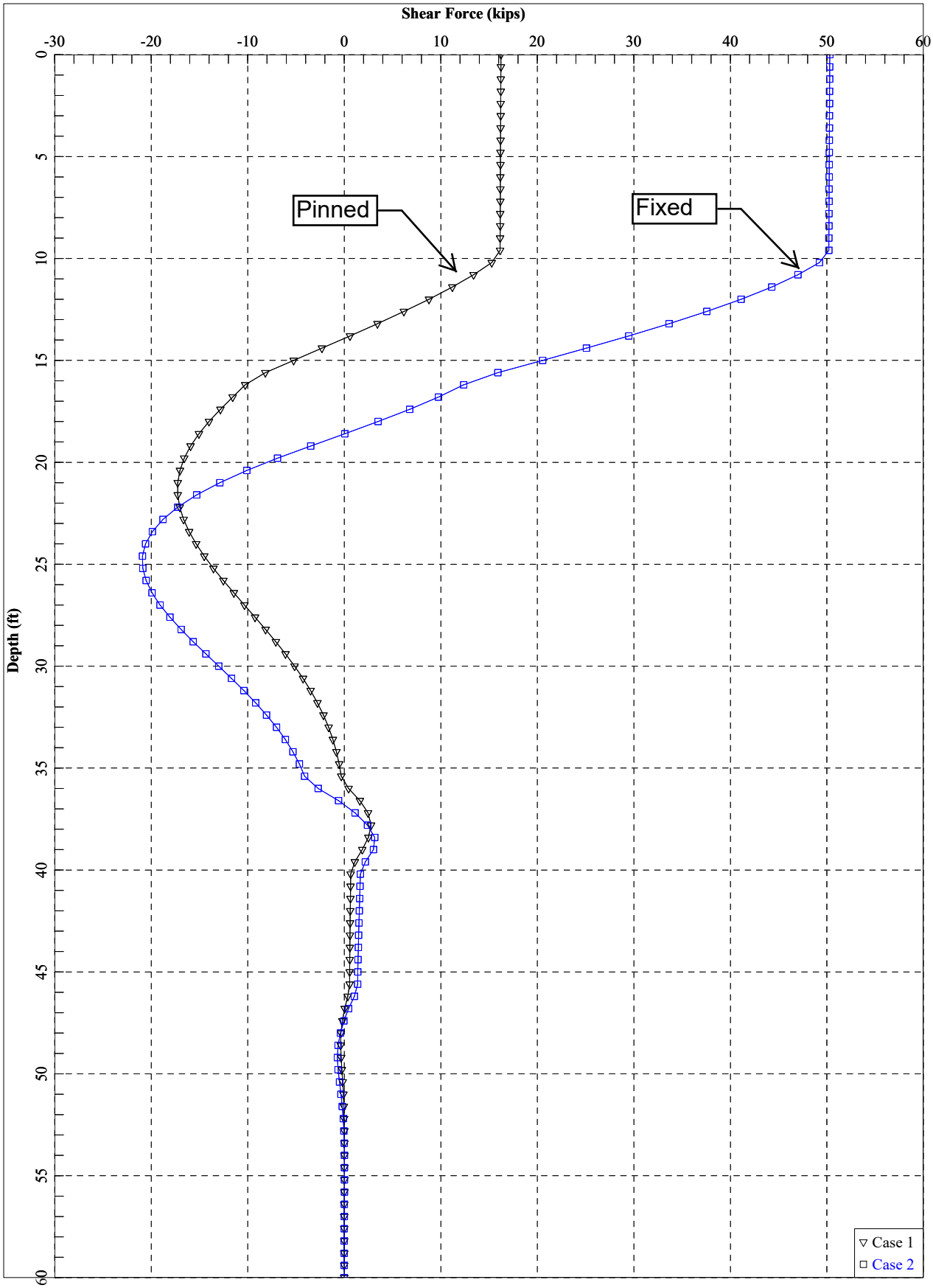

West Side
Mobilized Soil Reaction vs. Depth
30-Inch Pile

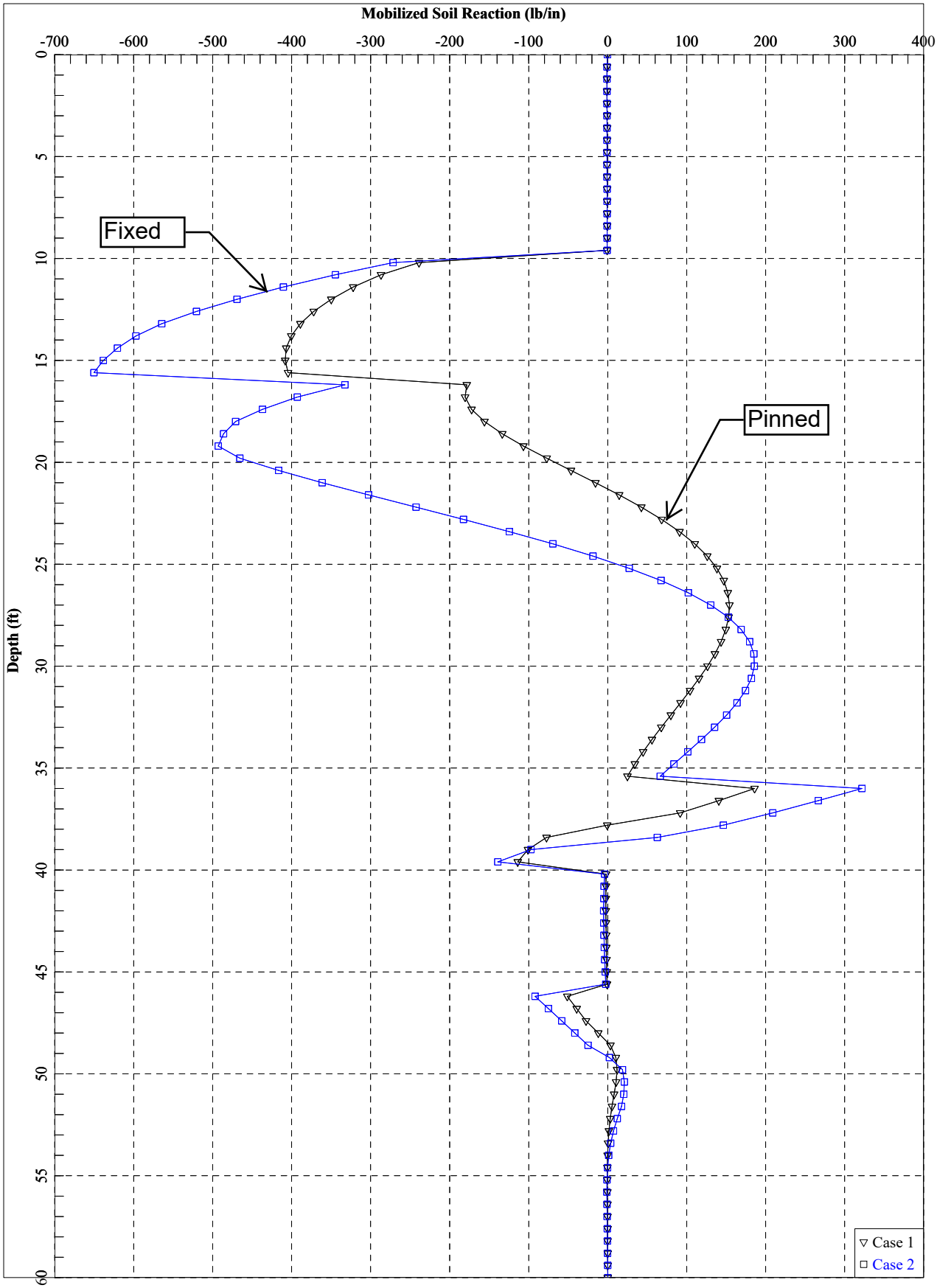

Building
Axial Capacity
18-Inch Pile

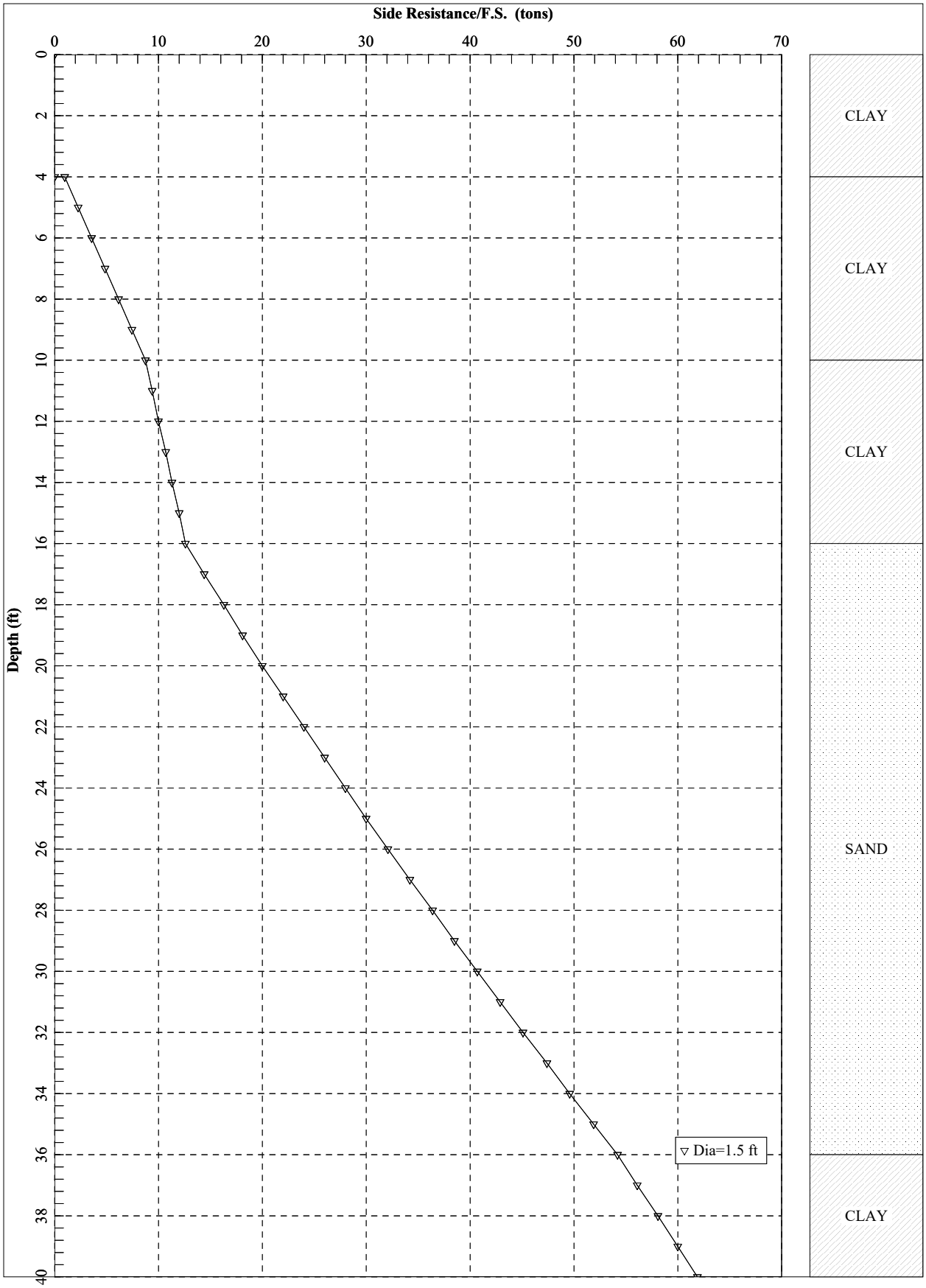

Building
Axial Capacity
30-Inch Pile

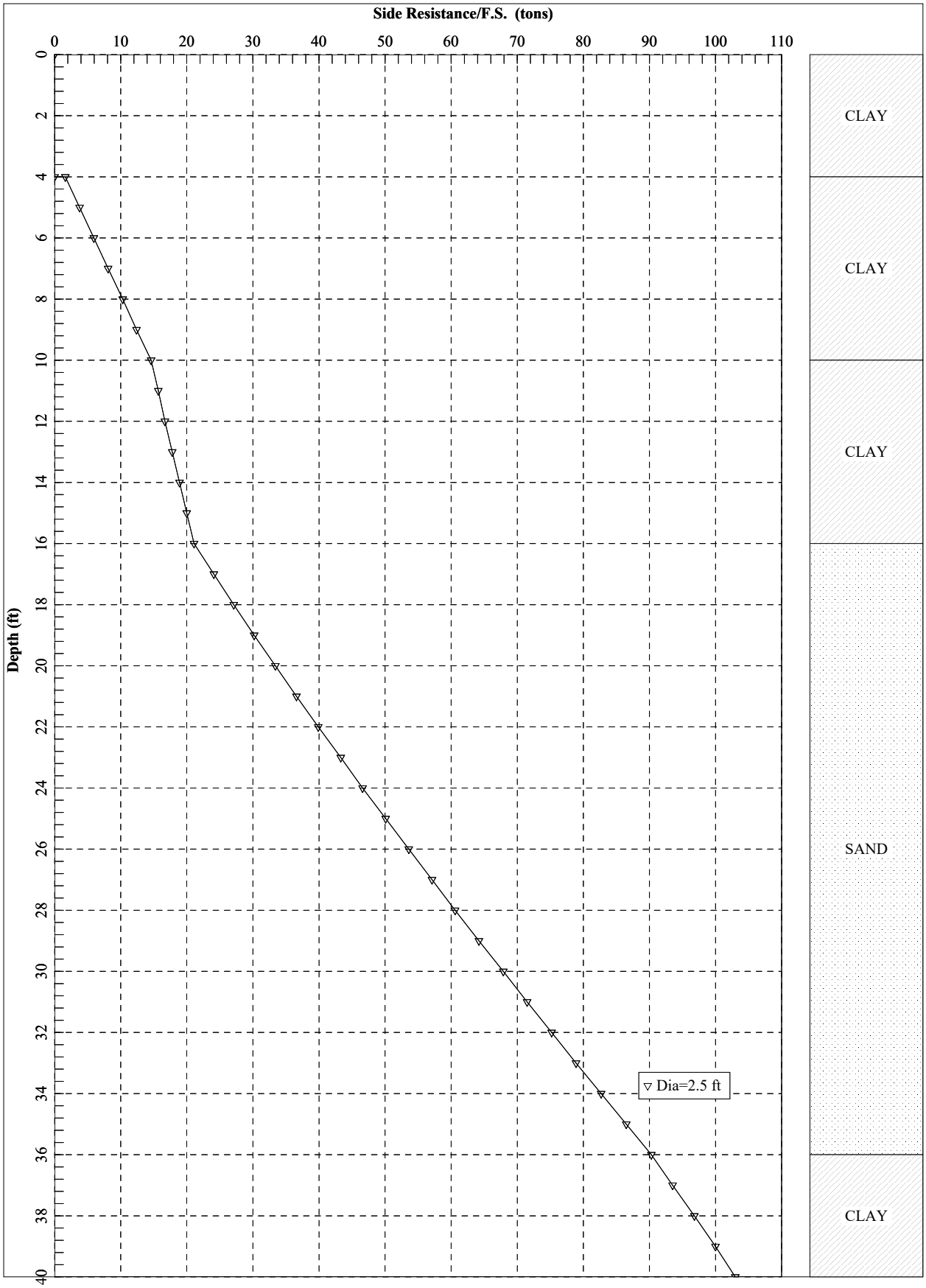

Building
Lateral Response - Bending Moment
18-Inch Pile

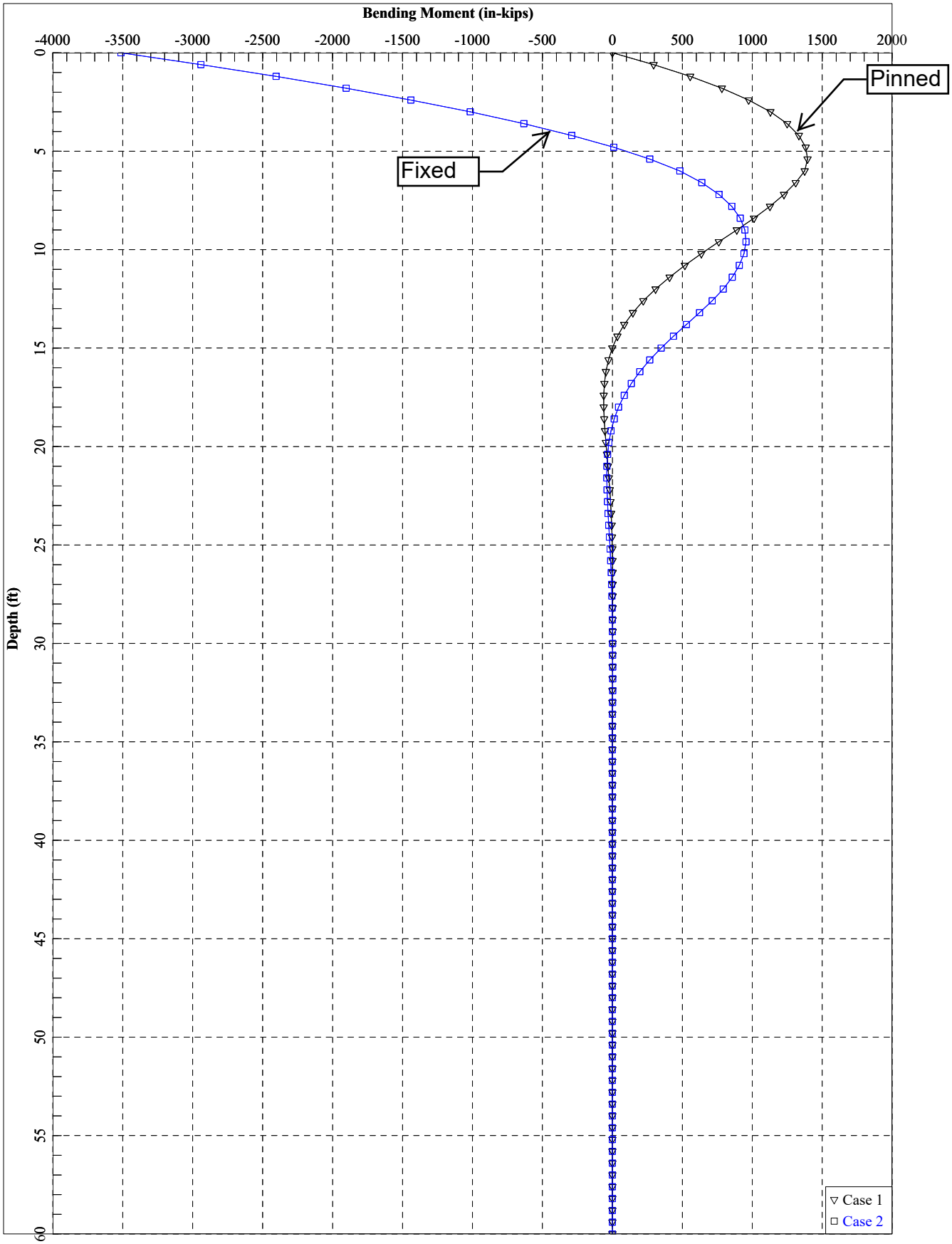

Building
Lateral Response - Shear Force
18-Inch Pile

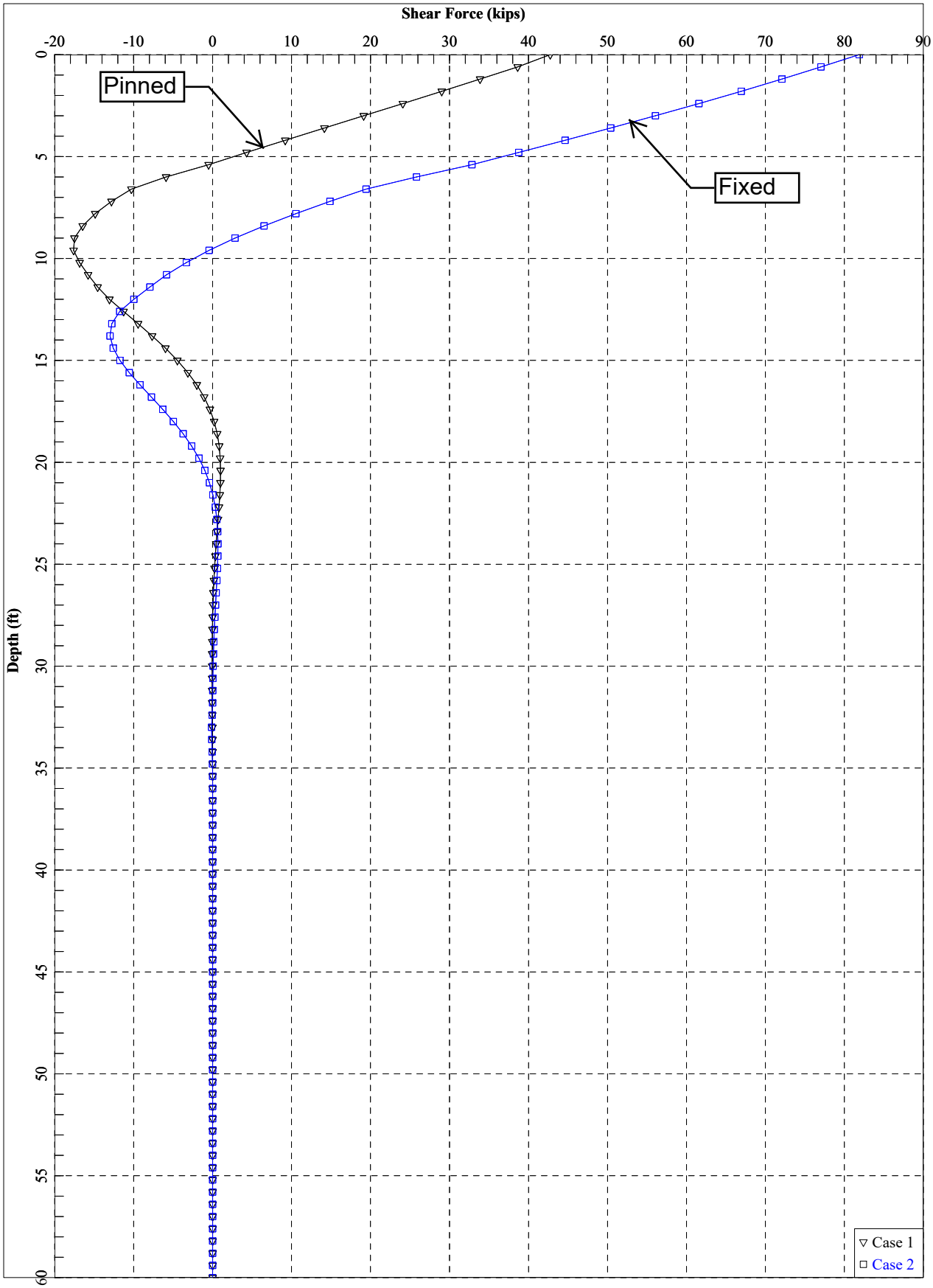

Building
Mobilized Soil Reaction vs. Depth
18-Inch Pile

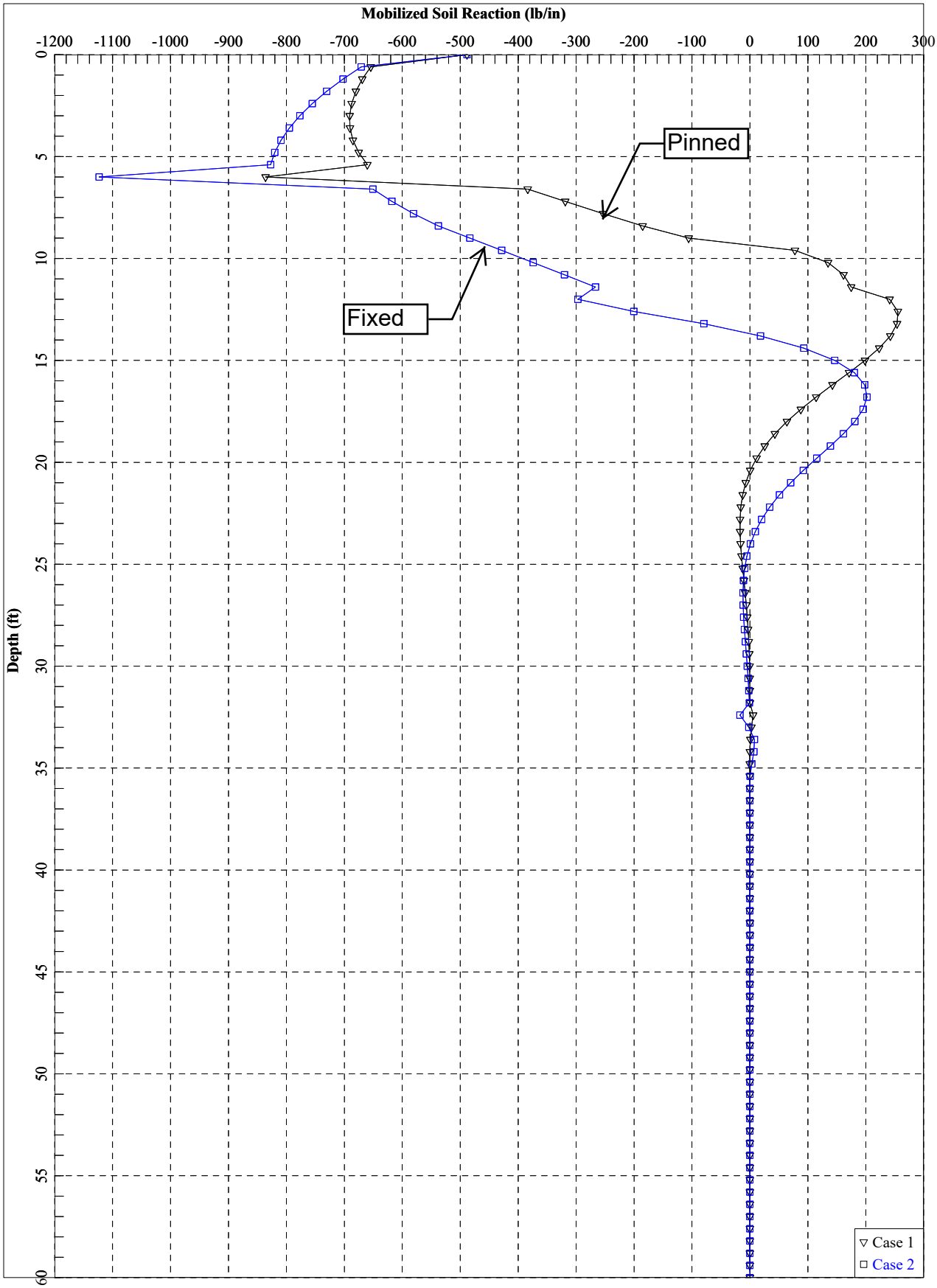

Building
Lateral Response - Bending Moment
30-Inch Pile

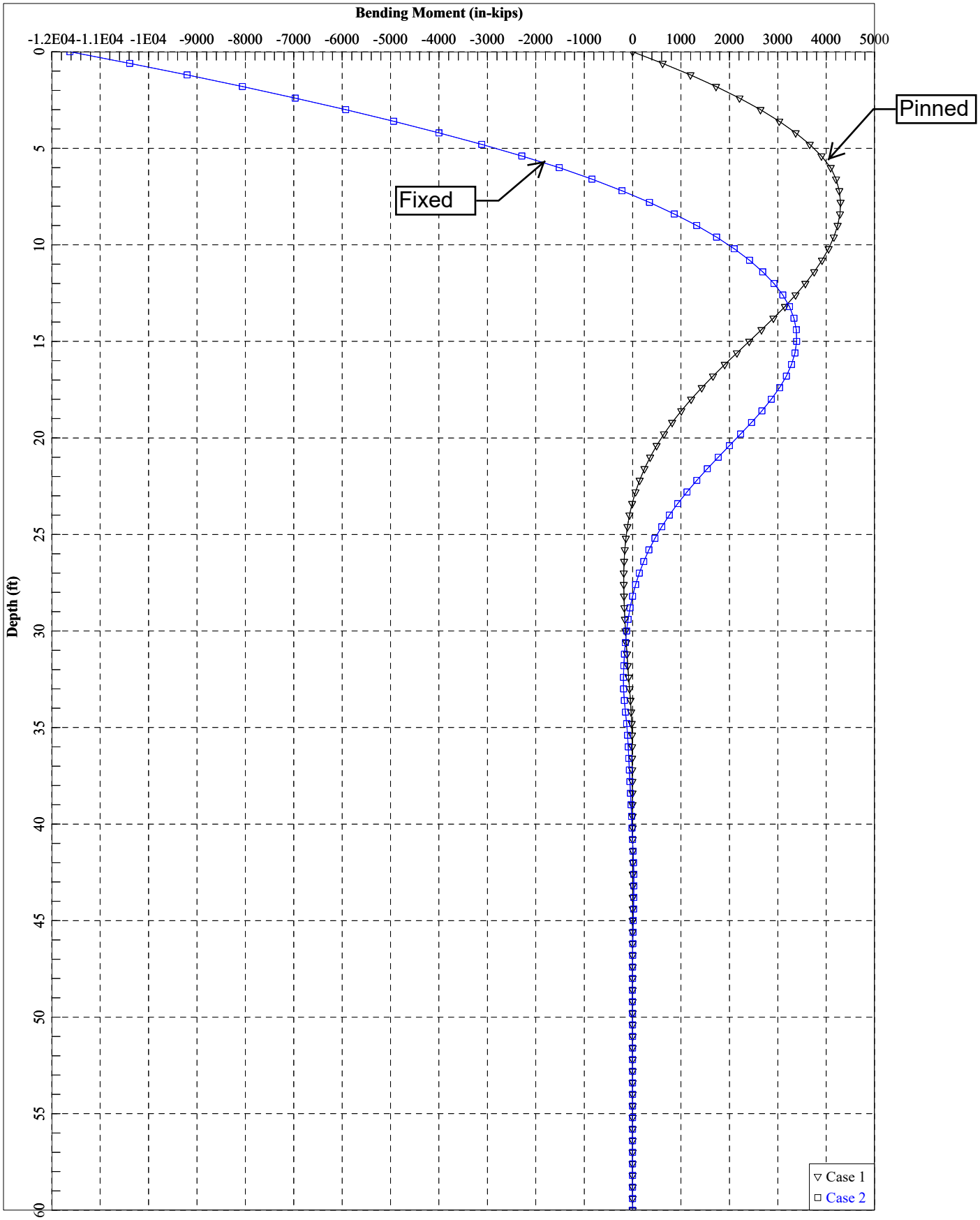

Building
Lateral Response - Shear Force
30-Inch Pile

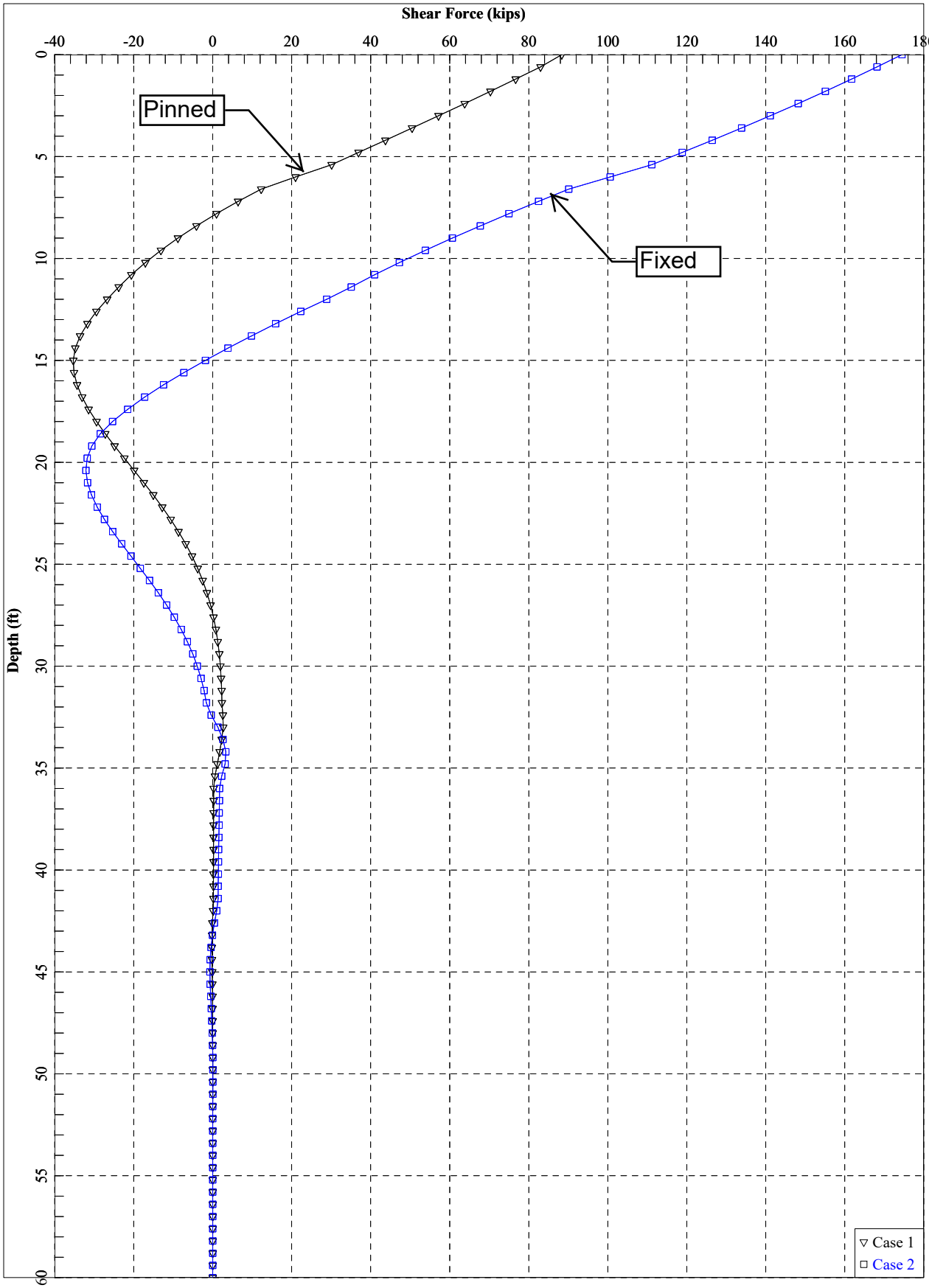

Building
Mobilized Soil Reaction vs. Depth
30-Inch Pile

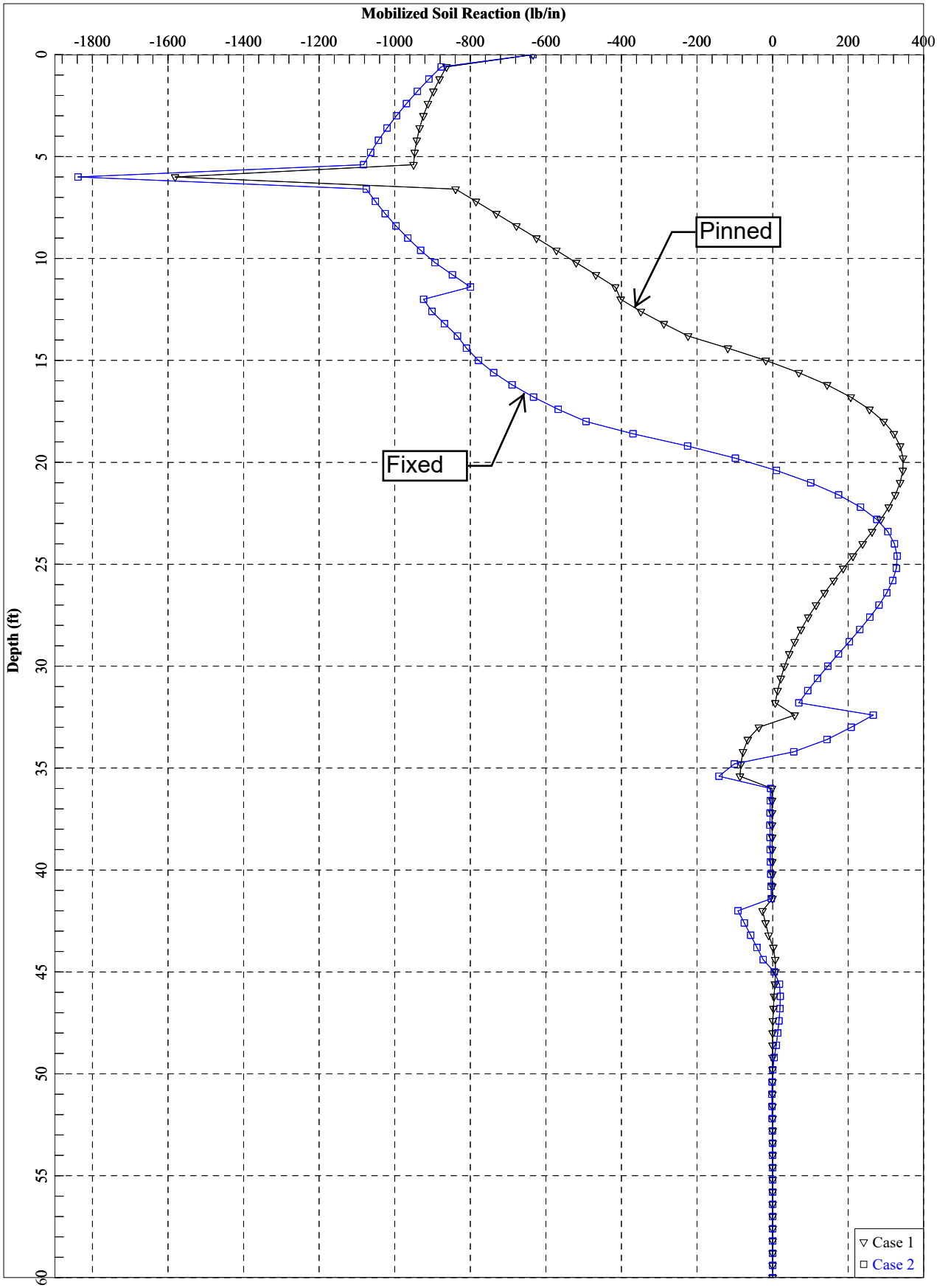

APPENDIX I

Modulus of Subgrade Reaction

Service LC: D: Max Soil Bearing Pressure Plan

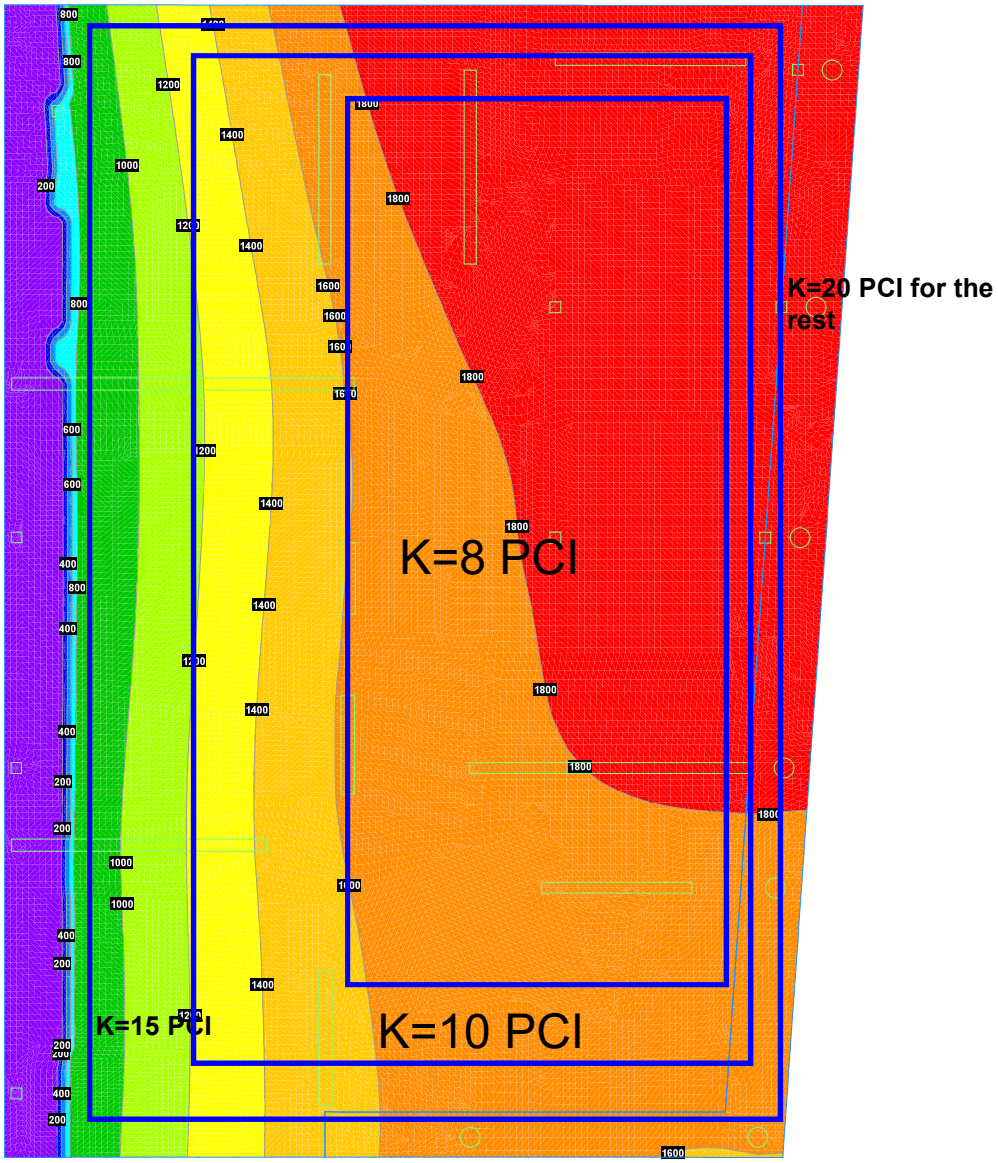

END OF REPORT